UNIVERSIDADE DE TAUBATÉ
PROGRAMA DE PÓS-GRADUAÇÃO EM CIÊNCIAS AMBIENTAIS
Revista Ambiente & Água
An Interdisciplinary Journal of Applied Science

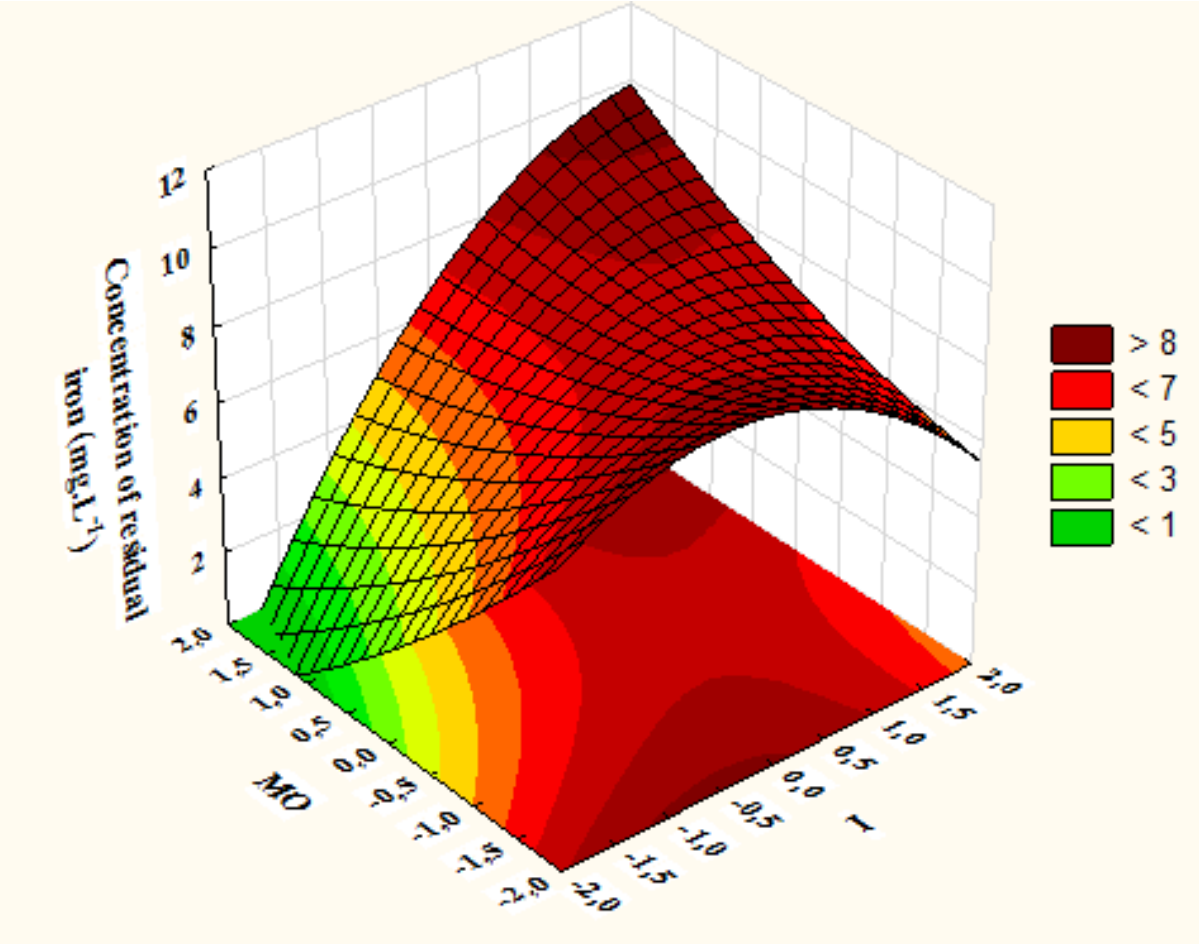

ISSN = 1980-993X (Online)
http://www.ambi-agua.net

Library catalog entry by Liliane Castro CRB/8-6748

Revista Ambiente & Água - An Interdisciplinary Journal of Applied Science / Instituto de Pesquisas Ambientais em Bacias Hidrográficas. Taubaté. v. 14, n.3 (2006) - Taubaté: IPABHi, 2019.
Quadrimestral (2006 – 2013), Trimestral (2014 – 2016), Bimestral (2017), Publicação Contínua a partir de Janeiro de 2018.

Resumo em português e inglês.
ISSN 1980-993X

1. Ciências ambientais. 2. Recursos hídricos. I. Instituto de Pesquisas Ambientais em Bacias Hidrográficas.

CDD - 333.705
CDU - (03)556.18

TABLE OF CONTENTS

COVER:

This research is based on the evidence that the extract of Moringa Oleífera Lam has shown excellent performance for water clarification, reaching 90-94% of turbidity removal. In order to verify such potential, this study focused on applying a hybrid treatment system to the removal of reactive dye Blue 5G from aqueous solutions. This figure shows the surface response for the concentration of residual iron. This surface shows that the lowest values for the concentration of residual iron are achieved when a high dose of aqueous extract of Moringa Oleífera Lam is used and low values of electric current intensity are employed. Source: SANTOS, B. S. de. et al. Continuous electrochemical reactor improved by the addition of Moringa oleífera lam extract: optimization of operational conditions for Blue 5G dye removal. **Rev. Ambient. Água,** Taubaté, vol. 14 n. 3, p. 1-14, 2019. ***doi:10.4136/ambi-agua.2290***

ARTICLES

Ambiente & Água - An Interdisciplinary Journal of Applied Science
ISSN 1980-993X – doi:10.4136/1980-993X
www.ambi-agua.net
E-mail: ambi.agua@gmail.com

Environmental services in watersheds with small declivity: fluvial marine plains

ARTICLES doi:10.4136/ambi-agua.2265

Received: 03 Apr. 2018; Accepted: 19 Feb. 2019

Mateus Marques Bueno[1*]; Ricardo Valcarcel[2]; Felipe Araújo Mateus[2]; Marcos Gervasio Pereira[3]

[1]Instituto Federal de Educação, Ciência e Tecnologia de Minas Gerais (IFMG), São João Evangelista, MG, Brasil
Departamento de Agronomia. E-mail: mateusjuruaia@gmail.com
[2]Universidade Federal Rural do Rio de Janeiro (UFRRJ), Seropédica, RJ, Brasil
Instituto de Florestas (IF). Departamento de Ciencias Ambientais (DCA).
E-mail: ricardo.valcarcel@gmail.com, felipearaujomateus@gmail.com
[3]Universidade Federal Rural do Rio de Janeiro (UFRRJ), Seropédica, RJ, Brasil
Instituto de Agronomia (IA). Departamento de Solos. E-mail: mgervasiopereira01@gmail.com
[*]Corresponding author

ABSTRACT

Fluvial marine plains harbor environments with reduced declivity, but with different environmental attributes that may be relevant ecosystem services in their watersheds, which can be transformed into opportunities for the development of environmental services payments. This study digitally spatialized part of the ecosystem services related to water availability in the microbasins of the Guandu Basin Hydrographic Basin, the main source of water supply for the metropolitan region of Rio de Janeiro, based on geo-environmental factors and the effects of transposition of watersheds, in order to facilitate the formulation of public policies regarding environmental services. The excerpts with the highest potential for producing environmental services from subsurface water flows, Topographic Wetness Index-ITU (ITU > 11), flat formation and low altimetry (< 40 m), are close to the old silted thalwegs, which can be potentialized by the effects of transposition, notably in the APA Guandu conservation unit. These areas should be prioritized in public and private water systems' preservation programs. The areas near the transposition canals feature environmental services that depend directly on the transposition, and may be subject to management, as found in Guandu conservation unit. Flat areas with (7<ITU< 11) have their ecosystem services transferred from subsurface water flows to surface water flows and are dependent more on meteorological phenomena and on ways to manage heavy rain showers through their use, especially as altimetry and slope increase.

Keywords: hydrogenetic areas, topographical index of wetness, water management.

Serviços ambientais em microbacias com baixa declividade: planícies fluvio-marinhas

RESUMO

Planícies fluvio-marinhas abrigam ambientes com reduzida declividade, porém com ofertas diferenciadas de atributos ambientais que podem constituir relevantes serviços

ecossistêmicos nas suas bacias hidrográficas, que podem ser transformadas em oportunidades para o desenvolvimento de pagamento de serviços ambientais. O estudo espacializou parte dos serviços ecossistêmicos relacionados a disponibilidade hídrica nas microbacias da Bacia Hidrográfica do Sistema Guandu, principal manancial de abastecimento da região metropolitana do Rio de Janeiro, com base em fatores geo-ambientais e efeitos de transposição de água entre bacias hidrográficas, a fim de facilitar a tomada de decisão das políticas públicas em relação aos serviços ambientais. Os trechos com maior potencial para a produção de serviços ambientais a partir de vazões subterrâneas, índice de umidade topográfica - ITU (ITU >11), formação plana e baixa altimetria (<40 m), estão próximo aos antigos talvegues assoreados, que podem ser potencializados pelos efeitos da transposição, notadamente na unidade de conservação APA Guandu. Áreas planas com (7 < UIT < 11) têm seus serviços ecossistêmicos transferidos dos fluxos de água sub-superficiais para os fluxos de águas superficiais e dependem mais dos fenômenos meteorológicos e das formas de manejo de chuvas intensas durante seu uso, especialmente quando a altimetria e inclinação aumentam.

Palavras-chave: áreas hidrogenéticas, índice topográfico de umidade, manejo hídrico.

1. INTRODUCTION

The region of fluvial marine plains in Sepetiba Rio de Janeiro, as with others along the Brazilian coastline, present environmental services related to water resources differently, because the variables of terrain, soil, climate, anthropogenic interventions and mountain ranges' influence allow the production and storage of water in the soil, altering the supply of this resource in drainage areas throughout the watershed.

In this way, Meireles and Campos (2010) studied different coastal regions, and affirm that there may be differentiation in the production capacity of ecosystem services. This differentiation in the production of water resource is caused by the variation of the constituents of the sediments that make up the plains, rainfall distribution and local relief (Costanza *et al.*, 1997). In addition, intensive and irregular soils use and recent climate changes, such as the increase in temperature and irregular distribution of rainfall, demand more efficient alternatives in the management of water resources in these places where there is already ample water availability.

Geoprocessing techniques, linked to environmental analyses, and the correct interpretation of the processes that occur in watersheds, allow the identification of hydrologically sensitive areas, leading to the knowledge of their aptitudes and potential. Therefore, with the technological advances of recent decades, the computerization of data is important to the work in environmental science, seeking to optimize from the planning stage to the processing and interpretation of data.

There is therefore a close relationship between technological development, the identification of ecosystem services and the sustainable development of a region (Tacconi, 2012). Thus, it is important to identify how contemporary geomorphological processes are working and how they will intervene in the future; this knowledge is essential for designing environmental policies based on the ecosystem, such as payment programs for environmental services (Gjorup *et al.*, 2016).

For that reason, the identification of natural ecosystem services will only be possible when human demands and planning tools to identify and spatialize areas to receive environmental services measures in a watershed are combined. The small watershed that composes the Guandu System is very important to the water supply of Rio de Janeiro. Therefore, this study used digital processing to infer ecosystem services that can be transformed at environmental service in the Guandu System.

2. METHODS AND MATERIAL

2.1. Characterization of the Fluvial Marine Plains Studied

The studied region comprises the Guandu Watershed System (BHSG), where one of several Brazilian fluvial marine plains is located. This watershed is of fundamental importance for the water supply of the city of Rio de Janeiro. Currently, Guandu channel is source of water for human use and for various productive sectors such as the steel industry, petrochemicals, food and beverages, clothing, among others. The total area of BHSG is 1,437.59 km^2. Considering Lajes' riverside as the main segment of the system, the total length of the Guandu River is 108.5 km.

The predominant climate in the region is the Köppen Aw. The rainfall regime is characterized by a rainy season, from December to March (summer), and dry season, from June to August (winter). The annual average rainfall is 1,270 mm, according to data from the meteorological station historical series A601-Agricultural Ecology, located in the city of Seropédica-RJ. However, there is no uniformity in the regime of rainfall along the watershed, which is related to the irregularity of the atmospheric systems. It causes a variation in the total volume of precipitation from 700 to 2,400 mm per year.

Sepetiba Bay Watershed's lithological units occur generally disseminated among themselves, Proterozoic age lithologies show clear structural direction NE-SW and Neogenous sediments scattered throughout the low formation points. Some units occur in isolation, especially the units of Cenozoic age, and some of Proterozoic age. The fluvial marine sediments of Neogenous age are spread along low areas and around elevations composed by Proterozoic rocks, forming Fluvial Marine Plains (Garcia *et al.*, 2015).

According to a survey conducted by Santos *et al.* (2013), adapted on Figure 1, the lower parts of the watershed and near the coast (upwelling zone) are composed by Ultisols (Albaquults) and represent 33.92% of the watershed's total area. In addition, the Ultisols dominate almost the entire remainder of the watershed, or 63.45%.

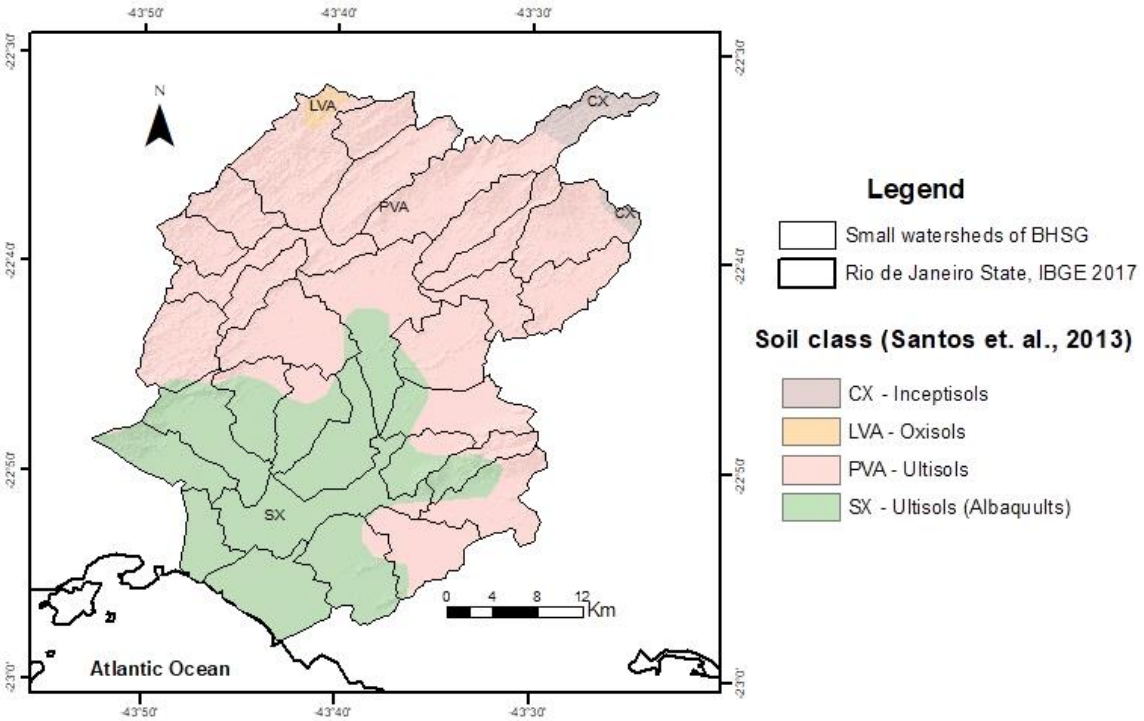

Figure 1. Soil classes for the Guandu Watershed System (BHSG), adapted by Santos *et al.* (2013).

2.2. BHSG's Morphometric Characterization

The Digital Model of Hydrologically Consistent Elevation (MDE-HC) of the area was obtained by processing the cartographic database from the Brazilian Institute of Geography and Statistics (IBGE), with contour levels offsets of 10 m, hydrography and quoted points, on a scale of 1:25,000. The interpolation of elevation's data was performed with spatial resolution of 10 m, via the Software ArcGIS 10.2.1, using the spatial analysis tool. From the MDE-HC were obtained altimetry classes (reclassify tool), slope (surface and slope tools), aspect (surface and aspect tools), and curvature surfaces (surface and curvature tools).

The physical parameters of the BHSG of all small watersheds (area, perimeter, channels' lengths, drainage density, form factor, index of circularity [Ke], compactness index [Kc], and sinuosity index [Is]) were computed as described by the methodology of Hajam *et al.* (2013), using the MDE-HC and the limits provided by the hydrographic basin tool from the ArcGIS. These parameters Ke, Kc and Is, are important to compare different watersheds. Using area, perimeter and length it is possible to create a standardization and compare the characteristics of the watershed with standard forms and with one another.

Drainage obtained by automatic interpolation of MDE-HC, was compared with the official IBGE and overlapped to high-resolution satellite imagery from Landsat 5 TM satellite, 2006, acquired from the National Space Research Institute (INPE)'s database website.

2.3. Floodplain and Water Dynamics

The automatic delimitation refers to the detection of floodplains through the classification of a regional (not local) topographic variable, recognized as an indicator, by means of the Topographic Wetness Index (ITU). The methodology consisted in obtaining regional topographic variables from the MDE-HC, based on the developments of the ITU. The data processing was carried out by SAGA GIS 2.1.2 software. The UTI characterizes the surface water saturation zones and the water content in the soils. (Prates *et al.*, 2012) found that for well-drained soils, the index varies between 4 and 5, in moderately drained soils it varies between 5 and 7 and in poorly drained soils, the indices oscillate between 7 and 12. This index can also be associated with soil thickness, structural grade and permeability (Lin *et al.*, 2006).

The local water dynamics was characterized from the regional rainfall, with data obtained directly from INMET's conventional and automatic stations. The anthropized micro watersheds' water dynamics was determined by the characterization of contemporary geomorphological processes, simplified in hydrogenetic zones (Table 1).

Table 1. Parameters used to classify the hydrogenetic zones of Guandu's Hydrographic Watershed System (BHSG).

Hydrogenetic zones	Description
Capitation	Areas with high elevations (reference to the lowest elevation of the watershed). This areas start from the top of the watershed, with small and varying angular inclination, deeper soils, infiltration prevail and subsurface flow.
Transition	Areas with intermediate elevations and high slope. Shallow soils with frequent processes of surface layer movement. Region favorable to the occurrence of surface runoff and mass displacement processes.
Outcrop	Areas of lower relative elevation and low slope. Region of sediment accumulation, with presence of soils with greater water storage capacity. Prevalence of subsurface flow processes.

Finally, the interference of the construction of Guandu's canal and other drainages in the region were compared with the identified plains, in order to infer about their interference in the availability of the watershed's environmental services. The checking of the results was made

using high-resolution satellite imagery from Landsat 5 TM satellite, 2006; in addition to the historical series of images available on Google Earth Pro program for the years 2002 to 2016. The processing of maps and images was performed in ArcGIS 10.2.1.

3. RESULTS AND DISCUSSION

The small watersheds (MB1 to MB33 - less MB 18 e MB 19) and the topography classes can be seen in Figure 2. The physical indexes of BHSG (Table 2) indicate a variation, since the Ke and Kc values point to the presence of more rounded forms in the central south region and more elongated forms in the surroundings. Similarly to what was verified by analyses of Dd and Is indexes, showing that the small surrounding watersheds are more drained (values above average, 2.26) and with sinuosity index further from the unit. Ferrari *et al.* (2013) indicated that the more elongated and the more efficient the drainage conditions are, the more likely is water loss through the watershed's outflow.

In the area, the geological and climatic conditioners markedly influenced the effects of geomorphological factors, allowing formation of sites with high climate variation. This variability causes differences in the provision of environmental services available in small BHSG, noted in the variability observed in values of obtained for the ITU (Figure 3), which occur preferentially in non-consolidated sand, gravel, silt, clay and peat deposits.

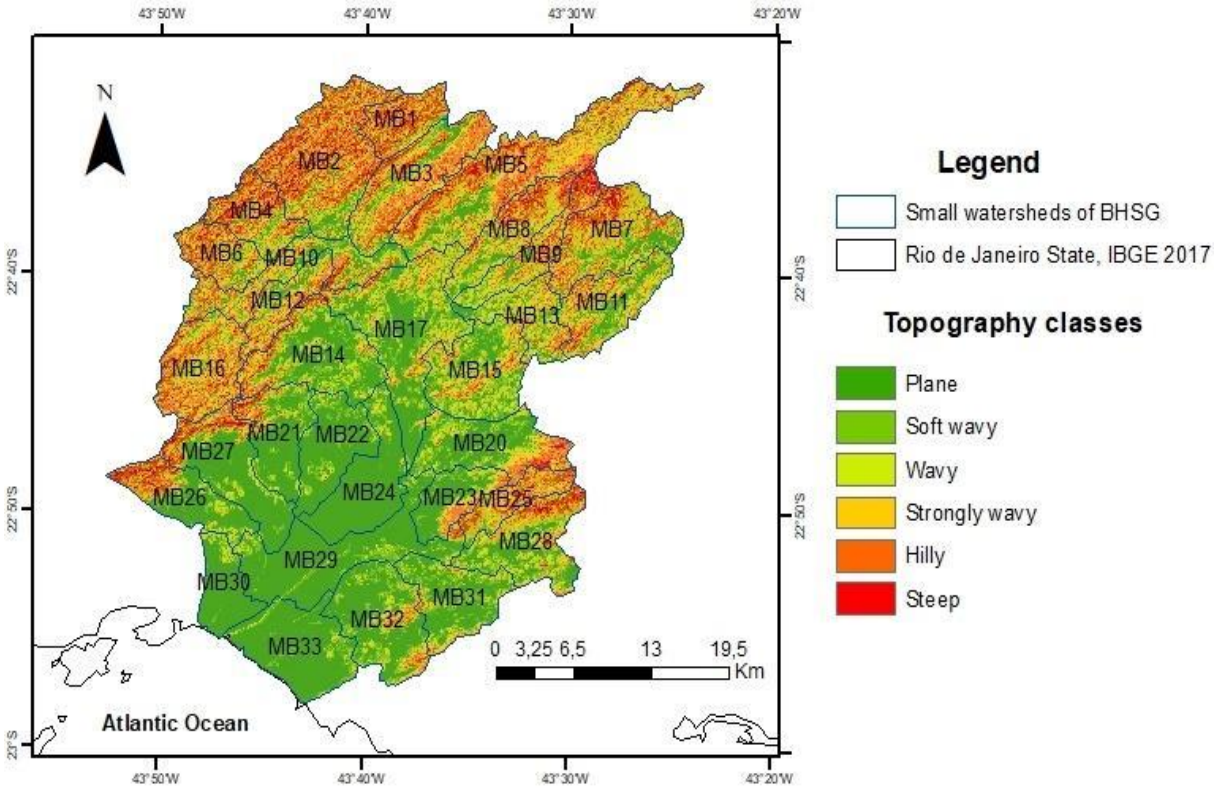

Figure 2. Topographic classes and small watersheds of the Guandu Watershed System (BHSG).

Table 2. Physical Parameters of Guandu's Hydrographic Watershed System (BHSG).

Item	A	P	∑ L	L	L	Dd	Ke	KC	Is
	km²	km		M		m/m²	-	-	m/m
BHSG	1,437.59	1,177.77	3,034.50	75,584.85	58,439.59	2.11	0.01	8.70	1.29
MB1	24.98	22.69	57.26	12,096.05	2,763.63	2.29	0.61	1.27	1.38
MB2	80.60	47.45	182.82	18,546.54	12,990.15	2.27	0.45	1.48	1.43
MB3	55.38	38.38	124.63	14,394.31	12,990.19	2.25	0.47	1.44	1.11
MB4	31.16	27.69	70.02	9,058.68	6,287.42	2.25	0.51	1.39	1.44
MB5	97.62	73.40	231.78	32,277.88	27,662.56	2.37	0.23	2.08	1.17
MB6	25.85	23.66	57.62	8,418.06	5,795.10	2.23	0.58	1.30	1.45
MB7	55.66	37.51	146.30	12,141.25	6,287.42	2.63	0.50	1.41	1.93
MB8	36.96	33.49	95.10	16,378.08	13,779.65	2.57	0.41	1.54	1.19
MB9	29.79	37.33	74.31	17,519.94	15,084.21	2.49	0.27	1.91	1.16
MB10	43.50	58.38	108.79	20,100.51	16,042.07	2.50	0.16	2.48	1.25
MB11	40.68	34.09	92.44	13,998.92	11,730.74	2.27	0.44	1.50	1.19
MB12	24.13	28.38	56.69	12,027.80	9,919.56	2.35	0.38	1.62	1.21
MB13	29.23	36.15	70.06	7,829.59	6,294.58	2.40	0.28	1.87	1.24
MB14	61.21	39.57	140.10	14,572.89	11,441.41	2.29	0.49	1.42	1.27
MB15	52.94	34.02	116.64	10,195.36	9,394.11	2.20	0.57	1.31	1.09
MB16	47.44	28.75	115.33	11,436.97	9,167.53	2.43	0.72	1.17	1.25
MB17	85.01	61.37	198.30	20,652.88	16,280.15	2.33	0.28	1.86	1.27
MB20	50.06	41.27	115.55	17,178.21	13,590.73	2.31	0.37	1.63	1.26
MB21	38.03	31.52	82.35	9,770.26	9,047.23	2.17	0.48	1.43	1.08
MB22	39.36	32.02	87.02	8,813.97	7,630.04	2.21	0.48	1.43	1.16
MB23	26.05	24.49	55.57	8,636.09	7,382.69	2.13	0.55	1.34	1.17
MB24	48.01	39.31	84.55	15,657.08	12,654.35	1.76	0.39	1.59	1.24
MB25	22.75	28.17	48.41	11,628.15	10,023.34	2.13	0.36	1.65	1.16
MB26	37.82	34.30	89.80	13,017.75	12,265.06	2.37	0.40	1.56	1.06
MB27	53.08	43.02	130.23	14,513.62	11,668.40	2.45	0.36	1.65	1.24
MB28	48.53	40.09	103.68	13,132.87	11,021.79	2.14	0.38	1.61	1.19
MB29	72.87	70.59	169.50	15,216.71	14,738.26	2.33	0.18	2.32	1.03
MB30	26.17	25.81	45.69	5,742.56	5,142.08	1.75	0.49	1.41	1.12
MB31	42.39	33.59	92.29	9,686.88	8,811.01	2.18	0.47	1.44	1.10
MB32	55.81	34.66	112.79	11,144.91	7,727.16	2.02	0.58	1.30	1.44
MB33	54.52	36.63	110.73	12,631.90	6,815.07	2.03	0.51	1.39	1.85

Legend: A – hydrographical watershed area; P - perimeter of the hydrographical watershed area; A - watershed area; ∑L - length of all watershed drains; L - length of the main drain of the watershed; l - vectorial length of watershed' main drain; DD - drainage density; Ke – circularity index; KC – compactness index; Is – sinuosity index; BHSG - Guandu Watershed System and M1 to M33 – small watershed of the BHSG.

About 50% (720.81 km²) of the area of BHSG is less than 40 m in altitude and 36% (511.49 km²) presents a flat surface (Figure 1). These areas are located in the central region of the watershed, where 91.21 km² presents ITU above 11 units; they are humid plains, with maximum expression of natural ecosystem services. Immediately adjacent to these areas, there are saturated areas with less intensity, with ITU values of between 5 to 11 units, totaling 580.97 km², 40.41% of the BHSG's total area. The surface in this area is characterized as soft wavy, wavy and strong wavy. The driest areas represent 53.24% (765.40 km²) and are located in peripheral areas that are not in contact with the sea. The surface is predominantly mountainous and rugged in small portions.

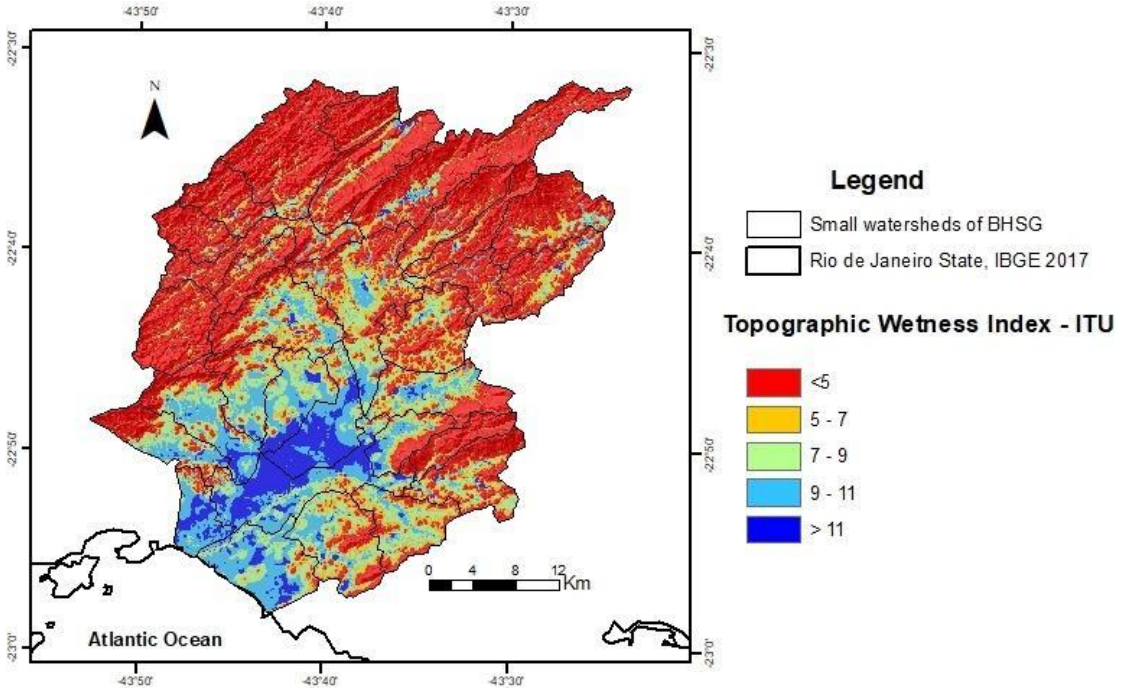

Figure 3. Topographic Wetness Index (ITU), to the watershed of the Guandu System (BHSG).

The soil distribution indicates the prevalence of Ultisols (Albaquults) in low areas and in part of the transitional areas. The other areas feature mostly Ultisols in the transition areas and with rugged relief. Oxisols and Inceptisols are evidenced in areas with greater altimetry and irregular topography, and represent less than 3% of the total area of the watershed.

The Ultisols (Albaquults), for having a low amount of clay on the surface, have less surface water storage capacity (Dondeyne *et al.*, 2014). In this way, the water flow is influenced by other factors, mainly by relief and the upstream and downstream hydraulic potential. The predominance of Ultisols (Albaquults) in the flat regions, where there was the deposition in the channels that drain to the sea, with low hydraulic gradient, indicating selective sedimentation, with coarse sediments in high and fine parts in low. In the transition to the mountains, there are some areas of low elevation (about 40 m). These area are slightly undulate to undulate hills, shaped as a "half orange". This configuration shows the differentiation of storage and water flow capacities in the watershed, as well as the distribution of morphological features.

Reis *et al.* (2014) by studying the effect of different uses on Ultisols (Albaquults), found that the formation and stabilization of aggregates occur simultaneously with the influence of physical, chemical and biological processes in the soil. These aggregates, which are agents of soil structuring, store water and are predominated by horizontal flows of water. The influence of the salinas wedges occur in the opposite direction, often in the mains canal (paleo channels). Salamene *et al.* (2011) studied this areas and found influence of the sea water for 20 km in the main Guandu channel.

It is important to point out that the land use promotes changes in the land's physical attributes, mainly in soil structure, which may promote or hinder the water storage in the soil (Ortigara *et al.*, 2014). Intensive cultivation, without the development of conservation practices, for several years, as occurred in the transitional region, can degrade the soil, altering its water retention.

The river influence on soil's water storage of fluvial marine plains is related to the peculiarities of these sites and their management. When there is an imbalance generated by changes in land use or even by periods of restriction, the influence of the sea can prevail. On the other hand, in the case of preservation and climate normality, the greatest influence is given by rainwater.

The relationship between the ITU and the soil's water pressure is positive and is variable in time and space for a natural forest catchment watershed (Liang and Chan, 2017). In this way, ITU can be correlated with depth and capacity of the soil to keep water over time. A similar assessment, but in agricultural soils, performed by Buchanan *et al.* (2014) demonstrated that the ITU can be correlated with superficial and deep soil wetness segments and can coexist.

The wetness areas operate hydrologically in a harmonious way with the transitional areas, working as the great aquifers that reach the surface of the flood plain's soil. These areas when saturated extend laterally. As observed by Baptista *et al.* (2014), in their study in areas of an old paleo canal (thalwegs) embedded by sediments of fluvial influence, the current and former sites of sand accumulation are present in the plains and exhibit a particle size stratification, which is related to the distance from the source of emission and the reduction of transport energy. This evidence refers to the geomorphological role of the basins in the formation of fluvial-marine plains near the coast, where we developed the study. The ecosystem services prevalent in wet areas arise from the impoundment of the sub surface and deep streams, depending on the influence of tidal oscillations. In the part closest to the sea, there is an interdependence of the effects of saline intrusion, which causes a high degree of salinity up to 8 km on the river surface and is introduced to the interior of the continent by the lines of drainage channels (Salamene *et al.*, 2011).

These factors show that there is a wide variation in the dynamics of this system, and confirm that in the flat area there is a strong influence of the water table in the water control system of the watershed, which gives these areas a predominance of vertical and horizontal movements of subsurface water. In the mountainous areas, there is a predominance of horizontal and vertical movements on the surface, and both are found in the areas of transmission.

In this sense, the slope is the expression of the mass movement potential, water flow velocity and other erosion processes (Pinheiro *et al.*, 2012), and determines the amount of water a soil can hold, the potential for erosion or deposition, among other fundamental processes (Wilson and Gallant, 2000). In this way, it can be verified that most of the area has its natural potential reduced due to erosion processes.

Similarly, curvature, plan and profile data aid in the interpretation of morphological characteristics of landscape such as susceptibility to erosion, surface runoff, storage and flow of water. In the BHSG, three different hydrogenetic zones were identified: Outcrop, Transition and Capitation (Figure 4). In the Outcrop zone, there is a predominance of a plane topographic profile followed by the convex form. in the transition zone also there is a predominance of the convex form, but with soft wavy, wavy and strongly wavy reliefs. The Capitation zone represents small areas in this watershed, so the hydric dynamic is more important for the two other zones.

These indicators show that there is a differentiation in dynamics of water flows along the watershed; in the upwelling area horizontal flows predominate and in transmission areas there is the interference of horizontal and vertical streams. This pattern shows that there is a differentiation of environmental service capacity in these areas.

On the other hand, orientation of the relief is important because it allows the visualization of the face of sun exposure, thus making it possible to infer about the local micro-climate (temperature, precipitation and humidity), and about the differentiation of the evapotranspiration process of the areas (Valeriano, 2003). The BHSG presents only a slight northern predominance (about 28%); other orientations are distributed evenly. Little variation indicates that there is homogeneity with respect to sun exposure and, consequently with respect to the ability of wetness loss. However, the evaluation of this parameter to specific watersheds shows differences in exposure and, as a result, in the water production capacity.

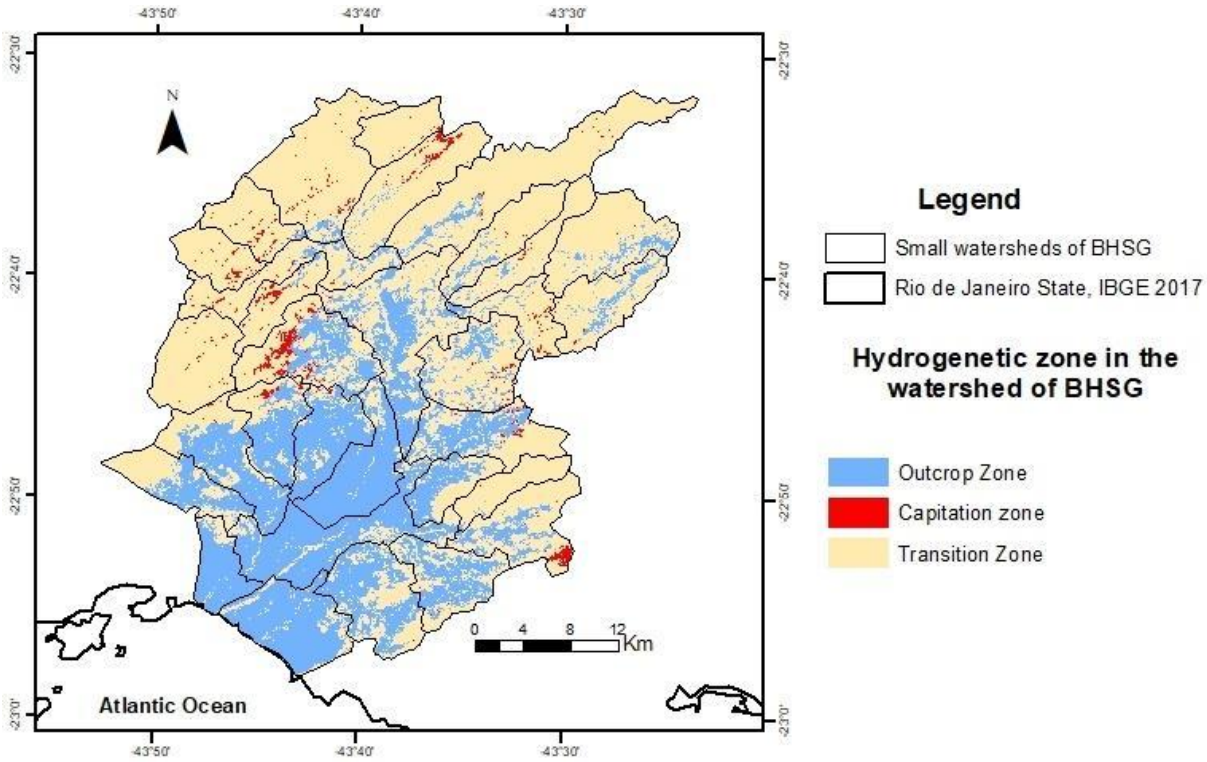

Figure 4. Hydrogenetic zone of the watershed of the Guandu System (BHSG).

Salamene *et al.* (2011) studied the Guandu channel gutter and its interaction with a buffer of 100 m across the central line. This paper shows that after the construction of the artificial canal in the BHSG, there was a lowering of the water table. This alteration led to the increase of the area of outcropping upstream and the decrease of the area downstream. Consequently, there was a change in the local water dynamics, causing the regulatory areas to change. The impact of this alteration should be taken into account in public policies related to Guandu's protection area, since the preservation of this resource is of fundamental importance to government policies.

4. CONCLUSIONS

The variation in precipitation constitutes an important factor for the planning in the small watersheds; however, the constant inward flow of 160 $m^3 s^{-1}$ transposition that encompasses the BHSG in terms of environmental services made the storage areas in the water table more important. The morphological characterization and development of the ITU allowed for the segregation areas that serve as supply and catchment areas and of the floodplain system. These areas are located mainly in the surrounding areas of the ancient beds of natural paleo channels, traversed by Guandu's canal, both upstream and downstream, and should be prioritized in public and private water system preservation programs. In the areas occupied by the floodplain, the ITU has enabled the identification of differentiated areas regarding water production.

The Guandu's canal passage through the areas of floodplain influence affects positively the upwelling areas upstream. On the contrary, downstream a modification can be perceived in order to decrease the water flow and cause a deficit, mainly from the demotion of the water table and the modification in the drainage system. In areas above the elevation of 40 m, the effects of the floodplain and transposing channel are barely noted. The micro-watersheds located in these areas need to be hydrologically determined; that is, they depend on rain and on the system's water storage and output.

The inability of water supply to meet the growing demand in the metropolitan region of Rio de Janeiro highlights the need for alternative management strategies of the BHSG. Among them, we highlight the renaturalization on the outcrop zone functions, in order to take advantage of water storage capacity during the full season so that it may be utilized during the dry season.

5. ACKNOWLEDGEMENTS

We thank the Federal Rural University of Rio de Janeiro, specifically the PPGCAF, LMBH and LGCS. We recognize CNPq and the Petra Agregados mining company for the financial support.

6. REFERENCES

BAPTISTA, M. N.; VALCARCEL, R.; MAYA, V.; CANTO, F. Selection of Preferred Floodplains for the Renaturalization of Hydrologic Functions: A Case Study of the Paraíba do Sul River Basin, Brazil. **Water resources management**, v. 28, n. 13, p. 4781-4793, 2014. https://doi.org/10.1007/s11269-014-0775-z

BUCHANAN, B. P.; FLEMING, M.; SCHNEIDER, R. L.; RICHARDS, B. K.; ARCHIBALD, J.; QIU, Z.; WALTER, M. T. Evaluating topographic wetness indices across central New York agricultural landscapes. **Hydrology and Earth System Sciences**, v. 18, n. 8, p. 3279, 2014. https://dx.doi.org/10.5194/hess-18-3279-2014

COSTANZA, R.; D'ARGE, R.; DE GROOT, R.; FARBER, S.; GRASSO, M.; HANNON, B.; RASKIN, R. G. The Value of the World's Ecosystem Services and Natural Capital. **Nature**, v. 387, p. 253-260, 1997. https://doi.org/10.1038/387253a0

DONDEYNE, S.; VANIERSCHOT, L.; LANGOHR, R.; VAN RANST, E.; DECKERS, J. **The Soil Map of the Flemish Region Converted to the 3rd Edition of the World Reference Base for Soil Resources**. Brussels: Departement Leefmilieu, Natuur & Energie, 2014.

FERRARI, J. L.; SILVA, S. F.; SANTOS, A. R.; GARCIA, R. F. Análise morfométrica da sub-bacia hidrográfica do córrego Horizonte Alegre, ES. **Revista Brasileira de Ciências Agrárias**, v. 8, n. 2, p. 181–188, 2013. https://dx.doi.org/10.5039/agraria.v8i2a1575

GARCIA, M. G. M.; BRILHA, J.; LIMA, F. F.; VARGAS, J. C.; AGUILAR, A. P.; DULEBA, W.; FERNANDES, L. A.; FIERZ, M.; MARTINS, L.; RAPOSO, M. I. B.; RICARDI-BRANCO, F.; ROSS, J.; SALLUN, W. The inventory of geological heritage of the State of São Paulo, Brazil: methodological basis and preliminary results. In: INTERNATIONAL SYMPOSIUM OF PROGEO, 8., 2015, Reyjavik, IS. **Anais[...]** Uppsala: Progeo, 2015. p. 32-33.

GJORUP, A. F.; FIDALGO, E. C. C.; PRADO, R. B.; SCHULER, A. E. Análise de procedimentos para seleção de áreas prioritárias em programas de pagamento por serviços ambientais hídricos. **Revista Ambiente & Água**, v. 11, n. 1, p. 225, 2016. https://dx.doi.org/10.4136/ambi-agua.1782

HAJAM, R. A.; HAMID, A.; BHAT, S. Application of morphometric analysis for geohydrological studies using geo-spatial technology - A case study of Vishav drainage watershed. **Hydrology Current Research**, v. 4, n. 3, p. 1-12, 2013.

LIANG, W. L.; CHAN, M. C. Spatial and temporal variations in the effects of soil depth and topographic wetness index of bedrock topography on subsurface saturation generation in a steep natural forested headwater catchment. **Journal of Hydrology**, v. 546, p. 405-418, 2017. https://doi.org/10.1016/j.jhydrol.2017.01.033

LIN, H. S.; KOGELMANN, W.; WALKER, C.; BRUNS, M. A. Soil moisture patterns in a forested catchment: A hydropedological perspective. **Geoderma**, v. 131, p. 345-368, 2006. https://doi.org/10.1016/j.geoderma.2005.03.013

MEIRELES, A. J. A.; CAMPOS, A. A. **Componentes Geomorfológicos, Funções e Serviços Ambientais de Complexos Estuarinos no Nordeste do Brasil**. Revista da ANPEGE, v. 6, n. 6, p. 89-107, 2010. https://doi.org/10.5418/RA2010.0606.000

ORTIGARA, C.; KOPPE, E.; LUZ, F. B.; BERTOLLO, A. M.; KAISER, D. R.; SILVA, V. R. Uso do solo e propriedades físico-mecânicas de Latossolo Vermelho. **Revista Brasileira de Ciência do Solo**, v. 38, n. 2, p. 619-626, 2014.

PINHEIRO, H. S. K.; DA SILVA CHAGAS, C.; DE CARVALHO JÚNIOR, W.; DOS ANJOS, L. H. C. Modelos de elevação para obtenção de atributos topográficos utilizados em mapeamento digital de solos. **Pesquisa Agropecuária Brasileira**, v. 47, n. 9, p. 1384-1394, 2012.

PRATES, V.; SOUZA, L. C. D. P.; OLIVEIRA JUNIOR, J. C. D. Índices para a representação da paisagem como apoio para levantamento pedológico em ambiente de geoprocessamento. **Revista Brasileira de Engenharia Agrícola e Ambiental**, v. 16, n. 4, p. 408-414, 2012.

REIS, D. A.; LIMA, C. L. R.; PAULETTO, E. A. Resistência tênsil de agregados e compressibilidade de um solo construído com plantas de cobertura em área de mineração de carvão em Candiota, RS. **Revista Brasileira de Ciência do Solo**, v. 38, p. 669-78, 2014.

SALAMENE, S.; FRANCELINO, M. R.; VALCARCEL, R.; LANI, J. L.; SÁ, M. M. F. Estratificação e caracterização ambiental da área de preservação permanente do Rio Guandu/RJ. **Revista Árvore**, v. 35, n. 2, p. 221-231, 2011.

SANTOS, H. D.; JACOMINE, P. K. T.; ANJOS, L. D.; OLIVEIRA, V. D.; OLIVEIRA, J. D.; COELHO, M. R.; CUNHA, T. D. **Sistema brasileiro de classificação de solos**. 3. ed. Rio de Janeiro: Embrapa Solos, 2013.

TACCONI, L. Redefining payments for environmental services. **Ecological Economics**, v. 73, p. 29-36, 2012. https://doi.org/10.1016/j.ecolecon.2011.09.028

VALERIANO, M. D. M. Curvatura vertical de vertentes em microbacias pela análise de modelos digitais de elevação. **Revista Brasileira de Engenharia Agrícola e Ambiental**, v. 7, n. 3, p. 539-546, 2003.

WILSON, J. P.; GALLANT, J. C. Digital terrain analysis. *In:* WILSON, J. P.; GALLANT, J. C. (Eds.). **Terrain analysis**: Principles and applications. New York: Wiley, 2000. p. 1-27.

Ambiente & Água - An Interdisciplinary Journal of Applied Science
ISSN 1980-993X – doi:10.4136/1980-993X
www.ambi-agua.net
E-mail: ambi.agua@gmail.com

Diversity of the riparian vegetation of high Andean wetlands of the Junín region, Peru

ARTICLES doi:10.4136/ambi-agua.2271

Received: 21 Apr. 2018; Accepted: 19 Feb. 2019

Fernán Cosme Chanamé-Zapata*; María Custodio-Villanueva; Raúl Marino Yaranga-Cano; Rafael Antonio Pantoja-Esquivel

Universidad Nacional del Centro del Perú (UNCP), Huancayo, Junín, Peru
Facultad de Zootecnia. Instituto de Investigación en Alta Montaña (IIAM).
E-mail: fernan_chz@hotmail.com, mcustodio@uncp.edu.pe,
raul_yaranga@yahoo.es, centrozoot@hotmail.com
*Corresponding author

ABSTRACT

The diversity of the riparian vegetation of five high Andean lagoons of the Junin region was evaluated between March and December of 2017. The sampling of the riparian vegetation was carried out by means of the transect method. The unidentified species were collected for later identification in the herbarium. The diversity was determined by floristic composition, abundance and frequency, and by species richness indices of Simpson and Shannon-Wiener. In the Pomacocha Lagoon, the floristic composition was represented by 43 species, distributed in 15 families, with the most abundant species being *Aciachne pulvinata*, *Azorella crenata* and *Geranium sessiliflorum* and the most frequent *Aciachne pulvinata.* In the Laguna Tragadero, the floristic composition was represented by 17 species, distributed in 10 families, with the most abundant species being *Pennisetum clandestinum and Eleocharis sp* and the most frequent *Polypogon interruptus*. In the Cucancocha Lagoon, the floristic composition was represented by 19 species, distributed in 7 families, with the most abundant species being *Calamagrostis sp* and *Wernberia humbellata* and the one of most frequent *Carex ecuadorica*. In the Incacocha Lagoon, the floristic composition was represented by 22 species, distributed in 11 families, with the most abundant and frequent species being *Alchemilla pinnata*. In the Ñahuinpuquio Lagoon, the floristic composition was represented by 20 species, distributed in 9 families, with the most abundant species being *Pennisetum clandestinum* and the most frequent species *Pennisetum clandestinum, Juncus arcticus* and *Muhlenbergia andina*. The results obtained contribute data on the diversity of riparian vegetation of high Andean wetlands in the Junin region, Peru.

Keywords: biodiversity indexes, floristic composition, high Andean wetlands, riparian vegetation.

Diversidade da vegetação ripária das áreas alagadas andinas altas na região de Junín, Peru

RESUMO

Avaliou-se a diversidade da vegetação ripária de cinco lagos altos andinos da região de Junin entre março e dezembro de 2017. A amostragem da vegetação ripária foi realizada por meio do método de transectos. As espécies não identificadas foram coletadas para posterior

identificação no herbário. A diversidade foi determinada pela composição florística, abundância e frequência e pelos índices de riqueza de espécies, Simpson e Shannon-Wiener. Na lagoa Pomacocha a composição florística foi representada por 43 espécies, distribuídas em 15 famílias, as espécies mais abundantes foram *Aciachne pulvinata, Azorella crenata* e *Geranium sessiliflorum* e a mais frequente *Aciachne pulvinata*. Na lagoa Tragadero a composição florística foi representada por 17 espécies, distribuídas em 10 famílias, as espécies mais abundantes foram *Pennisetum clandestinum* e *Eleocharis sp* e a mais frequente *Polypogon interruptus*. Na lagoa Cucancocha a composição florística foi representada por 19 espécies, distribuídos em 7 famílias, as espécies mais abundantes foram *Calamagrostis sp* e *Wernberia humbellata* e a mais frequente *Carex ecuadorica*. Na lagoa Incacocha a composição florística foi representada por 22 espécies, distribuídas em 11 famílias, sendo a espécie mais abundante e freqüente *Alchemilla pinnata*. Na lagoa Ñahuinpuquio a composição florística foi representada por 20 espécies em 9 famílias, sendo a espécie mais abundante *Pennisetum clandestinum* e as espécies mais freqüentes *Pennisetum clandestinum*, *Juncus articus* e *Muhlenbergia andina*. Os resultados obtidos contribuem com dados sobre a diversidade da vegetação ripária das áreas úmidas andinas da região de Junin, no Peru.

Palavras-chave: altiplano andino alto, composição florística, índices alfa-biodiversidade, vegetação ripária.

1. INTRODUCTION

The high Andean wetlands play a vital role in the development of the Andean basins, as well as other hydrographic systems, since their waters flow towards the slopes of the Amazon and towards the coasts of the Pacific and the Caribbean. These wetlands and wetland complexes maintain a unique biological diversity and are characterized by a high level of endemism of plants and animals. In addition, they are fundamental components of the habitat of species of notable economic and ecological importance such as the vicuña, the guanaco or the chinchilla, among others (Ramsar, 2005). High Andean wetlands are ecosystems that include a wide variety of environments, which share as a fundamental characteristic the presence of water. They have a unique biological diversity and are considered ecosystems of great fragility (Gonzales, 2015) due to natural (extreme conditions) and anthropogenic pressures (unsustainable agriculture, overgrazing and unsustainable mining in the páramo and puna). Understanding of the importance of biodiversity has developed over the years that followed the report of the World Commission on Environment and Development (Brundtland Report). It is increasingly recognized that human beings are part of the ecosystems in which they live, that they are not an independent part of them and that they are affected by changes in these ecosystems (Ash and Fazel, 2007).

It is estimated that the diversity of plant species and their distribution in space have important effects on the function of wetland ecosystems. However, knowledge of the relationships between plant species and spatial diversity remains incomplete (Brandt *et al.*, 2015).

Studies of wetlands in Western Europe and other terrestrial ecosystems in North America often show that nutrient enrichment causes changes in the composition of the species, decrease in the diversity of plant species in general and loss of rare species and uncommon ones (Bedford *et al.*, 1999).

The Andes are the richest center of species biodiversity in the world. Most of the conservation research and attention in the Andes has focused on biomes such as rainforest, cloud forest and paramo, where the diversity of plant species is the result of the rapid speciation associated with the recent Andean orogeny (Pennington *et al.*, 2010).

Peru is one of the most valuable countries on our planet, due to its high ecological diversity of climates, altitudinal band of vegetation and productive ecosystems. The high diversity of ecosystems has allowed the development of numerous human groups (Brack, 2014). However, the high Andean continental aquatic ecosystems are still the least studied and represent one of the most-threatened and least-managed systems (Acosta, 2009).

There are initiatives by different governmental and non-governmental organizations to inventory biological resources, including the National Service of Natural Protected Areas of Peru, national universities and NGOs. However, these initiatives are scattered; there is no coordination between them and existing studies are scarce.

Studies have been carried out on the Poaceae in the Huancavelica-Peru region, such as the works of Tovar (1957, 1960, 1965 and 1972) in the provinces of Huancavelica, Tayacaja and Castrovirreyna (Gutiérrez Peralta and Castañeda Sifuentes, 2014). However the information on the diversity of the riparian vegetation of high Andean wetlands of the Junín region is scarce; becoming one of the first research works at the regional level.

The definition of the diversity of species considers both the number of species and the number of individuals (abundance of each species existing in a certain place). It is evaluated by means of indices, which are tools used in floristic and ecological studies to compare the diversity of species, whether between habitat types, forest types, etc. (Mostacedo and Fredericksen, 2000), the Andes being the richest biodiversity point of species in the world (Pennington *et al.*, 2010). In this sense, it is necessary to carry out inventories of riparian vegetation to understand the diversity and the state of conservation in which they are found in order to complement the efforts to reduce the uncertainty about the knowledge of biodiversity in these ecosystems. Therefore, the objective of the study was to evaluate the diversity of riparian vegetation of five high Andean wetlands of the Junín region.

2. MATERIAL AND METHODS

2.1. Study area

The study area included five high Andean lagoons located in the Junín region, in Peru, which present regular riverine vegetation, around which extensive cattle ranching (sheep, bovine and camelids) is developed. The Pomacocha lagoon is located in the district of Apata, Concepción province at 4486 masl (473139 E, 8697593 N). The Tragadero lagoon in the district of Paca, province of Jauja at 3465 masl (441171 E, 8699215 N). The Cucancocha lagoon in the district of San José de Quero, Chupaca province at 4481 masl (488791 E, 8668186 N). The Incacocha lagoon in the district of Yanacancha, Chupaca province at 4420 masl (417825 E, 8669695 N). The Ñahuinpuquio in the district of Ahuac, Chupaca province at 3372 masl (463131 E, 8665631 N). (Figure 1).

The productive activities of the high Andean wetlands are associated with the altitude in which they are located. In the areas of the puna, jalca and paramo, the predominant activities are livestock of cattle, sheep and camelids, mining, fishing and industrial afforestation. Subsistence activity is the extraction of plants and peat as fuel, since in many areas a good part of the rural population depends on firewood to cook their food. At lower altitudes, crops of potatoes and other tubers and Andean cereals are produced. Extensive cattle ranching is favored in the high Andean wetlands because they are associated with the generation of fodder for wild and domesticated species such as alpacas, lamas, goats, sheep and cattle (Ramsar, 2005).

2.2. Methods

The sampling stations were selected according to the morphometry of the water bodies. Four samplings were carried out in April, May, September and October of 2017. The sampling method applied in each of the stations was the transect method, because it is a very used method

to inventory and evaluate grasslands, especially pastures, due to its advantages over the method of plots with fixed dimensions, mainly because it is fast and allows to capture greater variability in the terrain and therefore the dispersion of the species. Each registration point was defined by a survey ring 2.5 cm in diameter, held by a 60 cm long bronze rod (Flórez, 2005).

The diversity of the riparian vegetation was determined by the floristic composition, abundance and frequency, according to the guide of evaluation of the wild flora of the MINAM (Perú, 2011) and through the indices of species richness of Simpson and by Shannon-Wiener.

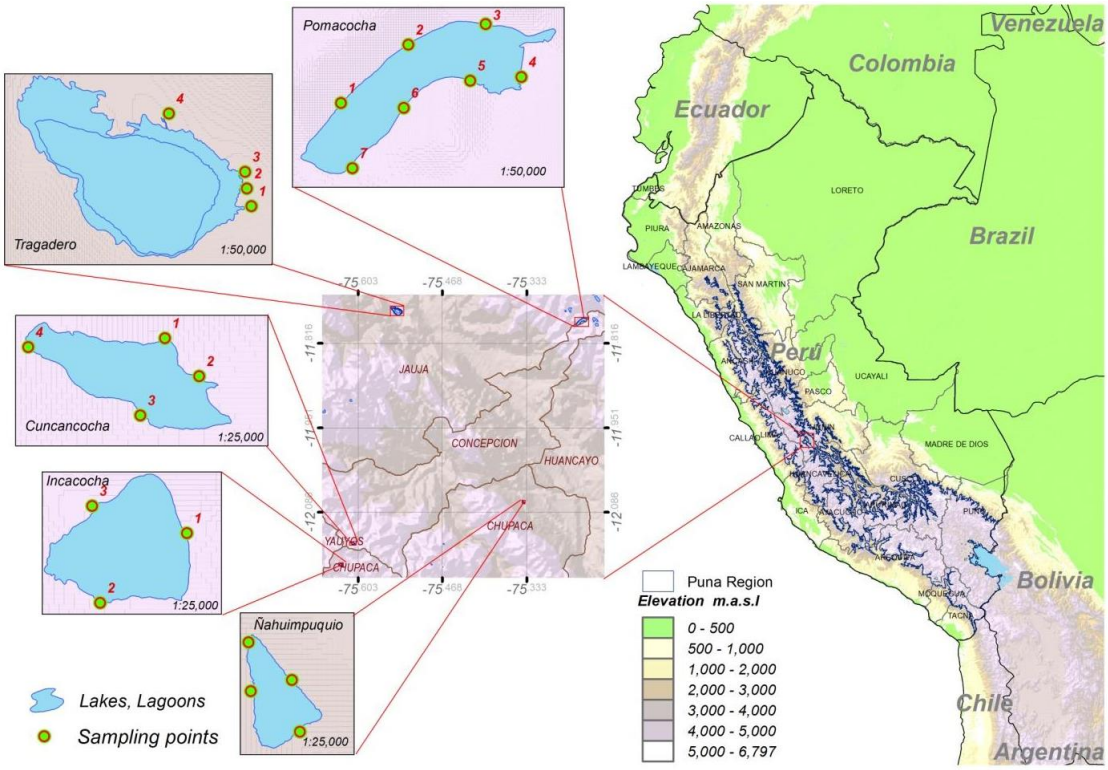

Figure 1. Location of the high Andean lagoons of the Junín region – Peru.

The floristic composition is the list of species registered in the totality of samples raised. The absolute abundance is the number of individuals of each species existing in a certain type of vegetation or area and relative abundance is expressed as a percentage of the total number of individuals. The absolute frequency is the number of times that a species is present in the total of sampling points raised and relative frequency is expressed as a percentage of the total number of sampling points surveyed.

The index of species richness (S) is the simplest way to measure biodiversity, since it is based solely on the number of species present, without taking into account the value of importance of them.

The Simpson Index is an index based on dominance; it is a reverse parameter to the concept of uniformity or equity of the community. It takes into account the representativeness of the species with greater importance value without evaluating the contribution of the rest of the species.

Carr *et al.* (2007) cited in Moreno (2001) state that the Simpson index is a measure of dominance that is strongly influenced by the importance of the most dominant species, and as the index increases, the diversity decreases; that is, when this probability is higher, less diverse is the plant community. That's why the Simpson index has the tendency to be smaller when the community is more diverse. Its formula is (Equation 1):

$$D_{Si} = \frac{\sum_{i=1}^{S} n(n-1)}{N\,(N-1)} \quad (1)$$

The Shannon-Wiener Index is the most-recognized index that is based mainly on the concept of equity.

Mayr (1992) mentions that the Shannon-Wiener Index expresses the uniformity of values of importance across all species in the sample. Acquire values between zero, when there is only one species, and the logarithm of S, when all species are represented by the same number of individuals (Magurran, 1988, cited in Moreno 2001). This index requires that all species are represented in the sample and is very susceptible to abundance; normally it takes values between 1 and 4.5. Values above 3 are typically interpreted as diverse (Barajas-Gea, 2005). Its formula is (Equation 2):

$$H' = -\Sigma\ pi \times \ln pi \quad (2)$$

The data of abundance, frequency and alpha diversity indices of species richness, Simpson and Shannon-Wiener, were analyzed through the statistical program Past 3.17.

3. RESULTS AND DISCUSSION

3.1. Floristic composition, abundance and frequency of the Pomacocha Lagoon

The floristic composition was represented by 43 species identified in the riparian vegetation of the Pomacocha Lagoon, distributed in 15 families. The most representative families are Poaceae and Asteraceae with 9 species each, followed by Cyperaceae (4), Plantaginaceae (3), Caryophyllaceae (3), Apiaceae (3), Geraniaceae (2), Ranunculaceae (2), Gentianaceae (2), Rosaceae (1), Isoetaceae (1), Polygonaceae (1), Fabaceae (1), Oxalidaceae (1) and Juncaceae (1).

The most abundant species are *Aciachne pulvinata, Azorella crenata and Geranium sessiliflorum*, representing 15.90%, 8.92% and 8.79%, respectively. The less abundant species are *Eleocharis sp* and *Luzula racemosa*, where each species represents 0.13%.

The species with more frequency is *Aciachne pulvinata*, which represents 8.05%. This species has characteristics adapted to the environment and is frequent in the lagoon of Pomacocha. There are several less frequent species, possibly due to the demand of environmental factors, among which are *Geranium weddelli, Oreithales sp, Dactilis glomerata*, among others, where each species represents 1.15% (Table 1).

3.2. Floristic composition, abundance and frequency of the Tragadero Lagoon

The floristic composition consisted of 17 identified species in the riparian vegetation of the Tragadero Lagoon, distributed in 10 families. The most representative families are Asteraceae and Fabaceae with 3 species each, followed by Apiaceae (2), Cyperaceae (2), Poaceae (2), Rosaceae (1) Juncaceae (1), Oxalidaceae (1), Caryophyllaceae (1) and Gentianaceae (1).

The most abundant species are *Pennisetum clandestinum* and *Eleocharis sp*, representing 38.46% and 20.36%. The least abundant species are *Oxalis sp* and Polypogon *interruptu*s, which represent 0.11%.

Table 1. Floristic composition, abundance and frequency of the Pomacocha Lagoon.

Floristic Composition		Absolute Abundance	Relative Abundance (%)	Absolute Frequency	Relative Frequency (%)
Family	**Species**				
Poaceae	*Aciachne pulvinata*	*117*	*14.904459*	7	8.045977
Apiaceae	*Azorella crenata*	*70*	*8.917197*	4	4.597701
Geraniaceae	*Geranium sessiliflorum*	*69*	*8.789809*	4	4.597701
Cyperaceae	*Scirpus rigidus*	*52*	*6.624204*	3	3.448276
Poaceae	*Dactylis glomerata*	*35*	*4.458599*	1	1.149425
Asteraceae	*Misbrookea strigosissima*	*30*	*3.821656*	2	2.298851
Fabaceae	*Lupinus chlorolepis*	*24*	*3.057325*	2	2.298851
Poaceae	*Muhlenbergia ligularis*	*23*	*2.929936*	2	2.298851
Poaceae	*Poa aequigluma*	*22*	*2.802548*	2	2.298851
Polygonaceae	*Rumex acetosella*	*21*	*2.675159*	2	2.298851
Ranunculaceae	*Oreithales integrifolia*	*20*	*2.547771*	1	1.149425
Cyperaceae	*Cyperus sp*	*18*	*2.292994*	1	1.149425
Isoetaceae	*Isoetes lacustris*	*17*	*2.165605*	4	4.597701
Asteraceae	*Hypochaeris taraxacoides*	*17*	*2.165605*	1	1.149425
Asteraceae	*Liabum bullatum*	*17*	*2.165605*	2	2.298851
Gentianaceae	*Gentiana prostrata*	*16*	*2.038217*	1	1.149425
Asteraceae	*Werneria nubígena*	*16*	*2.038217*	3	3.448276
Plantaginaceae	*Plantago rígida*	*15*	*1.910828*	3	3.448276
Asteraceae	*Werneria caespitosa*	*13*	*1.656051*	1	1.149425
Poaceae	*Stipa brachyphylla*	*12*	*1.528662*	2	2.298851
Poaceae	*Calamagrostis spicigera*	*12*	*1.528662*	1	1.149425
Asteraceae	*Werneria humbellata*	*12*	*1.528662*	2	2.298851
Poaceae	*Calamagrostis curvula*	*12*	*1.528662*	1	1.149425
Geraniaceae	*Geranium weddellii*	*10*	*1.273885*	1	1.149425
Asteraceae	*Werneria pinnatifida*	*10*	*1.273885*	3	3.448276
Oxalidaceae	*Oxalis sp*	*10*	*1.273885*	3	3.448276
Ranunculaceae	*Oreithales sp*	*9*	*1.146497*	1	1.149425
Caryophyllaceae	*Arenaria acaulis*	*9*	*1.146497*	1	1.149425
Cyperaceae	*Carex ecuadorica*	*9*	*1.146497*	3	3.448276
Plantaginaceae	*Plantago sp*	*8*	*1.019108*	2	2.298851
Caryophyllaceae	*Paronychia andina*	*8*	*1.019108*	3	3.448276
Asteraceae	*Baccharis tricuneata*	*8*	*1.019108*	1	1.149425
Poaceae	*Calamagrostis vicunarum*	*7*	*0.891720*	2	2.298851
Caryophyllaceae	*Paronychia aretioides*	*7*	*0.891720*	2	2.298851
Poaceae	*Poa candamoana*	*7*	*0.891720*	2	2.298851
Apiaceae	*Azorella compacta*	*5*	*0.636943*	1	1.149425
Rosaceae	*Alchemilla pinnata*	*4*	*0.509554*	4	4.597701
Plantaginaceae	*Plantago tubulosa*	*3*	*0.382166*	1	1.149425
Gentianaceae	*Gentiana sedifolia*	*3*	*0.382166*	1	1.149425
Apiaceae	*Azorella biloba*	*3*	*0.382166*	1	1.149425
Asteraceae	*Gnaphalium supinum*	*3*	*0.382166*	1	1.149425
Cyperaceae	*Eleocharis sp*	*1*	*0.127389*	1	1.149425
Juncaceae	*Luzula racemosa*	*1*	*0.127389*	1	1.149425
	Total	**785**	**100**	**87**	**100**

The most frequent species is Polypogon *interruptus*, representing 13.79% and is frequent in the Tragadero Lagoon. There are several less frequent species, among which are *Lilaeopsis andina, Oxalis sp, Werneria humbellata*, among others, where each species represents 3.45% (Table 2).

Table 2. Floristic composition, abundance and frequency of the Tragadero Lagoon.

Floristic Composition		Absolute Abundance	Relative Abundance (%)	Absolute Frequency	Relative Frequency (%)
Family	**Species**				
Poaceae	*Pennisetum clandestinum*	340	38.461538	4	13.793103
Cyperaceae	*Eleocharis sp*	180	20.361991	2	6.896552
Apiaceae	*Hydrocotile bowlesioides*	102	11.538462	2	6.896552
Cyperaceae	*Eleocharis albi bracteata*	100	11.312217	1	3.448276
Juncaceae	*Juncus arcticus*	37	4.18552	3	10.344828
Rosaceae	*Alchemilla pinnata*	32	3.61991	2	6.896552
Fabaceae	*Medicago hispida*	18	2.036199	3	10.344828
Fabaceae	*Trifolium amabile*	18	2.036199	1	3.448276
Apiaceae	*Lilaeopsis andina*	15	1.696833	1	3.448276
Asteraceae	*Gamochaeta purpurea*	14	1.58371	2	6.896552
Caryophyllaceae	*Paronychia aretioides*	13	1.470588	1	3.448276
Gentianaceae	*Gentianella bellidifolia*	7	0.791855	1	3.448276
Asteraceae	*Taraxacum officinale*	3	0.339367	2	6.896552
Asteraceae	*Werneria humbellata*	2	0.226244	1	3.448276
Oxalidaceae	*Oxalis sp*	1	0.113122	1	3.448276
Poaceae	*Polypogon interruptus*	1	0.113122	1	3.448276
Fabaceae	*Medicago lupulina*	1	0.113122	1	3.448276
Total		**884**	**100**	**29**	**100**

3.3. Floristic composition, abundance and frequency of the Cucancocha Lagoon

The floristic composition consisted of 19 species identified in the riparian vegetation of the Cucancocha Lagoon, distributed in 7 families. The most representative families are Asteraceae with 7 species and Poaceae with 6 species, followed by Cyperaceae (2), Rosaceae (1), Apiaceae (1), Gentianaceae (1) and Isoetaceae (1).

The most abundant species are *Calamagrostis* sp and *Wernberia humbella*ta, representing 30.48% and 14.74%. The least abundant species are *Passiflora tripartita* and *Podocarpus glomeratus*, which represent 0.11%.

Carex ecuadorica, is the most frequent species, representing 11.33%, being frequent in the Cuicocha Lagoon. There are several less frequent species, among which are *Festuca dolichophylla, Taraxacum officinale*, among others, representing 3.33% (Table 3).

3.4. Floristic composition, abundance and frequency of the Incacocha Lagoon

The floristic composition was represented by 22 species identified in the riparian vegetation of the Incacocha Lagoon, distributed in 11 families. The most representative family is Poaceae, with 6 species, followed by Asteraceae (3), Cyperaceae (3), Rosaceae (2), Apiaceae (2), Onagraceae (1), Fabaceae (1), Geraniaceae (1), Caryophyllaceae (1), Valerianaceae (1) and Malvaceae (1).

The most abundant species in the Incacocha lagoon are *Alchemilla pinnata*, and *Festuca humilior*, representing 26.10% and 16.54%. The least abundant species is *Nototriche acaulis*, representing 0.37%, as well as *Lupinus chlorolepis* and *Arenaria acaulis*, among others, where each species represents 0.74%.

The species with greatest frequency is *Alchemilla pinnata*, which represents 11.54%, being frequent in the Incacocha Lagoon. There are several less frequent species, among which are *Oenothera multicaulis*, *Lupinus chlorolepis*, *Baccharis caespitosa*, among others, where each species represents 3.85% (Table 4).

Table 3. Floristic composition, abundance and frequency of the Cucancocha Lagoon.

Floristic Composition		Absolute Abundance	Relative Abundance (%)	Absolute Frequency	Relative Frequency (%)
Family	**Specie**				
Poaceae	*Calamagrostis sp*	153	30.478088	2	6.666667
Asteraceae	*Wernberia umbellata*	74	14.741036	3	10
Cyperaceae	*Carex ecuadorica*	41	8.167331	4	13.333333
Asteraceae	Bella *sp*	41	8.167331	1	3.333333
Poaceae	*Festuca dolichophylla*	36	7.171315	1	3.333333
Poaceae	*Stipa depauperata*	35	6.972112	1	3.333333
Asteraceae	*Hypochaeris taraxacoides*	33	6.573705	2	6.666667
Poaceae	*Calamagrostis vicunarum*	25	4.98008	2	6.666667
Asteraceae	*Paranephelius uniflorus*	20	3.984064	1	3.333333
Rosaceae	*Alchemilla pinnata*	14	2.788845	2	6.666667
Cyperaceae	*Cyperus sp*	12	2.390438	1	3.333333
Gentianaceae	*Gentiana sedifolia*	4	0.796813	2	6.666667
Isoetaceae	*Isoetes lacustris*	4	0.796813	1	3.333333
Asteraceae	*Werneria pygmaea*	3	0.59761	1	3.333333
Poaceae	*Bromus lanatus*	2	0.398406	2	6.666667
Poaceae	*Festuca sp*	2	0.398406	1	3.333333
Asteraceae	*Taraxacum officinale*	1	0.199203	1	3.333333
Asteraceae	*Baccharis tricuneata*	1	0.199203	1	3.333333
Apiaceae	*Oreomyrrhis andicola*	1	0.199203	1	3.333333
Total		**502**	**100**	**30**	**100**

Table 4. Floristic composition, abundance and frequency of the Incacocha Lagoon.

Floristic composition		Absolute abundance	Relative Abundance (%)	Absolute Frequency	Relative Frequency (%)
Family	**Specie**				
Rosaceae	*Alchemilla pinnata*	71	26.102941	3	11.538462
Poaceae	*Festuca humilior*	45	16.544118	2	7.692308
Onagraceae	*Oenothera multicaulis*	25	9.191176	1	3.846154
Apiaceae	*Azorella compacta*	21	7.720588	1	3.846154
Cyperaceae	*Cyperus sp*	20	7.352941	1	3.846154
Poaceae	*Calamagrostis sp*	18	6.617647	1	3.846154
Poaceae	*Muhlenbergia fastigiata*	14	5.147059	1	3.846154
Poaceae	*Stipa brachyphylla*	8	2.941176	1	3.846154
Asteraceae	*Baccharis caespitosa*	7	2.573529	1	3.846154
Poaceae	*Poa aequigluma*	6	2.205882	1	3.846154
Rosaceae	*Alchemilla diplophylla*	5	1.838235	2	7.692308
Poaceae	*Festuca rígida*	5	1.838235	1	3.846154
Valerianaceae	*Valeriana sp*	4	1.470588	1	3.846154
Cyperaceae	*Eleocharis sp*	4	1.470588	1	3.846154
Geraniaceae	*Geranium sessiliflorum*	3	1.102941	1	3.846154
Cyperaceae	*Carex ecuadorica*	3	1.102941	1	3.846154
Apiaceae	*Oreomyrrhis andicola*	3	1.102941	1	3.846154
Asteraceae	Bella *sp*	3	1.102941	1	3.846154
Fabaceae	*Lupinus chlorolepis*	2	0.735294	1	3.846154
Caryophyllaceae	*Arenaria acaulis*	2	0.735294	1	3.846154
Asteraceae	*Werneria humbellata*	2	0.735294	1	3.846154
Malvaceae	*Nototriche acaulis*	1	0.367647	1	3.846154
Total		**272**	**100**	**26**	**100**

3.5. Floristic composition, abundance and frequency of the Ñahuinpuquio lagoon

The floristic composition was represented by 20 identified species in the riparian vegetation of the Ñahuinpuquio Lagoon, distributed in 9 families. The most representative family is Poaceae, with 7 species, followed by Fabaceae (3), Asteraceae (2), Brassicaceae (2), Plantaginaceae (2), Juncaceae (1), Polygonaceae (1), Rosaceae (1) and Apiaceae (1). The most abundant species is *Pennisetum clandestinum*, representing 40.93%. The least abundant species are *Calamagrostis* sp and *Rumex crispus*, where each species represents 0.14%.

The species with greater frequency are *Pennisetum clandestinum, Juncus arcticus, Muhlenbergia andina,* among others, where each species represents 8.57% and is frequent in the Ñahuinpuquio Lagoon. There are several less frequent species, among which are *Calamagrostis sp, Rumex crispus, Cassia sp, Brayopsis calycina* among others, where each species represents 2.86% (Table 5).

Table 5. Floristic composition, abundance and frequency of the Ñahuinpuquio lagoon.

Floristic composition		Absolute abundance	Relative Abundance (%)	Absolute Frequency	Relative Frequency (%)
Family	**Specie**				
Poaceae	*Pennisetum clandestinum*	300	40.927694	3	8.571429
Juncaceae	*Juncus articus*	70	9.549795	3	8.571429
Fabaceae	*Trifolium repens*	48	6.548431	2	5.714286
Plantaginaceae	*Plantago tubulosa*	45	6.139154	2	5.714286
Rosaceae	*Alchemilla pinnata*	38	5.184175	2	5.714286
Fabaceae	*Medicago hispida*	38	5.184175	1	2.857143
Poaceae	*Muhlenbergia andina*	37	5.047749	3	8.571429
Apiaceae	*Hydrocotile bowlesioides*	32	4.365621	1	2.857143
Poaceae	*Muhlenbergia ligularis*	28	3.819918	2	5.714286
Poaceae	*Lolium multiflorum*	21	2.864939	2	5.714286
Plantaginaceae	*Plantago major*	20	2.728513	2	5.714286
Asteraceae	*Bidens andicola*	20	2.728513	1	2.857143
Fabaceae	*Medicago lupulina*	15	2.046385	1	2.857143
Poaceae	*Poa gilgiana*	6	0.818554	2	5.714286
Asteraceae	*Taraxacum officinale*	5	0.682128	2	5.714286
Poaceae	*Polypogon interruptus*	3	0.409277	2	5.714286
Brassicaceae	Bryopsis *calycina*	3	0.409277	1	2.857143
Brassicaceae	*Nasturtium officinale*	2	0.272851	1	2.857143
Poaceae	*Calamagrostis sp*	1	0.136426	1	2.857143
Polygonaceae	*Rumex crispus*	1	0.136426	1	2.857143
Total		**733**	**100**	**35**	**100**

3.6. Analysis of floristic composition

The richness of the local species and the variation of composition among the high Andean wetlands, differ between the types of vegetation; however, the most representative species of the main wetlands of the region make important contributions to the diversity of the landscape (Flinn *et al.*, 2008). Since Pomacocha Lagoon presents the greatest number of species, in the case of the other lagoons the smaller number of species is possibly due to the culture of trout in floating cages (Cucancocha and Incacocha) where pelleted balanced foods are used, which, combined with fish excreta, constitute an important contribution of organic matter to aquatic ecosystems (Mariano *et al.*, 2010) and human activities, mainly tourism (Tragadero and Ñahuinpuquio).

It is estimated that the diversity of plant species and their distribution in space have important effects on the function of wetland ecosystems. We found that wetlands with a greater diversity of type of cover present a greater diversity of plant species than wetlands with less diversity of type of cover. We also found significant relationships between the diversity of plant

species and the spatial pattern of cover types, but the direction of the effect differs depending on the measure of diversity used (Brandt *et al.*, 2015).

Condori and Choquehuanca (2001) reported in Puno for Collao Province 45 plant species in high Andean wetlands, presenting a high floristic composition, being similar to the Pomacocha Lagoon; for Tarata 21 plant species were reported, similar respect to the Tragadero, Cucancocha, Incacocha and Ñahuinpuquio Lagoons. In Bolivia, Prieto *et al.* (2001) reported 58 plant species in high Andean wetlands. These results indicate that in the area of influence of our research there is a smaller distribution of species in front of the Bolivian wetland system. This result indicates that in our field of study, there is a lower number of species in wetlands.

Existing studies seem to confirm common generalizations: (1) changes in the type of community of plants across large nutrient gradients; (2) species richness decreases as several indicators of nutrient availability increase beyond a certain threshold; and (3) rare species are almost always associated with species-rich communities (Bedford *et al.*, 1999).

Tovar (1993), cited in Gutiérrez Peralta and Castañeda Sifuentes (2014), mentions that, the Poaceae family is widely distributed in the world; its species are present in all latitudes and altitudes, from sea level to above 5000 m.

Poaceae is one of the families with the highest number of species, with approximately 700 genre and 10,000 species distributed in almost all continents (Clayton and Renvoize, 1986). The Peruvian flora is represented by around 157 genera with 750 species (Brako and Zarucchi, 1993, Ulloa *et al.*, 2004), which are occupying all the bioclimatic levels, from the shores of the Pacific Ocean to the high peaks of the Andes and from these to the Amazon plain crossing the eastern Andes.

Gutiérrez Peralta and Castañeda Sifuentes (2014), for the district of Lircay, report a total of 46 species and one subspecies of the Poaceae family, grouped into 21 genres, 11 tribes and 6 subfamilies. The genus Calamagrostis is the most diverse with 9 species, followed by Poa with 5 species. Also, Aciachne acicularis "paccupaccu", Arundo donax "carrizo", Cortaderia hieronymi and Ortachne erectifolia "iruichu" are new reports for the region of Huancavelica.

Parra Rondinel *et al.* (2004), vegetation and floristic composition of the Pachachaca micro watershed, located in north western Huancavelica, were studied from 2001 to 2003. There were registered 180 species belonging to 57 families. Floristic composition shows a large richness in species. Asteraceae were most representative in the middle and lowland areas, Poaceae in the highlands, and Fabaceae in the middle and lowland areas of the watershed.

Gutiérrez Peralta and Castañeda Sifuentes (2014), a checklist of grasses (Poaceae) from Huancavelica is presented consisting of seven subfamilies, 21 tribes, 74 genres, 255 species, two subspecies, eight varieties, two forms and a hybrid. The checklist consolidates the agrostological flora from the Huancavelica region. Sources range from years of field collections to consultations from Peru herbal.

La Torre *et al.* (2004), recognize 81 endemic species in 19 genres. Peru endemic grasses have been found in practically all recognized ecological regions, although the majority is found in the Dry and Humid Puna, High Andean and Mesoandean regions, from sea level to 5500 m elevation. Twenty-five endemics have been reported to occur in Peru's protected areas.

In a taxonomic study of the Poaceae Family of the Yanachaga-Chemillén National Park and surrounding areas (Oxapampa, Pasco, Peru), 63 Poaceae species were recorded from the subfamilies Pooideae, Centothecoideae, Arundinoideae, Chloridoideae and Panicoideae, which are included in 37 genres and 12 tribes (La Torre *et al.*, 2004).

Gonzáles (2015) reports species of the family Asteraceae registered in wetlands and aquatic systems by floristic inventories made in the high Andean areas of the departments of Ancash, Apurímac, Arequipa, Ayacucho, Cusco, Cajamarca, Huancavelica, Huánuco, Junín, La Libertad, Lima, Moquegua, Pasco, Puno and Tacna, between 2009 and 2015. In this period

of time, 200 high Andean wetlands were explored, located in 30 locations, reporting a total of 25 species of the Asteraceae family for the high Andean wetlands. The Asteraceae of the high Andean wetlands are made up solely of herbaceous species and only two species are endemic to Peru, which coincides with the results of the research, since the Asteraceae family is one of the most representative families of the Andean highlands of the Junín region.

In the study, the most abundant species recorded in the lagoons of Pomacocha, Tragadero, Cucancocha, Incacocha and Ñahuinpuquio indicate that they are well adapted to the environment and distributed in the zones of life belonging to the Humid-Montane Tropical Forest (bh-MT) and to the Dry-Montane Low Tropical Forest (bs-MBT) (Alonso *et al.*, 2001), while the low abundance of several species in the aquatic ecosystem, possibly due to the selective use of these species and the presence of anthropogenic activities developed in the area of influence of the study area.

The most frequent species recorded in the five lagoons indicate that these species have characteristics adapted to the environment and are frequent in these wetlands; while the lower frequency of other species in the aquatic ecosystem is possibly due to the exigency of environmental factors (Martino and Zommers, 2007).

To guarantee the long-term conservation of the lentic wetlands (in this case, the high Andean wetlands), it is necessary to develop management and conservation strategies that take into account both natural and created wetlands (Murillo-Pacheco *et al.*, 2016).

3.7. Alpha diversity índices

The results of the investigation show that in the Pomacocha Lagoon species richness (S = 43) indicates that 43 species have been identified in the riparian vegetation; while the Simpson index ($1\text{-}D_{Si}$= 0.9446) indicates that diversity is high.

The Shannon Wiener index (H´= 3.3124) indicates that the diversity in the Pomacocha Lagoon has a high degree of species heterogeneity in plant communities.

In the Tragadero Lagoon, the species richness (S = 17) indicates that 17 species present in the riparian vegetation have been recorded in the study area; while the Simpson index ($1\text{-}D_{Si}$= 0.8227) indicates that diversity is high.

The Shannon Wiener index (H´= 2.2761) indicates that the diversity in the Tragadero Lagoon, has an intermediate degree of heterogeneity of species in the plant communities.

In the Cucancocha Lagoon, the richness of species (S = 19) indicates that 19 species have been identified in the riparian vegetation; while the Simpson index ($1\text{-}D_{Si}$= 0.8521) indicates that diversity is high.

The Shannon Wiener index ((H´= 2.2628) indicates that the diversity in the Cucancocha Lagoon has an intermediate degree of heterogeneity of species in plant communities.

In the Incacocha Lagoon, the species richness (S = 22) indicates that 22 species have been recorded in the riparian vegetation; while the Simpson index ($1\text{-}D_{Si}$= 0.8739) indicates that diversity is high.

The Shannon Wiener index (H´= 2.4706) indicates that the diversity in the Incacocha Lagoon has an intermediate degree of species heterogeneity in plant communities.

In the Ñahuinpuquio Lagoon, the richness of species (S = 20) indicates that 20 species present in the riparian vegetation have been identified, while the Simpson index ($1\text{-}D_{Si}$= 0.8011) indicates that the diversity is high.

The Shannon Wiener index (H´= 2.1891) indicates that the diversity in the Ñahuinpuquio lagoon has an intermediate degree of heterogeneity of species in the plant communities (Table 6).

Table 6. Alpha diversity indices in high Andean wetlands of the Junín region.

Indicators of Diversity	Lagoons				
	Pomacocha	Tragadero	Cucancocha	Incacocha	Ñahuinpuquio
Wealth of species (S)	43	17	19	22	20
Simpson Index (1-D_{Si})	0.9446	0.8227	0.8521	0.8739	0.8011
Shannon-Wiener Index (H')	3.3124	2.2761	2.2628	2.4706	2.1891

Yaranga *et al.* (2018), in the study of the Floristic diversity in grasslands according to plant formation in the Shullcas River subwatershed, Junin, Peru reports that the Shannon-Wiener index (H ') revealed that plant formations in the upper part have a high diversity of 3.12 to 3.41; while in the lower part they have an average diversity of 2.75 and 2.81. These results are close to that found in the páramos by Caranqui *et al.* (2016), which coincides with the highest H 'value in the case of grasslands with greater coverage (Zheng *et al.*, 2014). This fact reaffirms the theory that grassland ecosystems present heterogeneous diversity with the presence of different species among them (Habel *et al.*, 2013); this indicates that the location of the plots evaluated in each plant formation influences the obtained index (Janišová *et al.*, 2013).

The comparison of these indices with those obtained by other authors is difficult, due to the differences in the methods and sampling areas within the wetland. Therefore, it is necessary to establish the base elements and the conditions under which the indices must be calculated, so that aspects such as area and sampling area, habit (arboreal, shrub, herbaceous) and size categories, which allow comparisons between similar ecosystems (Cantillo *et al.*, 2004 cited in González-Pinto, 2017).

Alpha diversity indices are very useful in the description of ecological communities. Given that diversity in a community is an expression of the distribution of resources and energy, its study is one of the most useful approaches in the analysis of communities (Carranza, 2002).

Regarding the Wealth of Species (S) Carranza (2002) mentions that, the ideal form of measurement, it is to have a complete inventory that allows us to know the total number of species, obtained by a census of the community; however, in the research this index has been determined from a sampling of the riparian vegetation communities of the five high Andean lagoons, based solely on the number of species present in the study area.

The results of the biodiversity indices indicate that the diversity of riparian vegetation in the Pomacocha, Tragadero, Cucancocha, Incacocha and Ñahuinpuquio Lagoons present a low level of alteration, due to the different anthropogenic activities developed in the area of influence (livestock, fish farming, tourism); However, the Pomacocha Lagoon presents better indices of diversity, since in this aquatic ecosystem the anthropogenic activities are smaller. It is therefore necessary to consider the statements made by Peralta-Peláez *et al.* (2009), who indicate that management plans should be developed together with the communities that allow the use of these high Andean lagoons but that at the same time guarantee the permanence of the composition and structure of the riparian vegetation characteristic of these aquatic ecosystems.

4. CONCLUSIONS

Floristic composition, abundance and frequency, indicate that the most representative families of the Pomacocha Lagoon are Poaceae and Asteraceae, of Tragadero are Asteraceae and Fabaceae, of Cucancocha are Asteraceae and Poaceae, and of Incacocha and Ñahuinpuquio is Poaceae. The values of species richness indices, Simpson and Shannon-Wiener, indicate that the diversity of riparian vegetation of aquatic ecosystems still present a low level of alteration due to the different anthropogenic activities developed in the area of influence.

The use of these high Andean lagoons, through the development of management plans together with the communities, will guarantee the permanence of the composition and structure of the riparian vegetation characteristic of these aquatic ecosystems.

5. REFERENCES

ACOSTA, R. **Estudio de la cuenca altoandina del río Cañete (Perú**): distribución altitudinal de la comunidad de macroinvertebrados bentónicos y caracterización hidroquímica de sus cabeceras cárticas. 2009. 153f. Tesis (Doctoral) - Universidad de Barcelona, Barcelona, 2009.

ALONSO, A.; DALLMEIER, F.; CAMPBELL, P. **Urubamba**: the biodiversity of a Peruvian rainforest. Washington, D. C.: Smithsonian Institutional, 2001. 204 p.

ASH, N.; FAZEL, A. Biodiversidad. *In:* PNUMA. **Perspectivas del medio ambiente mundial GO4**. Nairobi, 2007. p. 157-194.

BARAJAS–GEA, C. I. Evaluación de la diversidad de la flora en el campus Juriquilla de la UNAM. **Bol-e: Órgano de comunicación electrónica del Centro de Geociencias de la UNAM**, v. 1, n. 2, 2005.

BEDFORD, B. L.; WALBRIDGE, M. R.; ALDOUS, A. Patterns in nutrient availability and plant diversity of temperate North American wetlands. **Ecology**, v. 80, n. 7, p. 2151–2169, 1999. https://doi.org/10.1890/0012-9658(1999)080[2151:pinaap]2.0.co;2

BRACK, A. Biodiversidad y desarrollo sostenible. *In:* INEI. **Anuario de Estadísticas Ambientales 2013**. Lima, 2014.

BRAKO, L.; ZARUCCHI, J. **Catalogue of the Flowering Plants and Gymnosperms of Peru**. St. Louis: Missouri Botanical Gardens, 1993. 1286 p.

BRANDT, E. C.; PETERSEN, J. E.; GROSSMAN, J. J.; ALLEN, G. A.; BENZING, D. H. Relationships between spatial metrics and plant diversity in constructed freshwater wetlands. **PLoS ONE**, v. 10, n. 8, 2015. https://doi.org/10.1371/journal.pone.0135917

CARANQUI, J.; LOZANO, P.; REYES, J. Composición y diversidad florística de los páramos en la Reserva de Producción de Fauna Chimborazo, Ecuador. Enfoque UTE, v. 7, n. 1, p. 33–45, 2016. http://dx.doi.org/10.29019/enfoqueute.v7n1.86

CARRANZA, J. **La Diversidad Biológica de Colombia**. Bogotá: Universidad Nacional de Colombia., 2002.

CLAYTON, W. D.; RENVOIZE, S. A. Genera Graminum: Grasses of the World. **Kew Bulletin Additional Series**, v. 13, p. 389, 1986.

CONDORI, E.; CHOQUEHUANCA, D. **Evaluación de las características y distribución de los bofedales en el ámbito peruano del sistema TDPS**. Puno: ALT; PNUD, 2001.

FLINN, K. M.; LECHOWICZ, M. J.; WATERWAY, M. J. Plant species diversity and composition of wetlands within an upland forest. **American Journal of Botany**, v. 95, n. 10, p. 1216–1224, 2008. https://doi.org/10.3732/ajb.0800098

FLÓREZ, A. **Manual de pastos y forrajes altoandinos**. Lima: Universidad Nacional Agraria La Molina, 2005. 51 p.

GONZÁLES, P. Diversidad de asteráceas en los humedales altoandinos del perú. **Científica**, v. 12, n. 2, p. 99–114, 2015. https://doi.org/10.21142/cient.v12i2.157

GONZÁLEZ-PINTO, A. Estructura y diversidad florística de la zona terrestre de un humedal urbano en Bogotá (Colombia). **Revista Luna Azul**, v. 45, p. 201- 226, 2017. http://dx.doi.org/10.17151/luaz.2017.45.11

GUTIÉRREZ PERALTA, H.; CASTAÑEDA SIFUENTES, R. Diversidad de las gramíneas (Poaceae) de Lircay (Angaraes, Huancavelica, Perú). **Ecología Aplicada**, v. 13, n. 1, p. 23–33, 2014.

HABEL, J. C.; DENGLER, J.; JANIŠOVÁ, M.; TÖRÖK, P.; WELLSTEIN, C.; WIEZIK, M. European grassland ecosystems: Threatened hotspots of biodiversity. **Biodiversity and Conservation**, v. 22, n. 10, p. 2131–2138, 2013. https://doi.org/10.1007/s10531-013-0537-x

JANIŠOVÁ, M.; MICHALCOVÁ, D.; BACARO, G.; GHISLA, A. Landscape effects on diversity of semi-natural grasslands. **Agriculture, Ecosystems & Environment**, v. 182, p. 47–58, 2013. https://doi.org/10.1016/j.agee.2013.05.022

LA TORRE, M.; CANO, A.; TOVAR, O. Las Poáceas del Parque Nacional Yanachaga-Chemillén (Oxapampa, Perú). Parte II: Pooideae, Centothecoideae, Arundinoideae, Chloridoideae y Panicoideae. **Revista Peruana de Biología**, v. 11, n. 1, p. 51–70, 2004.

LA TORRE, M.; ALEGRÍA, J.; SÁNCHEZ, I. Poaceae endémicas del Perú. **Revista Peruana de Biología**, v. 13, n. 2, p. 879s–891s, 2014.

MARIANO, M.; HUAMAN, P.; MAYTA, E.; MONTOYA, H.; CHANCO, M. Contaminación producida por piscicultura intensiva en lagunas andinas de Junín, Perú. **Revista Peruana de Biología**, v. 17, n. 1, p. 137–140, 2010.

MARTINO, D.; ZOMMERS, Z. Medio ambiente para el desarrollo. *In:* PNUMA. **Perspectivas del medio ambiente mundial GO4**. Nairobi, 2007.

MAYR, E. A local flora and the biological species concept. **American Journal of Botany**, v. 79, p. 222–238, 1992. https://doi.org/10.1002/j.1537-2197.1992.tb13641.x

MORENO, C. **Manual de métodos para medir la biodiversidad**. Xalapa: Universidad Veracruzana, 2001.

MOSTACEDO, B.; FREDERICKSEN, T. **Manual de métodos básicos de muestreo y análisis en ecología vegetal**. Santa Cruz: Bolfor, 2000. 87 p.

MURILLO-PACHECO, J. I.; RÖS, M.; ESCOBAR, F.; CASTRO-LIMA, F.; VERDÚ, J. R.; LÓPEZ-IBORRA, G. M. Effect of wetland management: are lentic wetlands refuges of plant-species diversity in the Andean–Orinoco Piedmont of Colombia? **PeerJ**, v. 4, n. e2267, 2016. https://doi.org/10.7717/peerj.2267

PARRA RONDINEL, F.; TORRES GUEVARA, J.; CERONI STUVA, A. Composición florística y vegetación de una microcuenca andina: el Pachachaca (Huancavelica). **Ecología Aplicada**, v. 13, n. 1–2, p. 9–16, 2004.

PENNINGTON, R. T.; LAVIN, M.; SARKINEN, T.; LEWIS, G. P.; KLITGAARD, B. B.; HUGHES, C. E. Contrasting plant diversification histories within the Andean biodiversity hotspot. **Proceedings of the National Academy of Sciences**, v. 107, n. 31, p. 13783–13787, 2010. https://doi.org/10.1073/pnas.1001317107

PERALTA-PELÁEZ, L. A. LA; MORENO-CASASOLA, P.; ALBERTO, L.; FLORÍSTICA, C.; LA, Y. D. D. E.; HUMEDALES, V. D. E. Composición florística y diversidad de la vegetación de humedales en los lagos interdunarios de Veracruz. **Boletín de La Sociedad Botánica de México**, v. 101, n. 85, p. 89–101, 2009.

PERU. Ministerio del Ambiente - MINAM. Dirección General de Evaluación, Valoración y Financiamiento del Patrimonio Natural. **Guía de evaluación de la flora silvestre**. Lima, 2011.

PRIETO, G.; ALZÉRRECA, H.; LAURA, J.; LUNA, D.; LAGUNA, S. **Características y distribución de los bofedales en el ámbito boliviano del sistema T.D.P.S**. 1. ed. La Paz, Editorial Plural Editores, 2001.

RAMSAR. Estrategia Regional de Conservación y Uso Sostenible de los Humedales Altoandinos. In: REUNIÓN DE LA CONFERENCIA DE LAS PARTES CONTRATANTES EN LA CONVENCIÓN SOBRE LOS HUMEDALES, 9., 2005, Kampala, Uganda. **Documentos[…]** Gland, 2005.

ULLOA, C.; ZARUCCHI, J.; LEÓN, B. Diez años de adiciones a la Flora del Perú: 1993-2003. **Arnaldoa**, ed. espec., p. 1-242, 2004.

YARANGA, R.; CUSTODIO, M.; CHANAMÉ, Z.; PANTOJA, R. Diversidad florística de pastizales según formación vegetal en la subcuenca del río Shullcas, Junín, Perú. **Scientia Agropecuaria**, v. 9, n. 4, p. 511–517, 2018. https://dx.doi.org/10.17268/sci.agropecu.2018.04.06

ZHENG, S.X., LI, W.H., LAN, Z.C., REN, H.Y., WANG, K.B. Y BAI, Y.F. Testing functional trait-based mechanisms underpinning plant responses to grazing and linkages to ecosystem functioning in grasslands. **Biogeosciences discussions**, v. 11, n. 9, p. 13157–13186, 2014. https://dx.doi.org/10.5194/bgd-11-13157-2014

Ambiente & Água - An Interdisciplinary Journal of Applied Science
ISSN 1980-993X – doi:10.4136/1980-993X
www.ambi-agua.net
E-mail: ambi.agua@gmail.com

Evaluation of methods for estimating atmospheric emissivity in Mato-Grossense Cerrado

ARTICLES doi:10.4136/ambi-agua.2288

Received: 05 Jun. 2018; Accepted: 06 Feb. 2019

Jonh Billy Silva[1,2]; Denilton Carlos Gaio[1,2]; Leone Francisco Amorim Curado[1,2]; José de Souza Nogueira[1,2]; Luiz Claudio Galvão Valle Júnior[3]; Thiago Rangel Rodrigues[4*]

[1]Universidade Federal de Mato Grosso (UFMT), Cuiabá, MT, Brasil
Programa de Pós-Graduação em Física Ambiental (PPGFA). E-mail: jonhbilly9@gmail.com, dcgaio@fisica.ufmt.br, leonecurado@gmail.com, nogueira@ufmt.br
[2]Universidade Federal de Mato Grosso (UFMT), Coxipó, MT, Brasil
Instituto de Física. E-mail: jonhbilly9@gmail.com, dcgaio@fisica.ufmt.br, leonecurado@gmail.com, nogueira@ufmt.br
[3]Universidade Federal do Mato Grosso do Sul (UFMS), Campo Grande, MT, Brasil
Programa de Pós-Graduação em Tecnologias Ambientais (PGTA). E-mail: luizvallejr@gmail.com
[4]Universidade Federal de Mato Grosso do Sul (UFMS), Campo Grande, MT, Brasil
Laboratório de Ciências Atmosféricas (LCA). E-mail: thiago.r.rodrigues@ufms.br
[*]Corresponding author

ABSTRACT

This study analyzed the performance of the Brunt (1932), Swinbank, (1963), Idso and Jackson (1969), Brutsaert (1975), Idso (1981), and Bignami *et al.* (1995) methods to estimate atmospheric emissivity under grass-dominated savannas (known as *campo sujo Cerrado*), in the region of Baixada Cuiabana. The estimates were compared with data obtained by energy balance equation in two seasons, dry season (May to August), and wet season (September to December) of 2009. The Swinbank and Idso and Jackson methods, that consider only air temperature, show better performances for the wet season. However, methods that consider water vapor pressure and air temperature (Brunt, Brutsaert, Bignami and Idso) show good performances for the dry season. The Idso and Brutsaert methods show the highest index of agreement and are recommended to estimate atmospheric emissivity for the region.

Keywords: air temperature, campo sujo Cerrado, water vapor pressure.

Avaliação de métodos para estimativa da emissividade atmosférica no cerrado Mato-Grossense

RESUMO

Este trabalho analisou o desempenho dos métodos de Brunt (1932), Swinbank (1963), Idso and Jackson (1969), Brutsaert (1975), Idso (1981) e Bignami *et al.* (1995) para estimativa da emissividade atmosférica para dados obtidos na região do Cerrado *Campo Sujo*, na baixada cuiabana. As estimativas foram comparadas com dados calculados pela equação do balanço de energia para dois períodos estudados, seco (maio a agosto) e chuvoso/úmido (setembro a dezembro) de 2009. Os métodos de Swinbank e Idso and Jackson, que levam em consideração

apenas a Temperara do ar, obtiveram melhor desempenho durante o período chuvoso. Em contrapartida, os métodos que levam em consideração a pressão de vapor d'água e a temperatura do ar (Brunt, Brutsaert, Bignami e Idso) tiveram melhor desempenho durante a estação seca, sendo as equações de Idso e Brutsaert que apresentaram melhor desempenho para o local e período estudados, obtendo os maiores índices de concordância, e sendo assim, as equações mais indicadas para a estimativa da emissividade atmosférica para o local de estudo.

Palavras-chave: campo sujo Cerrado, pressão de vapor d'água, temperatura do ar.

1. INTRODUCTION

Tropical savannas cover approximately 12% of the Earth's land area (Scholes and Archer, 1997) and are characterized by high plant species diversity (Giambelluca *et al.*, 2009). The Brazilian savanna (locally known as Cerrado) covers about 24% of the territory and is the dominant vegetation in areas subjected to a prolonged dry season (San José *et al.*, 1998). In the last decades, the anthropic activities in the Cerrado have been causing strong changes in this biome, in particular, in its conversion to pastures and the production of soybean and sugarcane (Klink and Moreira, 2002; Rodrigues *et al.*, 2014), besides the high rates of deforestation that are causing a mosaic of natural forests and arable land (Biudes *et al.*, 2015). That mosaic implies land cover changes, provoking changes in the distribution of solar energy that is available to the environment (Novais *et al.*, 2015; Faria *et al.*, 2018), which affects directly the biophysical process linked to regional energy balance (Rodrigues *et al.*, 2016).

One way to observe changes caused by anthropogenic action is by characterizing variations in surface radiation balance values, because the fluctuation of these values results in energy partitioning. For example, outgoing longwave radiation (OLR) is very important for meteorological studies, such as predicting diurnal temperature variations, frosts, and nighttime fog, as well as evaluations of radiation cooling of buildings at night (Jimenez *et al.*, 1987). However, it is the hardest variable of radiation balance components to measure (Aguiar *et al.*, 2011).

Since atmospheric emissivity (ε) is a determining factor for longwave radiation (OLR), many studies have been committed to analyze atmospheric behavior. Considering that atmospheric gases absorb and emit radiation, atmospheric emissivity (ε) can be presented as a function, the variation of which depends on water vapor content in the atmosphere and air temperature (Heitor *et al.*, 1991), as water vapor acts as a thermoregulator by absorbing infrared radiation.

According to the Stefan-Boltzmann Law (Equation 1), every body emits radiant energy, which depends on its temperature and emissivities, and the latter is calculated by a ratio of the energy radiated by the body to the energy radiated by a black body for the same wavelength. Any object that is not a real black body has an emissivity value under 1 and higher than 0 (Equation 1).

$$R = \sigma \varepsilon T^4 \quad (1)$$

Where $\sigma = 5.6697 \times 10^{-8}$ W m^{-2} K^{-4} is the Stefan-Boltzmann Constant, T (K) is the air temperature, ε is the emissivity, and R is the radiant energy.

Then, R can be considered as longwave radiation under clear sky conditions, being modelled as a function of air temperature (*Tar*), or actual water vapor pressure (e*a*), or both. Therefore, any method used to estimated of ORL can be rewritten using the Stefan-Boltzmann Law and estimates atmospheric emissivity (ε).

The majority of equations that estimate atmospheric emissivity using longwave radiation are only valid for clear sky days, and show better results when a daily basis or a long-term average is considered (Von Randow and Alvalá, 2006).

Curado *et al.* (2011), studying the Pantanal Mato Grossense, obtained higher atmospheric emissivity values during the wet season, because during this period there were a higher content of water in the atmosphere and quantity of clouds compared to the dry season. Following the same line of research, Nogueira and Lima (2011) assured that the higher radiation absorption by the clouds cause the rise of air temperature, and consequently raises its emission; i.e., the bodies that absorb more radiation also are the ones that emit more radiation (black body radiation law)

Considering how important is effect of *campo sujo* Cerrado on the climate of Mato Grosso state and the lack of information about atmospheric emissivity for this biome, the objective of this study was to assess the performance of the Brunt (1932), Swinbank (1963), Idso and Jackson (1969), Brutsaert (1975), Idso (1981), and Bignami *et al.* (1995) models on atmospheric emissivity (ε) estimates for *campo sujo* Cerrado from May to December 2009, compared with emissivity values obtained by the energy balance equation.

2. MATERIALS AND METHODS

2.1. Study Area

The study was conducted at the Fazenda Miranda (FM) in the region of Baixada Cuiabana, located 15 km away from Cuiaba, Mato Grosso, Brazil (15°43'53" S; 56°04'18" W; 157 m). The study site was a mixed forest-grassland (locally known as *campo sujo* or "dirty field") that was partially deforested approximately 35 years ago (Rodrigues *et al.*, 2014).

Vegetation consists predominantly of grasses and tree species *C. americana* and *Diospyros hispida* A. DC. According to the Köppen climate classification system, the climate in this area is Aw, tropical semi-humid, with dry winters and wet summers (Rodrigues *et al.*, 2016). Mean annual rainfall and temperature are 1420 mm and 26.5°C, respectively, and rainfall is seasonal (Vourlitis and Da Rocha, 2011). The range of mean monthly air temperature is wider than tropical and subtropical moist forests, with a minimum of 23.5°C in June and a maximum of 28.6°C in September (Vourlitis and Da Rocha, 2011). The research area is on a flat terrain at an elevation of 157 m above sea level. The soil type is a rocky, dystrophic red-yellow latosol locally known as *Solo Concrecionário Distrófico* (CPRM, 1982).

2.2. Instrumentation

Micrometeorological measurements were conducted between May to December 2009, where two local defined seasons can be observed: the dry season, with rainfall below 100 mm (May to August); and the wet season, with rainfall above 100 mm (September to December). A micrometeorological tower enabled the collection of data on air temperature (*Tar*), relative humidity (RH), wind speed (u), precipitation (Ppt), soil temperature (Ts), soil heat flux (G), net radiation (Rn) and solar radiation (Rs).

Tar and RH were measured 10 m above the ground level using a thermohygrometer (HMP45AC, Vaisala Inc., Woburn, MA, USA). Wind speed was measured 10 m above the ground level using anemometer (03101 R.M. Young Company), and G was measured using heat flux plates (HFP01-L20, Hukseflux Thermal Sensors BV, Delft, Netherlands) installed 1.0 cm below the soil surface, with one placed in a sandy soil type and the other placed in a laterite soil type, which were typical of the local soil in the tower footprint. Rn and Rs were measured 5 m above ground using a net radiometer (NR-LITE-L25, Kipp and Zonen, Delft, Netherlands) and a pyranometer (LI200X, LI-COR Biosciences, Inc., Lincoln, NE, USA), respectively. Precipitation was measured using a tipping bucket rainfall gauge (TR-525M, Texas Electronics, Inc., Dallas, TX, USA). The sensors were connected to a data logger

(CR1000, Campbell Scientific, Inc., Logan, UT, USA) that scanned each sensor every 30 s and stored average, and in the case of Ppt, total quantities every 30 min.

2.3. Atmospheric Emissivity Calculation

According to Duarte *et al.* (2006), since atmosphere does not have constant temperature, a local parametrization of atmospheric emissivity (ε) is necessary, which depends on air temperature.

We tested six different models that can be used in the local temperature range (Table 1). The first two models to estimate emissivity (ε) were proposed by Swinbank (1963), and Idso and Jackson (1969). Both models were chosen because they only consider temperature in their estimates, in a range of 2 to 29°C and -29 to 37°C, respectively. Table 1 also shows the models proposed by Brutsaert (1975), Brunt (1932), Bignami (1995) and Idso (1981), that were chosen because they work in a temperature range between -40 and 45°C and consider actual water vapor pressure (*ea*) in hPa (Equation 2) (Idso, 1981; Prata, 1996; Duarte *et al.*, 2006).

Table 1. Equations used to estimate atmospheric emissivity (ε), where σ is the Stefan-Boltzmann constant (5.6697x10^{-8} W m^{-2} K^{-4}), e_a is the actual water vapor pressure (hPa), and T*ar* is the air temperature (K) next to the surface.

Model	Equation
Brunt (1932)	$\varepsilon = 0{,}52 + 0{,}065\sqrt{e_a}$
Swinbank (1963)	$\varepsilon = 9{,}2 \,.\, 10^{-6}\, {T_{ar}}^2$
Idso and Jackson (1969)	$\varepsilon = 1 - 0{,}26\, exp[-7{,}77 \,.\, 10^{-4}\, (273 - T_{ar})]$
Brutsaert (1975)	$\varepsilon = 1{,}24\, (e_a/T_{ar})^{1/7}$
Idso (1981)	$\varepsilon = 0{,}7 + 5{,}95 \,.\, 10^{-5} e_a\, exp(1500/T_{ar})$
Bignami (1995)	$\varepsilon = 0{,}684 + 0{,}0056\, e_a$

Actual water vapor pressure (*ea)* is described as Equation 2.

$$e_a = \frac{e_s \,.\, RH}{100} \tag{2}$$

Where e_s is the saturation water vapor pressure determined by the Tetens Equation (Tetens, 1930) (Equation 3).

$$e_s = 6{,}1078 \,.\, 10^{\frac{7{,}5 \,.\, T_{ar}}{273{,}3 + T_{ar}}} \tag{3}$$

It is important to highlight that the methods used in this study were originally created to estimate ORL and by Equation 1 we could estimate ε.

The emissivity over fully vegetated surface show low variability, with its value usually ranging between 0.94 to 0.98 according to Food And Agriculture Organization Of The United Nations (1991). Nevertheless, the most-used value for surface emissivity is 1.

The atmospheric emissivity values estimated by the six methods presented in Table 1 were compared with emissivity values calculated by the energy balance equation (Equation 4). Its input data were measured during the study period by the instrumentation cited in Section 2.2.

$$\varepsilon = \frac{Rn - Rg + rRg + \sigma Ts^4}{\sigma Tar^4} \tag{4}$$

Where Rn (Wm^{-2}) is the net radiation, Rg (Wm^{-2}) is the incident global radiation, rRg (Wm^{-2}) is the surface albedo, σTar^4 (K^4) is the energy emitted by the atmosphere, σTs^4 (K^4) is the energy emitted by the soil, and ε is the atmospheric emissivity.

All the equations analyzed in this study make the assumption that ε is a function of temperature and/or vapor pressure near the ground.

2.4. Statistical analysis

The performance in atmospheric emissivity for each equation was assessed statistically using Mean Absolute Deviation (MAD), Mean Squared Error (MSE), and coefficient of determination (R^2) by linear regression without interception. Also were used Willmott's index of agreement (d), which indicates the estimation agreement level when compared with measured values (Willmott *et al.*, 1985), the Pearson correlation coefficient (r), which indicates the correlation level between observed and estimated values, and the confidence coefficient or Camargo and Sentelhas performance (c). The value of d and r must varies from 0 to 1, indicating non-concordance and perfect concordance, respectively (Machado *et al.*, 2015).

3. RESULTS AND DISCUSSION

3.1. Air temperature and relative humidity seasonal variation analysis

Sky conditions are directly related to atmospheric emissivity; therefore, a study of air temperature (*Tar*) and relative humidity (RH) seasonal variation is needed, since atmospheric conditions, as well as its components, mainly water vapor, have a strong influence on longwave radiation quantity that is irradiated to Earth's surface.

Mean monthly air temperature for the dry season varied from 11.22 to 31.95°C, with an average of 26.03°C. For the wet season, air temperature values ranged from 17.58 to 34.22°C, with an average of 28.33°C (Figure 1).

Relative humidity varied between 31.56% and 94.31% for the dry season and 35.21% and 94.75% for wet season, with average values of 60.59% and 64.99%, respectively. It was not possible to observe a pattern during the year, considering that its value in dry season decreases in comparison with wet season. This relation can be observed due to rainfall regularity, from September to March, and absence, from May to August.

Thus, it is expected for atmospheric emissivity values to be higher in the wet season than in the dry season, since higher values of relative humidity and air temperature can be observed during the wet season.

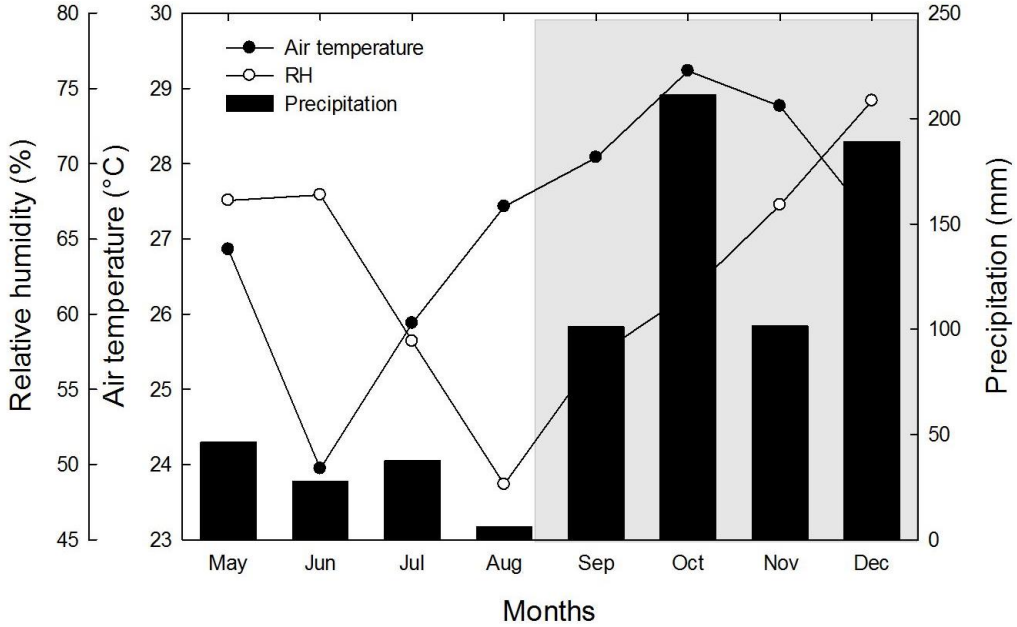

Figure 1. Mean monthly air temperature, relative humidity, and accumulated rainfall in 2009. The shaded area represents wet season, i.e., when rainfall > 100 mm.

Accumulated rainfall average value was equal to 29.38 mm for the dry season and 149.08 mm for the wet season. The lowest value was observed in August, 6.20 mm, while the highest was observed in October, 211 mm.

3.2. Atmospheric emissivity behavior analysis

The method used as reference in this study, the energy balance equation, has small instrumental errors inherent to micrometeorological data collection. Therefore, due to intrinsic errors related to the method, we found atmospheric emissivity values above 1.00, which is theoretically a black body emissivity. Table 2 shows the Mean Absolute Deviation (MAD) and Mean Squared Error (MSE) values.

Table 2. Minimum (Min), average (Avg), and maximum (Max) values of monthly atmospheric emissivity computed by energy balance (BE), Brutsaert (BT), Bignami (BG), Brunt (BR), Idso (ID), Idso and Jackson (IJ), and Swinbank (SW) equations under *campo sujo* Cerrado at the Fazenda Miranda.

Dry season												
	May			**June**			**July**			**August**		
	Min	**Avg**	**Max**	**Min**	**Avg**	**Max**	**Min**	**Avg**	**Max**	**Min**	**Avg**	**Max**
BE	0.93	0.98	1.06	0.88	0.95	1.05	0.88	0.94	1.00	0.86	0.93	1.08
IJ	0.79	0.85	0.87	0.80	0.84	0.86	0.76	0.84	0.87	0.74	0.83	0.89
SW	0.77	0.82	0.84	0.78	0.82	0.84	0.74	0.82	0.84	0.69	0.80	0.86
BT	0.84	0.88	0.91	0.82	0.87	0.91	0.82	0.86	0.91	0.80	0.83	0.89
BR	0.80	0.90	0.94	0.82	0.89	0.93	0.76	0.90	0.94	0.81	0.92	0.98
BG	0.77	0.83	0.85	0.78	0.82	0.85	0.76	0.81	0.84	0.77	0.80	0.84
ID	0.83	0.90	0.94	0.84	0.89	0.94	0.84	0.87	0.92	0.82	0.85	0.93
Wet Season												
	September			**October**			**November**			**December**		
	Min	**Avg**	**Max**	**Min**	**Avg**	**Max**	**Min**	**Avg**	**Max**	**Min**	**Avg**	**Max**
BE	0.89	1.03	1.11	0.97	1.04	1.09	0.92	1.04	1.12	0.85	1.03	1.09
IJ	0.80	0.86	0.90	0.85	0.87	0.89	0.83	0.86	0.88	0.83	0.87	1.00
SW	0.82	0.83	0.87	0.84	0.84	0.86	0.87	0.84	0.85	0.88	0.71	0.84
BT	0.81	0.86	0.90	0.90	0.87	0.89	0.86	0.88	0.91	0.69	0.76	0.91
BR	0.78	0.92	1.00	0.83	0.93	0.98	0.84	0.93	0.96	0.68	0.88	0.94
BG	0.78	0.82	0.85	0.82	0.85	0.87	0.82	0.86	0.87	0.82	0.83	0.87
ID	0.84	0.88	0.90	0.88	0.91	0.89	0.91	0.93	0.88	0.92	0.80	1.00

The energy balance method was adopted due to lack of local values of atmospheric emissivity in literature that could be considered as reference values, specifically for *campo sujo* Cerrado. Regarding the other six models, they have small instrumental errors too; they also show small errors related to each method, since the models have local parameters from where the model was initially proposed (constant values presented in each equation). Those parameters were not modified to the study area, as we wanted to evaluate the performance of each method in their original proposes.

Therefore, the results show that the six models have errors close to the instrumental errors used in this study, which makes this model an alternative to estimate atmospheric emissivity in the *campo sujo* Cerrado, using only two variables: air temperature (*Tar*) and relative humidity (RH).

These unique parameters (local constants) are extremely important to evaluate which method is more appropriate for *campo sujo* Cerrado. The Swinbank, and Idso and Jackson equations consider air temperature only, while the Brunt, Brutsaert, Idso, and Bignami equations consider, besides *T*, relative humidity, which is an effect of water vapor volume in the atmosphere. It is expected of those models that consider *T* only to estimate better values of atmospheric emissivity during dry seasons, considering the mean precipitation to be close to 0. For the other models, it is likely that they estimate better values of ε during wet seasons, because water volume in atmosphere increases significantly, raising RH values.

During the study period, the mean daily atmospheric emissivity (ε) calculated by the energy balance equation showed large variation during the dry season, ranging from 0.88 to 1.00, which is the maximum value. For Brutsaert and Brunt methods, emissivity values during the dry season varied from 0.80 to 0.91, and from 0.76 to 0.98, respectively, showing that those models estimate atmospheric emissivity within range of energy balance (Figure 2). That also happened during the wet season (Figure 3). The emissivity values by energy balance equation ranged from 0.85 to values higher than 1.00. Using the Bignami and Idso models, the values varied from 0.78 to 0.87, and 0.84 to 1.00, respectively. The average, minimum and maximum monthly values of atmospheric emissivity are shown in Table 2.

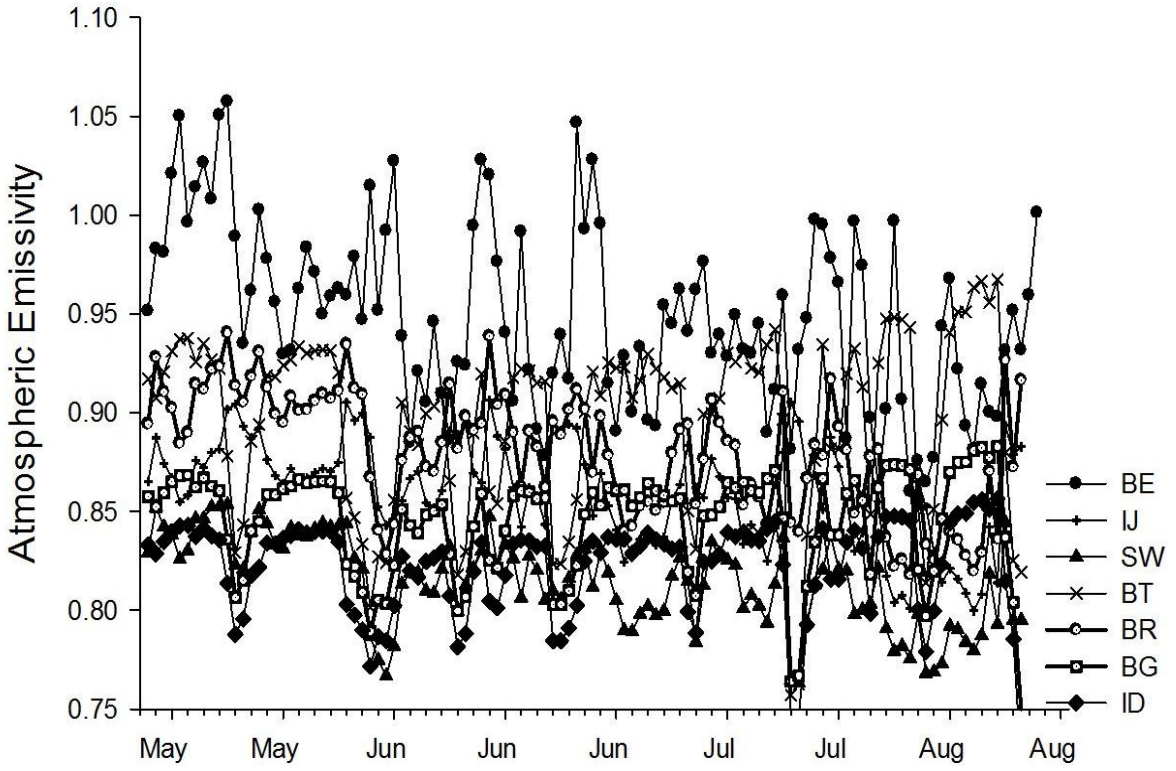

Figure 2. Mean daily atmospheric emissivity for the dry season computed by energy balance (BE), Brutsaert (BT), Bignami (BG), Brunt (BR), Idso (ID), Idso and Jackson (IJ), and Swinbank (SW) equations under *campo sujo* Cerrado at the Fazenda Miranda.

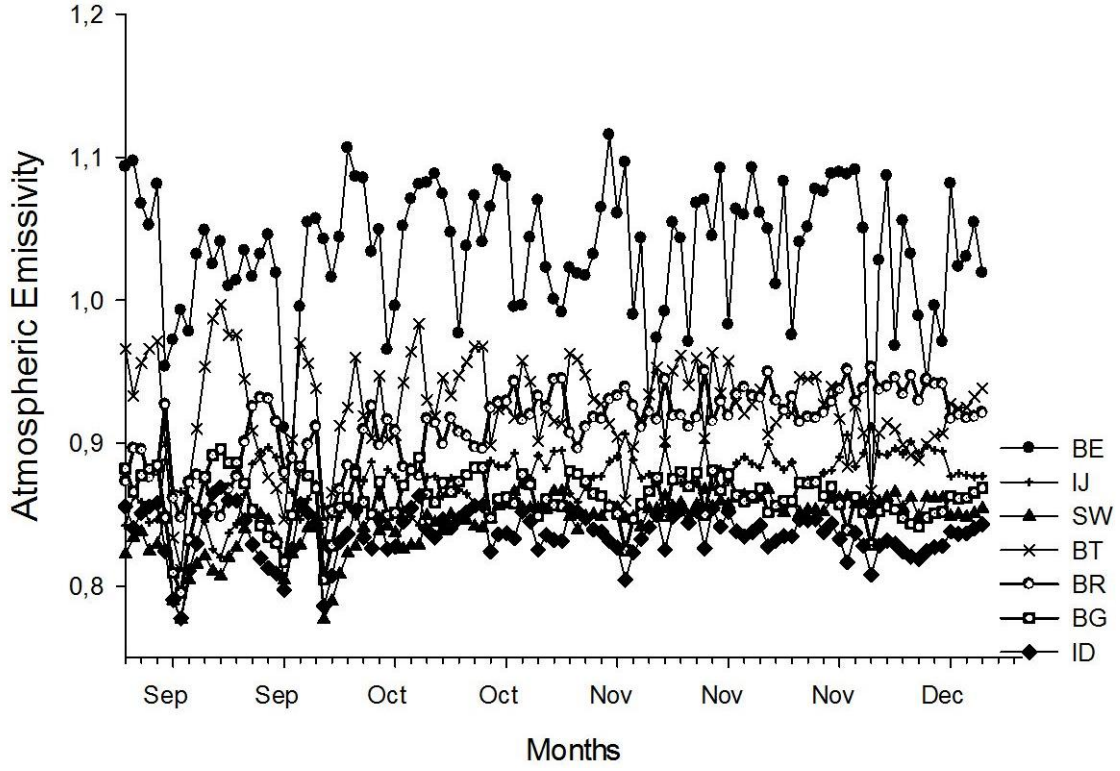

Figure 3. Mean daily atmospheric emissivity for the wet season computed by energy balance (BE), Brutsaert (BT), Bignami (BG), Brunt (BR), Idso (ID), Idso and Jackson (IJ), and Swinbank (SW) equations under *campo sujo* Cerrado at the Fazenda Miranda.

3.3. Atmospheric emissivity models performance

To evaluate the performance of the equations proposed by Brunt, Swinbank, Idso and Jackson, Brutsaert, Idso, and Bignami to estimate atmospheric emissivity (ε), mean ε daily values from May to August were used, covering a dry season and a part of the wet season, from September to December.

After estimations, the ε values were divided by periods and Mean Absolute Deviation (MAD), Mean Squared Error (MSE), and coefficient of determination (R^2) were calculated using linear regression without interception. Willmott's index of agreement (d), the Pearson correlation coefficient (r), and the confidence coefficient or Camargo and Sentelhas performance (c) were calculated as well, as shown in Table 3.

Low error values for the wet season (September to December) showed that the models adjust to the study area, where the variation ranges of MAD (-0.07 to -0.13), MSE (0.19 to 0.22), and R^2 (0.93 to 0.95) were lower than the values for the dry season. For the dry season, MAD ranged from -0.09 to -0.12, MSE ranged from 0.18 to 0.27, and R^2 varied from 0.89 to 0.96.

Negative MAD values indicate underestimation, while positive values indicate overestimation. We noted that the six models tend to underestimate atmospheric emissivity values. Due to lack of studies about atmospheric emissivity in literature, the performance of our estimates were compared to Von Randow and Alvalá (2006) and Aguiar *et al*. (2011). Those studies estimated ORL using the same models. This underestimation tendency was also found by to Von Randow and Alvalá (2006) and Aguiar *et al.* (2011), which indicated that the problems could be related to the coefficients used on the equations, which are adjusted to other regions.

It is possible to observe in Table 3 that the Pearson correlation coefficient (r) values for dry period are above 0.3, which are characterized as intermediate and high correlations,

indicating good precision when compared to monthly average. Idso and Jackson method obtained the lowest value for dry season, while Brutsaert, Bignami, and Idso models showed the best coefficient with a value of 0.59 each one.

For the wet season, the r values were very low and considered as low and very low. Idso and Jackson equation indicated the best effectiveness, with an r value of 0.31. The other methods obtained r values lower than 0.30 and were interpreted as low correlation.

About the confidence coefficient or Camargo and Sentelhas performance (c), for wet season, very poor performance were found for every method used. For dry season, the best results were found for Brutsaert, and Idso models, which indicated poor performance, and the other methods were determined as very poor.

Table 3. Statistical analyses of observed (computed by energy balance equation) and estimated atmospheric emissivity values.

Dry season								
Method	**MAD**	**MSE**	**R^2**	**d**	**r**	**Classification**	**c**	**Performance**
Idso and Jackson	-0.07	0.22	0.93	0.32	0.33	Intermediate	0.11	Very Poor
Swinbank	-0.09	0.22	0.93	0.38	0.41	Intermediate	0.15	Very Poor
Brutsaert	-0.09	0.20	0.94	0.72	0.59	High	0.42	Poor
Brunt	-0.05	0.20	0.95	0.71	0.55	High	0.39	Very Poor
Bignami	-0.13	0.22	0.93	0.68	0.59	High	0.40	Very Poor
Idso	-0.07	0.19	0.95	0.73	0.59	High	0.43	Poor
Wet season								
Method	**MAD**	**MSE**	**R^2**	**d**	**r**	**Classification**	**c**	**Performance**
Idso and Jackson	-0.09	0.18	0.96	0.31	0.31	Intermediate	0.09	Very Poor
Swinbank	-0.12	0.27	0.89	0.18	-0.12	Low	-0.02	Very Poor
Brutsaert	-0.10	0.24	0.92	0.16	-0.17	Low	-0.03	Very Poor
Brunt	-0.10	0.24	0.92	0.16	-0.17	Low	-0.03	Very Poor
Bignami	-0.10	0.20	0.94	0.26	-0.07	Very Low	-0.02	Very Poor
Idso	-0.08	0.22	0.94	0.16	-0.16	Low	-0.02	Very Poor

Idso equation obtained the highest R^2 value for the dry season, a high R^2 value of 0.94 for wet season, evidencing low error values compared to observed data, and the best r and c values for dry season, which represent the errors in comparison with regression equation.

For the wet season, the model with best performance was the Idso and Jackson equation, being the only method used with positive c and the highest R^2 value, 0.96.

The Brutsaert, Brunt, and Bignami equations had similar results. On the other hand, the Swinbank and Idso and Jackson methods results were very much alike too, and both models consider *Tar* only.

Figures 2 and 3 show values of daily average cycle of atmospheric emissivity, and it is possible to observe again that the values in the wet season are higher than in the dry season, and that the modelled values underestimate the emissivity found by energy balance equation.

For the dry season, Idso and Brutsaert equations showed the best model performances. On the other hand, the equation developed by Idso and Jackson results were more efficient for the wet season, where thermal amplitude is low, showing a sensitivity of this equation to the air temperature variation, since water vapor practically does not vary throughout the day.

Regarding the energy available to the environment, since atmospheric emissivity varied seasonally, with higher values observed during the wet season, the average energy of longwave radiation (ORL) that comes from the available atmosphere also varied from one period to another. Considering the higher emissivity during the wet season, during this period there was a higher availability of energy to the environment (Curado et al., 2011).

4. CONCLUSIONS

The equations evaluated in this study showed poor performance during the studied year, and only during the dry season was their performance acceptable. Those results were expected, since high cloudiness conditions negatively affected the models' performance for the wet season.

For dry season, the methods that consider water vapor pressure and air temperature show better performance than models that consider air temperature only, as with the Swinbank (1963) and Idso and Jackson (1969) equations. However, for the wet season, the Idso and Jackson (1969) model is more efficient, indicating a sensitivity associated to the air temperature.

The Idso (1981) and Brutsaert (1975) equations show better performance for the study area, obtaining higher indexes of agreement. Therefore, these models are the most suitable methods to estimate atmospheric emissivity for *campo sujo* Cerrado.

5. ACKNOWLEDGEMENTS

We acknowledge *Programa Pós-Graduação em Física Ambiental* (PPGFA) for provides data, and its professors for data collection, without their support, this study could not be developed. This study was financed in part by the *Coordenação de Aperfeiçoamento de Pessoal de Nível Superior* - Brasil (CAPES) - Finance Code 001. The authors are also grateful to Dr. Clovis Miranda and his family for allow this study to be developed at the Fazenda Miranda.

6. REFERENCES

AGUIAR, L. J. G.; FISCH, G. R.; FERREIRA, W. P. M.; COSTA, A. C. L. D.; COSTA, J. M. N. D.; AGUIAR, R. G. Estimativa da radiação de onda longa atmosférica em áreas de floresta e de pastagem no sudoeste da Amazônia. **Revista Brasileira de Meteorologia**, v. 26, n. 2, p. 215-224, 2011. https://dx.doi.org/10.1590/S0102-77862011000200006

BIGNAMI, F.; MARULLO, S.; SANTOLERI, R.; SCHIANO, M. E. Longwave radiation budget in the Mediterranean Sea. **Journal of Geophysical Research**, v. 100, n. C2, p. 2501-2514, 1995. https://doi.org/10.1029/94JC02496

BIUDES, M. S.; VOURLITIS, G. L.; MACHADO, N. G.; ARRUDA, P. H. Z.; NEVES, G. A. R.; ALMEIDA, L. F.; SOUZA, N. J. Patterns of energy exchange for tropical ecosystems across a climate gradient in Mato Grosso, Brazil. **Agricultural and Forest Meteorology**, v. 202, p. 112-124, 2015. http://dx.doi.org/10.1016/j.agrformet.2014.12.008

BRUNT, D. Notes on radiation in the atmosphere. I. **Quarterly Journal of the Royal Meteorological Society**, v. 58, n. 247, p. 389-420, 1932. https://doi.org/10.1002/qj.49705824704

BRUTSAERT, W. On a derivable formula for long-wave radiation from clear skies. **Water Resources Research,** v. 11, n. 5, p. 742-744, 1975. https://doi.org/10.1029/WR011i005p00742

CPRM. **Folha SD-21 Cuiabá**: atlas hidrogeológico do Brasil ao milionésimo. Projeto RadamBrasil. Brasília, 1982.

CURADO, L. F. A; RODRIGUES, T. R.; BIUDES, M. S.; DE PAULO, S. R.; DE PAULO, I. J. C.; DE SOUZA NOGUEIRA, J. Estimativa sazonal da emissividade atmosférica através da Equação de Brutsaert no norte do Pantanal Mato-grossense. **Ciência e Natura,** v. 33, n. 2, p. 167-180, 2011. http://dx.doi.org/10.5902/2179460X9368

DUARTE, F.; DIAS, L.; MAGGIOTTO, S. R. Assessing daytime downward longwave radiation estimates. **Agricultural and Forest Meteorology**, v. 139, p. 171-181, 2006. https://doi.org/10.1016/j.agrformet.2006.06.008

FARIA, T. O.; RODRIGUES, T. R.; CURADO, L. F. A.; GAIO, D. C.; NOGUEIRA, J. S. Surface albedo in different land-use and cover types in Amazon forest region. **Revista Ambiente e Água,** v. 13, p. 1-13, 2018. http://dx.doi.org/10.4136/ambi-agua.2120

FOOD AND AGRICULTURE ORGANIZATION OF THE UNITED NATIONS. **Report on the expert consultation on procedures for revision of FAO guidelines for prediction of crop water requirements**. Roma, 1991. p. 45.

GIAMBELLUCA, T. W.; SCHOLZ, F. G.; BUCCI, S. J.; MEINZER, F. C.; GOLDSTEIN, G.; HOFFMANN, W. A.; BUCHERT, M. P. Evapotranspiration and energy balance of Brazilian savannas with contrasting tree density. **Agricultural and forest meteorology**, v. 149, n. 8, p. 1365-1376, 2009. https://doi.org/10.1016/j.agrformet.2009.03.006

HEITOR, A.; BIGA, A. J.; ROSA, R. Thermal radiation components of the energy balance at the ground. **Agricultural and Forest Meteorology**, v. 54, n. 1, p. 29-48, 1991. https://doi.org/10.1016/0168-1923(91)90039-S

IDSO, S. B.; JACKSON, R. D. Thermal radiation from the atmosphere. **Journal Geophysical Research**, v. 74, n. 23, p. 5397-5403, 1969. https://doi.org/10.1029/JC074i023p05397

IDSO, S. B. A set of equations for full spectrum and 8 to 14 ìm and 10.5 to 12.5 μm thermal radiation from cloudless skies. **Water Resources Research,** v. 17, n. 2, p. 295 304, 1981. https://doi.org/10.1029/WR017i002p00295

JIMÉNEZ, J. I.; ALADOS-ARBOLEDAS, L.; CASTRO-DÍEZ, Y. *et al*. On the estimation of long-wave radiation flux from clear skies. **Theoretical and applied climatology**, v. 38, n. 1, p. 37-42, 1987. https://doi.org/10.1007/BF00866251

KLINK, C. A.; MOREIRA, A. G. Past and current human occupation, and land use. *In*: OLIVEIRA, P. S.; MARQUIS, R. J. (Eds.). **The cerrados of Brazi**l: ecology and natural history of a neotropical savanna. New York: Columbia University Press, 2002. p. 69-88.

MACHADO, N. G. *et al*. Estimation of rainfall by Neural Network Over A Neotropical Region. **Revista Brasileira de Climatologia**, v. 17, 2015. https://dx.doi.org/10.5380/abclima.v17i0.40799

NOGUEIRA, J. S.; LIMA, E. A. **Coletânea física ambiental I**. São Paulo: Baraúna, 2011.

NOVAIS, J. W. Z.; SANCHES, L.; MACHADO, N. G.; SILVA, L. B.; AQUINO, A. M.; RODRIGUES, T. R. Variação horária e sazonal da radiação solar incidida e refletida e suas relações com variáveis micrometeorológicas no Pantanal Norte Mato-grossense. **Revista Brasileira de Ciências Ambientais,** v. 38, p. 96-108, 2015. http://dx.doi.org/10.5327/Z2176-947820150053

PRATA, A. J. A new long wave formula for estimating downward clear sky radiation at the surface. **Quartely Journal of the Royal Meteorological Society,** v. 122, p. 1127 - 1151,1996. https://doi.org/10.1002/qj.49712253306

RODRIGUES, T. R.; VOURLITIS, G. L.; LOBO, F. A.; OLIVEIRA, R. G.; NOGUEIRA, J. D. S. Seasonal variation in energy balance and canopy conductance for a tropical savanna ecosystem of south central Mato Grosso, Brazil. **Journal of Geophysical Research: Biogeosciences**, v. 119, n. 1, p. 1-13, 2014. http://dx.doi.org/10.1002/2013JG002472

RODRIGUES, T. R.; CURADO, L. F. A.; PEREIRA, V. M. R.; SANCHES, L.; NOGUEIRA, J. S. Hourly interaction between wind speed and energy fluxes in Brazilian Wetlands – Mato Grosso - Brazil. **Anais da Academia Brasileira de Ciências**, v. 88, n. 4, p. 2195-2209, 2016. http://dx.doi.org/10.1590/0001-3765201620150130

SAN JOSÉ, J. J.; NIKONOVA, N.; BRACHO, R. Comparison of factors affecting water transfer in a cultivated paleotropical grass (Brachiaria decumbens Stapf) field and a neotropical savanna during the dry season of the Orinoco lowlands. **Journal of Applied Meteorology**, v. 37, n. 5, p. 509-522, 1998. https://doi.org/10.1175/1520-0450(1998)037%3C0509:COFAWT%3E2.0.CO;2

SCHOLES, R. J.; ARCHER, S. R. Tree-grass interactions in savannas. **Annual review of Ecology and Systematics**, v. 28, n. 1, p. 517-544, 1997. https://doi.org/10.1146/annurev.ecolsys.28.1.517

SWINBANK, W. C. Long-Wave Radiation from clear skies. **Quarterly Journal of the Royal Meteorological Society**, v. 89, n. 381, p. 339-348, 1963. https://doi.org/10.1002/qj.49708938105

TETENS, V. O. **Über einige meteorologische Begriffe**. Gesellschaft: Friedrich Vieweg & Sohn Akt, 1930. p. 297-309.

VON RANDOW, R. C. S.; ALVALÁ, R. C. S. Estimativa da radiação de onda longa atmosférica no pantanal sul mato-grossense durante os períodos secos de 1999 e 2000. **Revista Brasileira de Meteorologia**, v. 21, n. 3b, p. 398-412, 2006.

VOURLITIS, G. L.; DA ROCHA, H. R. Flux dynamics in the cerrado and cerrado-forest transition of Brazil. *In:* HILL, M. J.; HANAN, N. P. (Eds.). **Ecosystem function in global savannas**: measurement and modeling at landscape to global scales. Boca Raton: CRC Press, 2011. p. 97-116.

WILLMOTT, C. J.; ACKLESON, S. G.; DAVIS, J. J.; FEDDEMA, K. M.; KLINK, D. R. Statistics for the evaluation and comparison of models. **JGR Oceans**, v. 90, p. 8995-9005, 1985. https://doi.org/10.1029/JC090iC05p08995

Ambiente & Água - An Interdisciplinary Journal of Applied Science
ISSN 1980-993X – doi:10.4136/1980-993X
www.ambi-agua.net
E-mail: ambi.agua@gmail.com

Continuous electrochemical reactor improved by the addition of Moringa oleífera lam extract: optimization of operational conditions for Blue 5G dye removal

ARTICLES doi:10.4136/ambi-agua.2290

Received: 10 Jun. 2018; Accepted: 06 Feb. 2019

Bruna Souza dos Santos; Eduardo Eyng*; Paulo Rodrigo Stival Bittencourt; Laercio Mantovani Frare; Éder Lisandro de Moraes Flores; Michelle Budke Costa

Universidade Tecnológica Federal do Paraná (UTFPR), Medianeira, PR, Brasil
Programa de Pós-Graduação em Tecnologias Ambientais (PPGTAMB).
E-mail: brusouzasantos@hotmail.com, eduardoeyng@utfpr.edu.br, paulob@utfpr.edu.br, laercio@utfpr.edu.br, eder@utfpr.edu.br, michelleb@utfpr.edu.br
*Corresponding author

ABSTRACT

Wastewaters from textile industries are known for their difficulty to treat, several alternative technologies are applied for their treatment. In this context, the study examined a hybrid treatment system, composed of electrocoagulation combined with a natural coagulant (extract of Moringa oleífera lam seeds) to remove reactive dye Blue 5G aqueous solutions. The work evaluated the use of milder operating conditions to improve the efficiency of treatment, with reduced demands for electrical power and coagulant. The following factors were evaluated: electric current intensity, natural coagulant concentration and hydraulic retention time. A quadratic model was adjusted and validated at a 5% significance level. The overall optimization resulted in conditions of 0.28 A for electrical current intensity, 1000.00 mg L^{-1} of aqueous extract of Moringa oleífera lam and 5 min for hydraulic retention time. While operating under optimal conditions, the removal of 71.38% of color and 5.22 mg L^{-1} of iron residual concentration was achieved.

Keywords: central composite rotational design, global optimization of processes, natural coagulant, textile effluent, wastewater electrochemical treatment.

Reator eletroquímico contínuo potencializado pela adição de extrato de Moringa oleífera lam: otimização das condições operacionais para remoção do corante Blue 5G

RESUMO

Os efluentes das indústrias têxteis são conhecidos pela dificuldade de tratamento, constituindo um campo de aplicação de tecnologias alternativas para o tratamento. Neste contexto, um sistema de tratamento híbrido, composto por eletrocoagulação associada à adição de coagulante natural (extrato de sementes de Moringa oleífera lam), visa utilizar condições de operação mais suaves, que proporcionem eficiência de tratamento, com menor demanda de energia elétrica e coagulante. Assim, a remoção do corante reativo Azul 5G de soluções aquosas

foi estudada. Foram avaliados os efeitos dos fatores: intensidade da corrente elétrica, concentração de coagulantes naturais e tempo de retenção hidráulica. Um modelo quadrático foi ajustado e validado no nível de significância de 5%. A otimização global resultou em condições de 0,28 A para intensidade de corrente elétrica, 1000,00 mg L^{-1} de extrato aquoso de Moringa oleífera lam e 5 min para tempo de retenção hidráulica. Operando em condições ótimas, observou-se 71,38% de remoção de cor e 5,22 mg L^{-1} de concentração residual de ferro.

Palavras-chave: coagulante natural, delineamento composto central rotacional, efluentes têxteis, otimização global de processos, tratamento eletroquímico de águas residuárias.

1. INTRODUCTION

Despite current technological developments, many there are still many problems due to contamination and water pollution of waters. The development and improvement of technologies for effluent treatment are needed, not only from the perspective of the technical feasibility of pollutant removal, but also from the social-environmental viewpoint, since the minimization of treatment system waste is an important factor.

Industrial textile effluent is characterized by low biodegradability and relative toxicity. The study of alternative treatment technologies is therefore very important, since this sector consumes large volumes of water, and the need to reuse this water becomes increasingly important.

Among the physical-chemical treatment technologies of effluents, electrocoagulation is an interesting option. The technique can be more efficient than the coagulation/flocculation process normally used. This process uses the basic foundation of coagulation/flocculation, producing redox reactions, and also generates micro bubbles that ascend and eventually interact with whole system. The result is flocculation and flotation of the pollutant as a sludge, and consequently, optimization of treatment process effectiveness (Aquino Neto *et al.*, 2011).

There are in literature several studies that report the effectiveness of wastewater treatment by electrocoagulation, particularly, applications on textile effluent treatment (Pajootan *et al.*, 2012; Daneshvar *et al.*, 2006). In this context, electrocoagulation technology had been combined with other treatment technologies, such as, ozone (Asaithambi *et al.* 2012; Song *et al.*, 2007), fenton (Yavuz *et al.*, 2014), ultrasound agitation (Raschitor *et al.*, 2014; Vianney e Muthukumar, 2016) and adsorption (Secula *et al.*, 2012).

Another interesting work evaluated the efficiency of electrocoagulation process assisted by *Opuntia ficus indica* pad juice. The natural coagulant addition provided a 15.1% increase in turbidity removal from a synthetic solution (tap water with 300 mg L^{-1} and silica gel (Adjeroud *et al.*, 2015). Chemical coagulation and electrocoagulation techniques also have been explored for the removal of organic compounds from slaughterhouse effluent. The results showed that combined processes are inferred to be superior to electrocoagulation alone (Bazrafshan *et al.*, 2012).

Still in the field of alternative technologies for effluents treatment, the employment of the seed of Moringa Oleífera Lam as a natural coagulant deserves to be highlighted. The Moringa Oleífera Lam seed acts as an effective coagulant agent because it contains a cationic protein of low molecular weight which interacts with the organic material of the effluent, destroying the stability of colloidal structures and facilitating the removal of the material by sedimentation (Arantes *et al.*, 2012).

The analysis of the chemical composition of Moringa Oleífera Lam seeds reveals that the pulp contains proteins of low molecular weight and dissolution in water favors the attachment of colloids due to the neutralization of surface charges. The main reason for this coagulant action is the formation of bridges between the particles in suspension and specific organic

molecules present in Moringa Oleífera Lam extract (Barreto *et al.*, 2009).

The extract of Moringa Oleífera Lam has shown excellent performance for water clarification, reaching 90-94% of turbidity removal. This result is similar to substances traditionally used, such as Aluminum Sulphate ($Al_2 (SO_4)_3$), Ferric Chloride ($FeCl_3$) and Ferrous Sulphate ($FeSO_4$) (Paterniani *et al.*, 2009). Extracts from the pulp and the shell of the seed were also used for iron oxide removal from rainwater (Carvalho *et al.*, 2006).

The combination of these two techniques, electrocoagulation and the addition of a natural coagulant based on Moringa Oleífera Lam, as an hybrid system, may constitute a promising application for the treatment of textile effluent. This work therefore applied the hybrid treatment system to removal of reactive dye Blue 5G from aqueous solutions to evaluate whether the association of these treatment technologies, operated under milder treatment conditions, may provide an increase of performance.

2. MATERIALS AND METHODS

2.1. Analytical methodologies

The dye solutions used were prepared from the commercial reactive dye Blue 5G, with a concentration of 50 mg L^{-1}. Sodium Chloride was added to a concentration of 1 g L^{-1} to increase the solution electrical conductivity.

The color evaluation of samples was performed by light absorption (peak height) at 618 nm, which was previously determined by spectrum scanning on a PerkinElmer Spectrophotometer, dual beam, Lambda 45 model. This wavelength is in agreement with results reported in literature (Lambrecht *et al.*, 2015). Color removal was assessed by comparing the absorbance of the samples with treatment and without it.

The determination of the concentration of residual iron was carried out through spectrometry atomic absorption flame, using the direct method of air-acetylene flame. Before the residual iron determination, the samples were prepared by acid digestion. Therefore, 50 mL of sample was transferred to an Erlenmeyer and 5 mL of nitric acid (HNO_3) was added. The digestion was heated until the volume was reduced to 20 mL. The digested sample was transferred to a volumetric flask, and distilled water was added until the volume of 50 mL was reached. Atomic absorption measurements used the following conditions: Acetylene flow = 2 L min^{-1}; Air flow = 13.5 L min^{-1}; Lamp current = 10 mA; wave length 248.3 nm and slit = 0.2 m. The dilution of standard iron solution followed the concentrations: 0.5; 1.0; 2.5; 5.0 and 10.0 mg L^{-1}.

2.2. Method for obtain the extract of Moringa oleífera lam seed

The Moringa Oleífera Lam (MO) seeds used in this work, which were selected for uniformity in size and coloring, were from the municipality of Medianeira- PR Brazil, Latitude: 25 17'43" S and Longitude: 54 05'38" W and Marechal Cândido Rondon - PR Brazil, Latitude: 24 33'22" S and Longitude: 54 03'24" W.

Initially, the husks of MO seeds were removed and manually macerated so that a homogeneous material was obtained. This material was used in a natural coagulant solution preparation at a ratio of 5 g of MO to 100 mL of saline aqueous solution (20% sodium chloride concentration). This solution was then agitated for 20 s in an ultrasonic bath, at 80 kHz frequency and 150 W of power. After the extraction stage was finished, the solution was subjected to a vacuum filtration with filter paper of a 3-micrometer pore. After this procedure, the resulting solution can be used in coagulation/flocculation tests, presenting a ratio of 50.000 mg L^{-1} (solution matrix of coagulant).

2.3. System of treatment hybrid

Figure 1 is a schematic of the treatment system for synthetic textile effluent (reactive dye Blue 5G solution) operating under continuous flow, employing electrocoagulation technology as a hybrid arrangement with the addition of aqueous extract of Moringa oleífera lam seed.

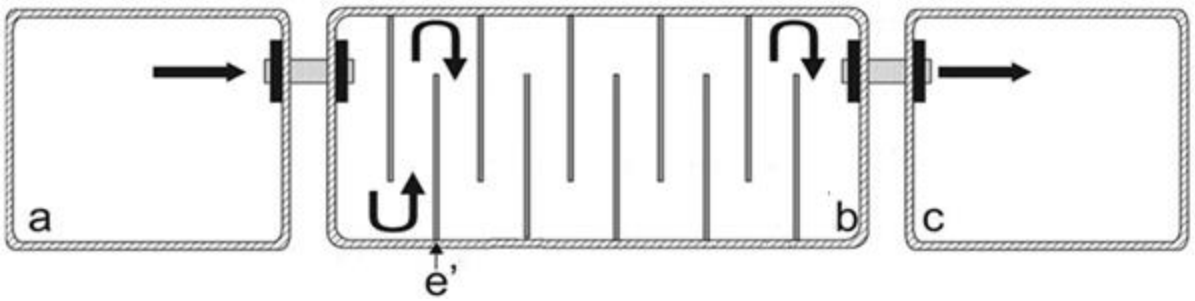

Figure 1. Schematic of the hybrid treatment system.

In first compartment, "a", the aqueous extract of Moringa oleífera lam seeds is mixed with dye reactive Blue 5G solution for a period of 3 min under high agitation. This section is equipped with a spindle, driven by a 12 V engine. The effluent is then pumped to the electrolytic chamber, "b" (18.5 cm of width x 58 cm of length x 20 cm of height, with effective volume of 16 L). In this compartment, the effluent comes into contact with iron sacrifice electrodes, which have two purposes: the viability of electrocoagulation, providing Fe^{3+} ions to solution, and also working as baffles, which help the hydraulic system. Finally, the treated effluent flows to the camera, "c", where it is stored. For the electrochemical treatment, the electrodes are connected to a DC-power source, in a parallel mode. Five pairs of iron electrodes were used, with a total area of 512 cm^2.

After the tests of electrocoagulation associated with addition of aqueous extract of Moringa Oleífera Lam, samples of treated effluent were collected in duplicate, and after an hour of stabilization were subjected to chemical analyses for color removal evaluation and determination of residual iron concentration.

2.4. Experimental Design

The effects of electric current intensity (I), concentration of Moringa Oleífera Lam coagulant (MO) and hydraulic retention time (HRT) on percentage color removal and concentration of residual iron on treated reactive dye Blue 5G solutions, were evaluated by a Central Composite Rotational Design – CCRD.

According to experimental design CCRD, 2^3 factorial tests were performed, with three repetitions at central point condition, and six tests were performed at axial points, totaling 17 runs, which were carried out in duplicate. The real values, corresponding to the range of the study variables, are presented in Table 1.

Table 1. Real and coded values corresponding to factors studied.

	-1.68	-1	0	1	+1.68
I (A)*	0.10	0.28	0.55	0.82	1.00
MO (mg L^{-1})	100.0	282.1	550.0	817.9	1000.0
HRT (min)	5.0	6.0	7.5	9.0	10.0

***Applied on each pair of sacrifice iron electrode.

3. RESULTS AND DISCUSSION

Table 2 presents the results of tests for color removal and concentration of residual iron by experimental design matrix execution. It should be noted that the data presented are mean values, because the tests were performed in duplicate.

Table 2. Experimental design matrix and results for color removal and concentration of residual iron.

Run	I (A)	MO (mg L^{-1})	HRT (min)	Color removal (%)	Concentration of residual iron (mg L^{-1})
1	-1 (0.28)	-1 (282.1)	-1(6)	76.92 ± 7.63	7.847 ± 0.013
2	+1 (0.82)	-1 (282.1)	-1(6)	86.80 ± 0.74	3.806 ± 0.054
3	-1 (0.28)	+1 (817.9)	-1(6)	73.89 ± 0.01	6.539 ± 0.343
4	+1 (0.82)	+1 (817.9)	-1(6)	36.01 ± 3.50	6.732 ± 0.813
5	-1 (0.28)	-1 (282.1)	+1(9)	81.94 ± 1.24	7.241 ± 0.610
6	+1 (0.82)	-1 (282.1)	+1(9)	65.20 ± 0.22	3.702 ± 0.241
7	-1 (0.28)	+1 (817.9)	+1(9)	50.28 ± 0.35	8.107 ± 0.314
8	+1 (0.82)	+1 (817.9)	+1(9)	23.91 ± 2.15	7.317 ± 0.552
9	0(0.55)	0 (550)	0 (7.5)	56.14 ± 2.20	8.492 ± 0.149
10	0 (0.55)	0 (550)	0 (7.5)	53.41 ± 0.53	7.066 ± 0.179
11	0 (0.55)	0 (550)	0 (7.5)	57.89 ± 0.46	7.072 ± 1.326
12	+1.68 (1.00)	0 (550)	0 (7.5)	90.25 ± 2.14	8.209 ± 0.942
13	-1.68 (0.10)	0 (550)	0 (7.5)	8.46 ± 3.39	3.871 ± 0.198
14	0 (0.55)	+1.68 (1000)	0 (7.5)	72.37 ± 0.45	7.478 ± 0.188
15	0 (0.55)	-1.68 (100)	0 (7.5)	20.66 ± 1.36	9.031 ± 2.658
16	0 (0.55)	0 (550)	+1.68 (10)	71.77 ± 0.63	5.332 ± 0.140
17	0 (0.55)	0 (550)	-1.68 (5)	58.08 ± 0.81	8.447 ± 0.031

Table 2 shows that the color removal ranged from 8.46% to 90.25%. In addition, the concentration of residual iron ranged from 3.70 mg L^{-1} to 9.03 mg. L^{-1}. Based on Brazilian legislation (Conama, 2011), the dissolved iron concentration limit for effluent discharge in water bodies is 15 mg. L^{-1}. This threshold was conformed to in all tests. The results obtained in this work with the hybrid treatment system are similar to those reported in the literature.

A techno-economic comparative between the use of chemical coagulants/flocculants and electrocoagulation in the treatment of textile industry wastewater was conducted. In this work the operating parameters analyzed were: pH, electric current density and time of electrolysis. Total Organic Carbon (TOC) and organic dye removal were used to evaluate treatment performance, in addition to energy and electrode consumption. In accordance with the optimal parameters found in this study, the percentage of removal achieved were 81% for COD, 85% for TOC, 93% for turbidity and 97.1% for Total Suspended Solids (TSS). The results showed that despite the costs of power, the electrochemical treatment minimized the production of sludge, which decreased the costs of the process.

The optimum operating conditions to maximize the percentage removal of color and turbidity from washing jeans effluent was found (Ströher *et al.*, 2012). The process parameters studied were: fast mixing time (ranged from 2 to 5 minutes), slow mixing time (from 20 to 30 minutes), and sedimentation time (from 20 to 30 minutes), with agitation fixed at 95 rpm for coagulation and 30 rpm for flocculation. The natural coagulant concentrations added were 1400, 1600, 1800, 2000, 2200, 2400 and 2600 mg L^{-1}. After coagulation/flocculation runs in Jar Test, the parameters of color and turbidity were analyzed and presented removals greater than 80.33% and 91,10%, respectively.

The variables that influence the efficiency of color removal from an azo dye solution (Reactive Black 5 - RB 5) by the combination of ozonation and electrocoagulation with iron electrodes were investigated (Song *et al.*, 2013). Various parameters were evaluated, such as

initial pH, initial dye concentration, electrical current density, salt concentration, temperature, ozone flow rate and distance between electrodes. The experimental results showed that the color of RB 5 in the aqueous phase was removed effectively. Under the conditions of initial dye concentration of 100 mg L^{-1}, initial pH of 5.5, electrical current density of 10 mA cm^{-2}, salt concentration of 5000 mg L^{-1}, temperature of 20 ^{0}C, ozone flow rate of 20 mL min^{-1} and distance between electrodes of 1 cm, the removal efficiency of color reached 94%, which corresponds to a COD reduction greater than 60%.

The effects of operating parameters, such as pH, initial dye concentration, electric current density, distance between electrodes and the electric conductivity in the treatment of a synthetic and real textile wastewater by electrocoagulation process were investigated (Merzouk *et al.*, 2010). The optimal conditions, which were determined from synthetic wastewater treatment, were applied to a real textile effluent. Initially, various current densities were tested ranging from 11.55 to 91.5 mA cm^{-2} and the distances of the electrodes 1, 2 and 3 cm. The application of ideal operating parameters showed a high removal efficiency. The best results provided 85.5% of suspended solids removal, 76.2% of turbidity, 88.9% of Biochemical Oxygen Demand (BOD_5^{20}), 79.7% of COD and 93% of color.

3.1. Empirical Modeling of color removal promoted by treatment hybrid system

Based on the results presented in Table 2, it was possible to evaluate the effects of the factors studied in response variable color removal. Analyzing Figure 2 (Pareto Diagram), it is possible to assess which of the terms relating to HRT was statistically significant (5% significance level), then these terms were excluded from the model and their contributions were incorporated into residuals. Despite the fact that the terms quadratics and the interaction between electric current intensity and concentration of Moringa Oleífera Lam coagulant have not been significant, these terms were kept in the model.

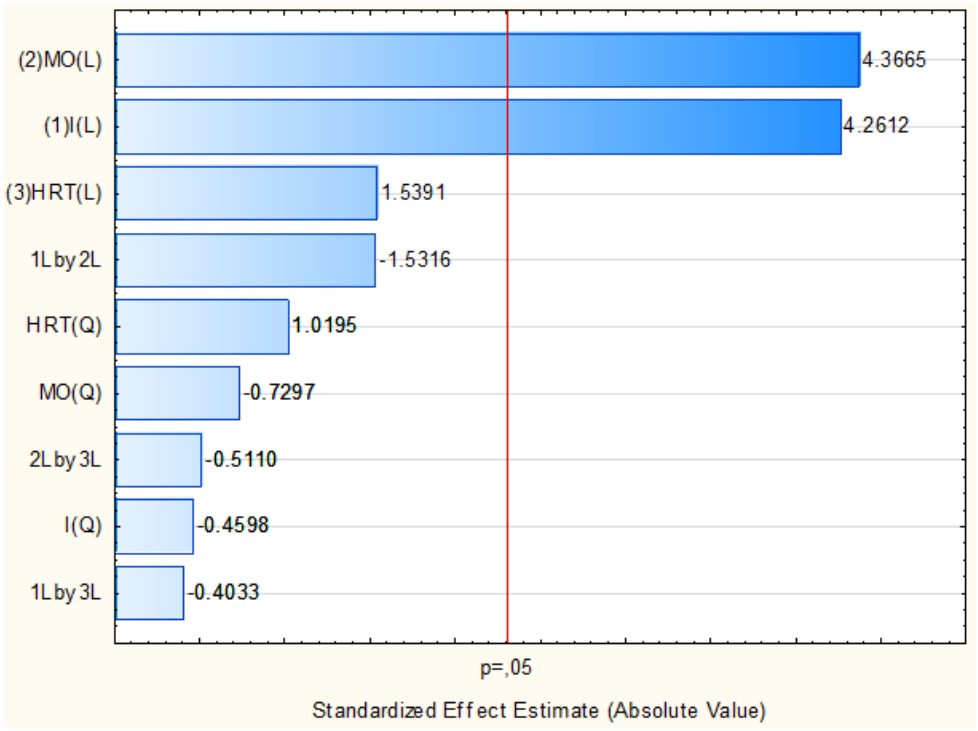

Figure 2. Pareto Diagram for color removal response.

Table 3 presents the regression coefficients of the model adjusted for color removal response.

Table 3. Regression coefficients for the model of color removal response.

	Effects	Coefficients	Standard Error	p-value
Mean		61.7628	5.8518	4.3E-07
I	30.5623	15.2812	3.6604	0.0016
I^2	-3.8291	-1.9145	3.8540	0.6291
MO	31.3174	15.6587	3.6604	0.0013
MO^2	-5.8427	-2.9213	3.8539	0.4644
I.MO	-14.3465	-7.1732	4.7805	0.1616

Table 4 presents the ANOVA for color removal response. At under a 5% significance level, the adjusted model is valid, with a determination coefficient of 77.85%.

Table 4. ANOVA for color removal response.

Source of Variation	Sum of Squares	Degrees of Freedom	Mean Squares	$F_{calculated}$	$F_{tabulated}$ $F_{0.05;5;11}$	p-value
Regression	7068.855	5	1413.771	7.733	3.204	0.0024
Residual	2011.049	11	182.823			
Total	9079.904	16				

R^2 = 77.85%.

Figure 3 presents the surface response for color removal, setting the HRT at -1.68 (encoded value), or 5 min (real value).

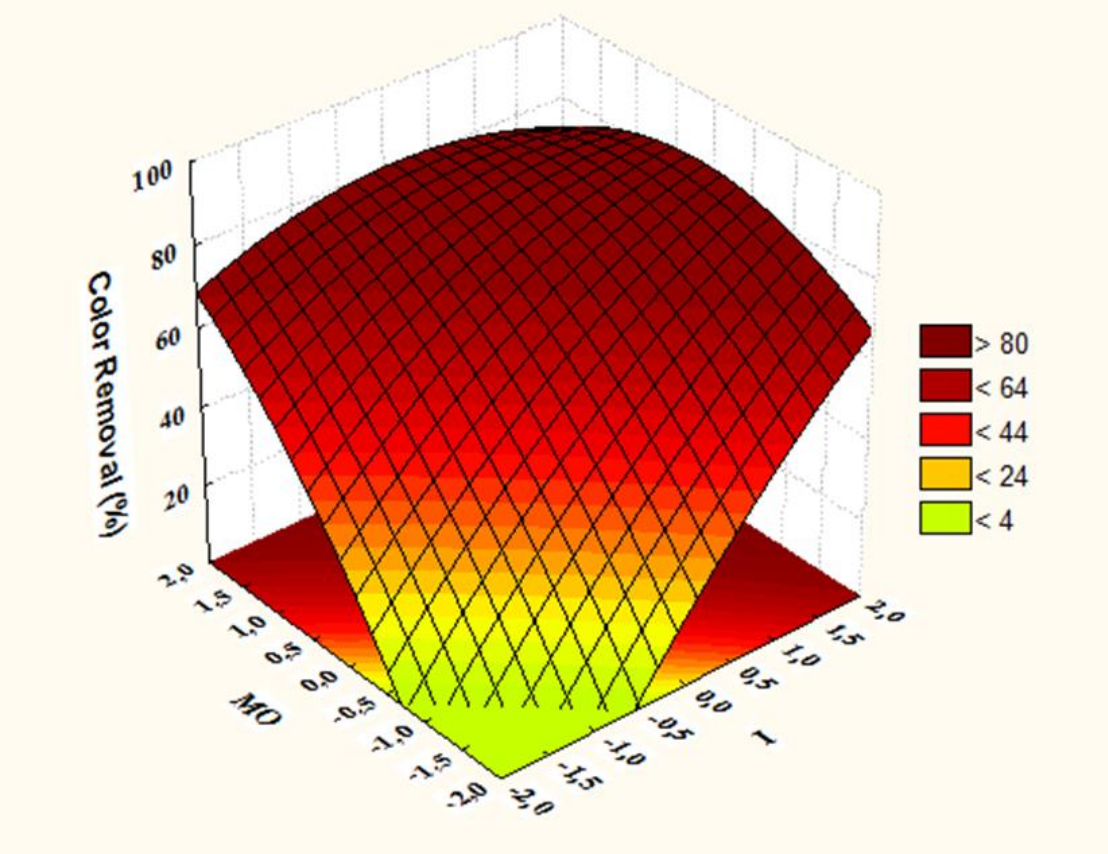

Figure 3. Surface response for color removal.

3.2. Empirical Modeling of concentration of residual iron

Based on the data presented in Table 2, the ANOVA for concentration of residual iron response was made. The results confirmed the statistical analysis performed for color removal response, where the model terms relating to HRT were not significant, under a 5% significance level. The effects of standardized terms can be observed in the Pareto Diagram (Figure 4).

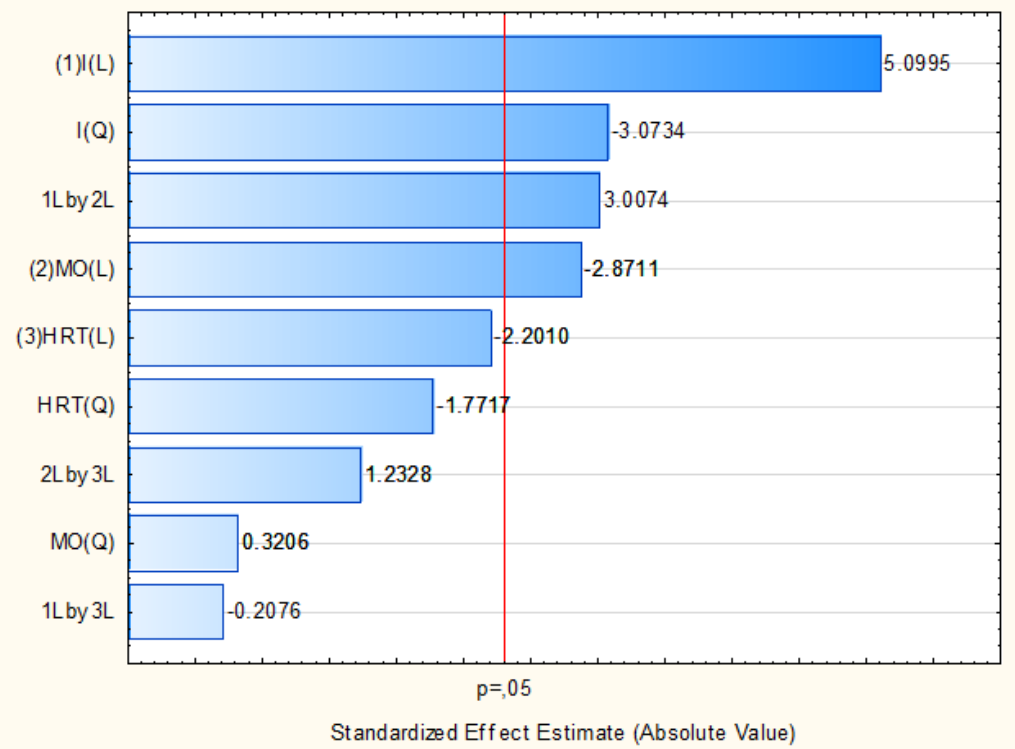

Figure 4. Pareto Diagram for concentration of residual iron response.

The terms relating to HRT were excluded from the model of concentration of residual iron, and their contributions were incorporated into residuals. The remaining terms were kept in the model. Table 5 shows the regression coefficients.

Table 5. Regression coefficients for concentration of residual iron response.

	Effects	Coefficients	Standard error	p - value
Mean		7.1129	0.4344	4.5E-09
I	2.2666	1.1333	0.2718	0.0016
I^2	-1.1239	-0.5619	0.2861	0.0753
MO	-1.2761	-0.6382	0.2718	0.0386
MO^2	0.4452	0.2227	0.2861	0.4530
I.MO	1.7457	0.8729	0.3549	0.0317

Table 6 presents the ANOVA for the concentration of residual iron response. It appears that for a 5% significance level, the adjusted model is valid, with a determination coefficient of 75.76%.

Figure 5 presents the surface response for concentration of residual iron, setting the HRT at -1.68 (encoded value), or 5 min (real value). According to the surface response, the lowest values for concentration of residual iron are achieved when a high dose of aqueous extract of Moringa Oleífera Lam is used and low values of electric current intensity are employed.

Table 6. ANOVA for concentration of residual iron response.

Source of Variation	Sum of Squares	Degrees of Freedom	Mean Squares	$F_{calculated}$	$F_{tabulated}$ $F_{0.05;5;11}$	p-value
Regression	34.655	5	6.931	6.878	3.204	0.0038
Residual	11.085	11	1.008			
Total	45.741	16				

R^2 = 75,76%.

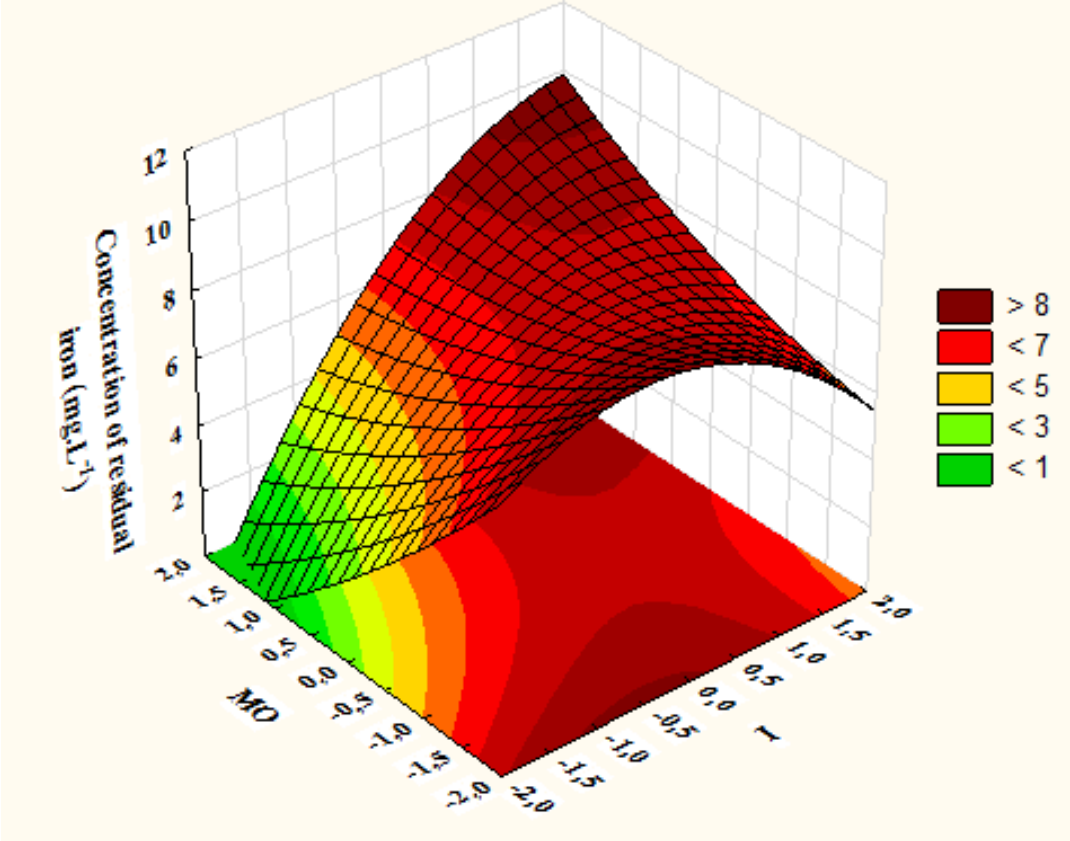

Figure 5. Surface response for concentration of residual iron.

3.3. Overall Optimization of hybrid treatment system and validation of empirical modeling

The optimal values of operating conditions for hybrid treatment system were found using the desirability function of Statistica™ software. This optimization tool searches for a unique solution, which satisfies both the maximization of color removal and the minimization of concentration of residual iron.

Figure 6 shows the optimum range of operating conditions obtained by the superposition of level curves for the responses evaluated in electrocoagulation tests in continuous flow. The best overall results were achieved with an electric current intensity of 0.28 A (encoded value of-1) and concentration of Moringa Oleífera Lam extract of 1000.00 mg L^{-1} (encoded value of +1,68). The HRT could be set at the minimum value (5 min), since it had no effect on the responses of the process.

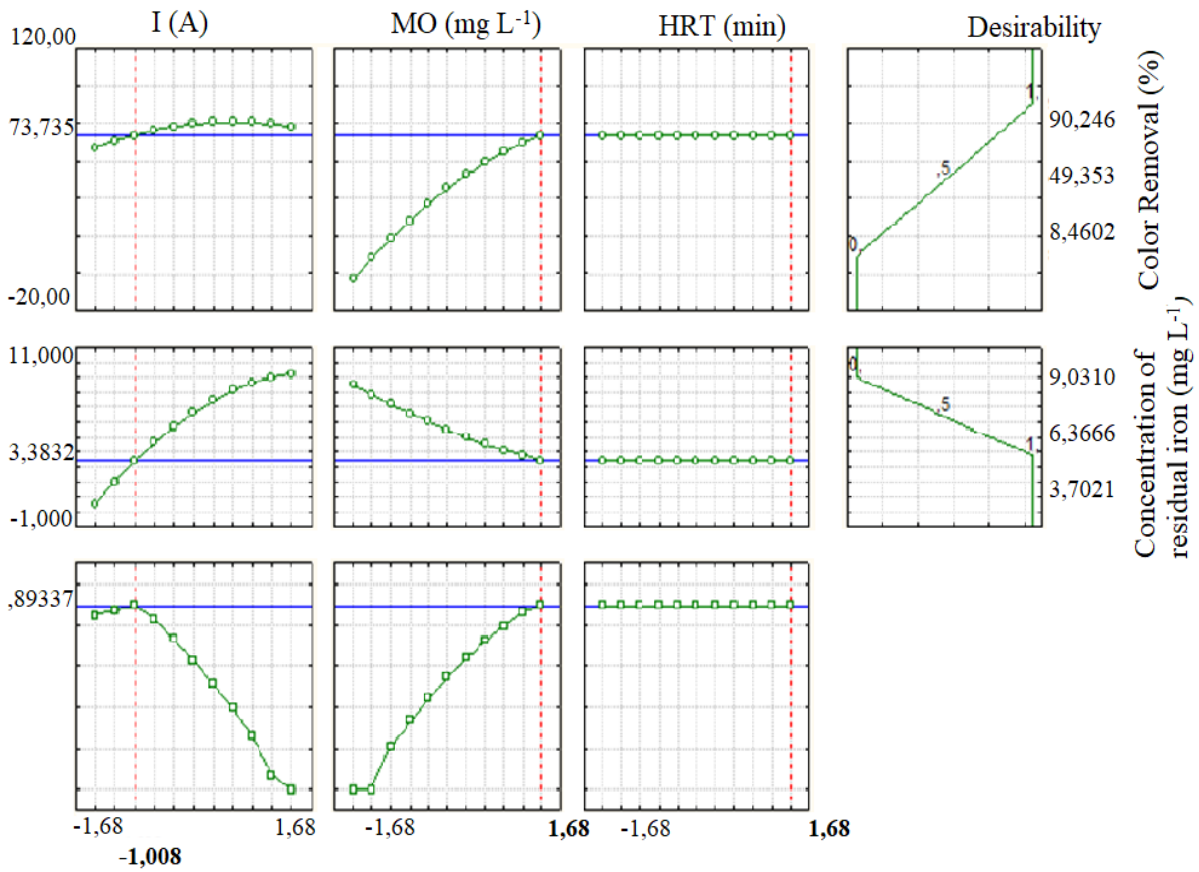

Figure 6. Overall optimization conditions for the hybrid treatment system.

After the optimal setting for the hybrid treatment system had been defined, the validation test was performed in triplicate. Table 7 presents the mean values of color removal and concentration of residual iron responses, in addition to the prediction errors of adjusted models.

Table 7. Validation test of models for color removal and concentration of residual iron.

Response	Predicted Value	Mean Value Observed	Mean Error
Color removal (%)	74.68	71.38± 1.44	4.62%
Concentration of residual iron (mg L^{-1})	3.5076	5.2237 ± 0.1069	32.85%

The results presented in Table 7 show that the model adjusted for color removal response can be used as a predictive model, because the presented mean error was less than 5%. However, the model for concentration of residual iron response presented high prediction error. The efficiency of hybrid treatment system was considered satisfactory, once it removed more than 70% of the color of Reactive Blue 5G dye solution, and the concentration of residual iron remained within allowable limits by Brazilian legislation (15 mg L^{-1}) (Conama, 2011).

Moreover, the association electrocoagulation with natural coagulant addition (Moringa Oleífera Lam extract) provided an interesting hybrid treatment system. Using both treatment technologies, it was possible to reduce the electric current intensity required, which is important for energy saving. Table 8 presents a summary of other study results for comparison.

Table 8. Treatment performance comparison.

Reference	Better results	Operating Conditions details
(Daneshvar *et al.*, 2006)	Almost 100% of color removal from dye mixture	6 a 8 mA cm^{-2}; Batch experiments; 5 min of electrolysis; 250 mL dye solution treated
(Song *et al.*, 2007)	Color removal of 94% and more than 60% of COD from Reactive Black 5 dye solution	10 mA cm^{-2} associated with 20 mL min^{-1} of ozone flow rate; Batch experiments with continuous ozone feed; 15 min of time reaction; 250 mL of dye solution treated (treatment efficiency evaluated after samples centrifugation)
(Yuksel *et al.*, 2011)	Color removal of 99.9% from Reactive Yellow RY 135 solution	4 mA cm^{-2}; Batch experiments; 1.5 L of dye solution treated; 10 min of electrolysis
(Merzouk *et al.*, 2010)	89.6% of turbidity removal from synthetic wastewater 85.5% of SS, 76.2% of turbidity, 88.9% of BOD, 79.7% of COD and 93% of color removal from real textile wastewater	11.55 mA cm^{-2}; Batch experiments; 10 min of electrolysis; 1 L of wastewater treated
(Mondal *et al.*, 2013)	99.7% of color removal and 94% of COD removal from an azo dye solution	19.51 mA cm^{-2}; Batch experiments; 102 min of electrolysis; 2 L of textile wastewater treated
(Valero *et al.*, 2008)	Color removal of 99.3% from Remazol Red RB 133 dye solution	10 mA cm^{-2}; Continuous electrochemical reactor; 250 mL of dye solution; 23 min of electrolysis
Current Paper	Better Results: Color removal of 90.25% and concentration of residual iron of 8.2 mg L^{-1}.	3.31 mA cm^{-2} associated with 550 mg L^{-1} of Moringa Oleífera Lam coagulant; continuous electrochemical reactor; 16 L of dye solution treated; 5 min of electrolysis
	Overall optimized conditions: Color removal of 71.38% and concentration of residual iron of 5.2 mg L^{-1}.	0.93 mA cm^{-2} associated with 1000 mg L^{-1} of Moringa Oleífera Lam coagulant. Continuous electrochemical reactor; 16 L of dye solution treated; 5 min of electrolysis.

Despite the different wastewaters tested, the current work used the least electric current and processed the largest volume of effluent.

4. CONCLUSIONS

The technique of electrocoagulation associated with the addition of Moringa Oleífera Lam extract applied in continuous flow presented excellent results for the removal of color, reaching a percentage of 90.25% for Reactive Blue 5G dye solutions. The concentration of residual iron was monitored for the effluent from the hybrid treatment system, and showed values from 3.702 to 9.031 mg L^{-1} (below the permissible limit by Brazilian legislation).

The overall optimization of the hybrid treatment system has been proceeding successfully. As a result of this analysis, electric current intensity of 0.28 A was achieved, at a concentration of Moringa Oleífera Lam extract of 1000.00 mg L^{-1} and a hydraulic retention time of 5 minutes. Tests using the optimal setting provided color mean removal of 71.38% and mean concentration of residual iron of 5.2237 mg L^{-1}.

The models adjusted for removal color and concentration of residual iron responses were validated statistically by ANOVA; however, only the model for color removal presented satisfactory results as a predictive model, because the prediction error evaluated was less than 5%, while the model for the concentration of residual iron response provided mean prediction error greater than 30%.

5. ACKNOWLEDGMENTS

This work was supported by the Fundação Araucaria, Fundação Parque Tecnológico Itaipú – Brasil and CNPq.

6. REFERENCES

ADJEROUD, N.; DAHMOUNE, F.; MERZOUK, B.; LECLERC, J.P.; MADANJ, K. Improvement of electrocoagulation–electroflotation treatment of effluent by addition of Opuntia ficusindica pad juice. **Separation and Purification Technology**, v. 144, p. 168-176, 2015. https://doi.org/10.1016/j.seppur.2015.02.018

AQUINO NETO, S.; MAGRI, T. C.; SILVA, G. M.; ANDRADE, A. R. Tratamento de Resíduos de Corante por Eletrofloculação: Um Experimento para Cursos de Graduação em Química. **Química Nova**, v. 34, p. 1468-1471, 2011. https://doi.org/10.1590/S0100-40422011000800030

ARANTES, C. C.; RIBEIRO, T. A. P.; PATERNIANI, J. E. S. Processamento de sementes de Moringa oleífera utilizando-se diferentes equipamentos para obtenção de solução coagulante. **Revista brasileira de Engenharia Agrícola e Ambiental**, v. 16, p. 661-666, 2012.

ASAITHAMBI, P.; SUSREE, M.; SARAVANATHAMIZHAN, R.; MATHESWARAN, M. Ozone assisted electrocoagulation for the treatment of distillery effluent. **Desalination**, v. 297, p. 1-7, 2012. https://doi.org/10.1016/j.desal.2012.04.011

BARRETO, M. B.; FREITAS, J. V. B.; SILVEIRA, E. R. Constituintes químicos voláteis e não voláteis de Moringa oleífera Lam, Moringaceae. **Revista Brasileira de Farmacognosia**, v. 19, p. 893-897, 2009.

BAZRAFSHAN, E.; MOSTAFAPOUR, F.K.; FARZADKJA, M.; OWNAGH, K.A.; MAHVI, A. H. Slaughterhouse wastewater treatment by combined chemical coagulation and electrocoagulation process. **Plos One**, v. 7, n. 6, p. e40108, 2012. https://doi.org/10.1371/journal.pone.0040108

CARVALHO, R. M.; PAIVA, J. F. de; GUEDES, C. D. Clarificação de águas pluviais ricas em óxidos de ferro acumuladas em cava de mineração através da utilização de um coagulante natural, a Moringa oleífera. **Revista Brasileira de Recursos Hídricos**, v. 11, p. 59-67, 2006.

CONAMA (Brasil). Resolução Nº 430 de 13 de maio de 2011. Dispõe sobre as condições e padrões de lançamento de efluentes, complementa e altera a Resolução no 357, de 17 de março de 2005, do Conselho Nacional do Meio Ambiente-CONAMA. **Diário Oficial [da] União**, n. 92, p. 89, 16 maio 2011.

DANESHVAR, N.; OLADEGARAGOZE, A.; DJAFARZADEH, N. Decolorization of basic dye solution by electrocoagulation: An investigation of the effect of operational parameters. **Journal of Hazardous Materials**, v. 129, p. 116-122, 2006. https://doi.org/10.1016/j.jhazmat.2005.08.033

LAMBRECHT, R.; BARROS, de M.A.S.D.; BORBA, C.E.; SILVA, E.A. Adsorption of the dye reactive blue 5G in retorted shale. **Brazilian Journal of Chemical Engineering**, v. 32, p. 269-281, 2015. http://dx.doi.org/10.1590/0104-6632.20150321s00001715

MERZOUK, B.; MADANI, K.; SEKKI, A. Using electrocoagulation-electroflotation technology to treat synthetic solution and textile wastewater, two case studies. **Desalination**, v. 250, p. 573-577, 2010. https://doi.org/10.1016/j.desal.2009.09.026

MONDAL, B.; SRIVASTAVA, V. C.; KUSHWAHA, J. P.; BHATNAGAR, R.; SINGH, S.; MALL, I. D. Parametric and multiple response optimization for the electrochemical treatment of textile printing dye-bath effluent. **Separation and Purification Technology**, v. 109, p. 135–143, 2013. https://doi.org/10.1016/j.seppur.2013.02.026

PAJOOTAN, E.; MOKHTAR, A.; NIYAZ, M. M. Binary system dye removal by electrocoagulation from synthetic and real colored wastewaters. **Journal of the Taiwan Institute of Chemical Engineers**, v. 43, n. 2, p. 282-290, 2012. https://doi.org/10.1016/j.jtice.2011.10.014

PATERNIANI, J. E. S.; MANTOVANI, M. C; SANT'ANNA, M. R. Uso de sementes de Moringa oleifera para tratamento de águas superficiais. **Revista Brasileira de Engenharia Agrícola e Ambiental**, v. 13, p. 765-771, 2009. https://dx.doi.org/10.1590/S1415-43662009000600015

RASCHITOR, A.; FERNANDEZ, C. M.; CRETESCU, I.; RODRIGO, M. A.; CAÑIZARES, P. Sono-electrocoagulation of wastewater polluted with Rhodamine 6G. **Separation and purification technology**, v. 135, p. 110-116, 2014. https://doi.org/10.1016/j.seppur.2014.08.003

SECULA, M. S.; CAGNON, B.; OLIVEIRA, T. F.; CHEDEVILLE, O.; FAUDUET, H. Removal of acid dye from aqueous solutions by electrocoagulation/GAC adsorption coupling: Kinetics and electrical operating costs. **Journal of the Taiwan Institute of Chemical Engineers**, v. 43, n. 5, p. 767-775, 2012. https://doi.org/10.1016/j.jtice.2012.03.003

SONG, S.; HE, S.; QIU, J.; XU, L.; CHEN, J. Ozone assisted electrocoagulation for decolorization of C.I. Reactive Black 5 in aqueous solution: An investigation of the effect of operational parameters. **Separation and Purification Technology**, v. 55, p. 238-245, 2007. https://doi.org/10.1016/j.seppur.2006.12.013

STRÖHER, A. P.; COUTO JUNIOR, O. M.; MENEZES, M. L.; BERGAMASCO, R.; PEREIRA, N. C. Aplicação de moringa oleífera lam no tratamento de efluente proveniente da lavagem de jeans. **Exacta**, v. 5, p. 61-66, 2012.

VALERO, D.; ORTIZ, J. M.; EXPÓSITO, E.; MONTIEL, V.; ALDAZ, A. Electrocoagulation of a synthetic textile effluent powered by photovoltaic energy without batteries: direct connection behavior. **Solar Energy Materials & Solar Cells**, v. 92, p. 291–297, 2008. https://doi.org/10.1016/j.solmat.2007.09.006

VIANNEY, M. J. M.; MUTHUKUMAR, K. Studies on Dye Decolorization by Ultrasound Assisted Electrocoagulation. **Clean–Soil, Air, Water**, v. 44, n. 3, p. 232-238, 2016. https://doi.org/10.1002/clen.201400011

YAVUZ, Y.; SHAHBAZI, R.; KOPARAL, A. S.; ÖĞÜTVEREN, Ü. B. Treatment of Basic Red 29 dye solution using iron-aluminum electrode pairs by electrocoagulation and electro-Fenton methods. **Environmental Science and Pollution Research**, v. 21, n. 14, p. 8603-8609, 2014. https://doi.org/10.1007/s11356-014-2789-8

YUKSEL, E.; GURBULAK, E.; EYVAZ, M. Decolorization of a Reactive Dye Solution and Treatment of a Textile Wastewater by Electrocoagulation and Chemical Coagulation: Techno-Economic Comparison. **Environmental Progress & Sustainable Energy**, v. 31, p. 524-535, 2011. https://doi.org/10.1002/ep.10574

Ambiente & Água - An Interdisciplinary Journal of Applied Science
ISSN 1980-993X – doi:10.4136/1980-993X
www.ambi-agua.net
E-mail: ambi.agua@gmail.com

Research on ecosystem services in Brazil: a systematic review

ARTICLES doi:10.4136/ambi-agua.2263

Received: 29 Mar. 2018; Accepted: 24 Mar. 2019

Lucilia Maria Parron[1*]; Elaine Cristina Cardoso Fidalgo[2]; Alessandra Polli Luz[3]; Monica Matoso Campanha[4]; Ana Paula Dias Turetta[2]; Bernadete Conceição Carvalho Gomes Pedreira[2]; Rachel Bardy Prado[2]

[1]Embrapa Florestas, Colombo, PR, Brasil
E-mail: lucilia.parron@embrapa.br
[2]Embrapa Solos, Rio de Janeiro, RJ, Brasil
E-mail: elaine.fidalgo@embrapa.br, ana.turetta@embrapa.br, bernadete.pedreira@embrapa.br, rachel.prado@embrapa.br
[3]Universidade Federal do Paraná (UFPR), Curitiba, PR, Brasil
Departamento de Engenharia Ambiental (DEA).
E-mail: alessandrapolliluz@gmail.com
[4]Embrapa Milho e Sorgo, Sete Lagoas, MG, Brasil
E-mail: monica.matoso@embrapa.br
[*]Corresponding author

ABSTRACT

Studies using the 'ecosystem services' (ES) approach developed in Brazil based on the framework of the Millennium Ecosystem Assessment (MEA), and range from quantitative and qualitative evaluation to the development of economic instruments for payment for ecosystem services (PES) or compensation for their maintenance, mainly for hydrological services. In order to summarize current knowledge regarding ES, the structure for teaching in ES, and also to provide a basis for future research in Brazil, we carried out a systematic review of publications on ES and a study on the availability of undergraduate and graduate courses related to ES. We found 282 publications for the 2006-2017 period, which included peer-reviewed articles, books, book chapters, theses, dissertations, articles in annals and technical publications. We identified current knowledge, knowledge gaps and trends in ES researches that may guide surveys and scenario analyses for future studies, in different biomes and regions of the country. Atlantic Forest and Amazon are the most-studied biome. Most of the studies were related to the evaluation of different types of ES and to the development of methodologies for their evaluation and monitoring. The most common ES are related to biodiversity, carbon sequestration and water.

Keywords: ecosystem services assessment, hydrological payment for ecosystem services, network analysis.

Pesquisa sobre serviços ecossistêmicos no Brasil: uma revisão sistemática

RESUMO

Estudos com a abordagem de serviços ecossistêmicos (ES) desenvolvidos no Brasil com base no quadro da Avaliação de Ecossistemas do Milênio (MEA) variam desde a avaliação

quantitativa e qualitativa até o desenvolvimento de instrumentos econômicos para pagamento por serviços ecossistêmicos (PES) ou compensação por sua manutenção, principalmente de serviços hidrológicos. Para sintetizar a atual produção de conhecimento e a estrutura de ensino em ES e também fornecer uma base para futuras pesquisas no Brasil, nós realizamos uma revisão sistemática de publicações sobre ES e uma pesquisa sobre a disponibilidade de cursos de graduação e pós-graduação relacionados aos ES. Nossa revisão sistemática encontrou 282 publicações para o período 2006-2017, que incluiu artigos revisados por pares, livros, capítulos de livros, teses, dissertações, artigos em anais e publicações técnicas. Identificamos o conhecimento atual, as interações entre instituições, lacunas de conhecimento e prioridades que deveriam ser consideradas em pesquisas futuras. O artigo fornece informações sobre estudos futuros e é um passo importante para considerar ES como uma abordagem para atingir os objetivos do desenvolvimento sustentável.

Palavras-chave: análises em rede, avaliação de serviços ecossistêmicos, pagamento por serviços ecossistêmicos hídricos.

1. INTRODUCTION

Ecosystem services (ES) can be defined as the benefits people obtain from ecosystems (MEA, 2005). The Millennium Ecosystem Assessment framework for ES identified that 15 of the 24 ES are declining at the global level, and can have a major negative impact on human well-being in the future.

Various classification systems for ES have been devised, such as those by De Groot *et al.* (2002), the Millennium Ecosystem Assessment (MEA, 2005) and The Economics of Ecosystem and Biodiversity (Kumar, 2010). The most common classification system divides ES into four categories: provisioning services, regulating services, habitat/supporting services and cultural services.

Since the Millennium Ecosystem Assessment, many research groups and papers have focused on ES (Martínez-Harms and Balvanera, 2012; Costanza *et al.*, 2016). An example is the IPBES (Intergovernmental Platform on Biodiversity and Ecosystem Services), a platform which assesses the state of biodiversity and the ES it provides to society, in response to requests from decision makers (http://ipbes.net/about-ipbes.html). Another example is the Ecosystem Service Partnership (ESP), which is a worldwide network of scientists, policy makers and practitioners who organize conferences and services to enhance the application of ES for nature conservation, ecosystem restoration and sustainable management (https://www.es-partnership.org/). In Brazil, the '*Rede de Serviços Ambientais'* (Ecosystem Services Network) is a research group acting in all biomes focused on research, development and public policy on ES (Prado *et al.*, 2015).

The integration produced by different research groups promote advancement of knowledge and stimulate new questions leading to a new cycle of investigations to answer them. The systematic review provides a broad overview of the literature, and from that point, are identified priorities and perspectives for the research. Besides, syntheses are increasingly demanded by scientific journals and funding agencies. Previous analyses of scientific research on ES focused on the global scale (Seppelt *et al.*, 2012), Latin America (Martínez-Harms and Balvanera, 2012), Africa (Egoh *et al.*, 2012), China (Jiang, 2017) and Australia (Plant and Ryan, 2013). However, there are no analyses of Brazilian literature on ES, although the Brazil is one of the most important producers of food, fiber and biofuel in the world and has great biodiversity and vital ecosystems services (Martinelli and Filoso, 2009). In order to combine and summarize Brazilian scientific studies of ES, the structure for teaching in ES and to provide a basis for future research in Brazil, we conducted a systematic review of publications on ES and the

availability of undergraduate and graduate courses related to ES. From the results obtained, we 1) characterized the published studies; 2) identified current knowledge and existing gaps; 3) identified the offer of disciplines in undergraduate and graduate courses in public universities; and 4) suggested priorities for future research.

2. METHODS

2.1. Systematic review of scientific production

This systematic review was based on published studies of Brazilian ES. To be included in the review, the publications should meet the criteria: a) to be in one of the electronic databases Capes, Scielo or Sabiia; b) to have the keywords 'ecosystem services' and 'environmental services' (in English and Portuguese) in their titles; c) have been published between the period 2006-2017; d) to be published in peer-reviewed journals, books, book chapters, theses, dissertations, articles in proceedings and technical publications. The Sabiia is a Brazilian database that gathers information about agriculture and related areas in peer-reviewed journals, book chapters, thesis and proceedings. The chosen period reveals the progress in previous experiences and reflects the most recent studies on the subject. From the initial research (533 publications), those that did not meet the criterion of the research described above and duplicated in more than one database were excluded. The remaining publications (n = 282) were analyzed by their abstracts and text and categorized within the ES to which they referred. We classified the results according to the following metadata: publication year; publication form (e.g. journal, book chapter); research focus (assessment, monitoring, mapping, modeling, methodological development, analysis and opinion, review and economic valuation); classification (provision, regulation, support/habitat and cultural); ES type; biome;approach to payment for ecosystem services (PES) programs; development of technologies and affiliation of authors. More than one ES type, classification and biome per publication was allowed. We used frequency and percentage of publications to show trends and relationships between the data. According to the method, publications which address ES in Brazil but do not have the key words in their titles were not included in the results of our compilation.

The publications were also considered to establish a network analysis between institutions. For this approach, the analysis considered the institution of the publication's authorship obtained by the systematic review. The aim was to identify the predominant players: institutions with the highest numbers of publications on the theme and their interactions. An undirected graph of the network (network analytic software Gephi 0.9.2) was developed considering the institution of the first author and its interaction with others and vice versa. The institutions that presented only one or two interactions were removed to facilitate visualization.

2.2. Survey of higher education institutions

First, the scope of the research was defined to identify undergraduate and graduate (lato-sensu and stricto-sensu) institutions working on the themes of ES and ecologic economy. The survey covered the Brazilian public education institutions, as the organized information was only available on the website of the Brazilian Ministry of Education, which provides data on these institutions.

The identification of the institutions was carried out using the online search system of the e-Mec website (http://emec.mec.gov.br/). The selected options for search were: a) active higher education institutions; b) all Brazilian states; and c) public federal, state or municipal administration. The result was an automatically generated spreadsheet containing the name and address of each institution meeting the conditions. A total of 317 institutions were identified.

The information obtained was used for a new search, this time on the websites of each institution to identify science areas related to ES. The selected areas were: Geography, Ecology, Biology, Environmental Engineering, Environmental Management, Forestry Engineering,

Agricultural Engineering, Civil Engineering and Agronomy. A search was then carried out to identify the undergraduate and graduate courses, their disciplines and the modules of these disciplines with the keywords: environmental services, ecosystem services, environmental economy and environmental value. Some complementary terms were considered, such as ecological economy, water resource economy, natural resource economy, forest economy, value of natural resources, economic value of the environment, and value of the environment. We collected information on the names of the module or discipline, their workload and the period of the course in which it was offered, the name of the course, its level and contact information.

Then, a form for the complementation of the missing data or the correction of the data on the site was sent by email to the contact of the courses and disciplines with the selected keywords in their programs. The email was sent on September 9, 2016 to 96 contacts and 33 responses were received. On April 13, 2017, the email was sent again to the contacts that had not responded to the previous one. The total forms answered reached 39. The geographical coordinates of the addresses of the institutions were used to display them on a map using ArcGIS10 from ESRI (http://www.esri.com/arcgis/about-arcgis).

3. RESULTS AND DISCUSSION

3.1. The publication trends

Two hundred and eighty-two publications were included in the database for the current study. The number of studies using the ES approach ranged from three in 2006 to fifty-nine in 2015 (Figure 1).

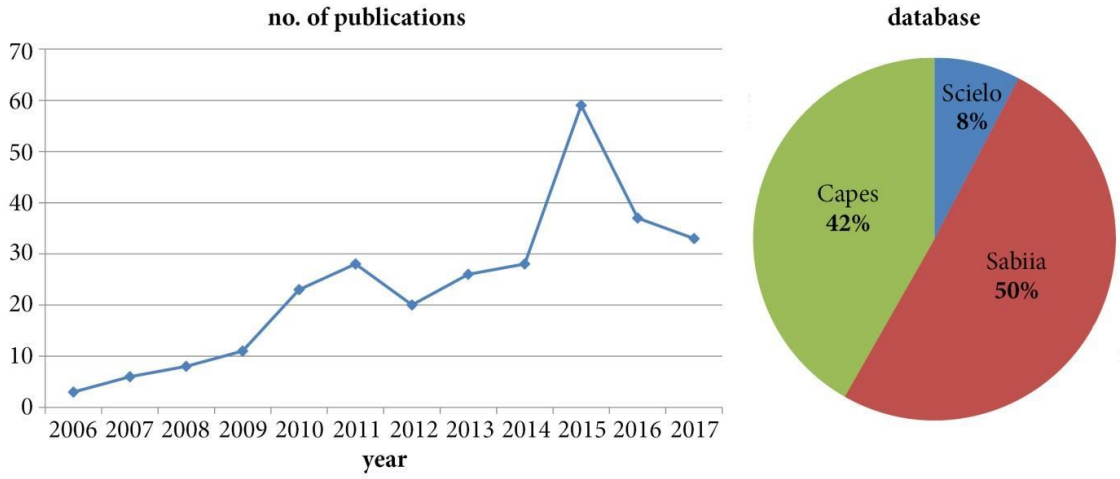

Figure 1. Number of publications according to year and biome.

The database covers six biomes. Most of the studies (37%) do not focus on a specific biome. The most frequent biomes are the Atlantic Forest (31%) and the Amazon (18%) (Figure 1). As a form of publication, peer-reviewed articles represent 54%, followed by book chapters (21%) and articles in proceedings (14%). The research focus is on analysis and opinion (19%), assessment (17%), economic valuation (16%), review (14%), methodological development (12%), modeling (11%), mapping (9%) and monitoring (2%) (Figure 2).

Regarding the classification of the Millennium Ecosystem Assessment our review found that most of the studies encompass all the ES or approach them in a general way (34%). The most frequent ES is regulation (30%), followed by provisioning (20%), supporting (14%), and cultural (2%) (Figure 3).

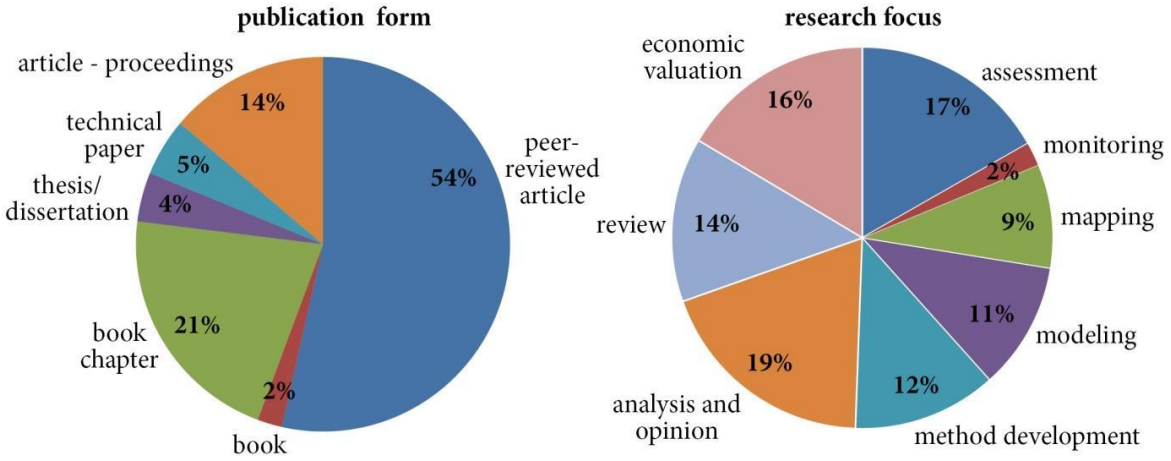

Figure 2. Percentage of publications by form and research focus.

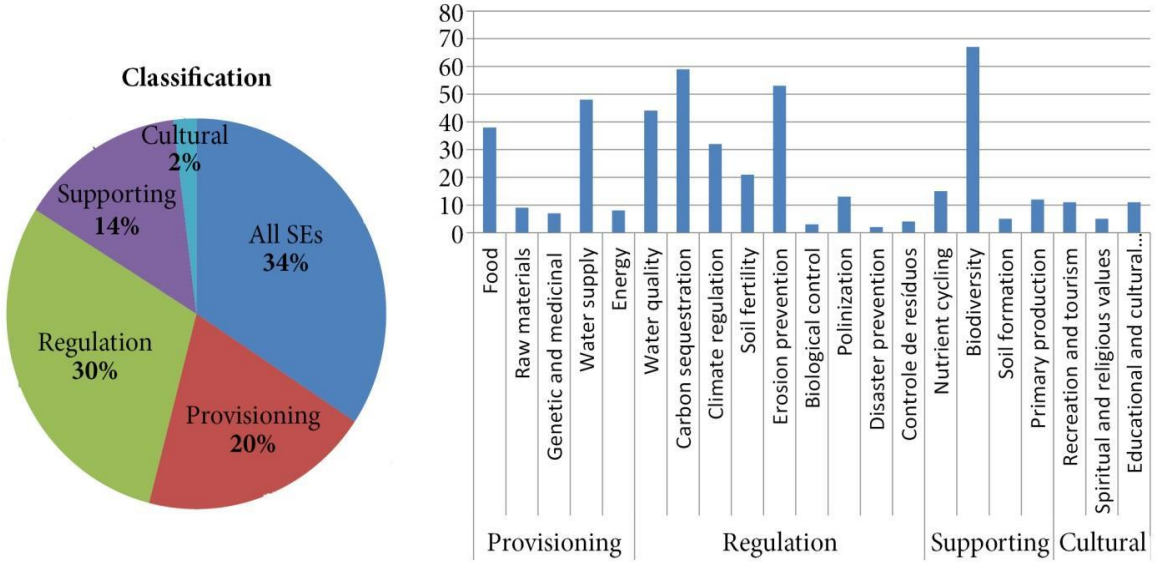

Figure 3. Percentage of publications and number of ecosystem services according to Millennium Ecosystem Assessment classification.

Among the ES, the most common are biodiversity (11.1%), carbon sequestration (9.8%), prevention and control of erosion (8.8%), water supply (8.0%), water quality (7.3%) and food (6.3%) (Figure 3). Few publications (n = 40) address a single service, 108 publications address 2 to 9 ES, while 134 publications address more than 10 ES or approach ES in a general way. Studies reporting PES mechanisms represent 44% of the publications. The ES approach with technological development represents only 9% of the publications. In the network analysis of the relationships among institutions, it is possible to identify four main clusters based on the degree of interaction, differentiated by colors (Figure 4).

The size of the nodes indicates the connections among institutions, i.e., the larger the number of connections, the larger the node size. It is also possible to observe a higher number of interactions among Brazilian institutions and foreign institutions. At the same time, the clusters show a tendency of interactions among institutions from the same geographic region. It is also possible to observe that most of the institutions are from the South and Southeast regions of Brazil, demonstrating that the knowledge and the scientific relationships are concentrated in these regions. 'Abroad' refers to publications whose first authors are from institutions outside Brazil.

The next section summarizes what we identified as the major ES studied to develop a current overview to drive future studies and research.

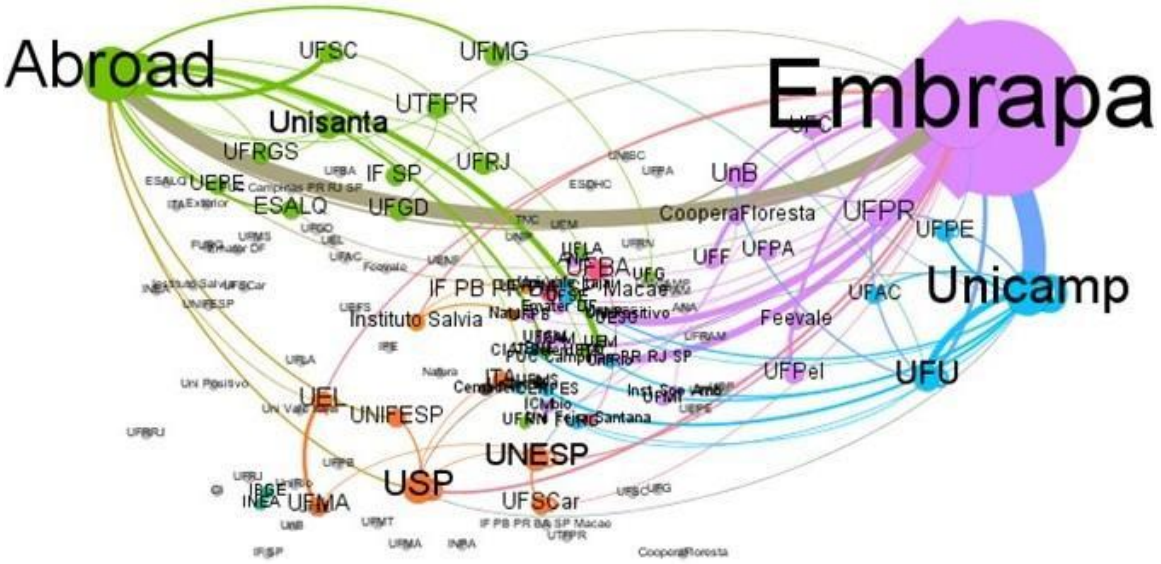

Figure 4. Network analysis of the relationships among publications.

3.2. Provisioning services

3.2.1. Food

Studies involving multiple ES generally include food production, which emphasizes the role of Brazil as an important producer of food, fiber and biofuels while holding mega biodiversity. Studies maintain that ES exist in productive systems only when natural ecosystems are able to keep them functioning, especially when they contain the source of genes that can help agricultural varieties become adapted to new climate conditions. To do so, it is essential to reduce the degradation of ES and promote the sustainable use of land and energy (Farley *et al.*, 2015; Martinelli and Filoso, 2009). Other studies also incorporate the concept of provision services for land use and management and show positive impacts on ecosystems and human well-being (Barrett *et al.*, 2013; Rosa and Sanchez, 2016). The approach from the economic point of view shows that the underpriced agricultural commodities lead to high environmental costs in the form of ES losses, largely borne by tropical countries, i.e., tropical nations subsidize the consumption of importing nations (Chang *et al.*, 2016). The ability of Brazilian farmers to generate ES in land uses will be enhanced by public policies, which increase their capacity to respond promptly to changes in production technology and market opportunities (technical assistance with new products and production technologies, agricultural credit, and quick access to information on relative prices) (Börner *et al.*, 2007).

3.2.2. Water supply

Land use, land-cover change scenarios, and hydrological models show problems related to water storage, food production and ES regulation, such as sediment control, water purification and retention (Koschke *et al.*, 2014; Lima *et al.*, 2014; Saad *et al.*, 2016). The studies show the impacts of ecosystem degradation on water resources and propose forest restoration to protect them and increase aquifer recharge, groundwater flows and river discharge equilibrium (Watanabe and Ortega, 2011; Young and Bakker, 2014). Proposals such as Payments for Ecosystem Services (PES) and Reducing Emissions from Deforestation and Forest Degradation (REDD), focus on compensation for local communities in exchange for the preservation of natural forests and their ES (Klemick, 2011).

3.2.3. Timber and non-timber resources

Studies that associate ES and raw materials, such as timber and non-timber resources, are scarce, and the few available use the economic valuation approach (Maciel *et al.*, 2010; Fasiaben *et al.*, 2015). Most of them are related to native forests and one study addresses trees in integrated production systems.

3.3. Regulating services

3.3.1. Carbon sequestration

The most common approach to carbon sequestration and carbon stocks is the mapping of multiple ES (Grimaldi *et al.*, 2014; Koschke, 2015; LeClec'h *et al.*, 2016), which includes an overview of several ES. More sophisticated models estimate the carbon flows or changes in carbon stocks as a result of changes in land use and land management (Watanabe and Ortega, 2014; 2011). Several studies also address the economic valuation of carbon (Mann *et al.*, 2012; Song *et al.*, 2014).

3.3.2. Regulation of water quality

Studies that associate regulating ES with water quality involve the maintenance and restoration of vegetation cover (Brancalion *et al.*, 2014) and the valuation and charge for water use, from economic-ecologic modeling (Andrade *et al.*, 2015; Garcia and Romeiro, 2015) and payment schemes for ecosystem services (PES) for water-resource protection (Young and Bakker, 2014; Zanella *et al.*, 2014). Studies involving multiple ES generally include regulation of water quality, water supply and erosion prevention and control, which emphasize the development of a spatial approach for the effects of land use/land cover on the capacity to provide or maintain ES (Lima *et al.*, 2017; Periotto and Tundisi, 2013).

3.3.3. Erosion prevention and control

Studies are focused on the quantification of several regulation ES as a land-use function (Ditt *et al.*, 2010; Ferraz *et al.*, 2014; Grimaldi *et al.*, 2014; LeClec'h *et al.*, 2016; Mathé and Rey-Valette, 2015). They also involve estimates of soil loss (Tôsto and Pereira, 2015), sediment input into water resources (Chaves, 2010) and the definition of conservation areas (Duarte *et al.*, 2016).

3.3.4. Maintenance of soil fertility

Studies are generally associated with ES of erosion prevention and control and encompass estimated soil nutrient loss using the Universal Soil Loss Equation model (USLE) (Tôsto and Pereira, 2015). Soil fertility is also used as an indicator to assess forest degradation (Celentano *et al.*, 2017). Few studies associate ES and production systems (Grimaldi *et al.*, 2014; Ditt *et al.*, 2010).

3.3.5. Pollination

Rrocesses that support pollination and their importance for human well-being and for agricultural productivity are well documented (Imperatriz-Fonseca and Nunes-Silva, 2010). The association with land use (Ferraz *et al.*, 2014), richness of pollinators (LeClec'h *et al.*, 2016), habitat connectivity (Giannini *et al.*, 2015) and crop production (Mangabeira *et al.*, 2015) are the most common approaches.

3.4. Supporting services

3.4.1. Biodiversity maintenance

The association between ecosystem functions and biodiversity is often used to assess and identify the consequences of human activities on the environment. Several ecosystem functions

are provided by soil fauna biodiversity (Marichal *et al.*, 2014; Nichols *et al.*, 2008). There are several studies that apply modeling and mapping to estimate the suitability of species habitat and the influence of the agricultural expansion in the maintenance of these habitats in order to analyze the distribution of species and its association with soil characteristics, climatic variables, topography and land use and cover (Brockerhoff *et al.*, 2013; Kennedy *et al.*, 2016; Leadley *et al.*, 2014).

3.4.2. Primary production (carbon)

Primary production refers to the production of organic matter and increase in the vegetal biomass. Studies that evaluate primary production quantify ES as a function of land use (LeClec'h *et al.*, 2016).

3.5. Cultural services

Cultural Services are services related to the aesthetic, spiritual, educational and recreational benefits offered by ecosystems. The research found few studies that evaluated people's perception of ES and the relationship they have with their environment (Mathé and Rey-Valette, 2015; Oliveira and Berkes, 2014) and with ecological restoration projects (Brancalion *et al.*, 2014). The studies apply qualitative (Pereira and Campos, 2009; Ribeiro and Ribeiro, 2016; Souza Filho *et al.*, 2014) and quantitative evaluations (Mariano *et al.*, 2015; Rares and Brandimarte, 2014) and economic valuation of ES (Mathé and Rey-Valette, 2015), to point out that aesthetic values and opportunities for recreation and tourism are the most commonly perceived ES.

3.6. Payment for ecosystem services programs (PES)

Based on the framework of the Millennium Ecosystem Assessment (2005), the first studies in ES in Brazil carried out with the payments for nature services approach addressed the relationship between people and their environment, and water, carbon and biodiversity conservation. These studies evaluated environmental policies and programs (legal reserve, Proambiente, *Bolsa* Floresta, mechanized patrols) used as a mechanism to encourage conservation practices and these studies proposed models to predict the effects of policy changes on land use (e.g. Börner *et al.*, 2007; Hall, 2008; Pereira, 2010). In addition, the studies focused on the assessment of how rural producers could receive payment for ES provided to the society to compensate for economic losses caused by the maintenance of ES (Begossi *et al.*, 2011; Lima *et al.*, 2014). Recently, studies have focused on the evaluation of adopted and successful PES mechanisms, which compensate landowners who agree to conserve natural forest areas associated with watershed protection (Lima *et al.*, 2017). These studies combine payment schemes with the opportunity cost of land (Alarcon *et al.*, 2016; 2017), indexes of quality and quantity of conservation and the relationships between the minimum amount of money that farmers would demand to get involved in PES programs for forest conservation and restoration (Young and Bakker, 2014; Zanella *et al.*, 2014). The impacts of such programs on economic (regarding opportunity costs) and non-economic factors (such as trust and participation in scheme design) play a crucial role in determining decisions by land users on whether to participate in PES schemes in a sustained way (Zanella *et al.*, 2014). The most successful programs are the hydrological. The project *Conservador das Águas* was created, with the support of ANA (Brazilian National Water Agency), stimulating PES. The project assists farmers that adopt soil conservation practices, apply rural sewage systems, and restore riparian zones, steep slopes and hilltops lands (Rosa *et al.*, 2014; 2016; Gjorup *et al.*, 2016). Watershed models like the AgES simulate stream flow at the outlet of the basin, and can be used for evaluating the particular hydrological responses (Cruz *et al.*, 2017). Articles also analyze the limitations of the approach which reconciles conservation and development,

using insights from transaction costs economics and PES, providing alternatives and novel theoretical approaches to the conceptualization and analysis of these programs (Muradian 2013; Gómez-Baggethun and Muradian, 2015; Muradian and Gómez-Baggethun, 2013).

3.7. Economic valuation

The valuation of ES uses economic-ecological modeling as a tool to understand the ecological dynamics involved in it and the incorporation of the values of ES that would otherwise not be considered, such as water regulation services (Andrade and Romeiro, 2013). Several studies use valuation as an estimate of the economic dimension of natural resources to guide a decision-making process involving the use of natural capital 'assets', along with financial instruments and institutional arrangements (Andrade *et al.*, 2015, 2012; Fasiaben *et al.*, 2015; Klemick, 2011; Tôsto and Pereira, 2015). Estimates generated from different sets of data, models and techniques allow for the comparison of ES values against the income obtained by agricultural commodities (Mann *et al.*, 2012). Other studies develop scenarios and simulation analyses based on geoprocessing, land use, climate and soil property models (e.g. InVest, MIMES). The models are generally comprised of biophysical and environmental assessment components, which convert input data into ES and economic benefits (Andrade *et al.*, 2015; Garcia and Romeiro, 2015; Saad *et al.*, 2016; Song *et al.*, 2014).

3.8. Technological development in ecosystem services

Here we present an approach on issues related to the use of technologies applied to ES. Technological processes, development and application of models with the potential for use in other ES studies were considered technologies (e.g. Britto *et al.*, 2012; Cruz *et al.*, 2017; Duarte *et al.*, 2016; Koschke *et al.*, 2014; Lima *et al.*, 2017). We found that most of the processes that could be considered technological were studies that applied some modeling tool associated with economic valuation. The systematic review pointed out that ES research in Brazil is more associated with the evaluation of natural resources and the analysis of their indicators and that there is a gap of technological packages for ES. This result shows that the research in ES in Brazil is still linked to scientific production, without advances in the direction of innovation and technological process.

3.9. Ecosystem services in brazilian education institutions

In the survey, 51 public institutions were identified. Altogether they have offered 93 disciplines which included in their program content the themes of environmental/ ecosystem services or economy/environmental value. The location of the institutions is shown in Figure 5.

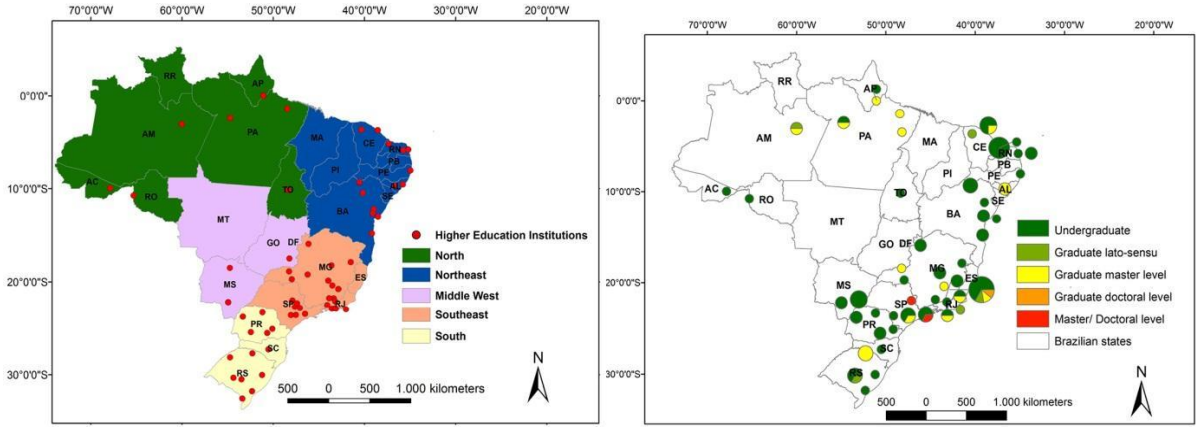

Figure 5. a) Brazilian higher education institutions that work on themes of ecosystem services and ecological economy; b) geographical distribution of the disciplines and the course level.

The distribution of the institutions in the regions of Brazil was: seventeen in the Southeast, fourteen in the Northeast, nine in the South, eight in the North, and three in the Middle West. The number of disciplines offered in each region followed the same sequence: the Southeast with 34, the Northeast with 27, the South with 15, the North with 10 and the Middle West with 7.

The data collected in the form filled-out by the institutions allowed us to verify the periodicity of the disciplines: ten annual, fifteen semiannual and nine with undetermined periodicity out of a total of 34 responses to this item. The average workload of the disciplines was 55.82 hours, the maximum was 80 hours and the minimum was 30 hours for a total of 29 responses.

The Federal University of Viçosa (UFV) showed nine disciplines related to the themes, which were taught in six undergraduate and three graduate courses. It was the institution with the largest number of disciplines, followed by the Federal Rural Semiarid University (UFERSA) with six disciplines offered at undergraduate level. Most of the undergraduate courses with disciplines in the selected themes were Environmental Management (14 subjects), Environmental Engineering (13), Biological Sciences (12) and Forest Engineering (11).

The results indicated that the great majority of the disciplines in environmental services or ecology economy were offered at the undergraduate level. Minas Gerais state had the greatest number of disciplines, and it was the only one with disciplines in the selected themes for all levels. It was also observed that only the states of Minas Gerais and São Paulo had disciplines at the doctoral level (Figure 5).

4. CONCLUSIONS

The study of ES has grown quickly in the last two decades, and Brazil followed this evolution with an increase in the number of publications and expansion of disciplines in undergraduate and graduate courses. Although Brazil is a large and environmentally diversified country, our results showed that this theme in educational institutions is still concentrated in the Southeastern region, which means that the research activity follows some socioeconomic characteristics. The Brazilian SE is the most populated region and most economically developed. Additionally, the Atlantic Forest, which appeared as the most-studied biome, is mainly located in this region. However, despite these characteristics, there are still several environmental problems that threat the biodiversity and natural resources in this area. The Amazon is the second most-studied biome and is the largest forested area in Brazil. It is also the most famous Brazilian biome, which attracts world interest for the richness of its biodiversity. That can be an advantage regarding research partnerships and financial resources to study this biome; but, on the other hand, some studies may support groups with specific interests. Most of the studies were related to the evaluation of different types of ES and to the development of methodologies for their evaluation and monitoring. The most common ES are related to biodiversity, carbon sequestration and water. This was expected due to the major problems related to ES such as the loss of biodiversity and the jeopardizing of its functions in ecosystems; the global concern about climate change and the efforts to mitigate its effects; and, lastly, the growing concern about the frequent water-related problems in various parts of the world. Although the other types of ES were less frequent, it is important to highlight the broad scope of the themes, showing the studies are not limited to the great themes. Most of the studies (33%) are analyses, opinion and revision, which is an indication that the SE theme is in full debate by the scientific community, probably because it is recent, and therefore reviews and analyses of work in this area must be consolidated so that consensus may be reached. Although these biomes are greatly important for the ES studies, the proportion of studies in Cerrado and Caatinga are much lower than the relative area they occupy in Brazil, indicating an imbalance.

There was also a small contribution to cultural services. Studies involving economic approaches tend to increase, since the PES tool, mainly hydrological PES, has become a support for public policies. The results presented here point to some gaps and trends in ES research that may guide surveys and scenario analyses for future studies in different biomes and regions of the country.

5. FUNDING

This research was supported by the Embrapa project 'Environmental services in the Brazilian rural landscape: construction and sharing of knowledge' (grant number 05.14.11.001.00.00).

6. REFERENCES

ALARCON, G. G.; FREITAS, L. A. S.; FOUNTOURA, G. O.; MACEDO, C. X.; RIBEIRO, D. C. The challenges of implementing a legal framework for Payment for Ecosystem Services in Santa Catarina, Brazil. **Natureza & Conservação**, v. 14, p. 132–136, 2016. https://dx.doi.org/10.1016/j.ncon.2016.05.003

ALARCON, G. G.; FANTINI, A. C.; SALVADOR, C. H.; FARLEY, J. Additionality is in detail: Farmers' choices regarding payment for ecosystem services programs in the Atlantic forest, Brazil. **Journal of Rural Studies**, v. 54, p. 177–186, 2017. https://dx.doi.org/10.1016/j.jrurstud.2017.06.008

ANDRADE, D. C.; ROMEIRO, A. R.; FASIABEN, M. C. R.; GARCIA, J. R. Dinâmica do uso do solo e valoração de serviços ecossistêmicos: notas de orientação para políticas ambientais. **Desenvolvimento e Meio Ambiente**, v. 25, p. 53–71, 2012. http://dx.doi.org/10.5380/dma.v25i0.26056

ANDRADE, D. C.; ROMEIRO, A. R. Valoração de serviços ecossistêmicos: por que e como avançar? **Sustentabilidade em Debate,** v. 4, p. 43–58, 2013.

ANDRADE, D. C.; TÔSTO, S. G.; SOBRINHO, R. P.; ROMEIRO, A. R. Avaliação do serviço ecossistêmico de regulação de água – aplicação do modelo Multi-scale Integrated Models of Ecosystem Services (Mimes) 1. *In:* TÔSTO, S. G.; BELARMINO, L. C.; ROMEIRO, A. R.; RODRIGUES, C. A. G. (Eds.). **Valoração de serviços ecossistêmicos**: metodologias e estudo de casos. Brasília, DF: Embrapa Territorial, 2015. p. 155–169.

BARRETT, K.; VALENTIM, J.; TURNER II, B. L. Ecosystem services from converted land: the importance of tree cover in Amazonian pastures. **Urban Ecosystem**, v. 16, p. 573–591, 2013. https://dx.doi.org/10.1007/s11252-012-0280-1

BEGOSSI, A.; MAY, P. H.; LOPES, P. F.; OLIVEIRA, L. E. C.; VINHA, V.; SILVANO, R. A. M. Compensation for environmental services from artisanal fisheries in SE Brazil: Policy and technical strategies. **Ecological Economics**, v. 71, p.25–32, 2011. https://dx.doi.org/10.1016/j.ecolecon.2011.09.008

BÖRNER, J.; MENDOZA, A.; VOSTI, S. A. Ecosystem services, agriculture, and rural poverty in the Eastern Brazilian Amazon: Interrelationships and policy prescriptions. **Ecological Economics**, v. 64, p. 356–373, 2007. https://dx.doi.org/10.1016/j.ecolecon.2007.03.001

BRANCALION, P. H. S.; CARDOZO, I. V.; CAMATTA, A.; ARONSON, J.; RODRIGUES, R. R. Cultural ecosystem services and popular perceptions of the benefits of an ecological restoration project in the Brazilian Atlantic Forest. **Restoration Ecology**, v. 22, p.65–71, 2014. https://dx.doi.org/10.1111/rec.12025

BRITTO, G. C.; KATO, O. R.; HERRERA, J. A. A prestação de serviços ambientais pode ser uma alternativa aos sistemas tradicionais da agricultura familiar no município de Pacajá, Amazônia Paraense – Brasil? **Sustentabilidade em Debate**, v. 3, p. 159–176, 2012.

BROCKERHOFF, E. G.; JACTEL, H.; PARROTTA, J. A.; FERRAZ, S. F. B. Management role of eucalypt and other planted forests in biodiversity conservation and the provision of biodiversity-related ecosystem services. **Forest Ecology and Management,** v. 301, p.43–50, 2013. https://doi.org/10.1016/j.foreco.2012.09.018

CELENTANO, D.; ROUSSEAU, G. X.; ENGEL, V. L.; ZELARAYÁN, M.; OLIVEIRA, E. C.; ARAUJO, A. C. M.; MOURA, E. G. Degradation of riparian forest affects soil properties and ecosystem services provision in eastern Amazon of Brazil. **Land Degradation & Development**, v. 493, p.482–493, 2017. https://dx.doi.org/10.1002/ldr.2547

CHANG, J.; SYMES, W. S.; LIM, F.; CARRASCO, L. R. International trade causes large net economic losses in tropical countries via the destruction of ecosystem services. **Ambio**, v. 45, p.387–397, 2016. https://dx.doi.org/10.1007/s13280-016-0768-7

CHAVES, H. M. L. Relações de aporte de sedimento e implicações de sua utilização no pagamento por serviço ambiental em bacias hidrográficas. **Revista Brasileira de Ciência do Solo**, v. 34, p.1469–1477, 2010. https://dx.doi.org/10.1590/S0100-06832010000400043

COSTANZA, R.; HOWARTH, R. B.; KUBISZEWSKI, I.; LIU, S.; MA, C.; PLUMECOCQ, G.; STERN, D. I. Influential publications in ecological economics revisited. **Ecological Economics**, v. 123, p.68–76, 2016. https://dx.doi.org/10.1016/j.ecolecon.2016.01.007

CRUZ, P. P. N.; GREEN, T. R.; FIGUEIREDO, R. O.; PEREIRA, A. S.; KIPKA, H.; SAAD, S. I.; SILVA, J. M.; GOMES, M. A. F. Hydrological modeling of the Ribeirão das Posses – An assessment based on the Agricultural Ecosystem Services (AgES) watershed model. **Revista Ambiente & Água**, v. 12, p. 351–364, 2017. https://dx.doi.org/10.4136/1980-993X

DE GROOT, R. S.; WILSON, M. A.; BOUMANS, R. MJ. A typology for the classification, description and valuation of ecosystem functions, goods and services. Ecological economics, v. 41, p. 393-408, 2002. https://doi.org/10.1016/S0921-8009(02)00089-7

DITT, E. H.; MOURATO, S.; GHAZOUL, J.; KNIGHT, J. Forest conversion and provision of ecosystem services in the Brazilian Atlantic Forest. **Land Degradation & Development**, v. 603, p. 591–603, 2010. https://doi.org/10.1002/ldr.1010

DUARTE, G. T.; RIBEIRO, M. C.; PAGLIA, A. P. Ecosystem services modeling as a tool for defining priority areas for conservation. **Plos One**, v. 11, p. 1–19, 2016. https://dx.doi.org/10.1371/journal.pone.0154573

EGOH, B. N.; O'FARRELL, P. J.; CHAREF, A.; JOSEPHINE GURNEY, L.; KOELLNER, T.; NIBAM ABI, H.; EGOH, M.; WILLEMEN, L. An African account of ecosystem service provision: use, threats and policy options for sustainable livelihoods. **Ecosystem Services**, v. 2, p. 71–81, 2012. https://dx.doi.org/10.1016/j.ecoser.2012.09.004

FARLEY, J.; SCHMITT, A.; BURKE, M.; FARR, M. Extending market allocation to ecosystem services: moral and practical implications on a full and unequal planet. **Ecological Economics**, v. 117, p. 244–252, 2015. https://dx.doi.org/10.1016/j.ecolecon.2014.06.021

FASIABEN, M. C. R.; ROMEIRO, A. R.; PERES, F. C.; MAIA, A. G. Impacto econômico da reserva legal sobre diferentes tipos de unidades de produção agropecuária. *In:* TÔSTO, S. G.; BELARMINO, L. C.; ROMEIRO, A. R.; RODRIGUES, C. A. G. (Eds.). **Valoração de serviços ecossistêmicos**: metodologias e estudo de casos. Brasília, DF: Embrapa Territorial, 2015. p. 279–313.

FERRAZ, S. F. B.; FERRAZ, K. M. P. M. B.; CASSIANO, C. C.; BRANCALION, P. H. S.; LUZ, D. T. A.; AZEVEDO, T. N.;TAMBOSI, L. R.; METZGER, J. P. How good are tropical forest patches for ecosystem services provisioning? **Landscape Ecology**, v. 29, p. 187–200, 2014. https://dx.doi.org/10.1007/s10980-014-9988-z

GARCIA, J. R.; ROMEIRO, A. R. Valoração e Cobrança pelo Uso da água: uma abordagem econômico-ecológica. *In:* TÔSTO, S. G.; BELARMINO, L. C.; ROMEIRO, A. R.; RODRIGUES, C. A. G. (Eds.). **Valoração de serviços ecossistêmicos**: metodologias e estudo de casos. Brasília, DF: Embrapa Territorial, 2015. p. 73–93.

GIANNINI, T. C.; TAMBOSI, L. R.; ACOSTA, A. L.; JAFFÉ, R. Safeguarding ecosystem services: a methodological framework to buffer the joint effect of habitat configuration and climate change. **Plos One**, v. 19, p. 1–19, 2015. https://dx.doi.org/10.1371/journal.pone.0129225

GJORUP, A. F.; FIDALGO, E. C. C.; PRADO, R. B.; SCHULER, A. E. Análise de procedimentos para seleção de áreas prioritárias em programas de pagamento por serviços ambientais hídricos. **Revista Ambiente & Água**, v. 11, p. 225–238, 2016. https://dx.doi.org/10.4136/ambi-agua.1782

GÓMEZ-BAGGETHUN, E.; MURADIAN, R. In markets we trust? Setting the boundaries of market-based Instruments in ecosystem services governance. **Ecological Economics**, v. 117, p. 217–224, 2015. https://dx.doi.org/10.1016/j.ecolecon.2015.03.016

GRIMALDI, M.; OSZWALD, J.; DOLÉDEC, S.; HURTADO, M.; MIRANDA, I.; SARTRE, X. A.; ASSIS, W. S.; CASTAÑEDA, E.; DESJARDINS, T.; DUBS, F.; GUEVARA, E.; GOND, V.; LIMA, T. T. S.; MARICHAL, R.; FERNANDO, M.; MITJA, D.; NORONHA, N.C.; OLIVEIRA, M.N.D.; RAMIREZ, B.; RODRIGUEZ, G.; SARRAZIN, M.; JUNIOR, M. L. S.; COSTA, L. G. S.; SOUZA, S. L.; VEIGA, I.; VELASQUEZ, E.; LAVELLE, P. Ecosystem services of regulation and support in Amazonian pioneer fronts : searching for landscape drivers. **Landscape Ecology**, v. 29, p. 311–328, 2014. https://dx.doi.org/10.1007/s10980-013-9981-y

HALL, A. Better RED than dead: paying the people for environmental services in Amazonia. **Philosophical Transactions of the Royal Society B: Biological Sciences**, v. 363, p. 1925–1932, 2008. https://dx.doi.org/10.1098/rstb.2007.0034

IMPERATRIZ-FONSECA, V. L.; NUNES-SILVA, P. As abelhas, os serviços ecossistêmicos e o Código Florestal Brasileiro. **Biota Neotropica**, v. 10, p. 59-62, 2010. https://dx.doi.org/10.1590/S1676-06032010000400008

JIANG, W. Ecosystem services research in China: A critical review. **Ecosystem services**, v. 26, p.10–16, 2017. https://dx.doi.org/10.1016/j.ecoser.2017.05.012

KENNEDY, C. M.; HAWTHORNE, P. L.; MITEVA, D. A.; BAUMGARTEN, L.; SOCHI, K.; MATSUMOTO, M.; EVANS, J. S.; POLASKY, S.; HAMEL, P.; VIEIRA, E. M.; FERREIRA, P.; SEKERCIOGLU, C. H.; DAVIDSON, A. D.; UHLHORN, E. M.; KIESECKER, J. Optimizing land use decision-making to sustain Brazilian agricultural profits, biodiversity and ecosystem services. **Biological Conservation**, v. 204, p. 221–230, 2016. https://dx.doi.org/10.1016/j.biocon.2016.10.039

KLEMICK, H. Shifting cultivation, forest fallow, and externalities in ecosystem services: Evidence from the Eastern Amazon. **Journal of Environmental Economics and Management**, v. 61, p. 95–106, 2011. https://dx.doi.org/10.1016/j.jeem.2010.07.003

KOSCHKE, L.; LORZ, C.; FÜRST, C.; LEHMANN, T.; MAKESCHIN, F. Assessing hydrological and provisioning ecosystem services in a case study in Western Central Brazil. **Ecological Process**, v. 3, p. 2-15, 2014. https://doi.org/10.1186/2192-1709-3-2

KOSCHKE, L. **The multi-criteria assessment of ecosystem services at a landscape level to support decision-making in regional and landscape planning**. 2015. 45p. Dissertation (Doctor) - Technische Universitat Dresden, Tharandt, 2015.

KUMAR, P. (Ed.). **TEEB The economics of ecosystems and biodiversity ecological and economic foundations**. London; Washington: Earthscan, 2010.

LEADLEY, P.; PROENÇA, V.; FERNÁNDEZ-MANJARRÉS, J.; PEREIRA, H.M.; ALKEMADE, R.; BIGGS, R.; BRULEY, E.; CHEUNG, W.; COOPER, D.; FIGUEIREDO, J.; GILMAN, E.; GUÉNETTE, S.; HURTT, G.; MBOW, C.; OBERDORFF, T.; REVENGA, C.; SCHARLEMANN, J. P. W.; SCHOLES, R.; SMITH, M. S.; SUMAILA, U. R.; WALPOLE, M. Interacting regional-scale regime shifts for biodiversity and ecosystem services. **BioScience**, v. 64, p. 665–679, 2014. https://dx.doi.org/10.1093/biosci/biu093

LECLEC'H, S.; OSZWALD, J.; DECAENS, T.; DESJARDINS, T.; DUFOUR, S.; GRIMALDI, M.; JEGOU, N.; LAVELLE, P. Mapping multiple ecosystem services indicator: Toward an objective-oriented approach. **Ecological Indicators**, v. 69, p. 508–521, 2016. https://dx.doi.org/10.1016/j.ecolind.2016.05.021

LIMA, J. E. F. W.; AQUINO, F.G.; CHAVES, T.A.; LORZ, C. Development of a spatially explicit approach for mapping ecosystem services in the Brazilian Savanna – MapES. **Ecological Indicators**, v. 82, p. 513–525, 2017. https://dx.doi.org/10.1016/j.ecolind.2017.07.028

LIMA, L. S.; COE, M. T.; SOARES FILHO, B. S.; CUADRA, S. V.; DIAS, L. C. P.; COSTA, M. H.; LIMA, L. S.; RODRIGUES, H. O. Feedbacks between deforestation, climate, and hydrology in the Southwestern Amazon: Implications for the provision of ecosystem services. **Landscape Ecology**, v. 29, p. 261–274, 2014. https://dx.doi.org/10.1007/s10980-013-9962-1

MACIEL, R. C. G.; REYDON, B. P.; COSTA, J. A.; SALES, G. O. Pagando pelos serviços ambientais: uma proposta para a Reserva Extrativista Chico Mendes. **Acta Amazonica**, v. 40, p. 489–498, 2010.

MANGABEIRA, J. A. C.; TÔSTO, S. G.; ROMEIRO, A. R.; GREGO, C. R. Análise espacial aplicada à valoração de serviços ecossistêmicos da agricultura: exemplo do café em Machadinho d'Oeste, RO. *In:* TÔSTO, S. G.; BELARMINO, L. C.; ROMEIRO, A. R.; RODRIGUES, C. A. G. (Eds.). **Valoração de serviços ecossistêmicos**: metodologias e estudo de casos. Brasília, DF: Embrapa Territorial, 2015. p. 55–71.

MANN, M. L.; KAUFMANN, R. K.; MARIE, D.; GOPAL, S.; BALDWIN, J. G.; DEL, M. Ecosystem service value and agricultural conversion in the Amazon: implications for policy intervention. **Environmental & Resource Economics**, v. 53, p.279–295, 2012. https://dx.doi.org/10.1007/s10640-012-9562-6

MARIANO, M. V.; AGOSTINHO, C. M. V. B. DE A.; BONILLA, S. H.; AGOSTINHO, F.; GIANNETTI, B. F. Avaliação em emergia como ferramenta de gestão nos parques urbanos de São Paulo. **Gestão & Produção**, v. 22, p. 443–458, 2015. https://dx.doi.org/10.1590/0104-530X712-13

MARICHAL, R.; GRIMALDI, M.; M, A.F.; OSZWALD, J.; PRAXEDES, C.; HERNAN, D.; COBO, R.; HURTADO, P.; DESJARDINS, T.; LOPES, M.; GONZAGA, L.; SOUZA, I.; NASCIMENTO, M.; OLIVEIRA, D.; BROWN, G.G.; TSÉLOUIKO, S.; BONIFACIO, M.; DECAËNS, T.; VELASQUEZ, E.; LAVELLE, P. Soil macroinvertebrate communities and ecosystem services in deforested landscapes of Amazonia. **Applied Soil Ecology**, v. 83, p. 177–185, 2014. https://dx.doi.org/10.1016/j.apsoil.2014.05.006

MARTINELLI, L. A.; FILOSO, S. Balance between food production, biodiversity and ecosystem services in Brazil: a challenge and an opportunity. **Biota Neotropica**, v. 9, p. 21–25, 2009. https://dx.doi.org/10.1590/S1676-06032009000400001

MARTÍNEZ-HARMS, M. J.; BALVANERA, P. Methods for mapping ecosystem service supply: a review. **International Journal of Biodiversidy Science, Ecosystem, Services & Management**, v. 8, p. 17–25, 2012. https://dx.doi.org/10.1080/21513732.2012.663792

MATHÉ, S.; REY-VALETTE, H. Local knowledge of pond fish-farming ecosystem services: management implications of stakeholders' perceptions in three different contexts (Brazil, France and Indonesia). **Sustainability**, v. 7, p. 7644–7666, 2015. https://dx.doi.org/10.3390/su7067644

MILLENNIUM ECOSYSTEM ASSESSMENT. **Ecosystems and human well-being**: synthesis. Washington, DC: Island Press: 2005.

MURADIAN, R. Payments for ecosystem services as incentives for collective action. **Society & Natural Resources**, v. 26, p.1155–1170, 2013. https://dx.doi.org/10.1080/08941920.2013.820816

MURADIAN, R.; GÓMEZ-BAGGETHUN, E. The institutional dimension of "market-based instruments" for governing ecosystem services: introduction to the special issue. **Society & Natural Resources**, v. 26, p. 1113–1121, 2013. https://dx.doi.org/10.1080/08941920.2013.829380

NICHOLS, E.; SPECTOR, S.; LOUZADA, J.; LARSEN, T.; AMEZQUITA, S.; FAVILA, M.E. Ecological functions and ecosystem services provided by Scarabaeinae dung beetles. **Biological Conservation**, v. 141, p. 1461-1474, 2008. https://dx.doi.org/10.1016/j.biocon.2008.04.011

OLIVEIRA, L. E. C.; BERKES, F. What value São Pedro's procession? Ecosystem services from local people's perceptions. **Ecological Economics**, v. 107, p. 114–121, 2014. https://dx.doi.org/10.1016/j.ecolecon.2014.08.008

PEREIRA, S. N. C. Payment for environmental services in the amazon forest: how can conservation and development be reconciled? **Journal of Environmental Development**, v. 19, p. 171–190, 2010. https://dx.doi.org/10.1177/1070496510368047

PEREIRA, M. A.; CAMPOS, W. G. de. Pagamento por serviços ambientais aliando conservação e ecoturismo. **Revista Brasileira do Ecoturismo**, v. 2, p. 255–272, 2009.

PERIOTTO, N. A; TUNDISI, J. G. Ecosystem services of UHE Carlos Botelho (Lobo/Broa): a new approach for management and planning of dams multiple-uses. **Brazilian Journal of Biology**, v. 73, p. 471–482, 2013. https://dx.doi.org/10.1590/S1519-69842013000300003

PLANT, R.; RYAN, P. Ecosystem services as a practicable concept for natural resource management: some lessons from Australia. **The International Journal of Biodiversity Science, Ecosystems Services & Management**, v. 9, p. 44–53, 2013. https://dx.doi.org/10.1080/21513732.2012.737372

PRADO, R. B.; FIDALGO, E. C. C.; FERREIRA, J. N.; CAMPANHA, M. M.; PARRON, L. M. V.; MATTOS, L. M.; PEDREIRA, B. C. C. G.; MONTEIRO, J. M. G; TURETTA, A. P. D.; MARTINS, A. L. S.; DONAGEMMA, G. K.; COUTINHO, H. L. C. Pesquisas em serviços ecossistêmicos e ambientais na paisagem rural do Brasil. **Revista Brasileira de Geografia Física**, v. 8, p. 610-622, 2015.

RARES, C. DE S.; BRANDIMARTE, A. L. O desafio da conservação de ambientes aquáticos e manutenção de serviços ambientais em áreas verdes urbanas: o caso do Parque Estadual da Cantareira. **Ambiente & Sociedade**, v. 17, p. 111–128, 2014.

RIBEIRO, F. P.; RIBEIRO, K. T. Participative mapping of cultural ecosystem services in Pedra Branca State Park, Brazil. **Natureza & Conservação**, v. 14, p. 120–127, 2016. https://doi.org/10.1016/j.ncon.2016.09.004

ROSA, F. S.; TONELLO, K. C.; VALENTE, R. O. A.; LOURENCO, R. W. Estrutura da paisagem, relevo e hidrografia de uma microbacia como suporte a um programa de pagamento por serviços ambientais relacionados à água. **Revista Ambiente & Água**, v. 9, p. 526-539, 2014. https://dx.doi.org/10.4136/ambi-agua.1326

ROSA, F. S.; TONELLO, K. C.; VALENTE, R. O. A.; LOURENCO, R. W. Selection of priority areas for payment of environmental services: an analysis at the watershed level. **Revista Ambiente & Água**, v. 11, p. 448-461, 2016. https://dx.doi.org/10.4136/ambi-agua.1809

ROSA, J. C. S.; SANCHEZ, L. E. Advances and challenges of incorporating ecosystem services into impact assessment. **Journal of Environmental Management**, v. 180, p. 485–492, 2016. https://dx.doi.org/10.1016/j.jenvman.2016.05.079

SAAD, S. I.; ROCHA, H. R.; SILVA, J. M. The impact of roads and sediment basins on simulated river discharge and sediment flux in an experimental catchment designed to improve ecosystem services. **Hydrology and Earth System Sciences Discussions**, p. 1-50, 2016. https://dx.doi.org/10.5194/hess-2015-490

SEPPELT, R.; FATH, B.; BURKHARD, B.; FISHER, J. L.; GRÊT-REGAMEY, A.; LAUTENBACH, S.; PERT, P.; HOTES, S.; SPANGENBERG, J.; VERBURG, P. H.; VAN OUDENHOVEN, A. P. E. Form follows function? Proposing a blueprint for ecosystem service assessments based on reviews and case studies. **Ecological Indicators**, v. 21, p. 145–154, 2012. https://dx.doi.org/10.1016/j.ecolind.2011.09.003

SONG, X. P.; HUANG, C.; TOWNSHEND, J. R. An integrated framework for evaluating the effects of deforestation on ecosystem services. **IOP Conference Series: Earth and Environmental Science**, v. 17, p. 1–6, 2014. https://dx.doi.org/10.1088/1755-1315/17/1/012061

SOUZA FILHO, J. R.; SANTOS, R. C.; SILVA, I. R.; ELLIFF, C. I. Evaluation of recreational quality, carrying capacity and ecosystem services supplied by sandy beaches of the municipality of Camaçari, northern coast of Bahia, Brazil. **Journal of Coastal Research**, v. 70, p. 527–532, 2014. https://dx.doi.org/10.2112/SI70-089.1

TÔSTO, S. G.; PEREIRA, L. C. A valoração ambiental da erosão do solo na cana-de-açúcar em São Paulo. *In:* TÔSTO, S. G.; BELARMINO, L. C.; ROMEIRO, A. R.; RODRIGUES, C. A. G. (Eds.). **Valoração de serviços ecossistêmicos**: metodologias e estudo de casos. Brasília, DF: Embrapa Territorial, 2015. p. 343–355.

WATANABE, M. D. B.; ORTEGA, E. Ecosystem services and biogeochemical cycles on a global scale: valuation of water, carbon and nitrogen processes. **Environmental Sciences & Policy**, v. 14, p. 594–604, 2011. https://dx.doi.org/10.1016/j.envsci.2011.05.013

WATANABE, M. D. B.; ORTEGA, E. Dynamic emergy accounting of water and carbon ecosystem services: A model to simulate the impacts of land-use change. **Ecological Modelling**, v. 271, p. 113–131, 2014. https://dx.doi.org/10.1016/j.ecolmodel.2013.03.006

YOUNG, C. E. F.; BAKKER, L. B. Payments for ecosystem services from watershed protection: a methodological assessment of the Oasis Project in Brazil. **Natureza & Conservação**, v. 12, p.71–78, 2014. https://dx.doi.org/10.4322/natcon.2014.013

ZANELLA, M. A.; SCHLEYER, C.; SPEELMAN, S. Why do farmers join Payments for Ecosystem Services (PES) schemes? An Assessment of PES water scheme participation in Brazil. **Ecological Economics**, v. 105, p.166–176, 2014.

Ambiente & Água - An Interdisciplinary Journal of Applied Science
ISSN 1980-993X – doi:10.4136/1980-993X
www.ambi-agua.net
E-mail: ambi.agua@gmail.com

Self-assembly modification of polyamide membrane by coating titanium dioxide nanoparticles for water treatment applications

ARTICLES doi:10.4136/ambi-agua.2297

Received: 09 Jul. 2018; Accepted: 19 Feb. 2019

Rosangela Bergamasco[1]; Priscila Ferri Coldebella[2]; Franciele Pereira Camacho[1]; Driano Rezende[1]; Natalia Ueda Yamaguchi[3*]; Márcia Regina Fagundes Klen[4]; Carlos José Macedo Tavares[5]; Maria Teresa Sousa Pessoa Amorim[6];

[1]Universidade Estadual de Maringá (UEM), Maringá, PR, Brasil
Departamento de Engenharia Química (DEQ). E-mail: ro.bergamasco@hotmail.com, franciele_camacho@hotmail.com, drirezend@gmail.com
[2]Centro Universitário Dinâmica das Cataratas (UDC), Foz do Iguaçu, PR, Brasil
Colegiado de Farmácia. E-mail: pricoldebella@gmail.com
[3]Centro Universitário de Maringá (Unicesumar/ICETI), Maringá, PR, Brasil
Departamento de Tecnologias Limpas. E-mail: nataliaueda@hotmail.com
[4]Universidade Estadual do Oeste do Paraná (UNIOESTE), Cascável, PR, Brasil
Centro de Engenharia e Ciências Exatas (CECE). E-mail: fagundes.klen@gmail.com
[5]Universidade do Minho (UMinho), Guimarães, Portugal
Departamento de Física (DF). E-mail: ctavares@fisica.uminho.pt
[6]Universidade do Minho (UMinho), Guimarães, Portugal
Departamento de Engenharia Têxtil (DET). E-mail: mtamorim@det.uminho.pt
[*]Corresponding author

ABSTRACT

This study modified the surface of a commercial polyamide membrane with the deposition of TiO_2 nanoparticles by the self-assembly method under pressure with high permeability and photocatalytic activity. Changes in membrane characteristics and its performance for photocatalytic properties were evaluated. The results indicated that both membrane hydrophilicity and photocatalytic performance were significantly improved by the presence of TiO_2 nanoparticles applied under a pressure of 1 bar. The deposition of the TiO_2 particles under pressure was able to maintain the particles on the surface of the membranes and their photocatalytic capacity for three cycles of use. The prepared TiO_2 photocatalytic membrane presented a great potential for wastewater treatment and for reuse wastewater systems due its ability to remove methylene blue (MB) dye solution by photocatalytic decomposition and physical separation.

Keywords: membrane filtration, methylene blue, organic photodegradation, photocatalysis, titanium dioxide.

Modificação self-assembly de membrana de poliamida pela deposição de nanopartículas de dióxido titânio para aplicações no tratamento de água

RESUMO

O principal objetivo do presente estudo foi modificar a superfície de uma membrana de poliamida comercial com a deposição de nanopartículas de TiO_2 pelo método self-assembly

sob pressão com alta permeabilidade e atividade fotocatalítica. Mudanças nas características da membrana e seu desempenho nas propriedades fotocatalíticas foram avaliados. Os resultados experimentais indicaram que tanto a hidrofilia da membrana quanto o desempenho fotocatalítico foram significativamente melhorados pela presença de nanopartículas de TiO_2 aplicadas sob uma pressão de 1 bar. A deposição das partículas de TiO_2 sob pressão foi capaz de manter as partículas na superfície das membranas e sua capacidade fotocatalítica por três ciclos de uso. A membrana fotocatalítica de TiO_2 preparada apresentou um grande potencial no tratamento de efluentes e sistemas de reuso devido à sua capacidade de remover o corante azul de metileno por decomposição fotocatalítica e separação física.

Palavras-chave: azul de metileno, dióxido de titânio, filtração por membrana, fotocatálise, fotodegradação orgânica.

1. INTRODUCTION

In recent years, titanium dioxide (TiO_2) has become an important semiconductor used in various industrialized products, including sunscreens, inks, ointments, toothpastes, and catalysts. Due to its photocatalytic properties in comparison to other semiconductor composites such as SiO_2, ZnO, Fe_2O_3, CuS, Al_2O_3, ZrO_2, TiO_2 has several advantages over their use in photocatalytic reactions, such as low cost due to its availability in nature, low toxicity, high chemical- and thermal stability and resistance to photocorrosion (Pan *et al.*, 2013).

Given these characteristics, since the 1970's, when it was proved that water could be decomposed into hydrogen and oxygen in the presence of ultraviolet light on a TiO_2 electrode in aqueous solution (Fujishima *et al.*, 1975), TiO_2 has received great attention for presenting photocatalytic properties for the decomposition of organic/inorganic materials. Thus the advanced oxidative processes (AOPs) through heterogeneous catalysis have been presented as an attractive processes for water and wastewater treatments.

However, the efficiency of TiO_2 as a photocatalyst depends on several factors, such as the type of contaminant, the initial concentration of the organic contaminant, the amount and duration of radiant light on the TiO_2 surface (Leong *et al.*, 2014). In addition, heterogeneous photocatalysis is favored by the increase of the specific area of the semiconductors, therefore its effects are more positive when they are synthesized in nanometric dimensions.

TiO_2 works as a catalyst; once organic matter has been degraded, TiO_2 can be reused for a further catalysis process (LEONG *et al.*, 2014). When TiO_2 is used in suspension, it is very difficult to separate it from the treated water, hindering its practical application (Leong *et al.*, 2014).

One of the most promising processes lies in the development of photocatalytic membranes, which are the combination of photocatalytic oxidation and membrane filtration. The advantage of this process is that two phenomena occur in a single treatment unit: the physical separation of the contaminant together with TiO_2 adhered to the membrane, as well as the organic photodegradation (Fischer *et al.*, 2015).

Once the pollutants are retained on the surface of the membrane, TiO_2 under UV radiation can degrade the pollutants, preventing the formation of a layer of cake on the surface of the membrane, thus reducing pore blockage, and drastically reducing the concentration of pollutants, consequently improving the quality of the permeate (Leong *et al.*, 2014).

You *et al.* (2012) and Shao *et al.* (2017) evaluated membranes modified with TiO_2 nanoparticles and verified that TiO_2 composite membranes showed better hydrophilicity, antifouling property and long-term flow stability.

This study proposes the deposition of TiO_2 nanoparticles on the surface of a polyamide commercial membrane using the self-assembly method under pressure to enable enhanced

photocatalytic properties under UV light. This study examines TiO_2-polyamide membrane properties by various characterization techniques, its permeability in water and photocatalytic activity for MB dye solution.

2. MATERIALS AND METHODS

2.1. Membrane modification

The characteristics of the commercial polyamide membrane of nanofiltration (Model TS-80, flat sheet nanofiltration membrane, 47 mm size, TriSep^{TM}, Sterlitech, Kent, WA, USA) used in this study were supplied by the manufacturer and are presented in Table 1.

Table 1. Commercial membrane characteristics.

Maximum Operating Pressure	41 bar
Maximum Operating Temperature	45°C 1.0 – 12.0
Cleaning pH Range	< 0.1 ppm
Chlorine Tolerance	1 bar per element
Maximum Pressure Drop	4 bar per housing
Maximum Silt density index	5.0
Maximum Turbidity	1 NTU

An innovative simple method was used to impregnate TiO_2 in a commercial membrane. In this method, the nanofiltration system itself was used to perform the impregnation process. The self-assembly method was used for membrane modification; the methodology was adapted from Ngo *et al.* (2016) and Shao *et al.* (2017). In summary, a solution of 0.5% (w/v) of TiO_2 nanoparticles was prepared in ultrapure water dispersion (Milli-Q® system, Millipore) under magnetic stirring for 1 hour followed by sonication for 1 hour at 37 KHz frequency (Model Elmasonic P30H, Elma Schmidbauer Gmbh). The commercial polyamide membrane of nanofiltration was placed in contact with 30 mL of TiO_2 solution under magnetic stirring and Nitrogen gas pressure at 1 bar for 90 minutes in a nanofiltration module (Model HP4750 StirredCell, Sterlitech ©, USA (Figure 1). After removal of the filtration module, the membrane was washed with ultrapure water under gentle stirring three times. The coated TiO_2 membranes were maintained in ultrapure water until used for characterization and filtration tests. Before the characterization tests the membranes were dried at 37°C for 24 hours and stored in a desiccator. To evaluate the reproducibility of the membrane modification process, 9 membranes were prepared: 3 membranes were separated for characterization studies, 3 membranes for permeability studies and 3 membranes for the photocatalytic activity evaluation.

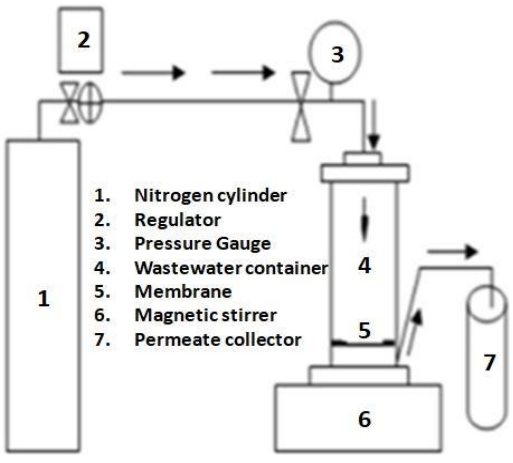

Figure 1. Nanofiltration module scheme

2.2. Membrane characterization

The morphological characteristics of the membranes were analyzed in a scanning electron microscope, Model SS 550 Superscan (Shimadzu, Japan), covering the samples with a thin layer of Au at a voltage of 20 kV.

Membrane functional groups were analyzed by attenuated total reflectance infrared (ATR-IR) spectroscopy, equipment Model Avatar 360 (ThermoNicolet). The spectral range was 4000 to 600 cm^{-1}. ATR-IR spectra were obtained after 32 scans with a resolution of 4 cm^{-1}. Measurements were performed at room temperature.

Differential Scanning Calorimetry (DSC) measurements were performed on Mettler-Toledo DSC28e equipment at a heating rate of 10°C min^{-1}, placing small pieces taken from the central region of the membrane in 40 μL aluminium containers. All assays were performed using nitrogen as purge gas. Samples were exposed to heating at a rate of 10°C min^{-1}, from 25 to 300°C.

Membranes samples (treated and untreated) were subjected to contact angle measurements to characterize their hydrophilicity/hydrophobicity. For this purpose, the Goniometer System OCA-15 was used, with SCA 20 software and CCD camera to record the image of the drop of distilled water on the sample. The tests were carried out under controlled environmental conditions at 19.3°C temperature. The volume of the water droplets used was 5 μL and at the rate of 5 μL/s. Five measurements were made at different points of the material, and the arithmetic mean was calculated. The behavior of the drop on the material as a function of time was also evaluated.

2.3. Photocatalytic activity

To evaluate the photocatalytic activity of TiO_2 impregnated in the membrane under UV radiation, a solution of the organic dye MB was used. The assays were performed with a 1.7 x 2.7 cm plate membrane (4.59 cm^2 area) placed in a quartz cell (40 mm × 40 mm × 10 mm), filled with MB solution (13 mL, 10^{-2} mM, pH = 6.8).

The membrane immersed in MB solution was initially held in the chamber for 30 minutes for adsorption/desorption until equilibrium of the concentration of MB solution was reached. The quartz cell was then irradiated with a high power LED lamp (Thorlabs, 700 mA) with a peak excitation at 365 nm (UV-A). The radiation incident on the membrane was measured with a light intensity meter and the mean radiation value was approximately 4mW.cm^2 (Marques *et al.*, 2013). The absorbance of the MB solution was monitored at 2-minute time intervals using a spectrophotometer (ScanSpec UV-Vis, ScanSci) with a wavelength scan of 300 to 900 nm. The photodegradation rate of the AM solution was analyzed by monitoring the peak energy absorption intensity at 662 nm.

The degradation reaction rate of the MB solution was calculated using the Langmuir-Hinshelwood model for pseudo-first-order reaction, expressed in Equation 1 (Yu *et al.*, 2007):

$$ln\left(\frac{C}{C_0}\right) = -kt \quad (1)$$

Where C_0 represents the concentration of the dye MB at time 0, C is the concentration of the dye MB at time t and k the first order constant of the reaction.

To evaluate the binding of the TiO_2 nanoparticles to the membrane surface, the photocatalytic assay was repeated 3 times with the same sample, intercalated by washing the membrane with water for 10 minutes under slow stirring (Fischer *et al.*, 2015).

2.4. Permeability experiments

The permeability experiments were performed in a "dead-end" membrane filtration system, consisting of a 300 cm^3 cylindrical steel cell, Model HP4750 StirredCell, Sterlitech © (USA), with a magnetic stirring system, connected to a cylinder of nitrogen gas, which has an effective filtration area of 12.254 cm^2 (Figure 1). All experiments were performed at room temperature.

Water permeability was determined after the steady flow was reached (when the flow value remained constant for 30 minutes) at different applied pressures (6, 8, 10, 12 and 14 bar). Initially, the membrane was compacted with ultrapure water at each pressure studied for 15 min (Ngo *et al.*, 2016). The water flow was determined by Equation 2:

$$J_w = \frac{V_w}{A \cdot t} \quad (2)$$

Where V_w is the ultrapure water volume (L) obtained by passing the membrane area A (m^2) at a filtration time of t (h).

The relation that governs the pure water flow to determine membrane permeability is (Ettori *et al.*, 2011) (Equation 3):

$$J_w = L_w \cdot \Delta P = \frac{1}{\mu R_m} \quad (3)$$

Where Jw (L h^{-1} m^{-2}) is the flux of ultrapure water, Lw is the ultrapure water permeability (L h^{-1} m^{-2} bar^{-1}), ΔP is the applied pressure (bar), μ is the dynamic viscosity of the water (1 Pa s^{-1}) and Rm is the hydraulic resistance of the membrane (m^{-1}).

3. RESULTS AND DISCUSSION

3.1. Membrane characterization

Figure 2 shows the comparison between the top surface images of the untreated membrane (A) and with self-assembled TiO_2 (B), respectively.

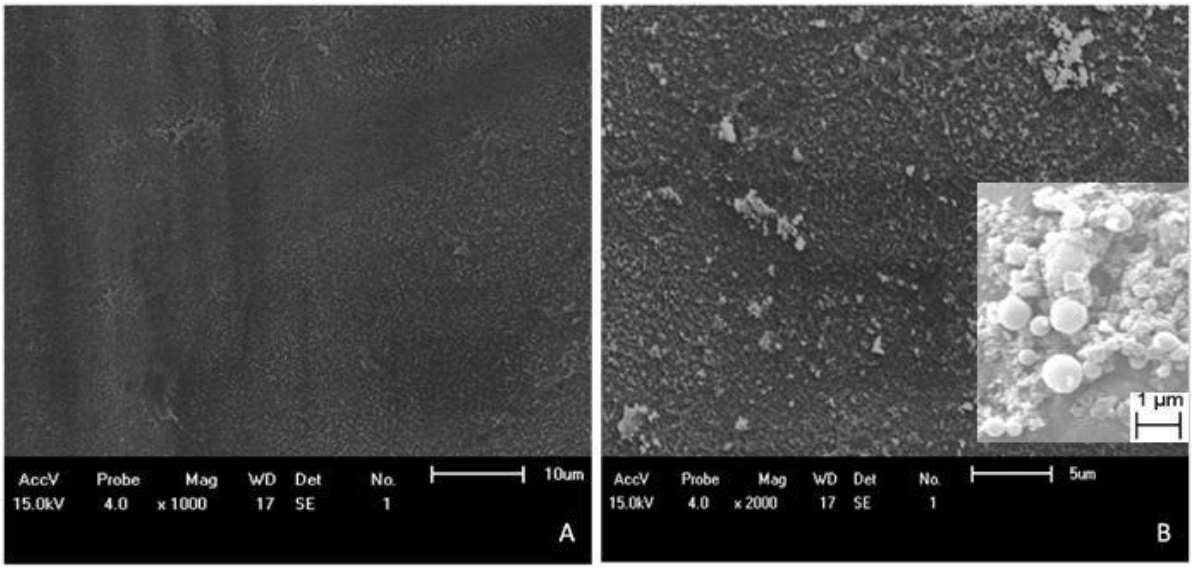

Figure 2. SEM images of the top surface of the untreated membrane (A) and with self-assembled TiO_2 nanoparticles (B).

The original and TiO_2-treated membrane when observed with naked eye has a smooth and flat surface; however, when increasing to a microscopic magnitude, a rough surface is observed

(see Figure 2A). According to Xiaoxiao *et al.* (2016) the morphology of the polyamide layer is typically of the "ridge and valley" type.

When observing Figure 2B, the presence of clusters of nanoparticles distributed on the surface of the membrane, resulting from deposited TiO_2 nanoparticles, is observed. The size differences of nanoparticles aggregated on the membrane surface are due to the sonication process of the colloidal solution of TiO_2, in which larger aggregated particles of TiO_2 were easily divided to form secondary particles from a few tens to a few hundred nanometers. In addition, at the time of deposition, the application of 1 bar pressure to the TiO_2 solution on the membrane possibly helped the adhesion of the nanoparticles to their surface.

Although SEM analysis can demonstrate the presence of TiO_2 nanoparticles on the membrane surface, differential scanning calorimetry was also performed. This analysis was able to identify the enthalpy change of the material when it undergoes physical and chemical changes. For monitoring variations in the behavior of chemical bonds that may have occurred due to the deposition of TiO_2 on the surface of the polyamide polymer membrane, attenuated total reflectance infrared spectroscopy (ATR-IR) was used.

Figure 3A shows non-isothermal DSC thermograms obtained for the untreated and TiO_2 treated membranes and Figure 3B shows the typical spectra of the original membrane (black solid line) and the TiO_2 modified membrane (red solid line).

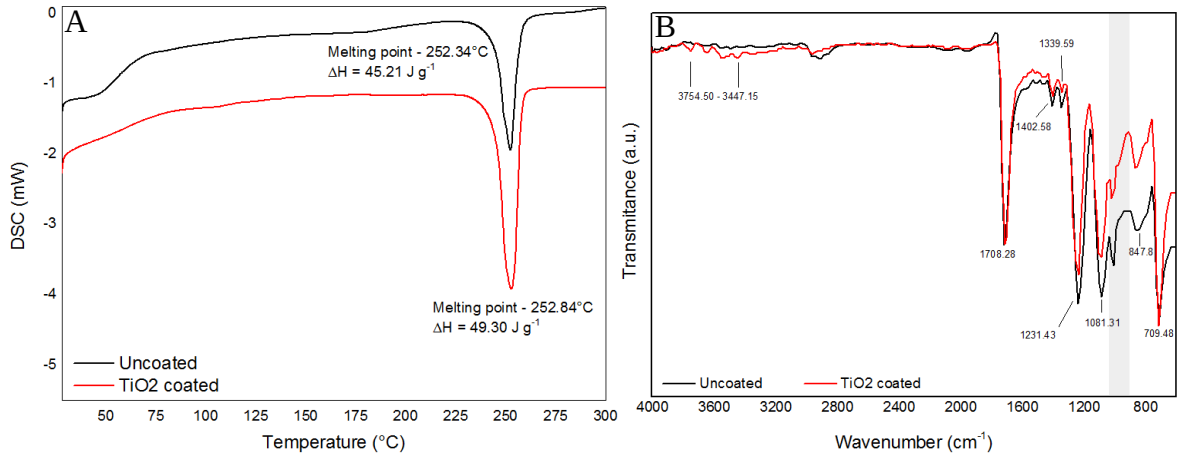

Figure 3. Thermograms of membranes untreated and treated with TiO_2. (A) and ATR-IR spectrum of untreated and treated membrane (B).

It can be observed in Figure 3A that the slope of the curve around 50°C for the treated membrane was not found, indicating the glassy transition state may have been affected by deposition of TiO_2 on the surface of the membrane. The glass transition of the polymer membrane occurs at a temperature around 50°C (Cossich *et al.*, 2015).

Comparing both curves of Figure 3A, the presence of an endothermic peak at 252.34°C for the untreated membrane and 252.84°C for the treated membrane is observed. This peak is associated with the melting process of the polymer. The presence of TiO_2 probably altered the crystalline behavior of the polymer matrix, making it difficult to crystallize. This can be observed by the increase of energy required in the transformation process, which for the untreated membrane required 45.21 J g^{-1}, and for the treated membrane, 49.30 J g^{-1} of energy was required, indicating that the presence of nanoparticles of TiO_2 increases the thermal stability of the membrane.

It was observed in Figure 3B that what characterizes the polyamide surface of the untreated membrane are: the presence of the strong bands at 1708.28 cm^{-1}, 1231.43 cm^{-1}, 1081.31 cm^{-1}, attributed to the stretching vibration of the amide II carbonyl, axial deformation vibrations of

the CN bond and the NH bond stretching of amide I (Li *et al.*, 2009). As the type of polyamide is aromatic, the ring can be detected by the vibration involving the elongation and contraction of carbon-carbon bonds in an aromatic ring at 1402.52 cm^{-1}. Another strong band that characterizes the membrane can be seen at 847.8 cm^{-1} and 709.48 cm^{-1}. According to Smith, such bands are caused by the out-of-plane C-H bond of an aromatic ring (Smith, 2016). Due to the planar aromatic rings, all hydrogens are in the plane of the molecule. When these hydrogens bend above and below the plane of the molecule, they are going through by the out-of-plane C-H bond out of the plane, which is sometimes called a "wag" because of the resemblance of the vibration to the swish of a dog's tail.

Comparing to the TiO_2-treated membrane in Figure 3B, it can be verified that the main bands were not altered, indicating that the polymer surface was not modified by the presence of TiO_2; however, a small modification in the spectrum in the regions of 3754.50 cm^{-1} to 3447.15 cm^{-1} (referring to OH groups) and in the region of 986.42 cm^{-1} (gray ragged region). According to different authors, there is a possibility that the bands in the region 3754.50 cm^{-1} to 3447.15 cm^{-1} indicate the interaction of Ti-OH and that of 986.42 cm^{-1} is attributed to Ti-O-Ti or C=O-Ti bond, confirming the occurrence of deposition/interaction of TiO_2 nanoparticles on the surface of the membrane (Ngo *et al.*, 2016).

The presence of OH bonds in the membrane coated with TiO_2 can lead to the hydrophilicity of the modified membrane, a characteristic that was proved by the analysis of the contact angle and permeability in water (Figure 4).

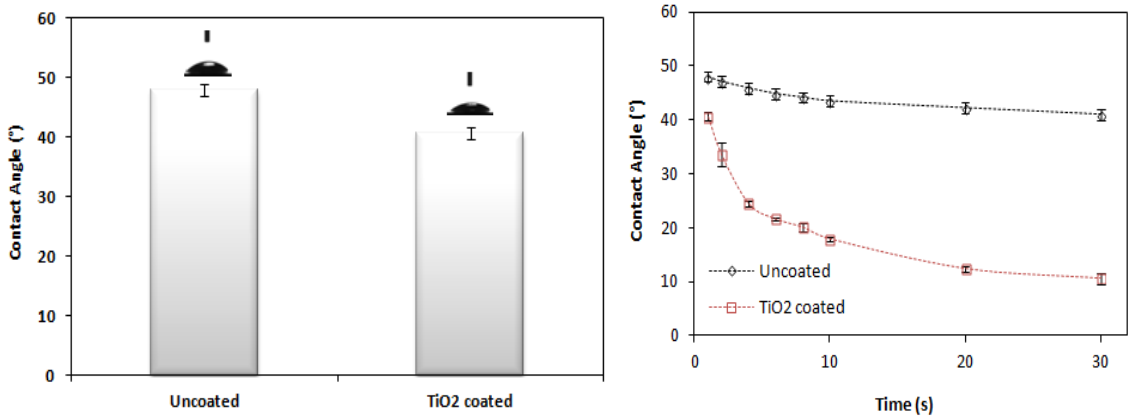

Figure 4. Contact angle between the membranes and ultrapure water droplet (A) and contact angle measurements as a function of time (B).

Surface hydrophilicity is one of the most important characteristics for a filtration membrane. One of the ways to obtain the relative hydrophilicity of the polymer membrane is the measurement of the contact angle (Li *et al.*, 2009). The "sessile drop" method was performed to examine the hydrophilicity of the membrane surfaces. If a drop of water comes in contact with a hydrophilic material, it spreads across the surface, resulting in a contact angle of zero or less. The wettability of the material is characterized by the contact angle between the surface of the solid and the tangent to the surface of the liquid from the point of contact (Cheryan, 1998).

As can be seen in Figure 4A, the contact angle of the untreated membrane was 48.03°C, which was slightly reduced to 40.64°C after the modification with TiO_2 nanoparticles. This reduction can be explained by the deposition of TiO_2 layer, making the surface area of the membrane more porous, facilitating the absorption of water and consequently increasing the hydrophilic property of the membrane (Verliefde *et al.*, 2009; Yamashita *et al.*, 2003).

To confirm the higher hydrophilicity of the TiO_2 treated surfaces, the dynamic contact angle was evaluated. The contact angle measurement was determined every second for 30 seconds, and the results are shown in Figure 4B.

The polyamide polymer leaves the membrane with hydrophilic characteristics; however we can see that the contact angles almost remain stable during the time of contact with the ultrapure water. For the membrane with TiO_2, it was noted that the contact angle was gradually reduced within the measurement time. This can be explained by the fact that TiO_2 has additional surface areas to absorb water more quickly and consequently leave the membrane more hydrophilic. The same behavior was observed by Li *et al.* (2009) and You *et al.* (2012) who evaluated Polyvinylidene fluoride membranes treated by self-assembly with TiO_2; and by Ngo *et al.* (2016) who modified the surface of commercial polyamide nanomembranes with TiO_2 nanoparticles.

3.2. Photocatalytic activity

The results obtained for the photodegradation of MB solution are presented in Figure 5.

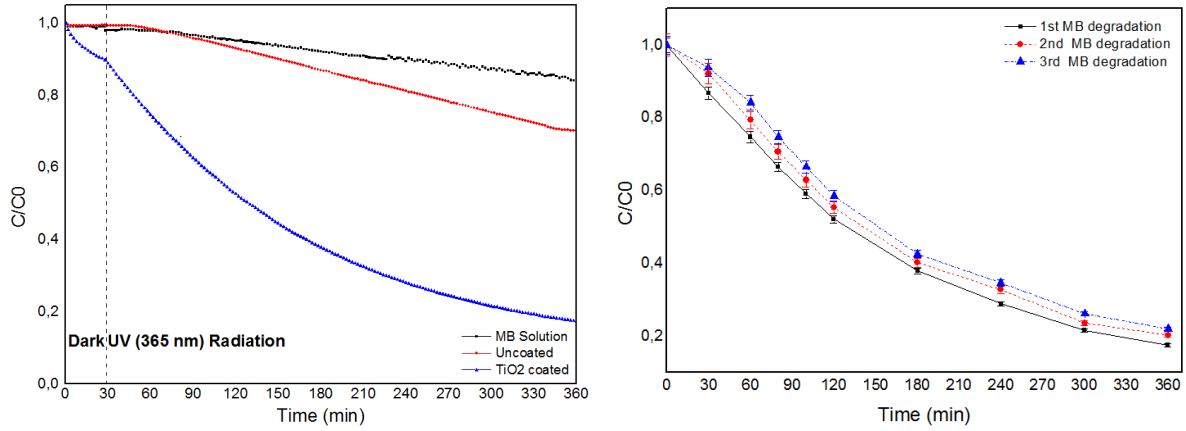

Figure 5. Degradation of MB (initial concentration = 10^{-2} mM) versus UV-A (A) and degradation of MB by 3 consecutive cycles with TiO_2 treated membrane (B).

It can be observed that in the first 30 minutes, without radiation incidence, there was no significant change in the concentration of dye for both treated membrane and untreated membrane. The small reduction of the observed concentration (~ 10% removal) is due to the presence of pores of the TiO_2 nanoparticles in which the adsorption process occurs. These pores will lead to a higher surface area on the membrane surface and, consequently, to a greater coverage for the dye adsorption (Tavares *et al.*, 2010).

The specific surface is one of the most important properties for photocatalytic activity, since photocatalytic reactions occur on the surface of the nanocatalyst. Thus, at the time of 30 minutes, in dark conditions, favours adsorption, exceeding the recombination fastness of the hole-electron pair (in nanoseconds), which usually results in excellent photocatalytic activities (Ochiai and Fujishima, 2012).

When analyzing the MB solution in contact with the TiO_2-treated membrane, after 6 hours under UV irradiation, it was found that MB degradation was approximately 91%. Table 1 shows the results of the photocatalytic assays of the MB solution in the presence and absence of the membranes (treated and untreated).

As can be observed, the of TiO_2 clearly improves the photocatalytic activity, since it presented a higher reaction rate (4.6 times higher than using the untreated membrane), lower half-life and higher efficiency of dye degradation. The data found in this study showed a photocatalytic behavior that is compatible with those reported in the literature (Cossich *et al.*, 2015; Li *et al.*, 2007; Yamashita *et al.*, 2003).

The mechanism of MB dye degradation may be explained by a adsorption-migration-photodegradation process. In this process, MB is first adsorbed by the dense polymer film, then

migrates to the TiO_2 nanoparticles and it is finally degraded by the TiO_2 catalyst under UV radiation (Cossich *et al.*, 2015; He *et al.*, 2009). Thus, the efficiency of the process is related to the combination of the membrane surface area (porosity) and the available TiO_2 surface area (Fischer *et al.*, 2014; Lombardi *et al.*, 2011)

In addition, it was found that the solution of MB that was in contact with the TiO_2 treated membrane had its color changed from bright blue to colorless during the photocatalysis process, indicating that an oxidation-reduction mechanism occurred on the surface of the thin films of titania, subsequently degrading the organic chromophore over time (Marques *et al.*, 2010).

Once dye was degraded, it was intended to verify the reusability of the TiO_2-treated membrane by repeating the MB photodegradation experiment for two more cycles, intercalated by washing the membrane with ultrapure water. The results can be seen in Figure 5B.

It was observed that the membrane treated with TiO_2 showed photocatalytic activity during the three cycles of radiation. This result indicates that the catalyst is regenerated and also was not lost during the washes with water, demonstrating that the application of the pressure of 1 bar during the treatment had a positive effect on the deposition process of the TiO_2 nanoparticles.

According to Fischer *et al.* (2015), the presence of TiO_2 on the surface of the membrane still has protective action since it avoids damage to the polymer membrane due to direct incidence of UV radiation on its surface.

These results indicate that a self-cleaning property was created by the TiO_2 particles deposited on the membrane surface (Madaeni and Ghaemi, 2007). This self-cleaning property can be explained both by the effect of increased membrane hydrophilicity, which may lead to a decrease in the hydrophobic interaction between the organic pollutants and the membrane surface (Bae and Tak, 2005), and by the photocatalytic effect under irradiation UV, of the TiO_2 particles in the decomposition of the pollutants.

3.3. Permeability experiments

Figure 6 shows the water flow changes caused by different pressures for the untreated and TiO_2 treated membrane. The water permeability (Lw) of the membranes can be found by determining the coefficient obtained by the linear regression of the graph of the pure water flux (Jw) versus transmembrane pressure (ΔP).

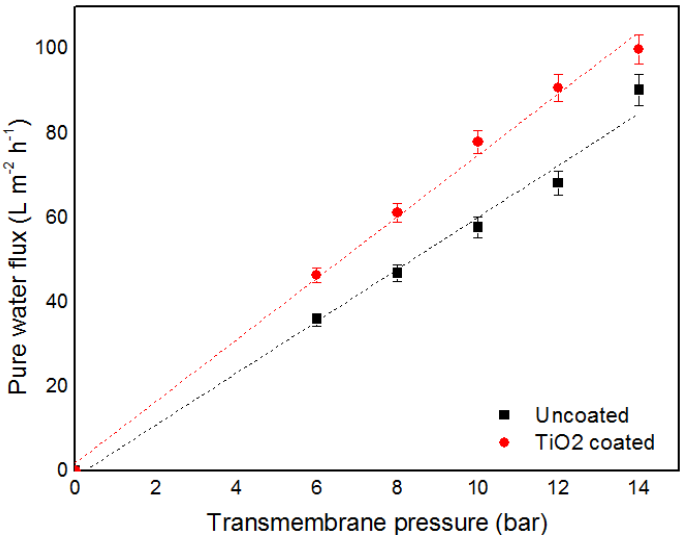

Figure 6. Variation of water flow at different pressures for untreated and TiO_2 treated membranes.

The nominal permeability of the membrane (supplied by the manufacturer) is 5.8 L h^{-1} m^{-2} $bar^{-1;}$ however, the value obtained with the filtration module used was 6.15 L h^{-1} m^{-2} bar^{-1}. The TiO_2 treated membrane presented a higher permeability of 7.28 L h^{-1} m^{-2} bar^{-1}, a result that corroborates with the results found in the contact angle analyses. The membrane becomes more hydrophilic with the presence of TiO_2 nanoparticles on the surface; consequently, it presents a lower contact angle and a higher flow of water. Titanium dioxide has been the focus of numerous investigations in recent years, because its high hydrophilicity, stable chemical property, innocuity and low cost, etc. The use of TiO_2 to increase the membrane hydrophilicity is observed by other researchers and is in accordance with the results founded in this study (Luo *et al.*, 2005; Vatanpour *et al.*, 2012).

4. CONCLUSIONS

The results of this study indicate that the impregnation of TiO_2 particles on the surface of a polyamide membrane by self-assembly under pressure was successful. ATR-IR analysis confirmed that the deposition process does not significantly alter the chemical structure of the polymer matrix of polyamide. Measurements of contact angle, as well as the determination of permeability, demonstrated that the hydrophilicity of the membrane increased. The photocatalytic performance of the membrane when depositing TiO_2 on surfaces has been improved, since the mechanism of degradation is established by the synergistic interaction of the TiO_2-dye membrane surface and UV irradiation. It is a simple technique for effective removal of recalcitrants of organic matter, such as dyes, phenols and humic acids, and can be reached by the photocatalytic membrane under UV irradiation.

5. ACKNOWLEDGEMENTS

This work was supported by the Portuguese National Fund, through the FCT - Fundação para a Ciência e a Tecnologia, under the project UID/CTM/00264/2013 and CAPES - Coordenação de Aperfeiçoamento Pessoal de Nível Superior - Agreement CAPES/FCT2014-2017. The authors thank the support of the researchers of surfaces laboratory of the Centre of Physics of the University of Minho, Portugal by the support analyzes.

6. REFERENCES

BAE, T.-H.; TAK, T.-M. Preparation of TiO_2 self-assembled polymeric nanocomposite membranes and examination of their fouling mitigation effects in a membrane bioreactor system. **Journal of Membrane Science,** v. 266, n. 1-2, p. 1-5, 2005. https://doi.org/10.1016/j.memsci.2005.08.014

CHERYAN, M. **Ultrafiltration and Microfiltration Handbook**. Lancaster: Technomic, 1998. 264 p.

COSSICH, E.; BERGAMASCO, R.; DE AMORIM, M. P.; MARTINS, P.; MARQUES, J.; TAVARES, C. J.; LANCEROS-MÉNDEZ, S.; SENCADAS, V. Development of electrospun photocatalytic TiO 2-polyamide-12 nanocomposites. **Materials Chemistry and Physics,** v. 164, p. 91-97, 2015. https://doi.org/10.1016/j.matchemphys.2015.08.029

ETTORI, A.; GAUDICHET-MAURIN, E.; SCHROTTER, J.-C.; AIMAR, P.; CAUSSERAND, C. Permeability and chemical analysis of aromatic polyamide-based membranes exposed to sodium hypochlorite. **Journal of Membrane Science,** v. 375, n. 1, p. 220-230, 2011. https://doi.org/10.1016/j.memsci.2011.03.044

FISCHER, K.; GLÄSER, R.; SCHULZE, A. Nanoneedle and nanotubular titanium dioxide – PES mixed matrix membrane for photocatalysis. **Applied Catalysis B: Environmental,** v. 160-161, p. 456-464, 2014. https://doi.org/10.1016/j.apcatb.2014.05.054

FISCHER, K.; GRIMM, M.; MEYERS, J.; DIETRICH, C.; GLÄSER, R.; SCHULZE, A. Photoactive microfiltration membranes via directed synthesis of TiO 2 nanoparticles on the polymer surface for removal of drugs from water. **Journal of Membrane Science,** v. 478, p. 49-57, 2015. https://doi.org/10.1016/j.memsci.2015.01.009

FUJISHIMA, A.; KOHAYAKAWA, K.; HONDA, K. Hydrogen production under sunlight with an electrochemical photocell. **Journal of the Electrochemical Society,** v. 122, p. 1487-1489, 1975.

HE, T.; ZHOU, Z.; XU, W.; REN, F.; MA, H.; WANG, J. Preparation and photocatalysis of TiO_2–fluoropolymer electrospun fiber nanocomposites. **Polymer,** v. 50, n. 13, p. 3031-3036, 2009. https://doi.org/10.1016/j.polymer.2009.04.015

LEONG, S.; RAZMJOU, A.; WANG, K.; HAPGOOD, K.; ZHANG, X.; WANG, H. TiO 2 based photocatalytic membranes: a review. **Journal of Membrane Science,** v. 472, p. 167-184, 2014. https://doi.org/10.1016/j.memsci.2014.08.016

LI, J.-B.; ZHU, J.-W.; ZHENG, M.-S. Morphologies and properties of poly (phthalazinone ether sulfone ketone) matrix ultrafiltration membranes with entrapped TiO_2 nanoparticles. **Journal of Applied Polymer Science,** v. 103, n. 6, p. 3623-3629, 2007. https://doi.org/10.1002/app.25428

LI, J.-H.; XU, Y.-Y.; ZHU, L.-P.; WANG, J.-H.; DU, C.-H. Fabrication and characterization of a novel TiO 2 nanoparticle self-assembly membrane with improved fouling resistance. **Journal of Membrane Science,** v. 326, n. 2, p. 659-666, 2009. https://doi.org/10.1016/j.memsci.2008.10.049

LOMBARDI, M.; PALMERO, P.; SANGERMANO, M.; VARESANO, A. Electrospun polyamide-6 membranes containing titanium dioxide as photocatalyst. **Polymer International,** v. 60, n. 2, p. 234-239, 2011. https://doi.org/10.1002/pi.2932

LUO, M.-L.; ZHAO, J.-Q.; TANG, W.; PU, C.-S. Hydrophilic modification of poly (ether sulfone) ultrafiltration membrane surface by self-assembly of TiO_2 nanoparticles. **Applied Surface Science,** v. 249, n. 1, p. 76-84, 2005. https://doi.org/10.1016/j.apsusc.2004.11.054

MADAENI, S.; GHAEMI, N. Characterization of self-cleaning RO membranes coated with TiO 2 particles under UV irradiation. **Journal of Membrane Science,** v. 303, n. 1, p. 221-233, 2007. https://doi.org/10.1016/j.memsci.2007.07.017

MARQUES, J.; OLIVEIRA, L.; PINTO, R.; COUTINHO, P. J.; PARPOT, P.; GÓIS, J.; COELHO, J.; MAGALHÃES, F.; TAVARES, C. Release of volatile compounds from polymeric microcapsules mediated by photocatalytic nanoparticles. **International Journal of Photoenergy,** v. 2013, 2013. http://dx.doi.org/10.1155/2013/712603

MARQUES, S.; TAVARES, C.; OLIVEIRA, L.; OLIVEIRA-CAMPOS, A. Photocatalytic degradation of CI Reactive Blue 19 with nitrogen-doped TiO_2 catalysts thin films under UV/visible light. **Journal of Molecular Structure,** v. 983, n. 1-3, p. 147-152, 2010. https://doi.org/10.1016/j.molstruc.2010.08.044

NGO, T. H. A.; NGUYEN, D. T.; DO, K. D.; NGUYEN, T. T. M.; MORI, S.; TRAN, D. T. Surface modification of polyamide thin film composite membrane by coating of titanium dioxide nanoparticles. **Journal of Science: Advanced Materials and Devices,** v. 1, n. 4, p. 468-475, 2016. https://doi.org/10.1016/j.jsamd.2016.10.002

OCHIAI, T.; FUJISHIMA, A. Photoelectrochemical properties of TiO_2 photocatalyst and its applications for environmental purification. **Journal of Photochemistry and Photobiology C: Photochemistry Reviews,** v. 13, n. 4, p. 247-262, 2012. https://doi.org/10.1016/j.jphotochemrev.2012.07.001

PAN, X.; YANG, M.-Q.; FU, X.; ZHANG, N.; XU, Y.-J. Defective TiO_2 with oxygen vacancies: synthesis, properties and photocatalytic applications. **Nanoscale**, v. 5, n. 9, p. 3601-3614, 2013. https://dx.doi.org/10.1039/C3NR00476G

SHAO, F.; XU, C.; JI, W.; DONG, H.; SUN, Q.; YU, L.; DONG, L. Layer-by-layer self-assembly TiO 2 and graphene oxide on polyamide reverse osmosis membranes with improved membrane durability. **Desalination**, v. 423, p. 21-29, 2017. https://doi.org/10.1016/j.desal.2017.09.007

SMITH, B. C. Group Wavenumbers and an Introduction to the Spectroscopy of Benzene Rings. **Spectroscopy,** v. 31, n. 3, p. 34-37, 2016.

TAVARES, C.; MARQUES, S.; LANCEROS-MÉNDEZ, S.; REBOUTA, L.; ALVES, E.; BARRADAS, N.; MUNNIK, F.; GIRARDEAU, T.; RIVIÈRE, J.-P. N-doped photocatalytic titania thin films on active polymer substrates. **Journal of Nanoscience and Nanotechnology,** v. 10, n. 2, p. 1072-1077, 2010. https://doi.org/10.1166/jnn.2010.1868

VATANPOUR, V.; MADAENI, S. S.; KHATAEE, A. R.; SALEHI, E.; ZINADINI, S.; MONFARED, H. A. TiO_2 embedded mixed matrix PES nanocomposite membranes: Influence of different sizes and types of nanoparticles on antifouling and performance. **Desalination,** v. 292, p. 19-29, 2012. https://doi.org/10.1016/j.desal.2012.02.006

VERLIEFDE, A. R. D.; CORNELISSEN, E. R.; HEIJMAN, S. G. J.; HOEK, E. M. V.; AMY, G. L.; BRUGGEN, B. V. D.; VAN DIJK, J. C. Influence of Solute−Membrane Affinity on Rejection of Uncharged Organic Solutes by Nanofiltration Membranes. **Environmental Science & Technology,** v. 43, n. 7, p. 2400-2406, 2009. https://dx.doi.org/10.1021/es803146r

XIAOXIAO, S.; JA, P.; SUN, D. D. Relating Water/Solute Permeability Coefficients to the Performance of Thin-Film Nanofiber Composite Forward Osmosis Membrane. **Journal of Membrane Science & Technology,** v. 6, n. 4, p. 1-10, 2016. https://dx.doi.org/10.4172/2155- 9589.1000167

YAMASHITA, H.; NAKAO, H.; TAKEUCHI, M.; NAKATANI, Y.; ANPO, M. Coating of TiO_2 photocatalysts on super-hydrophobic porous teflon membrane by an ion assisted deposition method and their self-cleaning performance. **Nuclear Instruments and Methods in Physics Research Section B: Beam Interactions with Materials and Atoms,** v. 206, p. 898-901, 2003. https://doi.org/10.1016/S0168-583X(03)00895-4

YOU, S.-J.; SEMBLANTE, G. U.; LU, S.-C.; DAMODAR, R. A.; WEI, T.-C. Evaluation of the antifouling and photocatalytic properties of poly (vinylidene fluoride) plasma-grafted poly (acrylic acid) membrane with self-assembled TiO 2. **Journal of Hazardous Materials,** v. 237, p. 10-19, 2012. https://doi.org/10.1016/j.jhazmat.2012.07.071

YU, J.; WANG, G.; CHENG, B.; ZHOU, M. Effects of hydrothermal temperature and time on the photocatalytic activity and microstructures of bimodal mesoporous TiO 2 powders. **Applied Catalysis B: Environmental,** v. 69, n. 3, p. 171-180, 2007. https://doi.org/10.1016/j.apcatb.2006.06.022

Ambiente & Água - An Interdisciplinary Journal of Applied Science
ISSN 1980-993X – doi:10.4136/1980-993X
www.ambi-agua.net
E-mail: ambi.agua@gmail.com

Contents of macronutrients and growth of 'BRS Marataoã' cowpea fertigated with yellow water and cassava wastewater

ARTICLES doi:10.4136/ambi-agua.2309

Received: 26 Jul. 2018; Accepted: 11 Mar. 2019

Narcísio Cabral de Araújo[1*]; Vera Lucia Antunes Lima[2]; Jailton Garcia Ramos[2]; Elysson Marcks Gonçalves Andrade[2]; Geovani Soares de Lima[3]; Suenildo Jósemo Costa Oliveira[4]

[1]Universidade Federal do Sul da Bahia (UFSB), Itabuna, BA, Brasil
Centro de Formação em Tecno-ciências e Inovação (CFTCI). E-mail: narcisioaraujo@gmail.com
[2]Universidade Federal de Campina Grande (UFCG), Campina Grande, PB, Brasil
Unidade Acadêmica de Engenharia Agrícola (CTRN). E-mail: antuneslima@gmail.com, jailtonbiossistemas@gmail.com, elyssonmarcks@yahoo.com.br
[3]Universidade Federal de Campina Grande (UFCG), Pombal, PB, Brasil
Unidade Acadêmica de Ciências Agrárias (UAGRA). E-mail: geovani.soares@pq.cnpq.br
[4]Universidade Estadual da Paraíba (UEPB), Lagoa Seca, PB, Brasil
Centro de Ciências Agrárias e Ambientais (CCAA). E-mail: suenildo@ccaa.uepb.edu.br
[*]Corresponding author

ABSTRACT

Agricultural utilization of yellow waters associated with cassava wastewater is a sustainable technique, since it allows reduction of costs related to acquisition of industrialized fertilizers and minimizes the environmental pollution caused by the inadequate disposal of these effluents. In this context, this study evaluated the macronutrient macronutrient content and growth of cowpea fertigated with yellow water associated with cassava wastewater and NPK as source of nutrients. The experiment was set up in a greenhouse located at Campus I of the Federal University of Campina Grande. The experimental design was completely randomized, composed of five treatments characterized by: fertigation with mineral fertilizers, in the form of NPK; organic fertigation composed of human urine, cassava wastewater, human urine plus cassava wastewater; and organo-mineral fertigation composed of urine, cassava wastewater and mineral phosphorus, with four replicates. At 36 days after sowing, the following parameters were determined: contents of nitrogen, phosphorus, potassium, sulfur and the variables number of leaves, plant height, stem diameter, leaf area, shoot fresh matter and shoot dry matter. The use of yellow waters promotes significant increases for growth and production variables for nitrogen and potassium contents mainly, as well as for growth and production variables. The contents of nitrogen, phosphorus and potassium were higher than the levels considered as adequate for the cowpea crop. The use of human urine and cassava wastewater have potential to meet the needs for the main macronutrients required by cowpea and the irrigation via fertigation with these biofertilizers positively influences the development of cowpea.

Keywords: agricultural use of wastes, human urine, *vigna unguiculata* (L.) Walp.

Teores de macronutrientes e crescimento do feijão vigna 'BRS Marataoã' fertirrigado com água amarela e manipueira

RESUMO

O uso agrícola de águas amarelas associadas à manipueira é uma técnica sustentável, uma vez que possibilita a redução de custos com a aquisição de fertilizantes industrializados e minimiza a poluição ambiental ocasionada pela destinação final inadequada desses efluentes. Neste contexto, objetivou-se com este trabalho avaliar os teores de macronutrientes e o crescimento do feijão vigna fertirrigado com águas amarela associada à manipueira e NPK como fonte de nutrientes. O experimento foi instalado em uma casa de vegetação localizada no Campus I da Universidade Federal de Campina Grande. Utilizou-se delineamento inteiramente casualizado composto por cinco tratamentos caracterizados por fertirrigações com fertilizantes minerais, na forma de NPK; orgânicos compostos por urina humana, manipueira, urina humana mais manipueira e organomineral composto por urina, manipueira e fósforo mineral e quatro repetições. Aos 36 dias após a semeadura foram avaliados os teores de nitrogênio, fósforo, potássio, enxofre e as variáveis: número de folhas, altura de planta, diâmetro caulinar, área foliar, massa fresca e seca da parte aérea. O uso de águas amarelas promove incrementos significativos para os teores de nitrogênio e potássio principalmente, assim como para as variáveis de crescimento e produção. Os teores de nitrogênio, fósforo e potássio apresentam valores superiores aos considerados adequados para o cultivo do feijão vigna. O uso de urina humana e a manipueira apresentam potencialidade para suprir as necessidades dos principais macronutrientes requeridos pela cultura do feijão vigna e a irrigação via fertirrigação com estes biofertilizantes pode influenciar positivamente o desenvolvimento dessa cultura.

Palavras-chave: urina humana, uso agrícola de resíduos, *Vigna unguiculata* (L.) Walp.

1. INTRODUCTION

Cowpea (*Vigna unguiculata* (L.) Walp.), also known as 'feijão-fradinho', 'feijão-macassar' or 'feijão-de-corda', is a source of income and food for many regions, especially the Brazilian Northeast (Benett *et al.*, 2013). In Brazil, cowpea has undergone great changes, in both the production sector, with expansion of its cultivation to other regions, and in the commercial sector, with the standardization of the best product, beginning of industrial processing and product entry in new markets in the country and abroad (Freire Filho *et al.*, 2011).

The recycling of nutrients contained in biodegradable wastes is a sustainable technique because it minimizes the use of synthetic mineral fertilizers and the negative impacts resulting from lack of environmental management in the exploitation of natural resources to produce fertilizers and pollution of waters due to uncontrolled disposal of wastes in the environment.

The increased costs of mineral fertilizers and increasing environmental pollution make the use of organic wastes in agriculture an attractive alternative from an economic point of view, due to the cycling of C (carbon) and nutrients (Silva *et al.*, 2010).

It is important to make it clear that yellow waters have high concentrations of nitrogen (N), phosphorus (P), potassium (K) and sulfur (S). Human urine has been used as a source of urea and cassava wastewater as a source of potassium since the concentration of these substitute mineral fertilizers (Ranasinghe *et al.*, 2016).

According to Sousa *et al.* (2008), various studied based on the separation of urine and feces have been carried out. Urine separation can provide a "free" hygienic fertilizer which can be used in agriculture (Kvarnström *et al.*, 2006). For Karak and Bhattacharyya (2011), urine is a

highly valuable source of nutrients which has been used in agriculture since ancient times.

Another effluent with great potential for recycling of nutrients through agricultural reuse is cassava wastewater because, according to Conceição *et al.* (2013), like human urine it is rich in macro and micronutrients, and can be used as fertilizer.

Recently, several studies have been conducted to evaluate the agricultural use of human urine. Araújo *et al.* (2015b) studied the cultivation components of hydroponic green fodder of corn fertilized with human urine as source of nutrients. Santos Júnior *et al.* (2015) evaluated grain and phytomass production in millet irrigated with human urine associated with domestic effluent. Bonvin *et al.* (2015) studied N and P absorption by ryegrass fertilized with synthetic urine. Santos *et al.* (2016) tested the use of human urine as source of nutrients for Bermuda grass and Botto *et al.* (2017) evaluated the yield of castor bean, cultivar 'BRS Nordestina', fertilized with human urine.

The human urine is rich in nitrogen in the form of urea, and cassava wastewater is rich in potassium; their use in agricultural production can reduce the use of mineral fertilizers that salinize the soil and water, destroy aquatic and terrestrial life, and which, during the process of manufacture, release into the air and water dioxins,, which are highly carcinogenic substances.

The use of wastewater in agricultural production reduces the use of mineral fertilizers, which generate negative impacts for water bodies, soil, air, etc. This happens because of the use of mineral fertilizers. This negatively affects the process of production, releasing POP'S (Persistent Organic Pollutants), as the dioxins, element high carcinogenic and smooth air and hydric flow. Regarding cassava wastewater, in the last seven years studies have been published analyzing the fertilizer potential of this effluent (Santos *et al.*, 2010; Schwengber *et al.*, 2010; Araújo *et al.*, 2012; 2015b; Duarte *et al.*, 2012; Silva Junior *et al.*, 2012; Barreto *et al.*, 2013; 2014; Dantas *et al.*, 2015; Leal *et al.*, 2015; Pessuti *et al.*, 2015). Based on the results obtained in the above-mentioned studies, the authors concluded that the agricultural use of human urine or cassava wastewater had positive effects on the variables of the crops analyzed.

Therefore, considering the lack of studies using yellow water and cassava wastewater in cowpea cultivation, the present study evaluated the contents of nitrogen (N), phosphorus (P), potassium (K) and sulfur (S) and the growth of *Vigna unguiculata* (L.) Walp., cultivar 'BRS Marataoã', fertigated with human urine combined with cassava wastewater as source of nutrients. These sources of organic fertilizer have little to no acquisition cost for small rural producers, and may increase production, particularly that based in family agricultural.

2. MATERIAL AND METHODS

The experiment was conducted in a greenhouse between November and December 2015, at Campus I of the Federal University of Campina Grande (UFCG), in the city of Campina Grande (7°13'50" S, 35°52'52" W, 551 m of altitude), Paraíba state, Brazil.

In the research environment, the experimental units consisted of 15-L plastic pots distributed at spacing of 0.80 m between rows and 0.50 m within the row, supported by a base made of bricks.

Each pot was perforated at the bottom to insert a drain, that is, a 15-cm long hose with nominal diameter of 6 mm, which was attached to a 2.0-L PET bottle to collect the drained effluent, allowing its recirculation in the original pot in order to reduce possible losses of nutrients leached by the excess of water volumes drained from irrigation. The pots were filled with a 0.50-kg layer of crushed stone (nº 0), covering the bottom, and a 15.0-kg layer of a Eutrophic Regolithic Neosol with sandy loam texture, properly pounded to break up clods and sieved, from the rural area of the municipality of Esperança, PB. Its analysis showed the following results: pH (H_2O) = 5.58; EC = 0.56 mmhos cm^{-1}; Al = 0.00 cmolc dm^{-3}; Mg = 2.78 cmolc dm^{-3}; Ca = 9.07 cmolc dm^{-3}; K = 0.33 cmolc dm^{-3}; Na = 1.64 cmolc dm^{-3};

P = 3.98 mg dm^{-3}; S = 13.72 cmolc dm^{-3}; OC = 1.70%; OM = 2.93% and d = 1.28 g cm^{-3}.

After the pots were filled, irrigation was applied to bring the soil to field capacity. Then, holes were opened and sowing was carried out by planting five seeds of the cowpea cultivar 'BRS Marataoã' per pot. 10 days after sowing (DAS), thinning was performed to leave two seedlings per pot.

Irrigation water volumes were estimated individually for each experimental plot with 2-day intervals based on water balance (difference between the mean volumes applied and drained sufficient to maintain the soil at field capacity, plus 20%, to meet water losses through evapotranspiration). The water used in irrigation was collected in the public supply network of Campina Grande, PB.

The experimental design was completely randomized, with four replicates and five treatments, totaling 20 experimental plots. Treatments consisted of fertigation with NPK (Treatment 1 - NPK); only human urine (Treatment 2 - U); only cassava wastewater (Treatment 3 - W); human urine plus cassava wastewater (Treatment 4 – U + W) and human urine plus cassava wastewater plus phosphorus (Treatment 5 – U + W + P). Mineral fertilizers consisted of urea (45.9% N), single superphosphate (18.9% P_2O_5) and potassium chloride (60% K_2O).

Treatments 1 and 5, in 10 fertirrigation treatments, were applied differently, because human urine and cassava wastewater must be diluted to soften the toxic effects that these effluents can cause in plants. If the concentrations of effluents applied via fertirrigation exceed the recommended limited by 10%, injuries may be caused to plants, such as burned leaves.

Fertigation began 10 days after sowing (DAS). Each plot received the equivalent of 100 mg N kg^{-1} of soil, 300 mg P kg^{-1} of soil and 150 mg K kg^{-1} of soil, according to the recommendations of Novais *et al.* (1991).

The amounts of human urine and cassava wastewater applied in each plot were estimated based on the concentrations of nitrogen and potassium in the effluents (Table 1) and the dose recommended by Novais *et al.* (1991) (100 mg N kg^{-1} of soil and 150 mg K kg^{-1} of soil).

The pots that received human urine were treated with 224.95 mL of this effluent to supply the nitrogen required by the cultivar, and 561.93 mL of cassava wastewater to supply the necessary potassium. To complete fertilization, phosphorus of mineral origin was applied in a portion of 23.83 g of P_2O_5 per pot.

Table 1. Physicochemical characterization of human urine (U) and cassava wastewater (W) used in the experiment.

Effluents	Parameters								
	TKN	NH_3-N	NO_3	P-PO_4^{-3}	K	Na	Ca + Mg	pH	EC
	g L^{-1}							-	mS cm^{-1}
U	6.668	5.257	0.002	0.325	1.558	2.509	0.034	9.12	42.7
W	1.199	0.336	0.019	0.338	4.004	0.096	2.800	3.75	11.75

Note: TKN: Total Kjeldahl Nitrogen; NH_3-N: Ammoniacal Nitrogen; NO_3: Nitrate; P – PO_4^{-3}: Soluble Orthophosphate; K: Potassium; Na: Sodium; Ca + Mg: total hardness; pH: Hydrogen potential and EC: Electrical Conductivity.

For treatments containing mineral fertilizers (Treatments 1 and 5), fertigation was split into 3 portions and applied at 10, 20 and 28 DAS. For treatments containing human urine (Treatment 2), cassava wastewater (Treatment 3) and human urine plus cassava wastewater (Treatments 4 and 5), fertigation was split into 10 portions and applied at 10, 12, 14, 16, 18, 20, 22, 24, 26 and 28 DAS.

Human urine was subjected to a treatment, which consisted of storage in a hermetically sealed 20-L plastic bucket for 60 days before being used. For cassava wastewater, the treatment

consisted of anaerobic digestion for 90 days in a 85-L plastic bucket, with an empty space of 10 cm inside it. The lid of the bucket was attached to a hose with the other tip immersed in a container with water up to 10 cm in depth, to release the gases generated during the effluent bio-digestion.

Regarding the presence of xenobiotics, everyone carries these in their bodies from food, drink, etc.; so the concentrations of xenobiotics would vary depending on the food habits of the individuals. The human urine utilized was from men who do not smoke and do not take any type of controlled medicine.

In relation to the use of cassava wastewater and human urine, these effluents harm only minimally, because they are a source of organic nutrients, with an easy assimilation into soil and plants. Moreover the applications followed a recommended method of fertilization which does not cause nutritional stress in the crop or eutrophic alterations in the hydric bodies and soil.

After treatment, the effluents were analyzed according to the methodology recommended by the Standard Methods for Wastewater (APHA *et al.*, 2005), and their parameters are presented in Table 1.

Human urine and cassava wastewater were submitted to pre-treatment to reduce the concentration of hydrocyanic acid in cassava wastewater and increase the pH of human urine to eliminate pathogenic microorganisms in the effluent.

It is known that treated cassava wastewater reduces pH (± 3.0), while human urine increases it (±9.0). In this way, the pH of the soil solution, in an interval between 5.5 and 6.5, promotes high nutrient availability for plants (Malavolta *et al.*, 1989).

At 36 days after sowing (DAS), a period in which plants were at a late vegetative stage and in early flowering, when they assimilate maximum quantities of nutrients, growth variables were evaluated: plant height (PH, cm), stem diameter (SD, mm), number of leaves (NL, leaves plant^{-1}), leaf area (LA, cm^2), shoot fresh matter (SFM, g plant^{-1}) and shoot dry matter (SDM, g plant^{-1}).

Plant height was determined using a tape measure graduated in centimeters from the collar to the apical bud. Stem diameter was measured using a digital caliper, graduated in millimeters, at approximately 2.0 cm from the collar. Number of leaves was determined by counting green leaves longer than 3.0 cm, disregarding dry leaves, from the basal leaves to the last open leaf in the plant. Leaf area was estimated by the mathematical model proposed by Lima *et al.* (2008), which consists in the sums of midrib length (L) and maximum width (W) of each leaflet, according to Equation 1:

$$LA = \sum(0.9915\ x\ (L\ x\ W)^{0.9134}) \quad (1)$$

Where: LA is the leaf area of the cultivar (cm^2); W is the maximum width of each leaflet (cm); and L is the midrib length (cm).

To determine shoot fresh matter, one plant from each plot was cut close to the soil and weighed on a precision analytical scale. After weighing, the plants were placed in paper bags previously identified and dried in an oven at a controlled temperature of 65ºC for 72 hours to determine SDM.

After SDM determination, plants were ground in a Wiley-type mill and placed in identified packages to determine the contents of nitrogen (N, g kg^{-1}), phosphorus (P, g kg^{-1}), potassium (K, g kg^{-1}) and sulfur (S, mg kg^{-1}). These analyses were conducted following the methodology described by EMBRAPA (2009).

The results of the studied variables were subjected to analysis of variance and means were compared by Tukey test at a 0.05 probability level using the program ASSISTAT v. 7.7 Beta (Silva and Azevedo, 2016).

3. RESULTS AND DISCUSSION

Based on the results presented in Table 2, the analysis of variance showed significant effect ($p < 0.01$) on the contents of nitrogen (N), phosphorus (P) and sulfur (S) and non-significant effect ($p > 0.05$) on the content of potassium (K). Significant statistical difference was also found between the means of N, P and S.

Table 2. Summary of analysis of variance and mean contents of N (g kg^{-1}), P (g kg^{-1}), K (g kg^{-1}) and S (mg kg^{-1}) in the shoot of cowpea fertigated with human urine and cassava wastewater.

SV	Mean square				
	DF	N	P	K	S
Treatments	4	151.29567**	6.46752**	34.12312^{ns}	2895.89787**
Residual	15	4.63867	0.20291	13.75016	15.22620
CV%	-	4.39	8.78	11.82	6.53
Treatments	Means				
1 - (NPK)		52.50a	6.41a	36.38a	43.45cd
2 - (U)		52.50a	4.27b	27.60a	35.55d
3 - (W)		36.40b	4.27b	29.21a	51.84bc
4 - (U+W)		51.80a	3.69b	31.15a	54.19b
5 - (U+W+P)		52.27a	6.99a	32.56a	113.76a

Note: SV – Source of variation; DF – Degrees of freedom; CV – Coefficient of variation; NPK – Nitrogen, phosphorus and potassium; U – Human urine; W – Cassava wastewater; U + W – Human urine plus cassava wastewater; U+W+P – Human urine plus cassava wastewater plus phosphorus; ($^{ns,\ **,\ *}$) - Not significant, significant at 0.01 and 0.05 probability levels by F test; Means followed by the same letter in the column do not differ by Tukey test ($p > 0.05$).

For N contents, the means of Treatment 3 (fertigation with cassava wastewater) were different, whereas the means of the other treatments did not differ from one another. The maximum mean of N was 52.5 g kg^{-1}, obtained in plants fertigated with yellow water (Treatment 2 – U) and with mineral fertilizers (Treatment 1 – NPK). The minimum mean of N was 36.40 g kg^{-1}, obtained in plants fertigated with only cassava wastewater (Treatment 3 – W), but this value was still higher than the concentration range considered as adequate for common beans (30 to 35 g kg^{-1}) (Fageria *et al.*, 1996) and for cowpea (19.7 ± 1.3 g kg^{-1}) (Freire Filho *et al.*, 2005).

The maximum mean of P was 6.99 g kg^{-1}, obtained in plants fertigated with urine plus cassava wastewater associated with the mineral fertilizer P (5 – U+W+P). This value did not differ statistically from that of the treatment with NPK fertigation (control; 6.41 g kg^{-1}). The means of P also did not differ between Treatment 2 (fertigation with yellow water), 3 (fertigation with cassava wastewater) and 4 (fertigation with yellow water associated with cassava wastewater).

According to the results in Table 2, N and P contents obtained in the present study were higher than those found by Parry *et al.* (2008), who analyzed the contents of macronutrients in cowpea shoots in soil fertilized with two P doses and in different sowing periods and obtained maximum values of 24.5 g kg^{-1} and 1.7 g kg^{-1}, respectively. Means of K did not differ statistically, and the maximum value (36.38 g kg^{-1}) was obtained under fertigation with NPK.

Mean S contents were statistically different between treatments, and the maximum value was approximately 113.76 mg kg^{-1}, obtained under fertigation with human urine associated with

cassava wastewater and mineral fertilizer (5 – U+W+P). This value is within the range are considered as adequate for common beans according to EMBRAPA (2009), from 18 to 50 mg kg^{-1}, and below the adequate value for cowpea, which is 1.5 ± 0.4 g kg^{-1} according to Freire Filho *et al.* (2005).

Except for S contents, all treatments led to N, P and K contents considered as adequate for common beans (Fageria *et al.*, 1996). For cowpea, Freire Filho *et al.* (2005) state that adequate P and K contents should be 1.4 ± 0.3 and 32.0 ± 3.6 g kg^{-1}, respectively. Thus, according to Table 2, all treatments met the needs for N and P by cowpea plants and Treatments 1 (1 – NPK) and 5 (5 - U+W+P) also met the needs of K, indicating that fertigation management was satisfactory in the present study for the cowpea crop.

In a study carried out by (Upreti *et al.*, 2011) with different crops (onion, potatoes, wheat, radish, rice), using mineral (NPK) and organic fertilizations (human urine), and with distinct spaces, it was observed that human urine positively affected the evaluated crops.

According to the summary of analysis of variance (Table 3), there was significant statistical difference between treatments ($p < 0.05$) for stem diameter (SD), shoot fresh matter (SFM) and shoot dry matter (SDM), whereas the other variables did not differ statistically between treatments, and these results corroborate those found in the literature. Pereira *et al.* (2013) studied the effects of three sources of organic fertilization (bovine manure, goat manure and earthworm humus) on cowpea and found no significant effect on number of leaves and plant height. Sousa *et al.* (2013) evaluated the effect of increasing doses of bovine biofertilizer on cowpea growth at 4 days after sowing and obtained significant statistical difference for stem diameter (SD) and shoot dry matter (SDM). Alves *et al.* (2009), studying the effects of increasing doses of biofertilizer obtained by whey fermentation and applied through fertigation in cowpea, found significant effect on plant height and number of leaves and non-significant effect on stem diameter.

Table 3. Summary of analysis of variance and means for number of leaves per plant (NL, leaves $plant^{-1}$), plant height (PH, cm), stem diameter (SD, mm), leaf area (LA, cm^2), shoot fresh matter (SFM, g $plant^{-1}$) and shoot dry matter (SDM, g $plant^{-1}$) of cowpea fertigated with human urine and cassava wastewater.

SV	Mean Square						
	DF	NL	PH	SD	LA	SFM	SDM
Treatments	4	4.55000^{ns}	39.59375^{ns}	1.21923*	10136.66698^{ns}	130.99785*	2.01556*
Residual	15	5.65000	13.03750	0.26424	18187.72725	29.37111	0.49281
CV%	-	12.81	10.82	6.18	16.00	11.45	10.54
Treatments	Means						
1 - (NPK)		17.00a	28.87b	7.95ab	802.24a	47.88ab	6.96ab
2 - (U)		18.75a	37.50a	8.78a	874.18a	47.7ab	6.69ab
3 - (W)		18.00a	32.37ab	7.54b	860.66a	41.85b	5.98b
4 - (U+W)		19.50a	34.50ab	8.80a	898.96a	56.34a	7.67a
5 - (U+W+P)		19.50a	33.62ab	8.50ab	779.28a	42.93b	6.00b

Note: SV – Source of variation; DF – Degrees of freedom; CV – Coefficient of variation; NPK – Nitrogen, phosphorus and potassium; U – Human urine; W – Cassava wastewater; U + W – Human urine plus cassava wastewater; U+W+P – Human urine plus cassava wastewater plus phosphorus; (^{ns,} **, *) - Not significant, significant at 0.01 and 0.05 probability levels by F test; Means followed by the same letter in the column do not differ by Tukey test ($p > 0.05$).

Significant differences were observed for plant height (PH), stem diameter (SD), shoot fresh matter (SFM) and shoot dry matter (SDM).

No statistical difference was found in the means of number of leaves (NL) and leaf area

(LA). Except for the Treatment 5 (5 – U+W+P) for leaf area, the means of number of leaves and leaf area in the other treatments (2 – U, 3 – W, 4 – U+W and 5 – U+W+P) were higher than those in the control (1 – NPK). A probable explanation for that can be related to the supply of other nutrients contained in yellow water and cassava wastewater, which were available to be assimilated by cowpea plants.

The maximum mean of number of leaves was 19.50 leaves per plant, obtained under fertigation with yellow water associated with cassava wastewater (4 – U+W) and these effluents associated with phosphorus (5 – U+W+P). Similar results were found by Silva *et al.* (2010), who obtained on average 20.50 leaves per plant of cowpea fertigated with 30 L ha^{-1} day^{-1} of bovine biofertilizer, at 45 days.

For plant height, it can be observed that there were no differences between the means of plants fertigated with only cassava wastewater (3 – W), yellow water associated with cassava wastewater (4 – U+W) and these effluents associated with mineral phosphorus (5 – U+W+P). Minimum mean of PH (28.87 cm) was obtained with NPK fertigation, whereas maximum values (34.50 and 37.5 cm) were found in plants fertigated with yellow water associated with cassava wastewater (4 – U+W) and only yellow water (3 – U), respectively.

The means of stem diameter of plants fertigated with NPK and yellow water associated with cassava wastewater and these effluents associated with mineral P (5 – U+W+P) did not differ statistically, and the same occurred with Treatments 2 (yellow water) and 4 (yellow water associated with cassava wastewater). The minimum mean (7.54 mm) was obtained in plants fertigated with cassava wastewater, whereas the maximum values of 8.78 and 8.80 mm were obtained with fertigation using yellow water (2 – U) and yellow water associated with cassava wastewater (4 – U+W), respectively. Evaluating the effect of cassava wastewater applied by fertigation on cowpea, at 35 DAS, Schwengber *et al.* (2010) observed that the highest value of stem diameter (2.99 mm) was obtained with application of 100 m^3 ha^{-1}. Cruz *et al.* (2014), evaluating cowpea at 40 days after emergence under application of 4.0 L m^{-1} of organic biofertilizer produced by accelerated biodegradation of wastes of coconut straw and inflorescences, neem tree pruning and cashew tree pruning, observed stem diameter of more than 6.0 mm, which is lower than the value found in the present study.

For leaf area (LA), the maximum mean was 898.96 cm^2, observed in plants fertigated with yellow water associated with cassava wastewater. Studying the growth of cowpea fertigated with wastewater, Rebouças *et al.* (2010) found maximum leaf area of 943.0 cm^2, which is very close to that observed in the present study.

The values of shoot fresh matter (SFM) were statistically different between the treatments tested. Its minimum (41.85 g $plant^{-1}$) and maximum (56.34 g $plant^{-1}$) values were obtained in plants fertigated with cassava wastewater and with yellow water associated with cassava wastewater (4 – U+W), respectively.

For shoot dry matter (SDM), there was a statistical difference between the means of Treatments 3 (cassava wastewater), 4 (yellow water associated with cassava wastewater) and 5 (yellow water associated with cassava wastewater and mineral P), and the results were not significant for the Treatments 1 (NPK) and 2 (yellow water). Minimum and maximum means were 5.98 and 7.67 g $plant^{-1}$, obtained in plants fertigated with cassava wastewater (3 – W) and yellow water associated with cassava wastewater (4 – U+W), respectively.

In a study by Messa *et al.* (2016) to determine the release of fertilizers in clay soil, it was observed that most of the fertilizers used in the study were released into the soil solution more quickly when at a pH between 4.0 to 5.5.

There probably was influence of the pH of the soil solution; its fluctuation can determine the availability of nutrients for the plants.

Evaluating the use of bovine biofertilizer and treated wastewater in cowpea fertigation,

Sousa *et al.* (2013) and Rebouças *et al.* (2010) obtained positive response with gains in shoot dry matter. Using bovine manure to fertilize cowpea at 35 days after planting, Bastos *et al.* (2012) found fresh shoot matter of 27.30 g per plant.

According to the data in Table 3, although there was no significant statistical difference between the means of number of leaves (NL), plant height (PH) and leaf area (LA), when plants were fertigated with wastewaters the values were higher than those of plants fertigated with chemical fertilizer formulated with NPK. In other words, the nutrients present in the yellow water and cassava wastewater caused positive effects on the cowpea crop. Except for the number of leaves and plant height, fertigation with yellow water associated with cassava wastewater led to maximum means for the variables SD, LA, SFM and SDM. A probable explanation is that the nutrients present in the yellow water and cassava wastewater were well assimilated by the plants, indicating great nutritional potential for the associated use of these effluents in agricultural cultivation.

The fact of effect variables promoted different results for the response variables; this action possibly can be associated with the fact of synergism or nutritional antagonism in the soil.

According to Fageria (2001), excess ions in the soil solution, such as potassium, which is an abundant nutrient in the cassava wastewater, can affect the absorption of other essential nutrients by plants, such as calcium, magnesium, zinc and manganese, due to the antagonism between potassium and these elements.

4. CONCLUSIONS

N, P and S contents, stem diameter, shoot fresh matter and shoot dry matter of cowpea were influenced by the fertigation with yellow water, association between yellow water and cassava wastewater, and these effluents associated with the source of P;

Maximum contents of N, P, K and S were obtained by fertigation with NPK and human urine plus cassava wastewater associated with the mineral source of P;

Human urine and cassava wastewater applied by fertigation have potential to meet the needs of the cowpea crop for N, P and K; and

Maximum means of most growth variables were obtained in plants fertilized with human urine associated with cassava wastewater.

5. REFERENCES

APHA; AWWA; WEF. **Standard Methods for the examination of water and wastewater.** 21st ed. Washington DC, 2005.

ALVES, S. V.; ALVES, S. S. V.; CAVALCANTI, M. L. F.; DEMARTELAERE, A. C. F.; TEÓFILO, T. M. S. Desempenho produtivo do feijoeiro em função da aplicação de biofertilizante. **Revista Verde de Agroecologia e Desenvolvimento Sustentável**, v. 4, n. 2, p. 113–117, 2009.

ARAÚJO, N. C.; FERREIRA, T. C.; OLIVEIRA, S. J. C.; GONÇALVES, C. P.; ARAÚJO, F. A. C. Avaliação do uso de efluente de casas de farinha como fertilizante foliar na cultura do milho (*Zea mays* L.). **Engenharia na Agricultura**, v. 20, n .4, p. 340 - 349, 2012. http://dx.doi.org/10.13083/1414-3984.v20n04a06

ARAÚJO, N. C.; OLIVEIRA, S. J. C.; FERREIRA, T. C.; LIMA, V. L. A.; QUEIROZ, A. J. P.; ARAÚJO, F. A. C. Crescimento e Produtividade de Milho Fertilizado com Manipueira como Fonte Alternativa de Nutrientes. **Tecnologia e Ciência Agropecuária**, v. 9, n. 2, p. 31 - 35, 2015a.

ARAÚJO, N. C.; COURA, M. A.; OLIVEIRA, R.; SABINO, C. M. B.; OLIVEIRA, S. J. C. Cultivo hidropônico de milho fertirrigado com urina humana como fonte alternativa de nutrientes. **Irriga**, v. 20, n. 4, p. 718-729, 2015b. https://dx.doi.org/10.15809/irriga.2015v20n4p718

BARRETO, M. T. L.; ROLIM, M. M.; PEDROSA, E. M. R.; MAGALHÃES, A. G.; TAVARES, U. E.; DUARTE, A. S. Atributos químicos de dois solos submetidos à aplicação de manipueira. **Agrária - Revista Brasileira de Ciências Agrárias**, v. 8, n. 4, p. 528-534, 2013. https://dx.doi.org/10.5039/agraria.v8i4a2425

BARRETO, M. T. L.; MAGALHÃES, A. G.; ROLIM, M. M.; PEDROSA, E. M. R.; DUARTE, A. S.; TAVARES, U. E. Desenvolvimento e acúmulo de macronutrientes em plantas de milho biofertilizadas com manipueira. **Revista Brasileira de Engenharia Agrícola e Ambiental**, v. 18, n. 5, p. 487–494, 2014. http://dx.doi.org/10.1590/S1415-43662014000500004

BASTOS, V. J.; MELO, D. A.; ALVES, J. M. A.; UCHÔA, S. C. P.; SILVA, P. M. C.; TEIXEIRA JUNIOR, D. L. Avaliação da fixação biológica de nitrogênio em feijão-caupi submetido a diferentes manejos da vegetação natural na savana de Roraima. **Revista Agro@mbiente On-line**, v. 6, n. 2, p. 133-139, 2012. http://dx.doi.org/10.18227/1982-8470ragro.v6i2.851

BENETT, C. G. S.; LIMA, M. F.; BENETT, K. S. S.; CAIONE, G.; PELLOSO, M. F. Formas de aplicação e doses de nitrogênio em cobertura na cultura do feijão-caupi. **Revista Agrotecnologia**, v. 4, n. 1, p. 17-30, 2013. https://dx.doi.org/10.12971/1449

BONVIN, C.; ETTER, B.; UDERT, K. M.; FROSSARD, E.; NANZER, S.; TAMBURINI, F.; OBERSON, A. Plant uptake of phosphorus and nitrogen recycled from synthetic source-separated urine. **Ambio**, v. 44, n. 2, p. 217–227, 2015. http://dx.doi.org/10.1007/s13280-014-0616-6

BOTTO, M. P.; MUNIZ, L. F.; AQUINO, B.; SANTOS, A. B. Produtividade da mamona Cultivar BRS nordestina fertilizada com urina humana na agricultura de pequeno porte. **Revista AIDIS de Ingeniería y Ciencias Ambientales: investigación, desarrollo y práctica**, v. 10, n. 1, p. 113-124, 2017.

CONCEIÇÃO, A. A.; RÊGO, A. P. B.; SANTANA, H.; TEIXEIRA, I.; CORDEIRO MATIAS, A. G. C. Tratamento de efluentes resultantes do processamento da mandioca e seus principais usos. **Revista Meio Ambiente e Sustentabilidade**, v. 4, n. 2, p. 118–130, 2013.

CRUZ, J. S.; SOUSA, E. C.; BELTRÃO JÚNIOR, J. A.; ALMEIDA, J. M. U.; LUNA, N. S. Comportamento vegetativo do feijão caupi irrigado e adubado sob diferentes doses de biofertilizante orgânico. **Revista Brasileira de Agricultura Irrigada,** v. 8, n. 2, p. 154-160, 2014. https://dx.doi.org/10.7127/rbai.v8n200241

DANTAS, M. S. M.; ROLIM, M. M.; DUARTE, A. S.; PEDROSA, E. M. R.; TABOSA, J. N.; DANTAS, D. C. Crescimento do girassol adubado com resíduo líquido do processamento de mandioca. **Revista Brasileira de Engenharia Agrícola e Ambiental**, v.19, n.4, p.350–357, 2015. http://dx.doi.org/10.1590/1807-1929/agriambi.v19n4p350-357

DUARTE, A. S.; SILVA, Ê. F. F.; ROLIM, M. M.; FERREIRA, R. F. A. L.; MALHEIROS, S. M. M.; ALBUQUERQUE, F. S. Uso de diferentes doses de manipueira na cultura da alface em substituição à adubação mineral. **Revista Brasileira de Engenharia Agrícola e Ambiental,** v. 16, n. 3, p. 262–267, 2012.

EMBRAPA. **Manual de análise química de solos, plantas e fertilizantes**. 2. ed. Brasília, DF: Embrapa Informações Tecnológica, 2009, 627p.

FAGERIA, N. K.; OLIVEIRA, I. P.; DUTRA, L. G. **Deficiências nutricionais na cultura do feijoeiro e suas correções.** Goiânia: Embrapa-CNPAF-APA, 1996. 40 p. (Documentos, n. 65).

FAGERIA, V. D. Nutrient interactions in crop plants. **Journal of plant nutrition,** v. 24, n. 8, p. 1269-1290, 2001.

FREIRE FILHO, F. R.; LIMA, J. A. A.; RIBEIRO, V. Q. **Feijão-caupi**: Avanços tecnológicos. Brasília, DF: Embrapa Informações Tecnológicas, 2005. 519 p.

FREIRE FILHO, F. R.; RIBEIRO, V. Q.; ROCHA, M. M.; SILVA, K. J. D.; NOGUEIRA, M. S. R.; RODRIGUES, E. V. **Feijão-caupi no Brasil: produção, melhoramento genético, avanços e desafios**. Teresina: Embrapa Meio-Norte, 2011, 84 p.

KVARNSTRÖM, E.; EMILSSON, K.; STINTZING, A. R.; JOHANSSON, M.; JÖNSSON, H.; PETERSENS, E.; SCHÖNNING, C.; CHRISTENSEN, J.; HELLSTRÖM, D.; QVARNSTRÖM, L. RIDDERSTOLPE, P.; DRANGERT, JAN-O. **Separação de urina**: Um passo em direção ao saneamento sustentável. Estocolmo: Instituto Ambiental de Estocolmo, 2006. Available at: www.ecosanres.org. Access: 24 Jan. 2017.

KARAK, T.; BHATTACHARYYA, P. Human urine as a source of alternative natural fertilizer in agriculture: A flight of fancy or an achievable reality. **Resources, Conservation and Recycling**. v. 55, n. 4, p. 400 – 408, 2011.

LEAL, F. R. R.; LEAL, M. P. C.; ALBUQUERQUE, C. L. C. D. Avalição do efeito da manipueira em aplicação vias foliar e substrato na produção de coentro. **Cadernos de Agroecologia**, v. 10, n.3, 2015.

LIMA, C. J. G. S.; OLIVEIRA, F. A.; MEDEIROS, J. F.; OLIVEIRA, M. K. T.; FILHO, A. F. O.; Modelos matemáticos para estimativa de área foliar de feijão caupi. **Revista Caatinga**, v. 21, n. 1, p.120-127, 2008.

MALAVOLTA, E.; VITTI, G. C.; OLIVEIRA, A.S. **Avaliação do estado nutricional das plantas: princípios e aplicações**. Piracicaba: Associação Brasileira para Pesquisa da Potassa e do Fosfato, 1989. 201 p.

MESSA, L. L.; FROES, J. D.; SOUZA, C. F.; FAEZ, R. Chitosan-clay hybrid for encapsulation of fertilizers and release sustained of potassium nitrate fertilizer. **Química Nova**, v. 39, n. 10, p. 1215-1220, 2016.

NOVAIS, R. F.; NEVES, J. C. L.; BARROS, N. F. Ensaio em ambiente controlado. In: OLIVEIRA, A. J. (Ed.). **Métodos de pesquisa em fertilidade do solo**. Brasília: Embrapa-SEA p. 189-253, 1991.

PARRY, M. M.; KATO, M. S. A.; CARVALHO, J. G. Macronutrientes em caupi cultivado sob duas doses de fósforo em diferentes épocas de plantio. **Revista Brasileira de Engenharia Agrícola e Ambiental**, v. 12, n. 3, p. 236–242, 2008. http://dx.doi.org/10.1590/S1415-43662008000300003

PEREIRA, R. F; CAVALCANTE, S. N.; LIMA, A. S.; MAIA FILHO, F. C. F.; SANTOS, J. G. R. Crescimento e rendimento de feijão vigna submetido à adubação orgânica. **Revista Verde de Agroecologia e Desenvolvimento Sustentável**, v. 8, n. 3, p. 91 - 96, 2013.

PESSUTI, C. A. A.; HERMES, E.; NEVES, A. C.; SILVA, R. P.; PENACHIO, M. ZENATTI, D. C. Diferentes doses de biofertilizante proveniente da digestão anaeróbia de efluente de processamento de mandioca no cultivo de soja. **Revista Gestão & Sustentabilidade Ambiental**, v. 4, p. 556-564, 2015.

RANASINGHE, E. S. S.; KARUNARATHNE, C. L. S. M.; BENERAGAMA, C. K.; WIJESOORIYA, B. G. G. Human urine as a low cost and effective nitrogen fertilizer for bean production. **Procedia food science**, v. 6, p. 279-282, 2016.

REBOUÇAS, J. R. L.; DIAS, N. S.; GONZAGA, M. I. S.; GHEYI, H. R.; SOUSA NETO, O. N. Crescimento do feijão-caupi irrigado com água residuária de esgoto doméstico tratado. **Revista Caatinga**, v. 23, n. 1, p. 97-102, 2010.

SANTOS, M. H. V.; ARAÚJO, A. C.; SANTOS, D. M. R.; LIMA, N. S.; LIMA, C. L. C.; SANTIAGO, A. D. Uso da manipueira como fonte de potássio na cultura da alface (*Lactuca sativa* L.) cultivada em casa-de-vegetação. **Acta Scientiarum Agronomy**, Maringá, v. 32, n. 4, p. 729-733, 2010. https://dx.doi.org/10.4025/actasciagron.v32i4.4819

SANTOS JÚNIOR, J. A.; SOUZA, C. F.; PÉREZ-MARIN, A. M.; CAVALCANTE, A. R.; MEDEIROS, S. S. Interação urina e efluente doméstico na produção do milheto cultivado em solos do semiárido paraibano. **Revista Brasileira de Engenharia Agrícola e Ambiental,** v. 19, n. 5, p. 456–463, 2015. https://dx.doi.org/10.1590/1807-1929/agriambi.v19n5p456-463

SANTOS, O. S. N.; TEIXEIRA, M. B.; QUEIROZ, L. M.; FADIGAS, F. S.; PAZ, V. P. S.; SILVA, A. J. P.; KIPERSTOK, A. Nitrogen recycling through fertilization of Bermuda grass using human urine diluted in water. **Revista Brasileira de Agroecologia**, v. 11, n. 3, p. 164-171, 2016.

SILVA, F. A. M.; VILAS-BOAS, R. L.; SILVA, R. B. Resposta da alface à adubação nitrogenada com diferentes compostos orgânicos em dois ciclos sucessivos. **Acta Scientiarum Agronomy**, v. 32, p. 131-137, 2010. https://dx.doi.org/10.4025/actasciagron.v32i1.1340

SILVA, F. A. S.; AZEVEDO, C. A. V. They assistat software version 7.7 and its use in the analysis of experimental data. **African Journal of Agricultural Research**, v. 11, n. 39, p. 3733 – 3740, 2016. https://dx.doi.org/10.5897/AJAR2016.11522

SILVA JUNIOR, J. J.; COELHO, E. F.; SANT'ANA, J. A. V.; SANTANA JUNIOR, E. B.; PAMPONET, A. J. M. Uso da manipueira na bananeira 'terra maranhão' e seus efeitos no solo e na produtividade. **Irriga**, v. 17, n. 3, p. 353 - 363, 2012.

SCHWENGBER, J. A. M.; SILVA, F. F.; SMIDERLE, O. J.; SCHWENGBER, D. R. Nodulação do feijão-caupi em função da aplicação de três águas de farinheira. **Revista em Agronegócios e Meio Ambiente**, v. 3, n. 2, p. 135-146, 2010.

SOUSA, J. T.; HENRIQUE, I. N.; LOPES, W. S.; LEITE, V. D. Gerenciamento Sustentável de Água Residuária Doméstica. **Health and Environment Journal**, v. 9, n. 1, 2008.

SOUSA, G. G.; SANTOS, E. M.; VIANA, T. V. A.; OLIVEIRA, C. M. B.; ALVINO, F. C. G.; AZEVEDO, B. M. Fertirrigação com biofertilizante bovino na cultura do feijoeiro. **ACSA – Agropecuária Científica no Semi-Árido**, v. 9, n. 4, p. 76 - 82, 2013.

UPRETI, H.; SHRESTHA, P.; PAUDEL, P. Effect of human urine as fertilizer on crop production. **Agronomy Journal of Nepal**, v. 2, p.168-172, 2011.

Ambiente & Água - An Interdisciplinary Journal of Applied Science
ISSN 1980-993X – doi:10.4136/1980-993X
www.ambi-agua.net
E-mail: ambi.agua@gmail.com

Sap flow in 'Tommy Atkins' mango trees under regulated deficit irrigation

ARTICLES doi:10.4136/ambi-agua.2316

Received: 17 Aug. 2018; Accepted: 06 Feb. 2019

Carlos Elizio Cotrim[1*]; Marcelo Rocha dos Santos[1]; Maurício Antônio Coelho Filho[2]; Eugênio Ferreira Coelho[2] João Abel da Silva[1]

[1]Instituto Federal de Educação, Ciência e Tecnologia Baiano (IFBaiano), Guanambi, BA, Brasil Setor de Agricultura. E-mail: carlos.cotrim@ifbaiano.edu.br, marcelo.rocha@ifbaiano.edu.br, joaoabelsilva@yahoo.com.br
[2]Embrapa Mandioca e Fruticultura, Cruz das Almas, BA, Brasil
E-mail: mauricio-antonio.coelho@embrapa.br, eugenio.coelho@embrapa.br
[*]Corresponding author

ABSTRACT

Knowledge of transpiration is of fundamental importance for improving irrigation management. This study measured sap flow of the 'Tommy Atkins' mango tree using Granier's thermal dissipation probe method under regulated deficit irrigation. The work was conducted in a 10-year-old 'Tommy Atkins' mango orchard, irrigated by micro sprinkler, located in the Irrigated Perimeter of Ceraíma, in Guanambi, Bahia, Brazil. Sap flow measurements were carried out on three consecutive days in plants under regulated deficit irrigation, with reductions of 30 and 60% of crop evapotranspiration in three phases of fruit development; beginning of flowering to early fruit growth (Phase I), fruit expansion (Phase II) and physiological maturation of fruits (Phase III). Regulated deficit irrigation led to reduced sap flow in 'Tommy Atkins' mango tree.

Keywords: irrigation management, Granier, transpiration, water use efficiency.

Fluxo de seiva em mangueiras 'Tommy Atkins' sob irrigação com déficit controlado

RESUMO

O conhecimento da transpiração é de fundamental importância para aprimoramento do manejo da irrigação. Objetivou-se com o presente trabalho determinar o fluxo de seiva da mangueira 'Tommy Atkins' utilizando o método da sonda de dissipação térmica de *Granier*, sob irrigação com déficit controlado. O trabalho foi desenvolvido em um pomar de mangueira 'Tommy Atkins' com 10 anos de idade, irrigado por microaspersão, localizada no Perímetro Irrigado de Ceraíma, no município de Guanambi, Bahia. A determinação do fluxo de seiva foi realizada em três dias consecutivos em plantas sob irrigação com déficit controlado, com redução de 30 e 60% da evapotranspiração da cultura em três fases de desenvolvimento do fruto, início da floração ao pegamento dos frutos (Fase I), fase de expansão do fruto (Fase II) e fase de maturação fisiológica do fruto (Fase III). Verificou-se que o déficit hídrico controlado causa redução no fluxo de seiva em mangueiras 'Tommy Atkins'.

Palavras-chave: eficiência de uso da água, Granier, manejo da irrigação, transpiração.

1. INTRODUCTION

The search for increasing yield and quality of fruits implies knowledge of parameters related to irrigation water management. Scarcity and irregularity of rainfall in the Northeast of Brazil indicate irrigation need over the whole year to guarantee production. Consoli *et al.* (2017) mention that climate change will impact water resources within a medium to long-term period. Water-use efficiency is therefore essential in irrigated agriculture due to less water requirement from water resources.

The increase in water-use efficiency might be attained by using high-efficient irrigation systems, such as trickle irrigation combined with the use of water-deficit irrigation strategies. Among these strategies, regulated deficit irrigation (RDI) and partial root-zone drying (PRD) stand out (Santos *et al.*, 2017; Cotrim *et al.*, 2017; Santos *et al.*, 2016a; Lima *et al.*, 2015; Santos *et al.*, 2015; Sampaio *et al.*, 2014).

Soil water conditions change when using water-deficit strategies; consequently, water conditions of plants, gas exchanges, and leaf temperature are also altered. These variables influence growth, developing, and yielding (Santos and Martinez, 2013). There is some research in the literature on the use of water-deficit strategies in mango trees grown in semi-arid regions of Brazil and how it relates to gas exchanges (Santos *et al.*, 2016b; 2016c; Santos and Martinez, 2013), to root distribution (Santos *et al.*, 2014a), to water uptake (Santos and Martinez, 2013), to flower induction (Faria *et al.*, 2016a), and to leaf nutrient content (Faria *et al.*, 2016b). Nonetheless, information regarding sap flow as an alternative to determine water demand of mangoes under deficit irrigation is lacking.

Among the methodologies used for measuring transpiration of trees, those based on the input of heat to plant stems (Heat Stem Balance Method, Thermal Dissipation Method, and the Heat-Pulse Method) have enabled advances in water relations and are tools for measuring transpiration (Boehringer *et al.*, 2013; Pinto Jr. *et al.*, 2013; Marin *et al.*, 2008; Coelho Filho *et al.*, 2005). These sap flow techniques are non-destructive (Hernandez-Santana *et al.*, 2016), are easy to install, and can simultaneously monitor several plants.

This study measured sap flow as an alternative to determine water demand of 'Tommy Atkins' mango trees under regulated deficit irrigation by using Granier's thermal dissipation probe method.

2. MATERIAL AND METHODS

The experiment was carried out in a 10-year-old 'Tommy Atkins' mango orchard, with trees spaced 8 x 8 meters apart, located at the Irrigated Perimeter of Ceraíma, in the municipality of Guanambi, Bahia state, Brazil (14º17'27'' S and 42º46'53'' W), from June to December 2007. The climate of the region is semi-arid, with altitude of 525 m, average annual rainfall of 680 mm, and average annual temperature of 26ºC. Main climate parameters were measured during the period of experiment from a weather station 500 m away from the experimental area (Table 1).

The soil of the experimental area is a sandy loam-textured Eutrophic Fulvic Neosol with high activity clay. At the depths of 0.00 to 0.20 and 0.20 to 0.40 m, the soil exhibited the following characteristics: density of 1,610 and 1,560 kg m^{-3}; particle density of 2,740 and 2,810 kg m^{-3}; sand, 0.507 and 0.485 kg kg^{-1}; silt, 0.296 and 0.300 kg kg^{-1}; clay, 0.197 and 0.215 kg kg^{-1}, respectively.

Table 1. Monthly precipitation values (P), mean air temperature (T), relative humidity (RH), reference evapotranspiration (ET_o), solar irradiance (SI) and wind speed (WS) for district of Ceraíma – Guanambi, in the year 2007.

Variables	Jun	Jul	Aug	Sep	Oct	Nov	Dec
P (mm)	0.00	0.00	0.00	0.00	0.00	170.00	129.10
T (ºC)	22.70	24.60	24.80	27.30	28.10	25.30	24.60
RH (%)	70.80	69.60	68.10	61.80	61.10	67.80	69.60
ET_o (mm day^{-1})	5.04	4.95	6.02	6.38	7.04	5.59	4.97
SI (h day^{-1})	8.68	8.64	9.39	9.17	8.05	6.45	6.53
WS (m s^{-1})	0.42	3.91	3.88	4.20	4.66	3.09	2.35

Tommy Atkins trees were watered to different irrigation depths (Table 2) from which regulated water deficits at two different percentages of crop evapotranspiration (ETc) were applied during three fruit-developing phases: fruit setting (Phase I), fruit growth (Phase II), and fruit ripening or physiological maturation (Phase III). Each treatment consisted of a single mango tree.

Table 2. Treatments: irrigation water depths applied at three fruit developing phases.

Treatment	Irrigation - % of ETc by phase		
	I	II	III
Rainfed – No irrigation at all phases	0	0	0
Full Irrigation – Irrigation with 100%ETc in all phases	100	100	100
RDI60PI – Irrigation with 60%ETc in phase I and full in phases II and III	60	100	100
RDI60PII – Irrigation with 60%ETc in phase II and full in phases I and III	100	60	100
RDI60PIII – Irrigation with 60%ETc in phase III and full in phases I and II	100	100	60
RDI30PI – Irrigation with 30%ETc in phase I and full in phases II and III	30	100	100
RDI30PII – Irrigation with 30%ETc in phase II and full in phases I and III	100	30	100
RDI30PIII– Irrigation with 30%ETc in phase III and full in phases I and II	100	100	30

Each tree was irrigated daily by a micro-sprinkler with a discharge rate of 56 l h^{-1}. Water depths were corrected to the respective percentage (30, 60, and 100% of ETc) by different valves installed at the beginning of the sub-mainline, so that the irrigation run-time could be regulated. Irrigation depth was determined by reference evapotranspiration, location coefficient (Kl = 0.80) and crop coefficients, as the latter varied from 0.45 to 0.87 from flowering to fruit ripening (Cotrim *et al.*, 2017; Santos *et al.*, 2014b). ET_o was measured by an automatic weather station through the Penman-Monteith method. The total amount of water applied for each treatment is shown in Figure 1.

After the data collection to calculate the sap flow using the Granier method, the leaf area of each branch where probe sensors were installed was estimated using the methodology proposed by Oliveira *et al.* (2005), described later.

The conducting sap flow area of the stem (xylem area) was estimated using its internal diameter (D_{int}), determined by Vellame *et al.* (2012), through the use of the destructive method with application of dyes in several trunks and branches of hose with different external diameters (D_{ext}), according to Equation 1.

$$D_{int} = 0.8746 \times D_{ext} \quad (1)$$

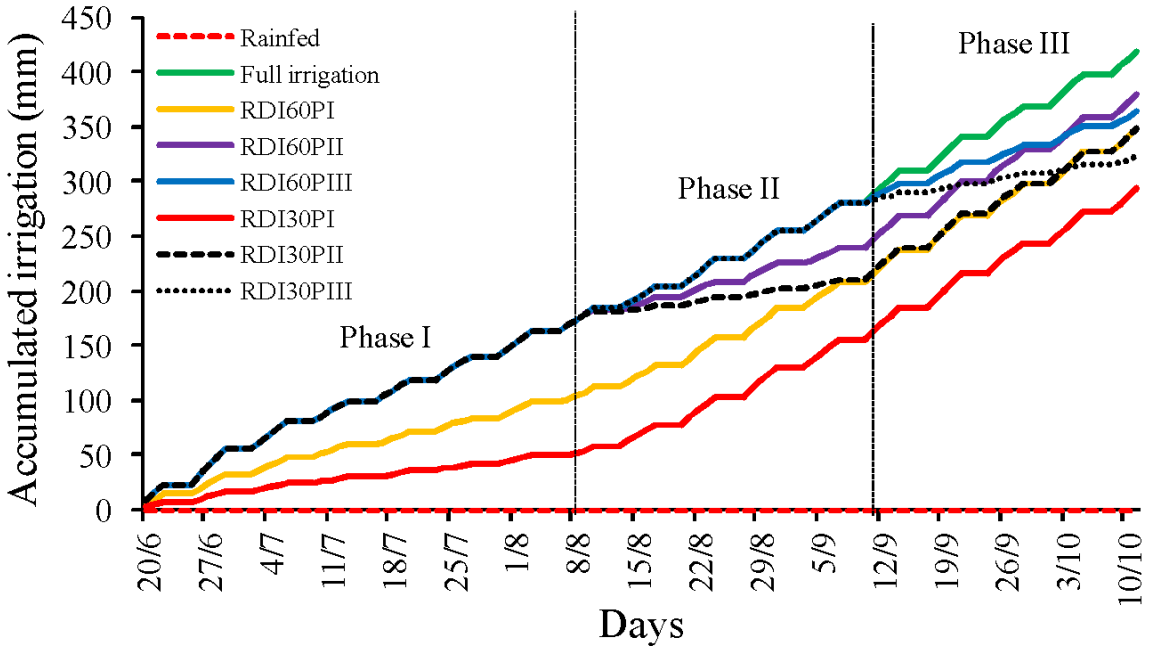

Figure 1. Total amount of water applied to 'Tommy Atkins' mango trees for different irrigation depths during the production cycle of the crop.

2.1. Estimation of sap flow density

Thermal dissipation probes (TDP) were installed at branches of similar diameters and located in the mid-section of tree crowns of eight mango trees, one for each treatment.

Probe sensors installed in the branches were completely insulated with neoprene and aluminum foil to prevent external interferences in the natural temperature gradient of the plant's branches. Besides the eight heated sensor probes, three additional unheated probes were installed to measure the ambient temperature of the wood during the experiment, which would be used afterwards as reference probes for correcting the estimated sap flow, following the methodology recommended by Granier (1985).

Probe sensors were made and calibrated in the Irrigation and Fertigation Laboratory of EMBRAPA Cassava and Tropical Fruits (Brazilian Agriculture Research Corporation) (Coelho Filho *et al.*, 2006; Vellame *et al.*, 2012). Each probe consisted of a continuously heated element at constant power of 0.1W per centimeter and an unheated probe (reference probe), which has an internal thermocouple.

2-cm-long probes needed a power of 0.2 W for the heating process. When making each thermal dissipation probe (TDP), we used two veterinary needles with a diameter of 1.6 mm, connected to one another by a thermocouple made of two copper wires (10 cm each) and a constantan wire (18 cm) with a diameter of 0.5 mm.

In the heated probe, a constantan wire of 0.5 mm of diameter and 25 cm long was put through the needle, and then, the wire's tip was wound around the needle. After that, the external part of the needle's tube was coated with resin, with 2 to 3-cm-long tips to be connected to the heating source with adjustable voltage.

2-cm-long probes were inserted into the mango's stem through bores made by a drill, 10 cm apart. The holes were covered by a cylinder made of brass with 3 mm in diameter and 2 cm in length. The empty space between the probes and cylinders was filled with thermal grease to improve the sensibility of the thermal sensors.

Regarding the recording of temperature differences between the two probes (heated and unheated probes) and the solar radiation, a system composed of a data logger (CR10X Campbell SCi) and a multiplexer (AM 416 Relay Multiplexer, CampbellSCi) was used.

To correct the stem's natural temperature gradient, temperature differences were measured by three unheated probes during the whole data-collecting period to measure sap flow. Natural temperature gradient data of the three unheated sensor probes were compared to natural temperature gradients generated by each one of the 8 probes over the period without heating; as a result, estimation models were created. These can estimate natural temperature gradients of heated probes as a function of natural temperature gradients of unheated probes, for each probe, individually.

Temperature differences of unheated probes were corrected by Equation 2.

$$\Delta T = \Delta T_{mesured} - \Delta TN_{estimated} \quad (2)$$

Where, ΔT is the corrected temperature difference (ºC); $\Delta T_{measured}$ is the temperature difference measured by the non-corrected probe (°C) and $\Delta T_{\text{estimated}}$ is the natural temperature difference estimated by the models (°C).

Flow index (*K*) is the relationship between sap flux density and temperature difference between probes installed in the trunk.*K* is defined using Equation 3, developed by Granier (1985):

$$K = \frac{(\Delta TM - \Delta T)}{\Delta T} = 0.0206 \times Js^{0.8124} \quad (3)$$

Where, ΔTM is the maximum temperature difference obtained by the probe on a given day, °C; ΔT is the current difference temperature, °C; and *Js* is sap flux density, $m^3m^{-2}day^{-1}$;

Sap flow was calculated by using the conducting sapwood area of the xylem, as described by Equation 4:

$$F = 118.99 \times 10^{-6} \times K^{1.231} \times AS \quad (4)$$

Where *F* is sap flow, L day^{-1} and *AS* is the area of the xylem, m^{-2}.

Two power supplies were used based on the total electrical resistance measured at the probes (multimeter) and on the voltage necessary, which was calculated by Equation 5, derived from Ohm's law.

$$V = \sqrt{P \times R} \quad (5)$$

Where *V* is the voltage of the adjustable power supply, volts; *P* is the power used to heat a 2- cm-long probe, watts; and *R* is the overall resistance of the collection of probes, ohms.

Leaf area of the branches were measured by counting the number of leaves and by estimating the average area per leaf. The latter was determined by measuring the length and width of three hundred leaves collected from approximately 30 randomly-selected plants (33% of the orchard), so that leaves of all sizes were measured. Leaf area was calculated through Equation 6, where 0.60 is a correction factor used for mango (Oliveira *et al.*, 2005).

$$LA = (L \times W \times 0.60) \times TNL \quad (6)$$

Where, *LA* is leaf area, m^2; *L* is the mean length of leaves, m; *W* is the mean width of the leaves, m; and *TNL* is the total number of leaves of the plant or branch.

Diameters of branches and trunks as well as leaf areas of the branch and the whole tree for each treatment are found in Table 3.

Table 3. Diameters of the branch and trunk and leaf area of the branch and the whole 'Tommy Atkins' mango tree where the thermal dissipation sensors probes were installed for each treatment.

Treatment	Diameter (cm)		Leaf area (m^2)	
	Branch	Trunk	Branch	Tree
Rainfed	11.46	83.00	9.33	82.12
Full Irrigation	11.52	85.00	5.34	96.38
RDI60PI	11.33	89.00	8.12	86.73
RDI60PII	11.40	84.00	6.67	92.94
RDI60PIII	11.46	96.00	6.12	74.15
RDI30PI	10.95	84.00	8.23	73.87
RDI30PII	11.52	87.00	6.07	79.66
RDI30PIII	10.38	85.00	8.67	111.62

Besides sap flow per square meter of leaf area, the following data were also analyzed by comparing one to another: sap flow per unit solar radiation (SR), and sap flow per unit reference evapotranspiration (ET_o), calculated by Penman-Monteith, using hourly data from an automatic weather station (Marin *et al.*, 2001).

Due to electrical problems with the sensor probes, sap flow had to be measured on different days during the same phase for some treatments. Therefore, to carry out statistical analysis of data, days on which the weather conditions were similar were selected; however, even under similar radiation conditions, other climate elements interfered with reference evapotranspiration, such as wind speed. Consequently, reference evapotranspiration, solar radiation, sap flow of branches, whole-tree sap flow, branch sap flow/ET_o ratio and branch sap flow/solar radiation ratio were measured on three different days, which were used as replicates. These data were subjected to a normality test, analysis of variance and the means were grouped by the Skott-Knott criteria at a significance level of 5%.

3. RESULTS AND DISCUSSION

Daily means of reference evapotranspiration (ET_o), solar radiation (Sr), sap flow of the branch (SPb), sap flow of the branch/radiation ratio (SPb/Sr), sap flow of the branch/ET_o (SPb/ET_o) and total sap flow of tree, in the fruit development Phases I, II, and III are shown in Table 4. Analysis of variance shows significant effects of treatments on ET_o because some of the data were measured on different days, as previously described. Nonetheless, it was only in Phase II of fruit development that ET_o, measured on days where sap flow measurements were performed at treatments with full irrigation (FI) and RDI at 60% of ETc, formed different groupings by Scott-Knott criteria, even with similar solar radiation. Rainfed plants exhibited the lowest estimated sap flow of the branch, as well as the lowest whole-tree sap flow in all phases (Table 4). This shows how much low soil water availability, due to water deficit, interferes with transpiration. When analyzing Phase I, we verified that sap flow in the branch, SFb/SR ratio, and SFb/ET_o ratio were higher for plants under full irrigation and lower for rainfed plants, which formed a grouping with the treatment RDI at 30% of ETc in phase II (RDI30PII).

Conditions under irrigation deficit in phase I (RDI60PI and RDI30PI) exhibited mean sap flow values of 0.798 and 0.914 L $m^{-2}day^{-1}$, respectively. These values are very close to the overall mean of the treatments that were not subjected to an irrigation deficit during Phase I (0.905 L m^{-2} day^{-1}). Therefore, irrigation deficit did not influence sap flow greatly; however,

there was formation of a grouping of different values of sap flow under the rainfed condition as well as under full-irrigation treatment (Table 4). Santos *et al.* (2014b) verified that partial water deficit in the soil as a result of RDI at 50% of ETc did not lead to a significant reduction in transpiration by the 'Tommy Atkins' mango in the first evaluation cycle under deficit; nevertheless, in the second cycle, both transpiration and stomatal conductance decreased. The authors reported that the reduction of these two parameters is likely to be related to the time of reading as these reductions only occurred at times of high water demand. In this study, however, sap flow was continuously monitored, which provides a better explanation for the effect of the deficit than non-continuous measurements.

Table 4. Reference evapotranspiration (ET_o), solar radiation (Sr), mean values of sap flow of the branch (SFb), sap flow of the branch/radiation ratio (SFb/Sr), sap flow of the branch/ET_o (SPb/ET_o) and total sap flow of tree (SFt), in fruit development Phases I, II, and III of 'Tommy Atkins' mango tree, irrigated by micro-sprinklers.

Phase	Treatment	ET_o	Sr	SFb	Ratio		SFt
		mm day^{-1}	MJm^{-2} day^{-1}	L m^{-2} day^{-1}	SFb/SR	SFb/ET_o	L day^{-1}
I	Rainfed	4.37	20.64	0.620c	0.030c	0.142c	50.93d
	Full Irrigation	4.37	20.64	1.255a	0.059a	0.280a	120.97a
	RDI60PI	4.37	20.64	0.798b	0.038b	0.183b	69.19c
	RDI60PII	4.37	20.64	0.776b	0.037b	0.177b	72.10c
	RDI60PIII	4.37	20.64	0.944b	0.046b	0.216b	70.02c
	RDI30PI	4.37	20.64	0.914b	0.044b	0.209b	67.46c
	RDI30PII	4.37	20.64	0.697c	0.034c	0.159c	55.49d
	RDI30PIII	4.37	20.64	0.852b	0.041c	0.195c	95.10b
II	Rainfed	5.16a	24.03	0.672e	0.028e	0.130d	55.20e
	Full Irrigation	4.59c	22.33	0.956c	0.043b	0.208a	92.14b
	RDI60PI	4.96b	23.20	0.845d	0.036c	0.170b	73.24d
	RDI60PII	5.16a	24.03	0.914c	0.038c	0.177b	84.94c
	RDI60PIII	5.16a	24.03	0.784d	0.033d	0.152c	58.17e
	RDI30PI	5.16a	24.03	1.111a	0.046a	0.215a	82.03c
	RDI30PII	5.16a	24.03	0.647e	0.027e	0.125d	51.53e
	RDI30PIII	5.16a	24.03	1.015b	0.042b	0.197a	113.34a
III	Rainfed	5.09	23.72	0.794c	0.033b	0.156b	65.16c
	Full Irrigation	5.15	23.81	1.117a	0.047a	0.217a	107.66a
	RDI60PI	5.19	24.80	0.899b	0.036b	0.173b	77.93b
	RDI60PII	5.09	23.72	0.844c	0.036b	0.166b	78.48b
	RDI60PIII	5.19	24.80	0.769c	0.031b	0.148b	57.02c
	RDI30PI	5.09	23.72	1.075a	0.045a	0.211a	79.44b
	RDI30PII	5.14	24.32	0.963b	0.040b	0.187b	76.71b
	RDI30PIII	5.09	23.72	0.926b	0.039b	0.182b	103.37a

Moreover, in Phase I, as for the whole-tree sap flow, there was formation of 4 groupings of SFt, following the same logic of sap flow in the branch, expect for the condition RDI30PIII, which exhibited the second highest value of SFt, likely on account of the highest leaf area of the plant (Table 3).

In Phase II of fruit development, rainfed condition and RDI30PII exhibited the lowest values of SFb, forming the same grouping, which is evidence that in this phase, water deficit at 30% of ETc affects transpiration, similarly to the rainfed condition. In regard to whole-tree sap flow, a behavior akin to that of Phase I was observed, in which the plant under the treatment RDI30PIII exhibited higher SFt.

Sap flow values varied in average from 0.784 to 1.111 L $m^{-2}day^{-1}$ in plants under the following conditions: Full Irrigation, RDI60PI, RDI60PIII, RDI30PI, and RDI30PIII. All of them were not subjected to water deficit during the fruit development Phase II. Their sap-flow values were comparable to those found in Phase I, thus, lower than those found by Oliveira *et al.* (2005), who used the heat balance method, and found values between 0.36 and 3.00 L $m^{-2}day^{-1}$. The analysis done of the sap flow in the branch (SFb), in L $m^{-2}day^{-1}$, was also valid for the values of SFb/SR ratio and SF/ET_o ratio, both of which exhibited similar behavior, even though the results were not obtained during the same period for all treatments.

Sap flow in the branch during the fruit development Phase III is lower under the rainfed condition, forming the same grouping with the condition RDI60PIII whereas the condition RDI30PIII, which also had a water deficit in the same phase, formed another grouping, with a higher sap flow value. As occurred in previous phases, whole-tree sap flow with water deficit at 30% of ETc was similar to the SFt of the treatment under full irrigation, which might be due to the leaf area of the tree.

Daily variations in estimated sap flow, for eight treatments, during Phases I, II, and III of mango fruit development, are depicted in Figure 2. It can be observed that sap flow values estimated by Granier's method follow the values of solar radiation measured over the course of three evaluation days for every treatment. This shows a typical behavior that has been also found in studies conducted by Vellame *et al.* (2012), Rojas (2003), and Paço (2003). Among the treatments Full Irrigation, RDI60PII, RDI60PIII, RDI30PII, and RDI30PIII, which were not subjected to any water deficit during the fruit development Phase I, only the treatment RDI30PII exhibited a value low of estimated sap flow (Table 4).

By looking at the results of sap flow in the three phases (Figures 2A, 2B, and 2C), a discrepancy is verified between profiles that describe the estimated sap flow of mango trees with the global solar radiation. Coelho Filho (2002) mentions that at the early hours of the morning, sap flow occurs due to the transpiration of water stored within plant tissues, and, at the end of the day, when transpiration tends to cease, sap flow continues to occur for the purpose of replenishing the water lost from the tissues during the day.

When analyzing the treatments Full Irrigation, RDI30PI, RDI30PII, RDI60PIII and RDI60PII, which were not under any irrigation deficit condition during Phase III of fruit development (Figure 2C), we could observe many similarities among them. Although, for treatments under water deficit during Phase III of fruit development, the rainfed condition and RDI60PIII exhibited lower estimated sap flow values than those aforementioned values recorded in treatments not subjected to irrigation deficit.

Estimated sap flow values varied from 0.697 and 1.255 L $m^{-2}day^{-1}$ under conditions that were not subjected to water deficit during the three phases of fruit development. These values are within the limits found by Oliveira *et al.* (2005), for four three-year-old mango cultivars (Tommy Atkins, Palmer, Haden, and Van Dyke), in Cruz das Almas, Bahia state, Brazil. This author used the heat balance method, and the sap flow values found varied from 0.36 to 3.00 L m^{-2} leaf day^{-1}.

4. CONCLUSIONS

Granier's thermal dissipation probe allows detecting fluctuations in sap flow by the lower water availability as a result of the application of irrigation deficit.

Regulated irrigation deficit reduces sap flow in 'Tommy Atkins' mango trees.

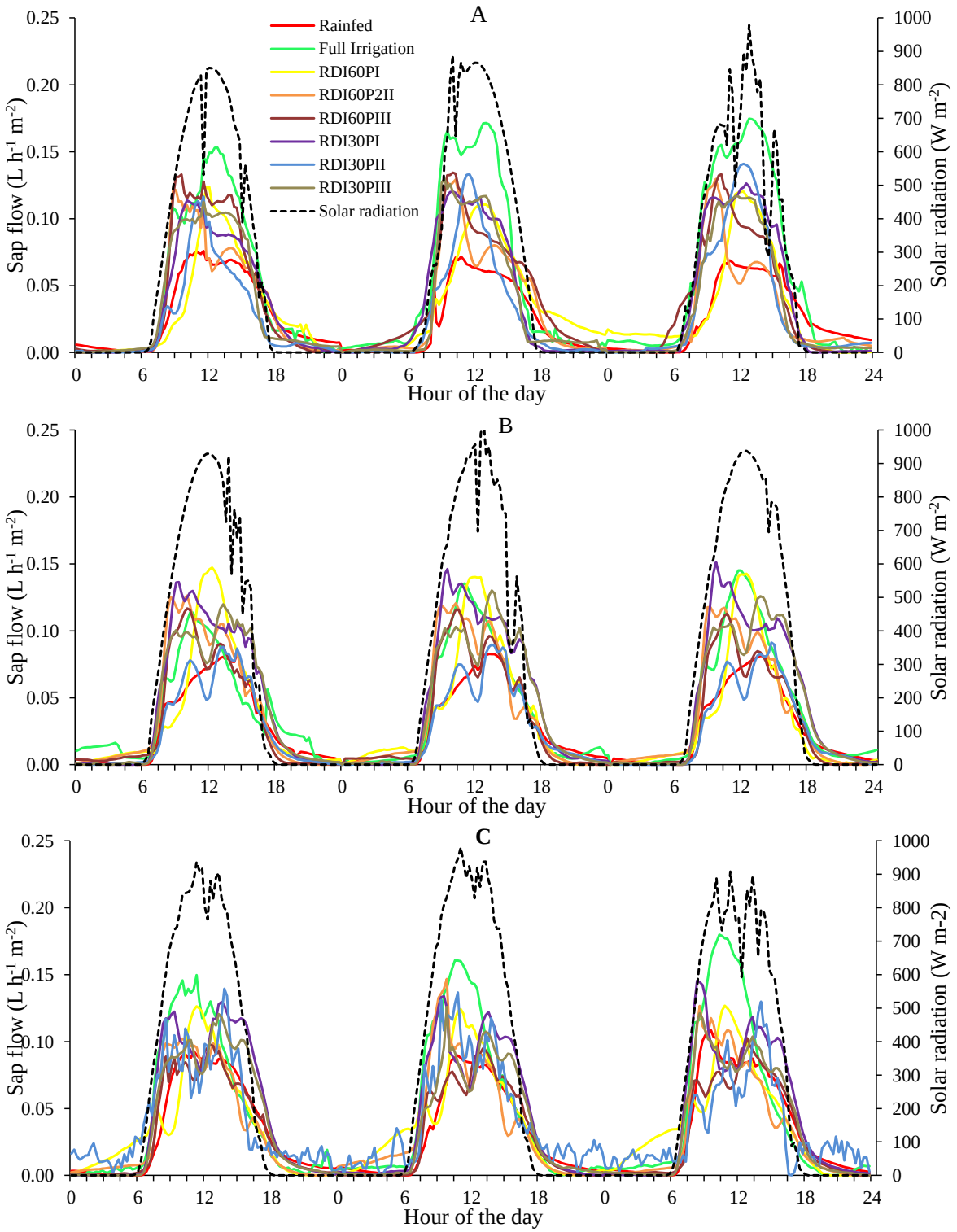

Figure 2. Daily variation in sap flow (SF) of 'Tommy Atkins' mango and solar radiation (SR), for the eight treatments during Phase I (A), Phase II (B), and Phase III (C) of fruit development, irrigated by micro-sprinklers.

5. REFERENCES

BOEHRINGER, D.; ZOLNIER, S.; RIBEIRO, A.; STEIDLE NETO, A. J. Determinação do fluxo de seiva na cana-de-açúcar pelo método do balanço de energia caulinar. **Engenharia Agrícola,** v. 33, n. 2, p. 237-248, 2013.

COELHO FILHO, M. A. **Determinação da transpiração máxima em um pomar jovem de lima ácida 'Tahiti' (Citrus latifólia Tan,) e sua relação com a evapotranspiração de referência.** 2002. 91f. Tese (Doutorado) - ESALQ-USP, Piracicaba.

COELHO FILHO, M. A.; VELAME, L. M.; COELHO, E. F.; CASTRO NETO, M. T.; PAZ, F. P. S. Uso de sensores Granier para determinação da transpiração de mangueiras In. CONGRESSO NACIONAL DE IRRIGAÇÃO E DRENAGEM, 16., Goiania, 2006. **Anais [...]** Goiania: ABID, 2006.

COELHO FILHO, M. A.; ANGELOCCI, L. R.; CAMPECHE, L. F. S. M.; FOLEGATTI, M. V.; BERNARDES, M. S. Field determination of young acid lime plants transpiration by the stem heat balance method**. Scientia Agricola**, v. 62, n. 3, p. 240-247, 2005. http://dx.doi.org/10.1590/S0103-90162005000300007

CONSOLI, S.; STAGNO, F.; VANELLA, D.; BOAGA, J.; CASSIANI, G.; ROCCUZZO, G. Partial root-zone drying irrigation in orange orchards: Effects on water use and crop production characteristics. **European Journal of Agronomy,** v. 82, p. 190–202, 2017. https://doi.org/10.1016/j.eja.2016.11.001

COTRIM, C. E.; COELHO, E. F.; SILVA, J. A.; SANTOS, M. R. Irrigação com déficit controlado e produtividade de mangueira 'Tommy Atkins' sob gotejamento. **Revista brasileira de Agricultura irrigada,** v. 11, p. 2229-2238, 2017. https://dx.doi.org/10.7127/rbai.v11n800728

FARIA, L. N.; SOARES, A. A.; DONATO, S. L. R.; SANTOS, M. R.; CASTRO, L. G. The effects of irrigation management on floral induction of 'Tommy Atkins' mango in Bahia semiarid. **Engenharia Agrícola,** v.36, p. 387-398, 2016a. http://dx.doi.org/10.1590/1809-4430-Eng.Agric.v36n3p387-398/2016

FARIA, L. N.; DONATO, S. L. R.; SANTOS, M. R.; CASTRO, L. G. Nutrient contents in 'Tommy Atkins' mango leaves at flowering and fruiting stages. **Engenharia Agrícola,** v. 36, p. 1073-1085, 2016b. http://dx.doi.org/10.1590/1809-4430-eng.agric.v36n6p1073-1085/2016

GRANIER, A. Une nouvelle méthode pour la mesure du flux de sève brute dans le tronc dês arbres. **Annales des Sciences Forestières**, v. 42, n. 2, p. 193-200, 1985.

HERNANDEZ-SANTANA, V.; FERNÁNDEZ, J.E.; RODRIGUEZ-DOMINGUEZ, C.M.; ROMERO, R.; DIAZ-ESPEJO, A. The dynamics of radial sap flux density reflects changes in stomatal conductance in response to soil and air water deficit. **Agricultural and Forest Meteorology**, v. 218–219, p. 92–101, 2016. https://doi.org/10.1016/j.agrformet.2015.11.013

LIMA, R. S. N.; FIGUEIREDO, F. A. M. M.; MARTINS, A. O.; DEUS, B. C. S.; FERRAZ, T. M.; GOMES, M. M. A.; SOUSA, E. F.; GLENN, D. M.; CAMPOSTRINI, E. Partial rootzone drying (PRD) and regulated deficit irrigation (RDI) effects on stomatal conductance, growth, photosynthetic capacity, and water-use efficiency of papaya. **Scientia Horticulturae,** v. 183, p. 13-22, 2015. https://doi.org/10.1016/j.scienta.2014.12.005

MARIN, F. R.; RIBEIRO, R. V.; ANGELOCCI, L. R.; RIGHI, E. Z. Fluxo de seiva pelo método do balanço de calor: base teórica, qualidade das medidas e aspectos práticos. **Bragantia,** v. 67, n. 1, p. 1-14, 2008.

MARIN, F. R.; ANGELOCCI, L. R.; PEREIRA, A. R.; VILLA NOVA, N. A.; SENTELHAS, P. C. Fluxo de seiva e evapotranspiração num pequeno pomar de citros irrigado. **Revista Brasileira de Agrometeorologia,** v. 9, n. 2, p. 219-226, 2001.

OLIVEIRA G. X. S.; COELHO FILHO, M. A.; PEREIRA, F. A. C.; CASTRO NETO, M. T.; COELHO, E. F. Relação entre transpiração máxima, evapotranspiração de referência e área foliar em quatro variedades de mangueira In: CONGRESSO NACIONAL DE IRRIGAÇÃO E DRENAGEM, 15., Teresina. **Anais [...]** Viçosa: ABID, 2005. 1 CD-ROM.

PAÇO, M. T. G. A. **Modelação da evapotranspiração em cobertos descontínuos. Programação da rega em pomar de pessegueiro.** 2003. 227 f. Tese (Doutorado) - Universidade Técnica de Lisboa, Instituto Superior de Agronomia, Lisboa, 2003.

PINTO JR., O. B.; VOURLITIS, G. L.; SANCHES, L.; DALMAGRO, H. J.; LOBO, F. A.; NOGUEIRA, J. S. Transpiração pelo método da sonda de dissipação térmica em floresta de transição Amazônica-Cerrado. **Revista Brasileira de Engenharia Agrícola e Ambiental**, v. 17, n. 3, p. 268–274, 2013.

ROJAS, J. S. D. R. **Avaliação do uso do fluxo de seiva e da variação do diâmetro do caule e de ramos na determinação das condições hídricas de citros, como base para o manejo de irrigação.** 2003. 110 f. Tese (Doutorado) - Escola Superior de Agricultura "Luís de Queiroz", Universidade de São Paulo, Piracicaba, 2003.

SAMPAIO, A. H. R.; COELHO FILHO, M. A.; COELHO, E. F.; DANIEL, R. Indicadores fisiológicos da lima ácida 'tahiti' submetida à irrigação deficitária com secamento parcial de raiz. **Irriga,** v. 19, n. 2, p. 292-301, 2014. https://doi.org/10.15809/irriga.2014v19n2p292

SANTOS, M. R.; DONATO, S. L. R.; ARANTES, A. M.; COELHO, E. F.; OLIVEIRA, P. M. Gas Exchange in 'BRS Princesa' banana (Musa spp.) under partial rootzone drying irrigation in the North of Minas Gerais, Brazil. **Acta Agronômica**, v. 66, p. 378-384, 2017. http://dx.doi.org/10.15446/acag.v66n3.55056

SANTOS, M. R.; DONATO, S. L. R.; COELHO, E. F.; ARANTES, A. M.; COELHO FILHO, M. A. Irrigação lateralmente alternada em lima ácida 'Tahiti' na região norte de Minas Gerais. **Irriga**, v. 1, n. 1, p. 71, 2016a. https://doi.org/10.15809/irriga.2016v1n01p71-88

SANTOS, M. R.; DONATO, S. L. R.; COELHO, E. F.; COTRIM JUNIOR, P. R. F.; CASTRO, I. N. Irrigation déficit strategiesonphysiologicalandproductiveparametersof'Tommy Atkins' mango. **Revista Caatinga,** v. 29, p. 173-182, 2016b. http://dx.doi.org/10.1590/1983-21252016v29n120rc

SANTOS, M. R.; DONATO, S. L. R.; FARIA, L. N.; COELHO, E. F.; COTRIM JUNIOR, P. R. F. Irrigation strategies with water deficit in 'Tommy Atkins' mango tree. **Engenharia Agrícola,** v. 36, p. 1096-1109, 2016c. http://dx.doi.org/10.1590/1809-4430-eng.agric.v36n6p1096-1109/2016

SANTOS, M. R.; NEVES, B. R.; SILVA, B. L.; DONATO, S. L. R. Yield, Water Use Efficiency and Physiological Characteristic of 'Tommy Atkins' Mango under Partial Rootzone Drying Irrigation System. **Journal of Water Resource and Protection,** v. 07, p. 1029-1037, 2015. http://dx.doi.org/10.4236/jwarp.2015.713084

SANTOS, M. R.; MARTINEZ, M. A.; DONATO, S. L. R.; COELHO, E. F. Fruit yield and root system distribution of ‘Tommy Atkins’ mango under different irrigation regimes. **Revista Brasileira de Engenharia Agrícola e Ambiental,** v. 18, p. 362-369, 2014a. http://dx.doi.org/10.1590/S1415-43662014000400002

SANTOS, M. R.; MARTINEZ, M. A.; DONATO, S. L. R.; COELHO, E. F. Produtividade e fotossíntese da mangueira ‘Tommy Atkins’ sob déficit hídrico em região semiárida da Bahia. **Revista Brasileira de Engenharia Agrícola e Ambiental,** v. 18, p. 899-907, 2014b. http://dx.doi.org/10.1590/1807-1929/agriambi.v18n09p899-907

SANTOS, M. R.; MARTINEZ, M. A. Soil water distribution and extraction by 'Tommy Atkins' mango (Mangifera Indica L.) trees under different irrigation regimes. **Idesia,** v. 31, p. 7-16, 2013.

VELLAME, L. M.; COELHO, R. D.; TOLENTINO, J. B. Transpiração de plantas jovens de laranjeira ‘valência’ sob porta-enxerto limão‘cravo’ e citrumelo ‘swingle’ em dois tipos de solo. **Revista Brasileira de Fruticultura**, v. 34, n. 1, p. 024-032, 2012.

Ambiente & Água - An Interdisciplinary Journal of Applied Science
ISSN 1980-993X – doi:10.4136/1980-993X
www.ambi-agua.net
E-mail: ambi.agua@gmail.com

Prioritization of pharmaceuticals in urban rivers: the case of oral contraceptives in the Belém River basin, Curitiba / PR, Brazil

ARTICLES doi:10.4136/ambi-agua.2334

Received: 01 Oct. 2018; Accepted: 15 Mar. 2019

Demian da Silveira Barcellos[1*]; Harry Alberto Bollmann[1]; Júlio César Rodrigues de Azevedo[2]

[1]Pontifícia Universidade Católica do Paraná (PUCPR), Curitiba, PR, Brasil
Programa de Pós-Graduação em Gestão Urbana (PPGTU)
E-mail: demian.barcellos@gmail.com, harry.bollmann@pucpr.br
[2]Universidade Tecnológica Federal do Paraná (UTFPR), Curitiba, PR, Brasil
Programa de Pós-Graduação em Ciência e Tecnologia Ambiental (PPGCTA)
E-mail: jcrazevedo.utfpr@gmail.com
[*]Corresponding author

ABSTRACT

Efforts to prioritize pharmaceutical products in urban rivers are still rare in Brazil. However, European and U.S. management experiences of pharmaceuticals in urban waters show that this has been one of the first steps necessary to reduce and control this type of pollution. The main objective of this research was to evaluate the presence of oral contraceptives in the catchment area of the Belém River in Curitiba based on the different criteria normally applied to prioritization. For this, in addition to a literature review, historical data on the concentrations of contraceptive hormones in the Belém River, data on pharmaceutical consumption in the basin (collected through interviews by random sampling in pharmacies and from the database of medicines provided by the City of Curitiba Health Units), and data from interviews conducted using intentional sampling with regional stakeholders. The results show that a consistent set of criteria supporting prioritization of ethinylestradiol and estradiol already exists, while the periodic monitoring of these two hormones has proved feasible and necessary in the waters of the region.

Keywords: female sex hormones, pharmaceutical management, prioritization of pharmaceuticals.

Priorização de fármacos nos rios urbanos: o caso dos contraceptivos orais na bacia do rio Belém, Curitiba/PR, Brasil

RESUMO

Esforços para priorizar produtos farmacêuticos em rios urbanos ainda são escassos no Brasil, mas as experiências europeia e norte-americana de gestão de produtos farmacêuticos em águas urbanas mostram que este foi um dos primeiros passos para reduzir e controlar este tipo de poluição. O objetivo principal desta pesquisa foi avaliar o caso de anticoncepcionais orais na área de abrangência do rio Belém, em Curitiba, sob a ótica das diferentes dimensões que têm sido consideradas no processo de priorização. Para isso, além da revisão da literatura, foram utilizados dados históricos sobre a concentração de hormônios contraceptivos nas águas do rio Belém, dados sobre o consumo de fármacos na área da bacia hidrográfica (coletados por meio

de entrevistas realizadas por amostragem aleatória em farmácias e pelo banco de dados de medicamentos fornecido pela Prefeitura de Curitiba por meio das Unidades de Saúde) e os dados das entrevistas feitas por amostragem intencional com *stakeholders* locais. Os resultados mostram que, em relação ao etinilestradiol e ao estradiol, já existe um conjunto consistente de critérios que apoiam sua priorização, enquanto que a regulamentação do monitoramento periódico desses dois hormônios se mostrou viável e necessária nas águas da região.

Palavras-chave: gestão de produtos farmacêuticos, hormônios sexuais femininos, priorização de fármacos.

1. INTRODUCTION

Prioritization methodology for controlling and reducing micropollutants in general, and pharmaceuticals in particular, in urban rivers has been a major management challenge given the wide variety of compounds reported in the literature (Berninger *et al.*, 2016; Aubakirova *et al.*, 2017). As a result, the assessment of the environmental and health risks related to the presence of such residues, alone or in combination, is very difficult (Voogt *et al.*, 2009; Riva *et al.*, 2015). Nevertheless, studies globally have reported a variety of prioritization methods to control micropollutants in the waters based on different criteria (Daouk *et al.*, 2015; Riva *et al.*, 2015; Mansour *et al.*, 2016; Aubakirova *et al.*, 2017; Burns *et al.*, 2018). Overall, the most important criteria considered by these methodologies have been: presence of the substance (assessed by consumption and identification in the environment); risk to environment or human health (tested for a range of organisms on various trophic levels); persistence in the environment (natural biodegradation and removal in wastewater treatment systems); and feasible monitoring (existing monitoring methods and appropriate equipment) (Helwig *et al.*, 2013; Daouk *et al.*, 2015; Mansour *et al.*, 2016; Burns *et al.*, 2018).

Two important examples of prioritization are the Norman Network and the European Watch-List. The prioritization methodology elaborated by the Norman Network is about the prioritization of emerging compounds that is included pharmaceuticals. The Norman Network is a global network of stakeholders whose goal is the exchange of information on emerging environmental substances. This network seeks to promote and benefit synergies among research teams from different countries (Norman Network, 2018). In this same direction, European legislation has used a Watch-List mechanism to prioritize emerging contaminants. This mechanism was added in the 2013 update of the Water Directive with the goal of obtaining monitoring data for the establishment of future priorities. This list focuses on pollutants for which available data to assess their risks are still insufficient to allow conclusions on their effects. This Watch-List Directive included several pharmaceuticals in an effort towards prioritization (European Union, 2013).

Given that prioritizing pharmaceuticals in urban rivers that receive domestic effluents is directly related to medicine consumption (a region-specific variable), there is an intrinsic dependence on information related to regional usage of pharmaceuticals, which presents a challenge to prioritization in several regions (Al-Khazrajy and Boxall, 2016; Mansour *et al.*, 2016). Prioritization efforts have been reported in North America, Europe, Australia, and East Asia (Voogt *et al.*, 2009; Guo *et al.*, 2016). However, most of these efforts have been concentrated in Europe and the United States (Al-Khazrajy and Boxall, 2016; Burns *et al.*, 2018), where some pharmaceuticals already undergo systematic monitoring regulated by law and where more advanced proposals are being prepared to control their concentration in water.

Management of urban catchment areas is very challenging due to the large numbers of people and diversity of local stakeholder sectors involved. Knowing stakeholder priorities for water management and the treatment of pharmaceuticals is essential since it is the stakeholders

that encourage, negotiate, and undertake these management initiatives.

Due to the lack of studies on pharmaceutical prioritization (Santos, 2015) and management in Brazil (Barcellos, 2018), this study sought to evaluate the different criteria that have been considered for prioritizing of pharmaceuticals, in case of oral contraceptive drugs in the Belém River basin, in Curitiba, State of Paraná, Brazil. The main active ingredients in these drugs, ethinylestradiol and estradiol, are already prioritized, and systematic monitoring is regulated by law in the United States and the European Union. Additionally, we sought to determine if enough evidence is already available to consider these hormones as priorities for water management in the study region.

2. METHODOLOGY

The study area was the Belém River catchment area (Figure 1), which is entirely located within the municipality of Curitiba, Paraná State and is completely urbanized. The river drainage area comprises 87.85 km², occupying 20% of the territory of the city and many of the main neighborhoods and architectural and landscape elements that represent Curitiba in a national and international context are located within the catchment area. According to data from the Brazilian Institute of Geography and Statistics (IBGE), the basin contained 475,606 of the 1,751,907 inhabitants of Curitiba in 2010, corresponding to 27% of the population. The institute (IBGE, 2017) estimates that the current population of Curitiba has reached 1,908,359 inhabitants, and the Belém River catchment area approximately 518,000 inhabitants. According to Lara (2014), approximately 43% of the properties in the catchment area are not properly connected to the sewage collection network, resulting in water containing high levels of domestic sewage pollution. In terms of the general quality of the Belém River water, there is ongoing degradation of the springs near the mouth due to habitual and diffuse sources of pollution, and approximately 90% of this pollution is derived from domestic sewage discharged through drainage networks (Bollmann and Edwiges, 2008).

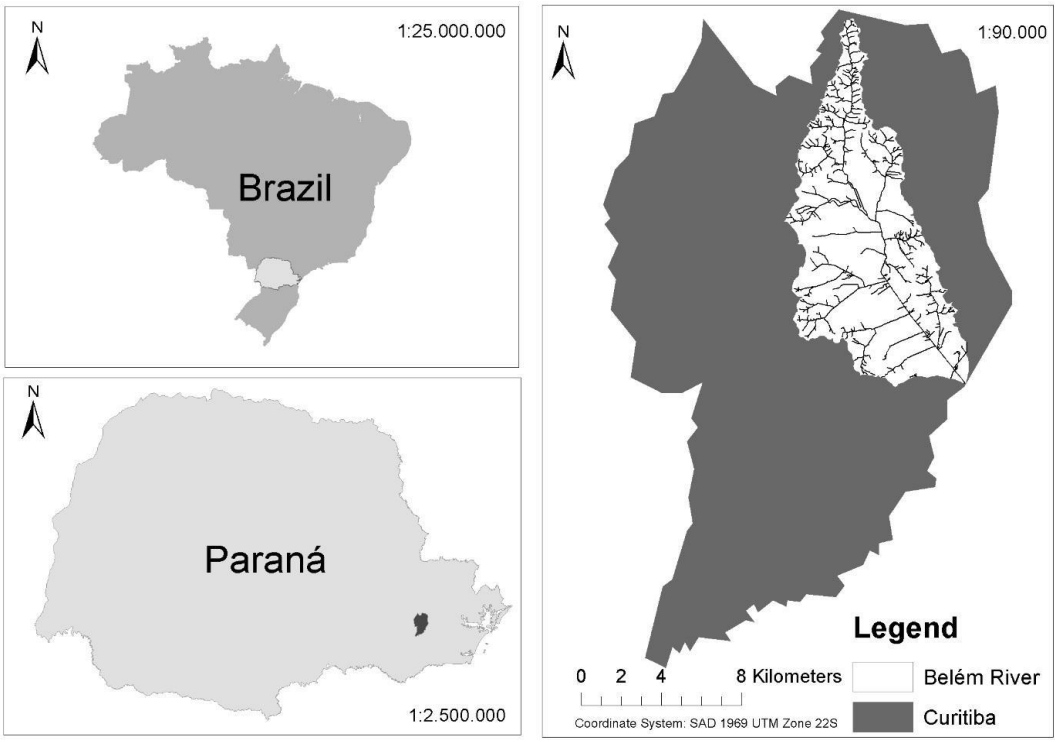

Figure 1. Macro-location of the Belém River basin.

Due to the complexity and variability of environmental characteristics and urban settlement of the Belém River catchment area, the region was divided into three parts: 1) Northern Belém, encompassing the region of the headwaters; 2) Central Belém, in the central region of the basin; and 3) Southern Belém, near the mouth of the basin (Figure 2).

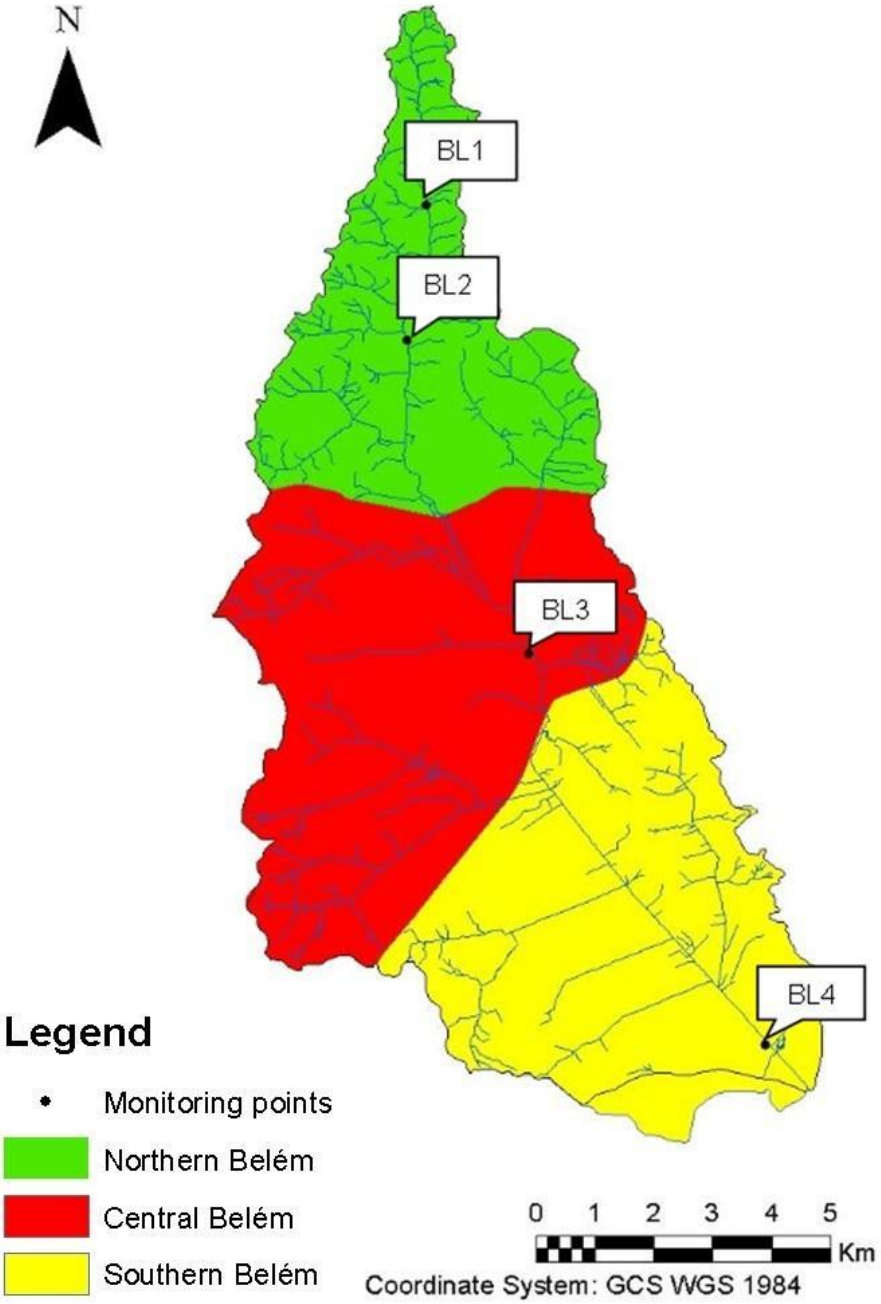

Figure 2. Demarcation of the regions: Northern Belém, Central Belém and Southern Belém, indicating the water quality monitoring points.

This division was based on the methodology proposed by Carvalho Junior (2007), and later also used by Knopki (2008), where the authors divided the catchment area into four major regions. However, in this study we combined Regions 1 and 2 reported by these authors, since they represent very small areas and, although they feature subtle distinctions, overall they present environmental and urban homogeneity. Notably, declivity, forest cover, water quality, and land use and occupation characteristics are similar in these regions.

The criteria considered for the prioritization of pharmaceuticals in this study were: the environmental and health risks of the compound; the presence and concentration of compounds in the water; consumption by the local population; and stakeholder priorities.

The following information was used for the evaluation of these dimensions: 1) pharmaceutical consumption in the Belém River catchment area, based on random interview data from 92 pharmacies between December, 2016 and June, 2017, as well as the distribution data for pharmaceuticals from the Municipal Health Units (UMSs) of the Municipal Health Department from June, 2015 to June, 2017; 2) data from interviews conducted with 32 local stakeholders, selected by intentional sampling, on their priorities for pharmaceutical management; 3) monitoring data on ethinylestradiol (EE2), estrone (E1), and estradiol (E2) from 2011 to 2017, available from the Laboratory of Advanced Studies in Environmental Chemistry (LEAQUA), from the Federal Technological University of Paraná (UTFPR); and 4) a literature review of micropollutant concentrations in the Belém River and information on the environmental effects of the studied compounds.

Hormone analysis was performed by high-performance liquid chromatography with diode array detector (HPLC-DAD). A 5L Van Dorn type bottle was used to collect water that was stored in 1L amber bottles. The extraction method for the hormones was developed using solid phase extraction (SPE). The sample was filtered through 0.45 µm cellulose acetate filters, after which the pH was adjusted to 3. 1 L of the filtered water sample was eluted through a preconditioned C18 SPE column (6 mL of hexane, 6 mL of ethyl acetate, 6 mL of methanol and 6 mL of ultrapure water) at a constant elution rate (10 mL min^{-1}). Then, the C18 SPE column was eluted with 12 mL of acetonitrile, the eluate was evaporated to dryness in a rotary evaporator and 1 mL of acetonitrile was added to re-dissolve the extract. Detailed analytical methodology and procedures are described elsewhere (Ide *et al.*, 2017; Machado *et al.*, 2017).

Purposive sampling was used to select the 32 interviewed stakeholders, considering their contributions to literature on micropollutants, involvement in initiatives for management of water pollution control applicable to pharmaceuticals, and referrals from institutional colleagues. The interviewees were not chosen randomly since the goal was not to generate information that could be generalized, but to know the points of view of a variety of stakeholders. This group included researchers from several universities (Positivo University, Pontifical Catholic University of Paraná, Federal University of Paraná, and Federal Technological University of Paraná), government sector staff (state and municipal departments of the environment, health and education, Environmental Institute of Paraná, and Water and Sanitation Company of Paraná State/SANEPAR), and representatives of the pharmaceutical industry (Pharmacy Council and unions), including the pharmaceutical manufacturing sector.

Interviews with stakeholders were conducted in person, by telephone, or by email (this was only in one case, because the selected person was studying abroad). Two questions were asked, an open question, which was the most important medicine for urban water management, and an objective question asking that classes of drugs (contraceptives, antibiotics, anti-inflammatories, analgesics, lipid and anti-hypertensive) were numbered in order of importance.

A shape file provided by the Department of Geoprocessing of the Institute of Research and Urban Planning of Curitiba (IPPUC) was used to select the sampled pharmacies in the Belém River basin; the file was compiled from permits issued by the Municipal Secretariat of Finance that contained the location of pharmacies. Using geoprocessing tools, 610 of the 1,352 pharmacies in Curitiba were found to be within the basin of the Belém River catchment area, representing the sampling universe. The Cochran formula (Cochran, 1977), Equation 1, was used to determine the sample size:

$$n = \frac{\frac{t^2 PQ}{d^2}}{1+\frac{1}{N}\left(\frac{t^2 PQ}{d^2}-1\right)} \quad (1)$$

Where:

n = sample size;

t = level of confidence chosen;

P = the percentage at which the phenomenon occurs;

Q = complementary percentage;

N = total number of pharmacies in the basin;

d = maximum error allowed.

For sample-size calculation, and taking N as 610, we set a confidence level of 90% (Student's *t*-value was 1.64), a maximum error of 8% (0.08), and the percentage at which the phenomenon occurs at 50% (0.5). The sample size for the catchment area studied was determined as 92 pharmacies, which were subsequently selected using a Random Number Generator. As pharmacies are not homogeneously distributed throughout the catchment area, the number of pharmacies in each of the 3 regions of the Belém River catchment area was recorded (Figure 2). Of the 610 pharmacies, 403 were found to be concentrated in Central Belém, which is in the central region of the city of Curitiba and has the most populated neighborhoods. Therefore, random selection of pharmacies was performed proportionally, per stratum (Northern, Central, and Southern Belém).

The interviews were carried out with the pharmacists or those responsible for the availability of medicines in pharmacies. The information requested in the interview was three selling rankings in ascending order: the ten best-selling drugs in the pharmacy (all classes of drugs including antibiotics and contraceptives), the best-selling antibiotics and the best-selling oral contraceptives.

3. RESULTS AND DISCUSSION

Estrone, estradiol, and ethinylestradiol are known to cause endocrine deregulation in marine animals and communities, with fish feminization observed even at very low concentrations (nanograms per liter). Table 1 shows the lowest observed effect concentration (LOEC) for which critical effects of estrone, estradiol and ethinylestradiol in water organisms have already been observed, according to WikiPharma, the Swedish digital database.

Although these three hormones can cause endocrine disruption, EE2 has a significantly higher individual endocrine disruption potency (Owen and Jobling, 2013), 10- to 50-fold higher than E2 and E1 (Nash *et al.*, 2004). According to Gilbert (2012), 5 – 6 ng L^{-1} of ethinylestradiol was enough to adversely affect aquatic populations and ecosystems, including collapsing fish communities, as shown in a study in an experimental lake in Canada (Kidd *et al.*, 2007); however, adverse effects were not observed in fish at concentrations below 0.2 – 0.1 ng L^{-1}. Nevertheless, the limit recommended by the European Commission is 0.035 ng L^{-1} in water, based on concentrations that European toxicologists consider safe for marine species (Gilbert, 2012).

The systematic monitoring of EE2, E2, and E1 hormones conducted by LEAQUA at UTFPR (Figure 3) showed that, although the concentrations of the three hormones in the Belém River are frequently below the detection limit (<48, <25 and <26 ng L^{-1}, respectively), concentration peaks of these pollutants can occur. The monitoring points in Central and Southern Belém (BL3 and BL4 in Figure 2) have been monitored since 2011, while monitoring of the points in Northern Belém (BL1 and BL2 in Figure 2) began in November, 2012.

Table 1. Lowest concentrations of female sex hormones tested with effects on aquatic organisms.

Compound	Animal	Critical effect	LOEC
EE2	Fish	Change in egg production	0.1 ng L^{-1}
	Fish	Change in sex/ increase of fertilization failure ratio	0.32 ng L^{-1}
	Fish	Feminization	0.96 ng L^{-1}
E2	Fish	Mortality	0.93 ng L^{-1}
	Fish	Increased body weight and length	2.86 ng L^{-1}
	Fish	Increase in the total length and vitellogenin/decreased fertility	8.66 ng L^{-1}
E1	Fish	Induction of plasma vitellogenin	31.8 ng L^{-1}
	Fish	Reduction in the gonadosomatic index	317.7 ng L^{-1}
	Fish	Induced intersex	100,000.00 ng L^{-1}

Source: WikiPharma (2017).

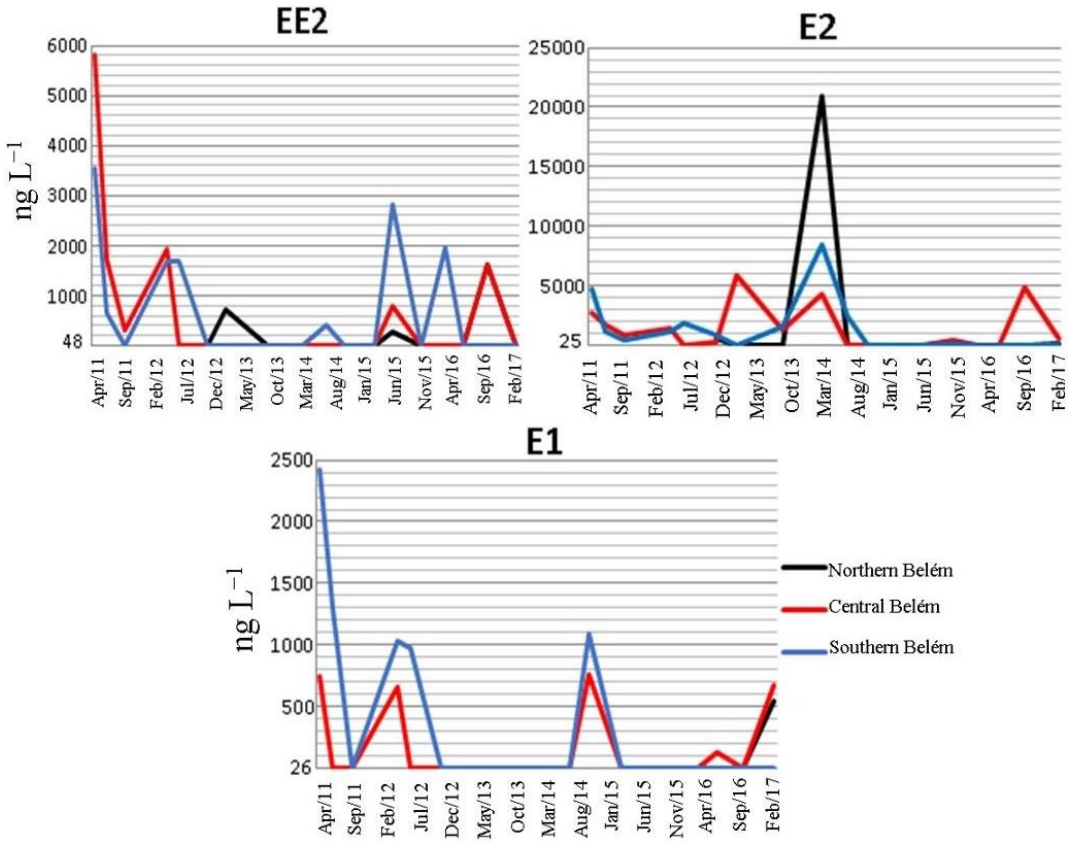

Figure 3. Temporal evolution of EE2, E2, and E1 concentrations in the waters of the Belém River.

The presence of oral contraceptive residues evidently pose an environmental risk given the significant concentrations confirmed in water, which additionally reflect the poor sanitation conditions in the urban area.

Although this catchment area is not a source of human water supply, this study on the concentration of female sex hormones in water is relevant since the Belém River flows directly into the Iguaçu River, which supplies municipalities downstream of the city of Curitiba. Given that the concentrations considered safe in natural waters are significantly lower than those found in the waters of the Belém River, this issue may be an important public health problem for the Curitiba region since the treatment systems employed to treat public water supply cannot remove them. Moreover, significant levels of female sex hormones have been found in the supply waters of the three most populous Brazilian cities (São Paulo, Rio de Janeiro and Belo

Horizonte), at concentrations that can have adverse effects on fish, as shown in the study by Dias (2014).

The analysis of pharmaceutical usage data indicated that oral contraceptives are accessed by the population mostly by purchase in pharmacies, since the amount distributed by UMS was approximately only 4.7% of the estimated amount consumed in Curitiba; this calculation took into account the relationship between a monthly average of 8,369 women who receive contraceptives in the UMSs and the expected monthly consumption in Curitiba, since estimates based on the IBGE census data of 2010 and information from the World Health Organization (Cunha, 2014) indicated that 179,564 (27% of the population) sexually active women (15–64 years) should consume these pharmaceuticals.

Contraceptives are the fourth most-sold class of pharmaceuticals in pharmacies in the region (Table 2), with injectable drugs being used significantly less than pills. The most-sold injectable drugs include Mesigyna (norethisterone enanthate + estradiol), ranked 76; Medroxyprogesterone acetate, ranked 77; and Perlutan (algestone + estradiol), ranked 91 in drug sales in pharmacies.

Table 2. Most sold therapeutic drug classes in pharmacies on the Belém River basin.

Sales Ranking	Therapeutic Classes
1	Analgesics
2	Anti-inflammatories
3	Antihypertensives
4	Contraceptives
5	Digestives
6	Antibiotics
7	Psychotropics
8	Antidiabetics
9	Nasal decongestants
10	Vitamins and supplements

The active ingredients in oral contraceptives with the highest relevance are ethinylestradiol, present in approximately 80% of the most sold contraceptives in pharmacies, and the compounds levonorgestrel, desogestrel, and drospiperone, present in 19% of the most sold contraceptives in pharmacies (Table 3). However, it should be stressed that if sales density is considered, the more relevant pharmaceuticals after ethinylestradiol are levonorgestrel (present in the morning-after pill), drospiperone, cyproterone, desogestrel, and estradiol (present in two of the three injectable contraceptives ranked among the most-sold pharmaceuticals in pharmacies).

Distribution of contraceptives by UMS strengthens the importance of levonorgestrel and estradiol, even though levels are substantially lower than acquisition from pharmacies. For example, the contraceptive most-distributed by UMS is an injectable drug containing estradiol as the active ingredient, ranking 68th among the most-distributed drugs, followed by a pill containing ethinylestradiol + levonorgestrel, ranking 70th among the drugs most-distributed by UMS.

Consequently, ethinylestradiol should be prioritized considering the strong evidence relating to the level of consumption. Although estradiol is consumed less than ethinylestradiol, and other active ingredients such as levonorgestrel, it should also be prioritized due to the high concentrations of these hormones in the Belém River and the proven associated environmental effects. However, E2 is also naturally excreted by the human body, partially explaining the high concentrations of E2 found in the environment.

Table 3. The most-sold oral contraceptives in pharmacies of the Belém River basin.

Formulation	Trade name	Intensity of sales[2]
0.15 mg levonorgestrel + 0.03 mg ethinylestradiol	Microvlar	2.80
0.15 mg levonorgestrel + 0.03 mg ethinylestradiol	Ciclo 21	2.90
3 mg drospirenone + 0.02 mg ethinylestradiol	Yaz	3.20
2 mg cyproterone acetate + 0.035 mg ethinylestradiol	Diane 35	3.51
3 mg drospirenone + 0.03 mg ethinylestradiol	Yasmin	3.57
0.075 mg desogestrel	Cerazette	3.92
3 or 2 or 1 mg estradiol + 2 or 3 mg dienogest	Qlaira	3.98
3 mg drospirenone + 0.03 mg ethinylestradiol	Elani ciclo	4.00
0.075 mg desogestrel	Desogestrel	4.01
3 mg drospirenone + 0.02 mg ethinylestradiol	Iumi	4.07
0.25 mg levonorgestrel + 0.05 mg ethinylestradiol	Neovlar	4.07
2.5 mg nomegestrol acetate + 1.5 mg estradiol	Stezza	4.12
2 mg cyproterone acetate + 0.035 mg ethinylestradiol	Selene	4.12
0.075 mg gestodene + 0.030 mg ethinylestradiol	Gynera	4.12
2 mg chlormadinone acetate + 0.03 mg ethinylestradiol	Belara	4.12
0.75 mg levonorgestrel	Diad[1]	4.13
0.1 mg levonorgestrel + 0.02 mg ethinylestradiol	Level	4.14
0.075 mg gestodene + 0.020 mg ethinylestradiol	Allestra 20	4.14
0.075 mg gestodene + 0.030 mg ethinylestradiol	Tamisa	4.14
0.75 mg levonorgestrel	Previdez[1]	4.14
0.15 mg desogestrel + 0.02 mg ethinylestradiol	Femina	4.15
0.06 gestodene + 0.015 ethinylestradiol	Sublima	4.15
1.5 mg levonorgestrel	Neodia[1]	4.15
0.15 mg desogestrel + 0.02 or 0.01 mg ethinylestradiol	Mercilon	4.16
0.15 mg desogestrel + 0.03 mg ethinylestradiol	Primera 30	4.16
2 mg cyproterone acetate + 0.035 mg ethinylestradiol	Diclin	4.16
0.15 mg levonorgestrel + 0.03 mg estradiol	Nordette	4.16
3 mg drospirenone + 0.02 mg ethinylestradiol	Drospirenone + ethinylestradiol	4.16
2 mg cyproterone acetate + 0.035 mg ethinylestradiol	Repopil	4.16

Note 1: abortifacients.
Note 2: average drug sales ranking among the 92 pharmacies.

Considering the level of consumption, the presence of levonorgestrel in the water should also be investigated, and the effect on aquatic communities should be monitored. Reports on the effects of levonorgestrel are scarce, according to the Swedish database Wiki Pharma. However, levonorgestrel levels are relevant from the point of view of consumption, particularly given the high dose present in contraceptive pills.

In addition to their importance in terms of consumption, contraceptives were also identified as important for the management of drugs by the 32 stakeholders interviewed, who further highlighted them as the most important therapeutic class of drugs (Table 4). Overall, therefore, oral contraceptives are considered a priority for drug management due to the high consumption, reported presence in the water, importance for the stakeholders involved in drug management, and the significant effects on aquatic communities.

Table 4. Prioritization of pharmaceutical products according to the 32 stakeholders interviewed.

Ranking of priorities	Therapeutic Class
1	Contraceptives
2	Antibiotics
3	Anti-inflammatories
4	Analgesics
5	Antihypertensives
6	Lipid Regulators
7	Others

4. CONCLUSIONS

With regard to ethinylestradiol and estradiol, a consistent set of criteria already exists that sustains prioritization for management strategies in the Curitiba region: the presence in the waters of the river at significant concentrations; consideration as priority pollutants among the therapeutic classes of drugs by stakeholders in the region; having a proven chronic deleterious environmental effect at concentrations found in the river; and, in terms of pharmaceutical consumption, forming part of a priority class of drugs, belonging to the fourth most-sold class in pharmacies.

As the analytical capacity to monitor these compounds already exists in the Curitiba region in terms of qualified personnel, equipment, and methodologies, systematic monitoring is feasible and necessary. However, given that only a few research centers are equipped to monitor compounds in Curitiba and the State of Paraná, systematic monitoring could at first be regulated from a health and environmental point of view in strategic hydrographic basins. Subsequently, as the technical capacity increases, systematic monitoring should encompass the whole region and standard methodology to determine concentrations using an adequate detection limit is required to set up official monitoring measures.

Once systematic monitoring is implemented with measures similar to those in the European Union and United States, safety levels can be established for these compounds in natural waters in Brazil, and the concentration limits in waters may subsequently be determined. However, prioritization studies on contraceptives and other medication must first be replicated in other regions in Brazil to meet this goal.

5. ACKNOWLEDGMENTS

The authors are grateful to the collaborators of the WENSI Project (Water Environment Micropollutant Science Initiative: A Collaboration to explore emergent pollutants in Brazilian watercourses) and their funders, the Brazilian Federal Agency for the Improvement of Higher Education through Edict PGCI n. 02/2015 of International Cooperation, Project no. 004/2016, and the British Council through the Newton Fund: Institutional Links, application ID 122728076. The authors also acknowledge the Laboratory of Advanced Studies in Environmental Chemistry (LEAQUA) of the UTFPR, for supplying unpublished historical hormone monitoring data and the Municipal Secretariat of Health of Curitiba for their participation in the study through provision of data on medications distributed by UMSs.

6. REFERENCES

AL-KHAZRAJY, O. S. A.; BOXALL, A. B. A. Risk-based prioritization of pharmaceuticals in the natural environment in Iraq. **Environmental Science and Pollution Research**, v. 23, p. 15712–15726, 2016. https://doi.org/10.1007/s11356-016-6679-0

AUBAKIROVA, B.; BEISENOVA, R.; BOXALL, A. B. Prioritization of pharmaceuticals based on risks to aquatic environments in Kazakhstan. **Integrated Environmental Assessment and Management**, v. 13, n. 5, p. 832–839, 2017. https://doi.org/10.1002/ieam.1895

BARCELLOS, D. S. **Gestão de micropoluentes em rios urbanos**: estudo de caso dos contraceptivos orais na bacia hidrográfica do rio Belém, Curitiba, Paraná. 2018. 193 p. Dissertation (MSc in Urban Management) - School of Architecture and Design, Pontifical Catholic University of Paraná, Curitiba, 2018.

BERNINGER, J. P.; LALONE, C. A.; VILLENEUVE, D. L.; ANKLEY, G. T. Prioritization of pharmaceuticals for potential environmental hazard through leveraging a large-scale mammalian pharmacological dataset. **Environmental Toxicology and Chemistry**, v. 35, n. 4, p. 1007–1020, 2016. https://doi.org/10.1002/etc.2965

BOLLMANN, H. A.; EDWIGES, T. Avaliação da qualidade das águas do Rio Belém, Curitiba-PR, com o emprego de indicadores quantitativos e perceptivos. **Engenharia Sanitária e Ambiental**, v. 13, p. 443–452, 2008. https://doi.org/10.1590/S1413-41522008000400013

BURNS, E. E.; CARTER, L. J.; SNAPE, J.; THOMAS-OATES, J.; BOXALL, A. B. A. Application of prioritization approaches to optimize environmental monitoring and testing of pharmaceuticals. **Journal of Toxicology and Environmental Health, Part B**, v. 21, p. 115-141, 2018. https://doi.org/10.1080/10937404.2018.1465873

CARVALHO JUNIOR, M. R. **O interesse popular na gestão dos recursos hídricos sob a ótica do desenvolvimento sustentável**: o caso da bacia do Rio Belém em Curitiba – PR. 2007. 268 p. Dissertation (MSc in Urban Management) - School of Architecture and Design, Pontifical Catholic University of Paraná, Curitiba, 2007.

COCHRAN, W. G. **Sampling Techniques**. 3. ed. New York: John Wiley & Sons, 1977.

CUNHA, D. L. **Avaliação do padrão de consumo do 17α – etinilestradiol no município de Santa Maria Madalena – RJ**. 2014. 86 p. Dissertation (MSc in Public Health) Oswaldo Cruz Foundation, Rio de Janeiro, 2014.

DAOUK, S.; CHEVRE, N.; VERNAZ, N.; BONNABRY, P.; DAYER, P.; DAALI, Y.; FLEURY-SOUVERAIN, S. Prioritization methodology for the monitoring of active pharmaceutical ingredients in hospital effluents. **Journal of Environmental Management**, v. 1, n. 160, p. 324-32, 2015. https://doi.org/10.1016/j.jenvman.2015.06.037

DIAS, R. V. A. **Avaliação da ocorrência de microcontaminantes emergentes em sistemas de abastecimento de água e da atividade estrogênica do estinilestradiol**. 2014. 148 p. Dissertation (MSc in Sanitation, Environment and Water Resources) - Federal University of Minas Gerais, Belo Horizonte, 2014.

EUROPEAN UNION. **Directive 2013/39/EC**. 12 Aug. 2013. Available at: https://eur-lex.europa.eu/legal-content/EN/TXT/PDF/?uri=CELEX:32013L0039&from=PT. Access: June 19, 2016.

GILBERT, N. Drug-pollution law all washed up. **Nature**, v. 491, p. 503–504, 2012. https://dx.doi.org/10.1038/491503a

GUO, J. H.; SINCLAIR, C. J.; SELBY, K.; BOXALL, A. B. A. Toxicological and ecotoxicological risk-based prioritization of pharmaceuticals in the natural environment. **Environmental Toxicology and Chemistry**, v. 35, n. 6, p. 1550–1559, 2016. https://doi.org/10.1002/etc.3319

HELWIG, K.; HUNTER, C.; MACLACHLAN, J.; MCNAUGHTAN, M.; ROBERTS, J.; CORNELISSEN, A.; DAGOT, C.; EVENBIJ, H.; KLEPISZEWSKI, K.; LYKO, S.; NAFO, I.; MCARDELL, C. S.; VENDITTI, S.; PAHL, O. Micropollutant Point Sources in the Built Environment: Identification and Monitoring of Priority Pharmaceutical Substances in Hospital Effluents. **Journal of Environmental & Analogic Toxicology**, v. 3, n. 4, p. 1–10, 2013. http://dx.doi.org/10.4172/2161-0525.1000177

IBGE. **Cidades**. 2017. Available at: https://cidades.ibge.gov.br/. Access: July 8, 2017.

IDE, A. H.; OSAWA, R. A.; MARCANTE, L. O.; PEREIRA, J. C.; AZEVEDO, J. C. R. Occurrence of pharmaceutical products, female sex hormones and caffeine in a subtropical region in Brazil. **Clean Soil Air Water**, v. 45, p. 1–9, 1600437, 2017. https://doi.org/10.1002/clen.201700334

KIDD, K. A.; BLANCHFIELD, P. J.; MILLS, K. H.; PALACE, V. P.; EVANS, R. E.; LAZORCHAK, J. M.; FLICK, R. W. Collapse of a fish population after exposure to a synthetic estrogen. **Proceedings of National Academy of Science of the USA**, v. 104, n. 21, p. 8897–8901, 2007. https://doi.org/10.1073/pnas.0609568104

KNOPKI, P. B. **Avaliação da qualidade de vida dos moradores da bacia hidrográfica do rio Belém, Curitiba – PR e sua relação com variáveis ambientais**. 2008. 89 p. Course Conclusion Work (Environmental Engineering) – Pontifical Catholic University of Paraná, Curitiba, 2008.

LARA, M. V. R. **Análise crítica de programas de revitalização de rios urbanos na bacia hidrográfica do Rio Belém em Curitiba – PR**. 2014. 150 p. Dissertation (MSc in Urban and Industrial Environment) - Technology Sector, Federal University of Paraná, Curitiba, 2014.

MACHADO, K. S.; AZEVEDO, J. C. R.; BRAGA, M. C. B.; FERREIRA, P. A. L.; FIGUEIRA, R. Distribution and Characterization of Sex Hormones in Sediment and Removal Estimate by Sewage Treatment Plant in South Brazil. **Environmental Pollution and Climate Change**, v. 1, p. 1–8, 2017.

MANSOUR, F.; AL-HINDI, M.; SAAD, W.; SALAM, D. Environmental risk analysis and prioritization of pharmaceuticals in a developing world context. **Science of The Total Environment**, 557-558, 31–43, 2016. https://doi.org/10.1016/j.scitotenv.2016.03.023

NASH, J. P.; KIME, D. E.; VAN DER VEN, L. T. M.; WESTER, P. W.; BRION, F.; MAACK, G.; STAHLSCHMIDT-ALLNER, P.; TYLER, C. R. Long-Term Exposure to Environmental concentrations of the pharmaceutical ethinyloestradiol cause reproductive failure in fish. **Environ. Health Perspect.**, v. 112, n. 17, p. 1725–1733, 2004. https://doi.org/10.1289/ehp.7209

NORMAN NETWORK. **Website**. Available at: https://www.norman-network.net/. Access: December 17, 2018.

OWEN, R.; JOBLING, S. Ethinyl oestradiol: bitter pill for the precautionary principle. In: EUROPEAN ENVIRONMENT AGENCY (Orgs.) **Late Lessons from Early Warnings**: Science, Precaution, Innovation. Copenhagen, 2013. p. 279–307.

RIVA, F.; ZUCCATO, E.; CASTIGLIONI, S. Prioritization and analysis of pharmaceuticals for human use contaminating the aquatic ecosystem in Italy. **Journal of Pharmaceutical and Biomedical Analysis**, v. 106, p. 71–78, 2015. https://doi.org/10.1016/j.jpba.2014.10.003

SANTOS, C. E. M. **Priorização de fármacos em água destinada ao consumo humano baseada em avaliação da toxicidade e do comportamento ambiental por meio de modelos computacionais (in silico) para fins de gestão ambiental**. 2015. 118 p. Dissertation (MSc in Public Health) - Department of Environmental Health, University of São Paulo, São Paulo, 2015.

VOOGT, P.; JANEX-HABIBI, M. L.; SACHER, F.; PUIJKER, L.; MONS, M. Development of a common priority list of pharmaceuticals relevant for the water cycle. **Water Science & Technology**, v. 59, n. 1, p. 39–46, 2009. https://doi.org/10.2166/wst.2009.764

WIKIPHARMA. **WikiPharma database**. Available at: http://www.wikipharma.org/api_data.asp. Access: July 8, 2017.

Ambiente & Água - An Interdisciplinary Journal of Applied Science
ISSN 1980-993X – doi:10.4136/1980-993X
www.ambi-agua.net
E-mail: ambi.agua@gmail.com

Distribution of rainfall probability in the Tapajos River Basin, Amazonia, Brazil

ARTICLES doi:10.4136/ambi-agua.2284

Received: 30 May 2018; Accepted: 25 Feb. 2019

Vanessa Conceição dos Santos[1]; Claudio Blanco[2*]; José Francisco de Oliveira Júnior[3]

[1]Universidade Federal do Pará (UFPA), Belém, PA, Brasil
Programa de Pós-Graduação em Engenharia Civil (PPGEC).
E-mail: vanessasantos.esa@gmail.com
[2]Universidade Federal do Pará (UFPA), Belém, PA, Brasil
Faculdade de Engenharia Sanitária e Ambiental (FAESA).
E-mail: blanco@ufpa.br
[3]Universidade Federal de Alagoas (UFAL), Maceió, AL, Brasil
Instituto de Cieências Atmosféricas (ICAT).
E-mail: junior_inpe@hotmail.com
[*]Corresponding author

ABSTRACT

Studies on the probability of rainfall and its spatiotemporal variations are important for the planning of water resources and optimization of the calendar of agricultural activities. This study identifies the occurrence of rain by first-order Markov Chain (MC) and by two states in the Tapajos River Basin (TRB), Amazon, Brazil. Cluster analysis (CA), based on the *Ward* method, was used to classify homogeneous regions and select samples for checking the probability of rainfall occurrence by season. The historical series of daily rainfall data of 80 stations were used for the period 1990-2014. The CA technique identified 8 homogeneous regions and their probability of occurrence of rainfall, helping to determine which regions and periods have greater need of irrigation. Results of the probability of occurrence of dry and rainy periods in the TRB were used to define the dry (May thru September) and rainy seasons (October thru April). Elements of the matrix transition probabilities showed variability in relation to time and, in addition, the influence of geographical position of seasonal rainfall in determining dry and rainy periods at specific sites in the TRB.

Keywords: cluster analysis, dry and rainy days, Markov chains.

Distribuição da probabilidade de chuva na bacia do rio Tapajós, Amazônia, Brasil

RESUMO

Estudos sobre a probabilidade de chuvas e suas variações espaço-temporais são importantes para o planejamento de recursos hídricos e otimização do calendário de atividades agrícolas. O presente estudo identifica a ocorrência de chuvas pela cadeia de Markov de primeira ordem (CM) e por dois estados da bacia hidrográfica do rio Tapajós (BHRT), Amazônia, Brasil. A análise de agrupamento (AC), baseada no método de *Ward*, classificou

regiões homogêneas e selecionou a amostra para verificar a probabilidade de ocorrência de chuvas por estação. A série histórica de dados diários de precipitação de 80 estações compreendendo o período de 1990-2014 foi usada. A técnica AC identificou 8 regiões homogêneas e suas probabilidades de ocorrência de chuvas, auxiliando assim no estabelecimento de períodos com maior necessidade de agricultura irrigada de acordo com a região. Os resultados sobre a probabilidade de ocorrência de períodos secos e chuvosos na bacia definiram as estações seca (maio a setembro) e chuvosa (outubro a abril). Elementos das probabilidades da matriz de transição mostraram variabilidade em relação ao tempo e, além disso, a influência da posição geográfica da precipitação sazonal na determinação dos períodos seco e chuvoso em locais específicos na bacia do rio Tapajós.

Palavras-chave: análise de agrupamentos, cadeias de Markov, dias secos e chuvosos.

1. INTRODUCTION

Rainfall is a climatic factor of major environmental importance, especially in relation to floods and prolonged periods of drought (Marengo *et al.*, 2010). Rainfall regime impacts environmental conditions and almost all productive activities of society, since it is the main water supply for human and economic activities (Almeida *et al.*, 2011). An understanding of the potential occurrence of dry and rainy days can contribute decisively to the decision-making process regarding planting times, water deficit risk assessment and irrigation system design (Keller Filho *et al.*, 2006; Marcelino *et al.*, 2012; Carvalho *et al.*, 2017). According to Vela *et al.* (2007), historical rainfall data are highly relevant for monitoring the impacts caused by their excess or prolonged shortage within a specific region. Despite the great importance of pluviometric data in the planning and design of engineering works, prolonged rainy weather can be a limiting factor for the use of agricultural equipment, affecting previously established schedules (Fernandes *et al.*, 2002).

The Central-West region, for example, ranks first nationally in corn and soybean production, with the State of Mato Grosso as the main producer of both crops, producing approximately 64% of maize and 60% of soybeans, with more than 4,498,000 and 9,518,000 hectares planted, respectively (CONAB, 2019). According to Garcia *et al.* (2013), in a study carried out in the Sinop region (MT), the best growing season indicated for maize crop corresponds to the wet season during spring and summer, which favors high water availability to the soil due to rainfall and less probability of occurrence of consecutive dry days. The authors also affirm that in order to obtain a good income from the agricultural activity, it is important to know the conditions of the environment and the culture, from before planting until post-harvest, as the rainfall and the temperature of the air, together with the photoperiod, are the main meteorological variables for productivity.

Semenov (2008) and Martin *et al.* (2007) state that stochastic models applied in hydrology are often used to complement daily climatological data. In addition, the models assess the effect of climate change on daily precipitation (Yoo *et al.*, 2016). Markov Chain (MC) models are often proposed to rapidly obtain weather forecasts (dry or rainy) and their transition throughout the year (Lennartsson *et al.*, 2008; Breinl *et al.*, 2013). In the present work, the MC method is used to model the occurrence of daily precipitation, as occurs often in the literature (Sharif *et al.*, 2007, Damé *et al.*, 2007, Selvaraj and Selvi, 2010, Sukla *et al.*, 2016, Yoo *et al.*, 2016). The emphasis on the application of the Markov chain derives from the use of the information from the previous day (dry or rainy) to provide a prognosis about the possible occurrence of a dry or rainy day for a given region (Carvalho *et al.*, 2017). The daily precipitation model, based on MC, presents several advantages, such as the ease of parameter estimation and data generation when compared to other models also used in rainfall modeling. For example, the Poisson model

has more complex structures and greater difficulties in parameter estimation (Yoo *et al.*, 2016), while MC basically involves two components: the occurrence of binary precipitation (precipitation or absence of precipitation) and the quantity of precipitation on wet days (Breinl *et al.*, 2013). The MC are also the most-indicated models for the study of rainy- and dry-day sequences, since other models for probabilities have difficulty in describing the daily persistence of the occurrence conditions (Sukla *et al.*, 2016). Another factor is the rapid response made possible by the model, which may contribute to a greater economic return for rural producers, as it supports the identification of alternative sowing dates. This planning can be optimized if time distribution is associated with a spatial distribution of occurrences by characterizing regions with similar behaviors.

Thus, regions with hydrological similarities can be classified into groups. The literature reports that the multivariate cluster analysis (CA) method provides striking results to determine homogeneity (Yang *et al.*, 2010; Cabrera *et al.*, 2012; Lyra *et al.*, 2014). This study sought to determine the distribution of rainfall probability using first-order Markov chains and two states (dry and rainy days), grouped by Cluster analysis to identify pluviometrically homogeneous regions in the Tapajos River Basin, Amazonia, Brazil. Other authors have used rainfall (daily, monthly or annual) and other information in their studies (Raziei *et al.*, 2012; Gonçalves *et al.*, 2016).

2. MATERIALS AND METHODS

2.1. Study area and data

The Tapajos River Basin (TRB) drains an area of 493,200 km^2 and comprises 6% of Brazilian territory. It occupies areas in the states of Mato Grosso (MT), Pará (PA) and a small part of the Amazon (AM), and lies between 2° and 15° S and between 53° and 61° W. According to Kottek *et al.* (2006), the TRB presents two climatic typologies by Köppen-Geiger´s climatic classification. The predominant climate from the headwaters to the center of the basin is classified as *"Aw"*, that is, rainfall in the summer, the characteristic climate of the savannahs. From the center to the mouth, climate is classified *"Am"*, or rather, tropical monsoon climate, with a dry season and intense rains for the rest of the year. In the study by Santos *et al*. (2014) in the TRB, within the *"Am"* climate area, the months with the lowest rainfall are from May to October. In the *"Aw"* climate, the dry season runs from April to September, with July being the month with the lowest rainfall value in both climates, with mean values of 36 mm / year and 6 mm / year, respectively.

Daily rainfall data provided by 80 gauge stations used in this study were retrieved from the National Water Agency (ANA) database, via HIDROWEB (http://hidroweb.ana.gov.br), and from the National Institute of Meteorology (INMET), via BDMET (http://www.inmet.gov.br/projetos/rede/pesquisa/). Because they were daily data, they were not submitted to any statistical treatment to fill in the flaws. Bertoni and Tucci (2007) present in their studies several methodologies used to fill in flaws and also comment that none is indicated to fill in daily failures, being more recommended to fill monthly or annual failures. In selecting the periods of the historical rainfall series, the admissible fault limit of up to 1.8% in each data series was applied as a criterion. This limit of failures was adopted based on the study by Baú *et al.* (2013), where the stochastic model chosen (Markov Chains) admitted, with good reasonableness, its application, but does not rule out the possibility of negative, albeit small, interference in the accuracy of the results. Figure 1 shows the site of the study area and the distribution of rainfall gauge stations. Table 1 provides information on the same.

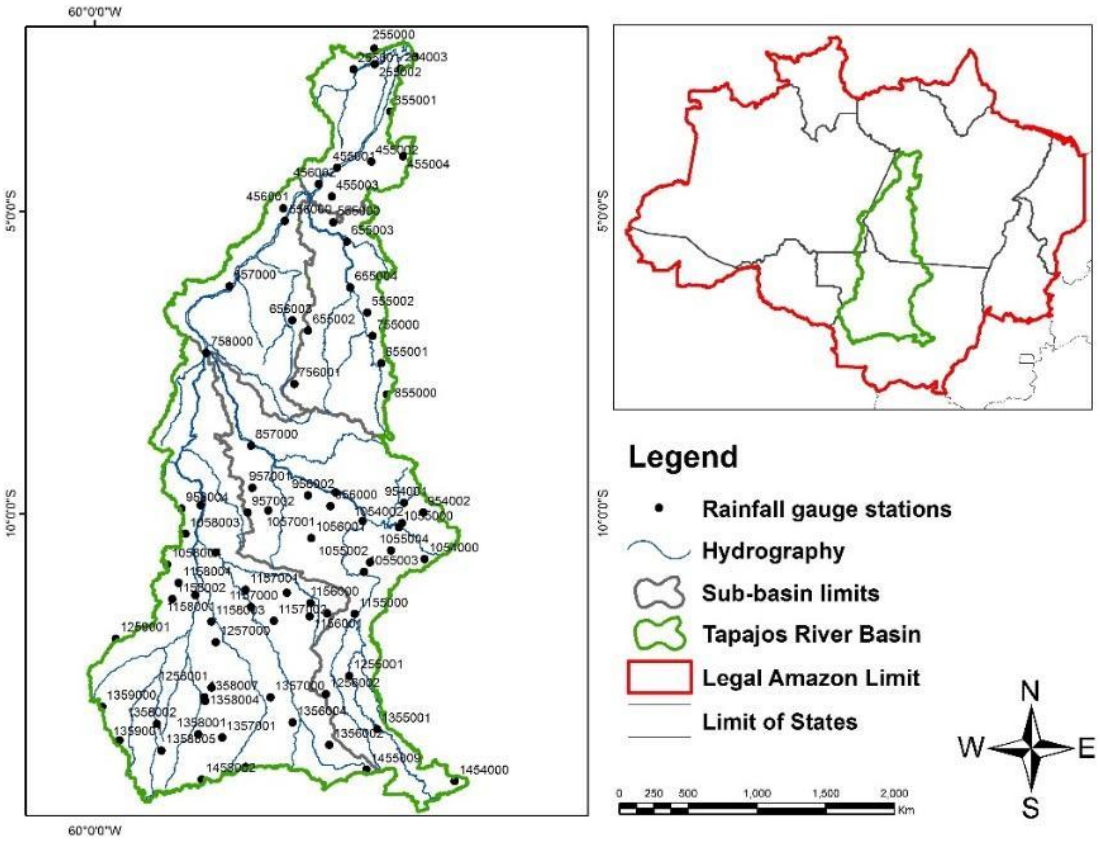

Figure 1. Location map of the area under analysis: Tapajos River Basin, with code of 80 rainfall gauge stations.

Table 1. Rainfall gauge stations in current study, with geographical coordinates (latitude and longitude, °), identifier (ID), code and start / end of time series.

ID	Code	Lat. (S)	Long. (W)	Start	End	Annual mean precipitation (mm)
01	756001	-7.8503	-56.7000	01/01/2000	31/12/2002	1707.3
02	255000	-2.2683	-55.4806	01/01/2002	31/12/2010	2578.3
03	855000	-8.1872	-55.1194	01/01/1992	28/02/2002	2607.8
04	1359001	-13.7781	-59.7675	22/02/1992	31/12/2014	1922.1
05	1358004	-13.0944	-58.1764	01/01/1997	31/12/1999	1523.3
06	254000	-2.4431	-54.7075	04/06/1995	30/11/2010	2375.9
07	1259001	-12.0603	-59.6503	01/01/1990	31/12/2001	1902.9
08	254003	-2.6419	-54.9439	01/01/1990	31/12/1998	1667.2
09	455001	-4.2772	-55.9931	01/01/1990	30/06/2014	2092.0
10	255002	-2.5644	-55.3742	01/01/2005	31/12/2014	2347.4
11	255001	-2.6508	-55.7206	01/01/1998	31/12/2014	1934.2
12	355001	-3.3500	-55.1167	01/03/2004	31/12/2014	2087.7
13	455004	-4.0894	-54.9028	01/01/1990	30/09/2003	1807.6
14	455002	-4.1750	-55.4269	01/03/2004	31/12/2014	2188.9
15	456002	-4.5500	-56.3000	01/03/2004	31/03/2014	2418.5
16	455003	-4.7547	-56.0794	01/01/1990	30/09/2003	1972.2
17	456001	-4.9469	-56.8822	01/01/1990	30/09/2003	1972.2
18	556000	-5.1542	-56.8556	01/03/2004	31/12/2012	2425.0
19	555000	-5.1825	-56.0578	01/01/1990	30/09/2003	2356.9
20	655003	-5.5000	-55.8333	01/03/2004	31/10/2012	2373.9
21	657000	-6.2358	-57.7756	01/03/2004	31/12/2014	2142.6
22	655004	-6.2575	-55.7733	01/03/2004	31/03/2013	1766.5
23	555002	-6.6714	-55.4958	01/03/2004	31/05/2014	2241.2

Continue...

Continued...

24	656003	-6.8000	-56.7333	01/03/2004	31/03/2013	2348.3
25	655002	-6.9678	-56.4728	01/03/2004	30/11/2012	1985.9
26	755000	-7.0606	-55.4078	01/03/2004	28/02/2013	2246.8
27	758000	-7.3389	-58.1550	01/03/2004	31/12/2014	2891.9
28	655001	-7.5067	-55.2614	01/01/1990	31/08/2002	2060.7
29	857000	-8.8703	-57.4164	01/03/2004	28/02/2013	2067.3
30	957001	-9.5664	-57.3947	01/09/1993	31/12/2013	1888.8
31	956001	-9.6425	-56.0183	01/10/1994	31/12/2013	2243.0
32	956002	-9.6939	-56.4742	01/11/1999	31/12/2014	2299.1
33	954001	-9.8172	-54.8858	01/04/1993	31/12/2014	2185.3
34	1058002	-9.8561	-58.2469	01/11/1994	31/08/2007	1920.2
35	956000	-9.8703	-56.1022	01/07/1998	30/11/2003	1898.3
36	958004	-9.9133	-58.5642	15/09/2004	31/12/2014	2085.3
37	1057001	-9.9414	-57.1319	01/09/1994	31/12/2014	2177.8
38	954002	-9.9758	-54.5653	01/01/2005	31/12/2014	1762.5
39	957002	-9.9761	-57.4736	01/07/2000	31/12/2014	2248.9
40	1055001	-10.1125	-55.5700	01/05/1995	31/12/2014	1940.9
41	1054002	-10.1500	-54.9186	13/12/2004	31/12/2014	2052.1
42	1055000	-10.2194	-54.9703	01/02/2004	31/10/2008	1673.1
43	1058003	-10.3286	-58.5003	01/01/1990	31/10/2004	1947.7
44	1056001	-10.3975	-56.4192	01/07/2005	31/12/2014	2119.9
45	1055004	-10.6044	-55.1033	01/08/2000	31/08/2012	1992.9
46	1058006	-10.6397	-58.0039	01/05/2001	31/01/2011	1951.6
47	1054000	-10.7461	-54.5461	01/05/1995	31/12/2014	1784.3
48	1055002	-10.7986	-55.4486	01/09/1993	31/12/2014	1734.5
49	1058004	-10.8342	-58.8033	03/07/2001	31/12/2014	2073.1
50	1055003	-10.9558	-55.5486	01/08/1994	31/12/2014	1990.7
51	1158004	-11.1392	-58.6150	01/10/2004	31/12/2014	1801.5
52	1157001	-11.2531	-57.5067	01/01/1997	31/08/2014	1934.3
53	1156002	-11.3047	-56.8250	01/08/2004	31/12/2014	2056.9
54	1158001	-11.3417	-58.3383	01/11/1991	31/12/2014	1785.5
55	1158002	-11.4081	-58.7186	01/01/1990	31/03/2006	1921.0
56	1156000	-11.4714	-56.4333	01/06/1992	31/12/2014	1845.2
57	1157000	-11.5358	-57.4172	01/03/1999	31/07/2011	1789.0
58	1156003	-11.6447	-56.1572	01/02/2008	31/12/2012	1967.4
59	1155000	-11.6531	-55.7017	01/08/2004	31/12/2014	1868.8
60	1156001	-11.6914	-56.4486	01/08/1992	31/12/2014	1843.1
61	1157002	-11.7650	-57.0419	04/12/1999	31/12/2014	1939.9
62	1158003	-11.7772	-58.0725	01/01/2008	31/08/2014	1832.8
63	1257000	-12.1169	-57.9992	01/03/1996	31/12/2014	1778.2
64	1255001	-12.6750	-55.7931	10/09/1996	31/12/2014	1667.9
65	1258001	-12.8675	-58.0703	01/10/2008	31/12/2014	1983.8
66	1256002	-12.9797	-56.1806	04/12/1999	31/12/2014	1795.7
67	1358007	-13.0267	-58.1881	01/03/2008	31/01/2014	1615.0
68	1357000	-13.0292	-57.0925	01/10/1996	31/12/2014	1642.3
69	1359000	-13.1831	-59.8769	07/10/1993	31/12/2014	2152.4
70	1356004	-13.4450	-56.7275	02/11/2004	31/12/2014	1623.0
71	1358002	-13.4667	-58.9750	01/11/1990	31/12/2014	2244.7
72	1355001	-13.5564	-55.3317	01/01/1992	31/10/2011	1721.6
73	1358001	-13.6414	-58.2892	19/04/1993	31/12/2014	1728.8
74	1357001	-13.6922	-57.8944	15/05/2000	30/09/2013	1760.6
75	1356002	-13.8156	-56.1222	01/08/2006	31/12/2014	1723.0
76	1358005	-13.9100	-58.8981	18/10/1999	31/12/2014	1929.8
77	1457003	-14.1847	-57.5069	01/01/1990	31/01/2008	1921.3
78	1455009	-14.2214	-55.5067	01/04/2006	31/03/2014	1671.9
79	1458002	-14.3842	-58.2344	01/09/2004	31/12/2014	1803.1
80	1454000	-14.4178	-54.0494	01/06/1994	31/08/2006	1742.4

2.2. Determination of rainy or dry days

Rainy or dry days are determined by applying the Markovian stochastic process, a widely used technique in the literature (Detzel and Mine, 2011; Dash, 2012; Stowasser, 2012;

Szyniszewska and Waylen, 2012; Baú *et al.*, 2013). The condition of rainy or dry state is associated with a probability of occurrence. The stochastic process adopted in the study was used to model rainfall occurrences by first-order MC (the probability of the rainfall state on the current day "*t*" depends only on the rainfall state of the previous day, *t-1*) and by two states (dry or rainy). Combination hypotheses for the determination of the probabilities of transition between states are carried out by a matrix of transition (MT) (Equation 1).

$$\mathrm{MT} = \begin{vmatrix} \mathrm{P}_{00} & \mathrm{P}_{01} \\ \mathrm{P}_{10} & \mathrm{P}_{11} \end{vmatrix} \quad (1)$$

The transition probabilities between states follow Equations 2 and 3:

$$P_{00} = P[X_{t+1} = 0/X_t = 0] \quad (2)$$

$$P_{11} = P[X_{t+1} = 1/X_t = 1] \quad (3)$$

In the case of defining rainfall states on day "*t*", current days are tagged as "X_t", with "0" for dry days and "1" for rainy days. First order MCs consider combinations of dry (0) and rainy (1) states as follows:

P_{00} is the probability of not raining today because it did not rain yesterday;

P_{01} is the probability of not raining today because it rained yesterday;

P_{10} it is likely to rain today because it did not rain yesterday;

P_{11} it is likely to rain today because it rained yesterday.

Calculation of probabilities is performed by counting the items in the historical records of the desired rainfall station, as described in Equations 4, 5, 6 and 7, where "*N*" represents the relation between the number of occurrences of combinations dry / rainy days of the historical series according to the rainfall station (j).

$$P_{00}(j) = \frac{N_{00}(j)}{N_{00}(j)+N_{10}(j)} \quad (4)$$

$$P_{01}(j) = \frac{N_{01}(j)}{N_{01}(j)+N_{11}(j)} = 1 - P_{11}(j) \quad (5)$$

$$P_{10}(j) = \frac{N_{10}(j)}{N_{00}(j)+N_{10}(j)} = 1 - P_{00}(j) \quad (6)$$

$$P_{11}(j) = \frac{N_{11}(j)}{N_{01}(j)+N_{11}(j)} \quad (7)$$

Where:

N_{00} – number of dry days with previous dry day;

N_{01} – number of dry days with previous rainy day;

N_{10} - number of rainy days with previous dry day;

N_{11} - number of rainy days with previous rainy day.

The values of daily rainfall as indicative of dry periods, also called minimum values, present a considerable variation among the authors found in the literature, such as, 0.3 mm (Baú *et al.*, 2013), 5.0 mm (Pizzato *et al.*, 2012; Viana *et al.*, 2002), 0.2 mm (Calgaro *et al.*, 2009),

0.1 mm (Dourado Neto *et al.*, 2005; Keller Filho *et al.*, 2006), 0.85 mm (Barron *et al.*, 2003) and 1 mm (Jeong *et al.*, 2013; Santos *et al.*, 2009), in which days with rainfall below these limits were classified as dry. Mehrotra and Sharma (2009) fined as a rainy day the one whose measured value reaches the threshold of 0.3 mm. Andrade Junior *et al.* (2001) and Viana *et al.* (2002) defined the day as dry, based on the occurrence of water deficit, that is, dry days are considered, those in which rainfall is less than the reference evapotranspiration. In the study by Vasconcellos *et al.* (2003), the authors defined the day as dry when the water storage in the soil, according to the water balance, is equal to or less than a certain critical value, conditioned by the atmospheric demand. However, the above rates depend on the study's aim, activity and type of environmental management under development. So that a day may be considered rainy, the criterion in current study is that minimum rainfall rate recorded in one day should be equal to or greater than 0.1 mm; therefore, if it is less than 0.1 mm, the day will be considered dry. This is the criterion used by INMET. This rate is equivalent to the smaller amount recorded by the pluviograph in conventional meteorological stations (CMS).

2.3. Sensitivity analysis

Sensitivity analysis was performed to determine the minimum period required for a given historical series of daily precipitation in order to estimate the probability of occurrence. In order to generate these probabilities, we verified the length of the historical series and their start and end date. In many studies applied to hydrological modeling there is a limitation in the available series, as well as in relation to the small period of observations and the low density of the data collection network. To analyze the behavior of pluviometric probabilities over time, a historical series of 30 years was selected, considering a failure limit of up to 1.8%. The four probabilities of monthly occurrences were generated for periods of 1, 2, 3, ..., 29 and 30 years. Thus, the station selected was station code 455001 (ID: 09), located in the state of the PA, in group 1 (G1) (Figure 1 and Table 1). The selected period was from 07/01/1984 to 06/30/2014 for 30 years and for the remaining periods (1 to 29 years) the final date was kept constant (day, month and year), varying only the start date and the year at each interval. To evaluate the behavior of the probabilities, a simple linear regression analysis was performed between the probabilities of occurrence generated for the 30-year series (keeping it as an independent variable in the regression analysis) and the respective probability of occurrence of each period of 1 to 29 years (dependent variables). Thus, for P00, P01, P10 and P11, the coefficient of determination (R2), the adjusted determination coefficient (R2a), the standard error, and the mean absolute and relative errors were obtained, considering p-value less than 0.05 at a significance level of 95%, with acceptance of the null hypothesis, that there is a correlation between the variables.

2.4. Cluster Analysis

The cluster analysis (CA) is a Multivariate Statistics technique that has the purpose of grouping individual items (such as objects, places or samples) into several groups, according to a classification criterion so that there is homogeneity within a group (or variables) and heterogeneity among the other groups formed based on their characteristics (Lyra *et al.*, 2014; Gonçalves *et al.*, 2016). The CA technique was used to determine the homogeneous pluviometric groups in the TRB, using all the values of the probability of occurrence of rainfall resulting from CM. The grouping criterion used was the method proposed by Ward Jr. (1963), which is a method of hierarchical data grouping that forms groups in such a way as to always achieve the smallest internal error between the vectors that make up each group and the average group vector. According to Johnson and Wichern (2007), this method is also called "minimal variance", because in each step of convergence of the method, the two clusters that have the smallest distance between them are combined to form a single group. For each phase, Ward's method uses Equation 8, which regulates the operation of the same and its convergence.

$$E_{(G1G2)} = \sum_{V}^{p} \sum_{\substack{i=1 \\ i \in G1}}^{n} (x_{iv} - \bar{x}_v)^2 \quad (8)$$

Where, $E_{(G1G2)}$ is the mean rate for two clusters; $\bar{x}_v$ is the cluster mean for each variable "v".

Euclidean distance, the geometric distance between two objects i and *i'* was employed to measure similarity between clusters. Let x_{ij} be the observation of *i-th* rainfall gauge station (i = 1, 2, ..., n), with reference to *j-th* variable in each class (j = 1, 2, ..., p) studied. Standardized Euclidean distance (DE) between two stations *i* and *i'* is calculated by Equation 9.

$$DE = \sum_{j=1}^{p} (x_{ij} - x_{i'j})^2 \quad (9)$$

Where, x_{ij} is the *j-th* characteristic of the *i-th* individual; x_{ij} is the j-th characteristic of the i-th individual.

Figure 2 shows the operational scheme of the methodology applied in this study, guiding the sequence of each step.

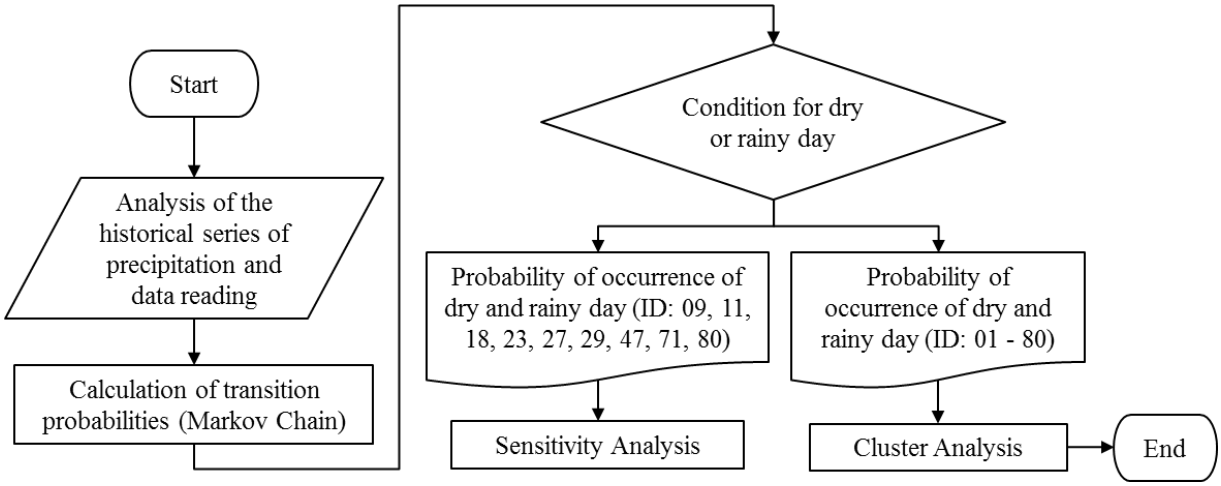

Figure 2. Methodology operational scheme.

3. RESULTS AND DISCUSSION

3.1. Sensitivity analysis

For the sensitivity analysis, the selected historical series was the one that presented values for R^2 and R^2_a equal to or greater than 0.8 in relation to the historical series of 30 years. From 3 years of data, considering the limit of failures in the registers equal to or lower than 1.8% for each analyzed period, it was possible to note that, with the exception of the linear coefficient (a), the angular coefficients determination (R^2) and adjusted determination (R^2_a) presented the same values (Table 2). This is due to the equation of the transition probabilities (Equation 2), since the behavior of P_{00} and P_{10} is complementary, as well as the behaviors of P_{01} and P_{11}. Therefore, these parameters tend to present the same slope of the regression line, although they cut the *x*-axis at different points.

Table 2. Linear regression analysis (linear coefficient (a), angular coefficient (b), determination (R^2) and adjusted determination (R^2_a)) between the probability of occurrence of rainfall data from Station 455001.

years	P_{00}				P_{01}				P_{10}				P_{11}			
	a	**b**	**R^2**	**R^2_a**	**a**	**b**	**R^2**	**R^2_a**	**a**	**b**	**R^2**	**R^2_a**	**a**	**b**	**R^2**	**R^2_a**
7	-0.05	1.02	0.97	0.97	-0.06	1.10	0.94	0.94	0.04	1.02	0.97	0.97	-0.05	1.10	0.94	0.94
6	-0.02	0.95	0.95	0.94	-0.06	1.11	0.93	0.93	0.06	0.95	0.95	0.94	-0.04	1.11	0.93	0.93
5	0.01	0.93	0.95	0.95	-0.05	1.08	0.90	0.89	0.06	0.93	0.95	0.95	-0.04	1.08	0.90	0.89
4	0.02	0.88	0.90	0.89	-0.02	1.00	0.88	0.87	0.10	0.88	0.90	0.89	0.02	1.00	0.88	0.87
3	0.11	0.72	**0.85**	**0.84**	-0.04	1.06	**0.94**	**0.93**	0.17	0.72	**0.85**	**0.84**	-0.02	1.06	**0.94**	**0.93**
2	0.12	0.69	0.77	0.75	0.00	1.01	0.96	0.95	0.19	0.69	0.77	0.75	-0.01	1.01	0.96	0.95
1	0.02	0.81	0.46	0.41	-0.05	1.14	0.85	0.84	0.17	0.81	0.46	0.41	-0.08	1.14	0.85	0.84

It was observed that R^2 and R^2_a presented values ranging from 0.8 to 0.9 in the historical series of 3, 4 and 5 years. From 6 years, the values of the coefficients are all above 0.9; therefore, the results of the other years were not shown in Table 2. Based on the analysis of the absolute and relative errors in each month for each probability of occurrence, it was verified that the highest values of these are found in the transition months (May and November) between the dry- and rainy period of the region where the rainfall season occurs.

As the period of the historical series available for generating the probabilities increases, the errors obtained in the estimates decrease. In Figure 3 (a, b, c and d), one can see the standard error and the mean absolute and relative errors for P_{00}, P_{01}, P_{10} and P_{11}, respectively. The level of significance was 95%, with a *p*-value of less than 0.05 in all analyses. The highest value was 0.0146 for the historical series of 1 year, indicating, therefore, strong statistical evidence of the relationship between the data. The range of inclination of the lines for 3 years of data, considering 95% confidence, presented the values 0.51 and 0.93 as lower and upper limit, respectively, in P_{00} and P_{10}. For P_{01} and P_{11}, the values were 0.86 and 1.26 as lower and upper limits, respectively. Since zero is not included in the confidence interval, it is possible to confirm the existence of a positive relationship between the analyzed data.

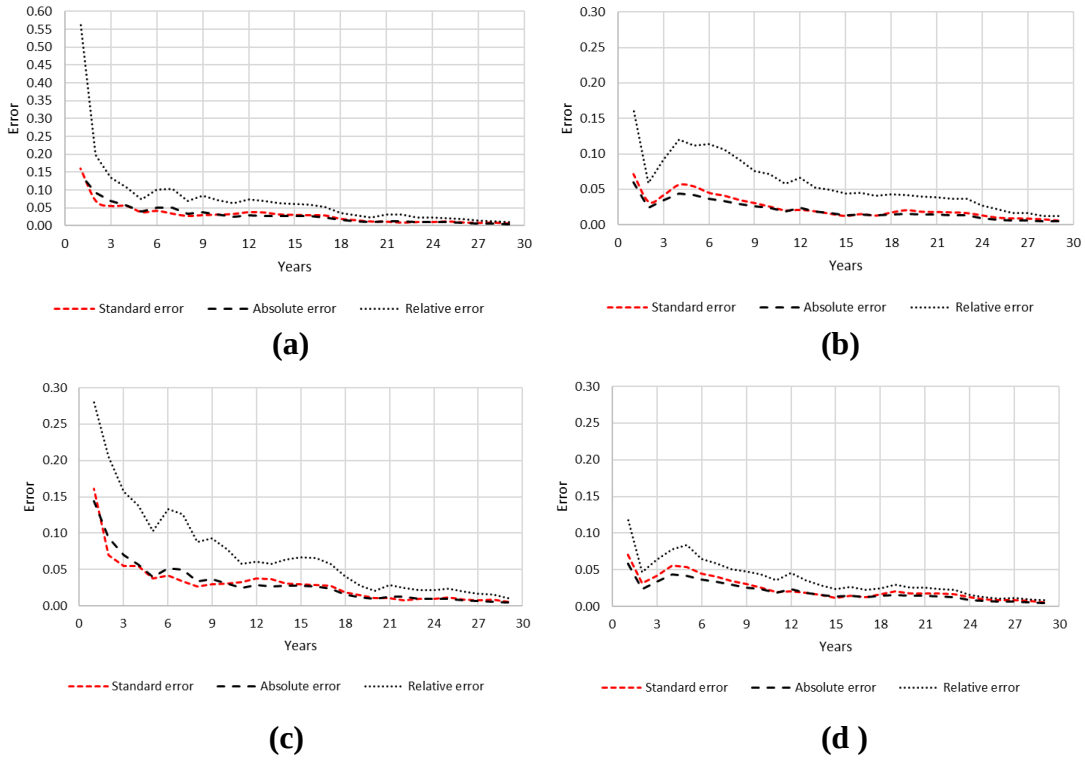

Figure 3 (a, b, c, d). Standard errors, absolute and relative sensitivity analysis of the probabilities of occurrence of rainfall data of 455001 Station for (a) P_{00}, (b) P_{01}, (c) P_{10} and (d) P_{11}.

In order to verify if this behavior could be applied in other stations, the analysis was performed this time for 8 distinct rain stations, with these codes: 758000 (ID: 27), 556000 (ID: 18), 555002 (ID: 23), 255001 (ID: 11), 857000 (ID: 29), 1454000 (ID: 80), 1358002 (ID: 71) and 1054000 (ID: 47). The starting date was the same as in Table 1, and from these the first 3 years of each historical series were separated, which were related to their maximum periods used in this study. In addition to the analyses performed at station code 455001 (ID: 09), the study also sought to verify possible interferences in the determination coefficients. The results appear in Figure 4.

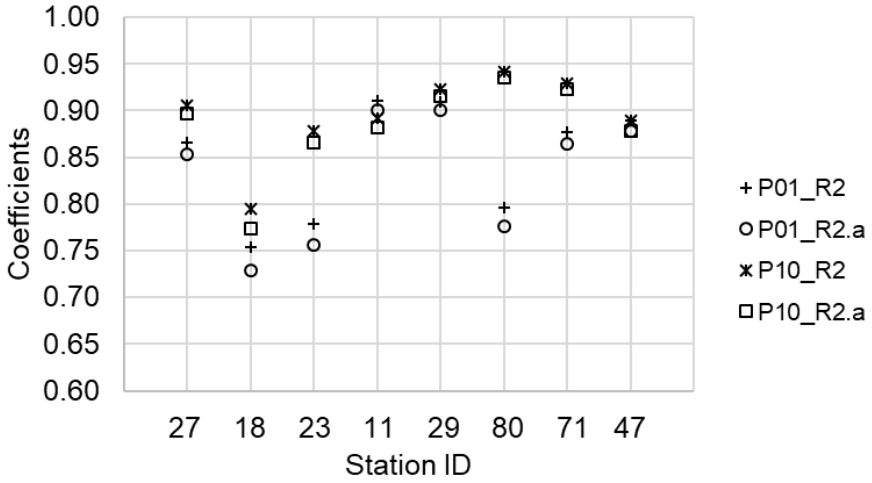

Figure 4. Coefficient of determination (R^2) and Adjusted Determination Coefficient (R^2_a) of the sensitivity analysis for the 8 rainy seasons.

Analyzing the results of both tests, the length of the historical series presented a greater influence on the results of the probabilities of occurrences when compared with the obtained Ps (simulated precipitation) if only the start and end dates are changed. This can be explained by MT itself, in that the larger the amount of information available to generate the Ps, the closer to 1 the coefficient of determination is presented (Table 2 and Figure 4).

In a historical series of 3 years, the limit of 1.8% corresponds to approximately 19 days of failure, being distributed throughout the 12 months, so that they do not present consecutively or concentrated in a single month. Otherwise, the lower the total available period, the greater the interference in the estimate of Ps in the month in question. Another possible interference is the occurrence of ENSO phenomena, since these will be related to the frequency and distribution of dry- and rainy days throughout the year, since the occurrence of the previous day is the information used to calculate the Ns of each probability. The occurrence of large-scale natural events (eg volcanic eruptions and forest fires) and low-frequency atmospheric-ocean phenomena (El Niño and La Niña) are pointed out by Salas *et al.* (2012) as factors that affect the statistical balance of hydrological series. In the study by Baú *et al.* (2013) in the Paraná Hydrographic Basin III, the analysis of the probability of occurrence results showed that the daily precipitation behavior maintained a pattern of quantity and occurrence simultaneously with the appearance of El Niño and La Niña phenomena. These possible interferences justify the reduction in the values found for the analyzed coefficients (R^2 and R^2_a), where the lowest coefficient obtained corresponds to 0.73 for R^2_a of P_{01} in station code 556000 (ID: 18), which, although less than the others, can still be considered as a good correlation between the data. The behavior of the *p*-value remained above 0.05 in all analyses. Thus, from 3 years of data, the probabilities of occurrence tend to present behavior statistically similar to the probabilities of the larger historical series, thus allowing the use of data with historical series from 3 years. It is worth mentioning that in the study are historical series ranging from 3 to 25 years, so it is not necessary to exclude any rainfall in this analysis.

3.2. Probability of rainfall occurrence and Cluster Analysis

The four probabilities of occurrence (P_{00}, P_{01}, P_{10} and P_{11}) were determined for each month of the historical series of the rainfall gauge stations of the TRB, calculated according to the number of dry and rainy days (Ns). Figures 5 and 6 show the boxplots of probabilities P_{10} and P_{01}, respectively, for the 80 stations studied. For each Boxplot (or box diagram), the vertical bar indicates the minimum and maximum value of the sample, the values being discrepant or outliers (if any) represented by circumferences. The horizontal lines of the gray box represent from bottom to top, respectively, the 1st quartile, the 2nd quartile or the median and the 3rd quartile. It may be observed that probability P_{01} presents less dispersion and asymmetry than probability P_{10}. The presence of outliers, especially in the transition months (May and October), may be explained by the individual behavior of each station along the TRB. Mean probability rates in the basin denote that the dry period occurs in the months between May and September and the rainy season from October to April. A similar result was obtained by Collischonn *et al.* (2008), who reported that the region had two well-defined seasons, a dry season from May to September and a rainy season from October to April, with annual rainfall rates varying between 1,600 mm and 2,700 mm. Figure 5, representing P_{10}, the month of February showed the lowest data variability. However, the lowest rainfall probabilities occurred in July, a fact confirmed by Figure 6 for P_{01}. Once more, dry days were a great probability in July. As a rule, May is considered the transition month between the dry and rainy periods in the TRB. Change is more pronounced in June because, depending on the rainy season and its location, rainfall probability approaches zero, confirming July and August as the driest months in the TRB.

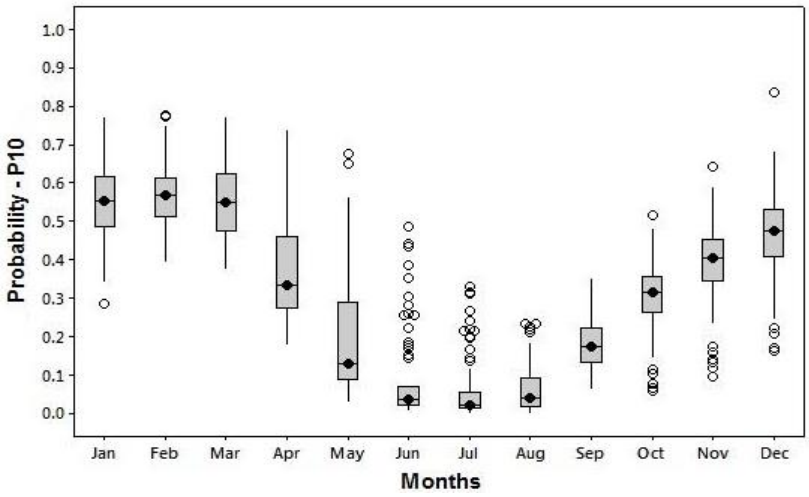

Figure 5. Boxplot of the probability of the sequence of rainy present day with previous dry (P_{10}) for the 80 rainy seasons of the TRB.

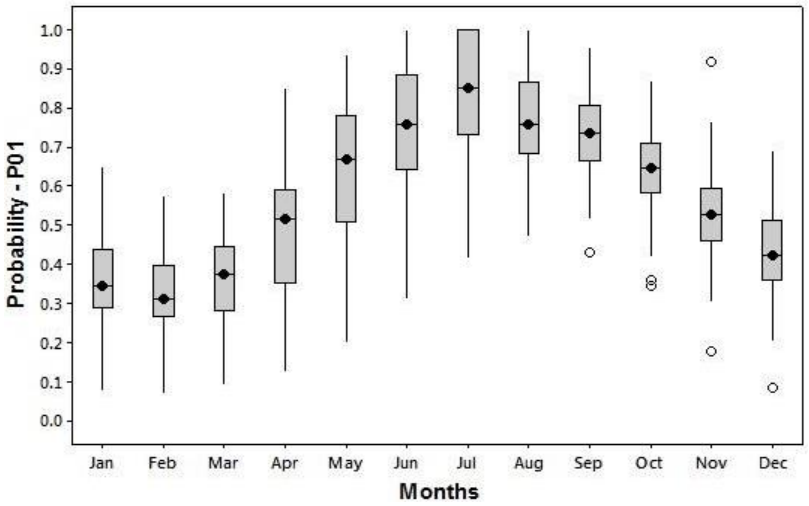

Figure 6. Boxplot of the probability of the current dry day sequence with previous rainy (P_{01}) for the 80 rainy seasons of the TRB.

Figure 7 shows the dendrogram with cluster formation and the results of the sensitivity analysis concerning the selection of Euclidean distance. Rainfall gauge stations, clustered according to similarity, are represented on the x-axis. The y-axis represents the measure of similarity for binding distances. The data used for the grouping were all 48 values of Ps obtained for each of the 80 rainfall stations. In the sensitivity analysis, the distance 3.5 was selected (red line) because it presented a better distribution of the formed clusters, resulting in 8 homogeneous ones. The stations of each cluster are identified in Table 3, while Figure 8 represents their distribution in the TRB.

After the use of the CA technique, the probability of rain occurrence was based on 8 rainy seasons, one station from each homogeneous cluster, as well as on their location in the TRB so that they could be located in different regions. The selected stations were: 555002 (ID: 23), 255001 (ID: 11), 556000 (ID: 18), 758000 (ID: 27), 1054000 (ID: 47), 857000 (ID: 29), 1358002 (ID: 71) and 1454000 (ID: 80) (Table 1). Only the probability of rainfall after a dry day (P10) and rainfall after a wet day (P11) was plotted. These two probabilities have been chosen because they are sufficient to define the Markovian process used in the model. Probabilities rates of P00 and P01 are not presented in these graphs because they are complementary to the probability rates of rain occurrence.

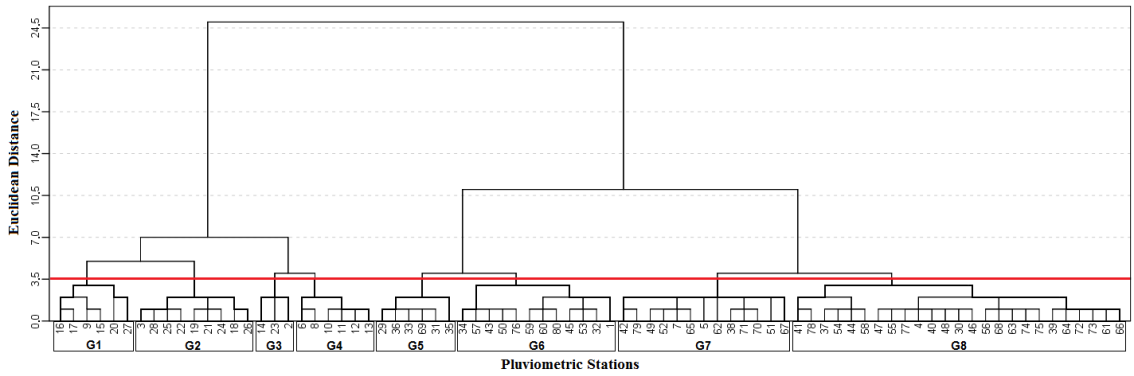

Figure 7. Dendrogram - Stations grouped according to their similarity, based on Euclidean distance.

Table 3. Identification of stations of the 8 homogeneous rainfall clusters (G_1, G_2, G_3, G_4, G_5, G_6, G_7 and G_8).

Cluster	Identification
1	16; 17; 9; 15; 20; 27.
2	3; 28; 25; 22; 19; 21; 24; 18; 26.
3	14; 23; 2.
4	6; 8; 10; 11; 12; 13.
5	29; 36; 33; 69; 31; 35.
6	34; 57; 43; 50; 76; 59; 60; 80; 45; 53; 32; 1.
7	42; 79; 49; 52; 7; 65; 5; 62; 38; 71; 70; 51; 67.
8	41; 78; 37; 54; 44; 58; 47; 55; 77; 4; 40; 48; 30; 46; 56; 68; 63; 74; 75; 39; 64; 72; 73; 61; 66.

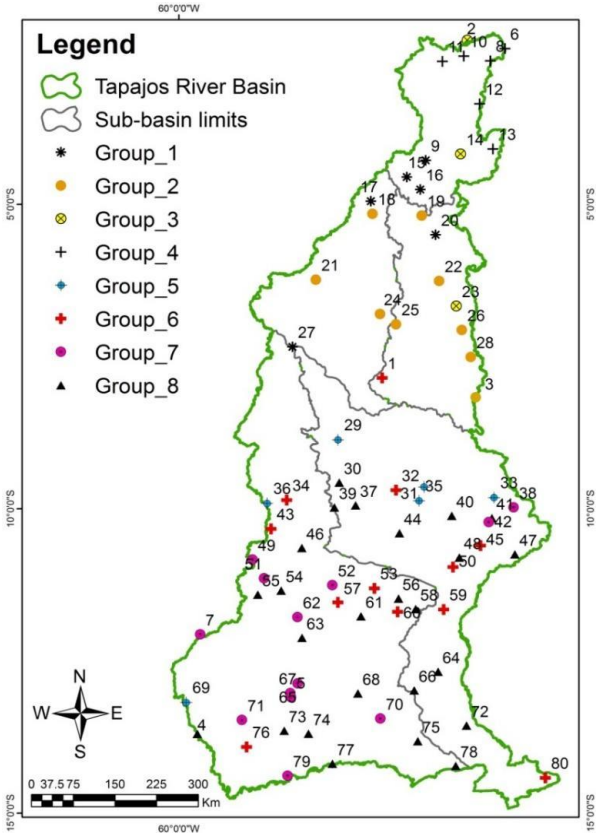

Figure 8. Spatial distribution of homogeneous rainfall clusters (G_1, G_2, G_3, G_4, G_5, G_6, G_7 and G_8) according to similarity.

Analyzing the distribution of clusters in the TRB area, it can be observed that clusters 1, 2, 3 and 4 are located in the northern region of the basin, while clusters 5, 6, 7 and 8 are distributed in the central and southern areas. It may be seen that the stations inserted in the same cluster, although presenting different rates for the occurrence of rains, have dry and rainy periods divided in a similar way in relation to the months. This fact can be verified in Figure 9 (a, b, c, d, e, f, g, h), in which the rates of clustered stations in the clusters were plotted, presenting in common the months of June, July and August as the driest; except in cluster 4, in which the smallest occurrences of rainy days occur in the months of August, September and October. For cluster 3, although the rainfall stations show relatively different values of P10, the dry period is the same (June to November). Figures 10 and 11 show the results for one station from each cluster.

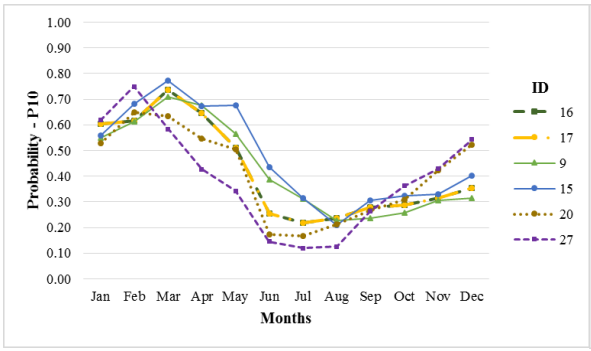

a) G_1

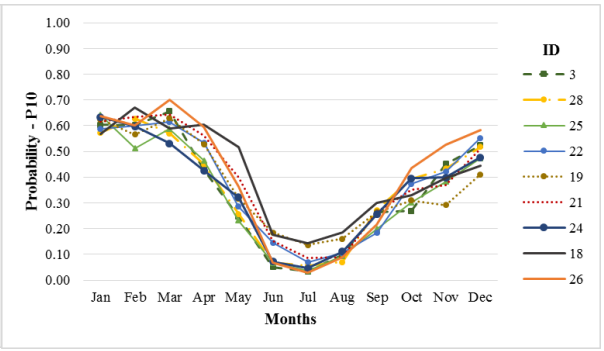

b) G_2

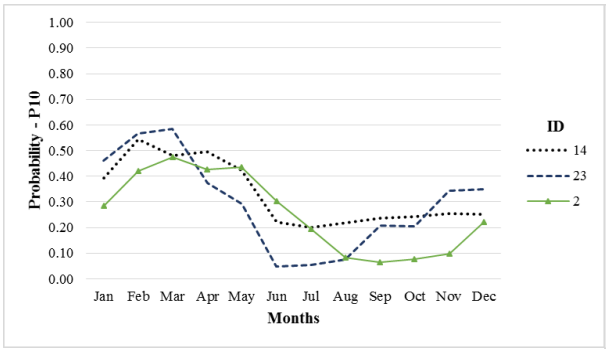

c) G_3

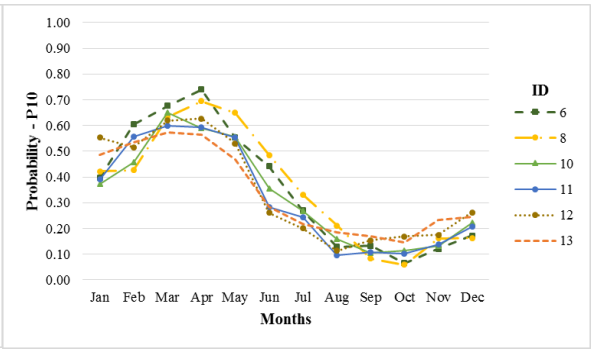

d) G_4

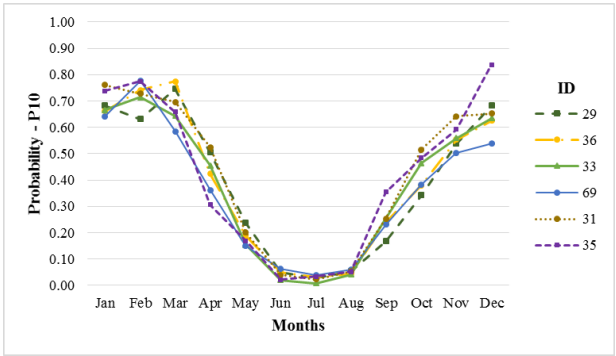

e) G_5

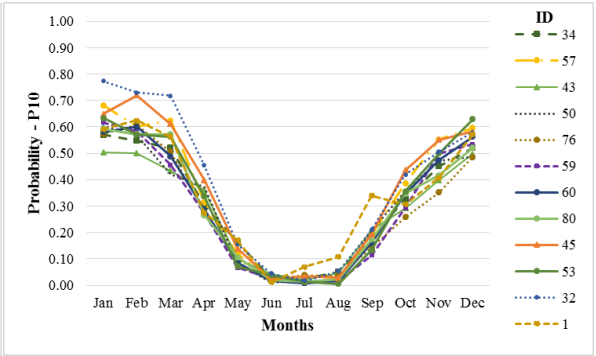

f) G_6

Figure 9 (a, b, c, d, e, f, g, h). Probabilities of transition - rainfall after a dry day (P_{10}) - rainfall gauge stations: clusters G_1, G_2, G_3, G_4, G_5, G_6, G_7 and G_8. Continue.

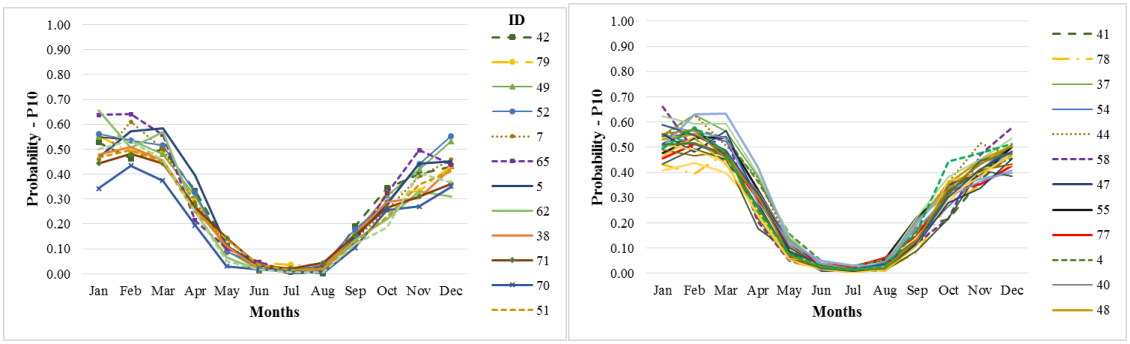

g) G_7 **h) G_8**

Figure 9 (a, b, c, d, e, f, g, h). Continued.

Figures 10 and 11 demonstrate that transition probabilities provide information on the dry or rainy periods of each season. It is possible to predict the magnitude of each period over each rainfall season. This may be noticed when comparing the probability rates in stations subjected to different climatic factors, for instance, stations 11 (code: 255001) and 80 (code: 1454000), located respectively north and south of TRB, where different biomes predominate, such as the Amazon biome at the mouth and the savannah biome at the headwaters (Mancuzzo *et al.*, 2011). This fact provides particular aspects with regard to climate and rainfall frequency. Climatic factors correspond to the static geographical features of the landscape, such as latitude, altitude, relief and vegetation (Mendonça and Danni-Oliveira, 2007).

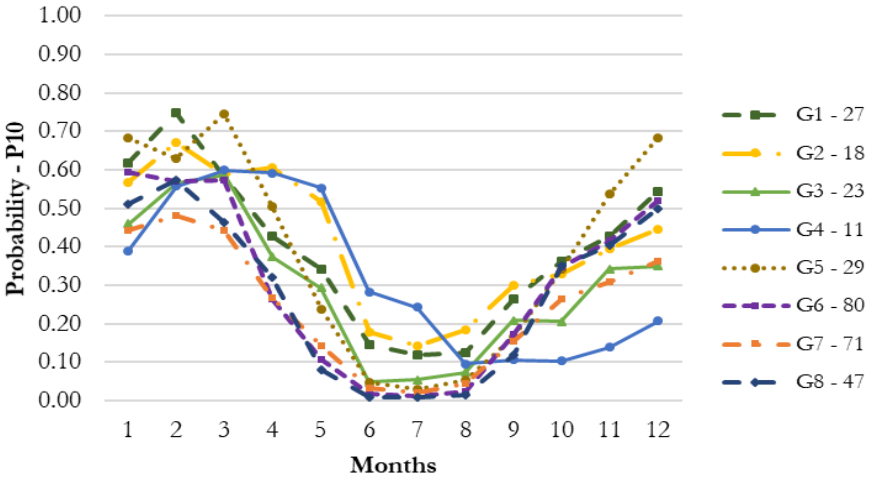

Figure 10. Transition Probabilities - Rain after a dry day (P_{10}) in 8 seasons.

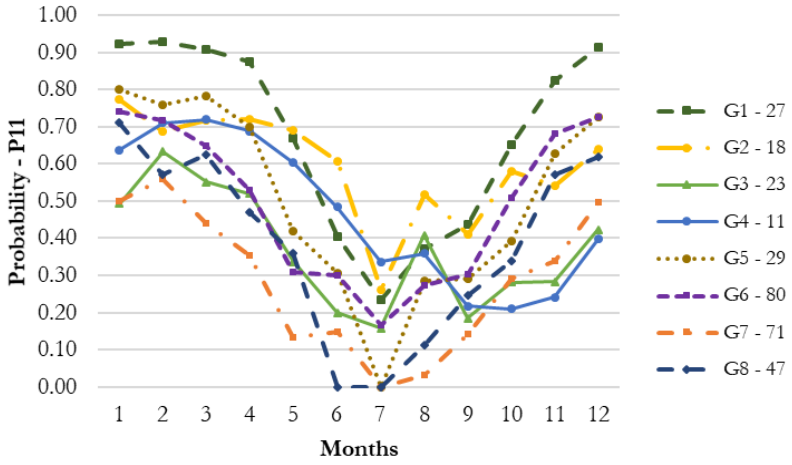

Figure 11. Transition Probabilities - Rain after a rainy day (P_{11}) in 8 seasons.

When the rates of P_{10} of stations 11 and 80 are compared, one may observe that the probability of rain after a dry day presented a rainy and dry period during a good part of the month. It was greater in the region where pluviometric station 255001 was installed. Similar results were reported by Mancuzzo *et al.* (2011) for the state of Mato Grosso (MT) where rainfall rates were higher in areas characterized by the Amazon biome and lowest for the Savannah and Pantanal biomes. According to Ziegler *et al.* (2004), the vegetation cover may influence the rainfall percentage of a given region, since, due to soil cover, the recharge of the surface and underground aquifers tend to increase or decrease due to the direct interference of the flow component. In their study conducted in Cáceres (MT), a municipality located in the south of the state of Mato Grosso, Pizzato *et al.* (2012) registered that rainfall behavior in this region differed from that in a study by Moreira *et al.* (2010) in Nova Maringá (MT) in the north of the same state. The authors concluded that, in the northern region, the drought period occurs earlier when compared to the Pantanal Matogrossense region.

In the case of the study by Moraes *et al.* (2005), the authors observed that December characterizes the beginning of the rainy season in most localities of the state of Pará (PA). However, in a small area south of the state, the beginning of the rainy season may occur in the month of October. However, in a wide range that goes from southwest to south-east, including center-south, the beginning of the rainy season occurs in November. This result does not differ from that found by Menezes *et al.* (2015) when they divided the state of PA into three homogeneous rainfall regions where the biggest rainfall rate (mm) occurred in the south-north region of the state. The occurrence of rainfall increases in most of the state of Pará in December also. In the case of annual rainfall distribution in the state of Pará, and taking into consideration the occurrence of El Niño and La Niña, results of a study by Gonçalves *et al.* (2016) showed that both events triggered the highest rainfall indexes, mainly in the northeast of the state, followed by the south region with the lowest rainfall rate.

In the case of station 255001, the period with the highest rainfall probability comprises the period between January and June, and the period with the lowest rainfall probability comprises the period between July and December, contrary to the result of Moraes *et al.* (2005). However, in the case of station 1454000, the period with the highest rainfall probability lies between October and March. Lowest rainfall probability is more pronounced between April and September. In most stations, especially those located between the headwaters and the center of the basin, probabilities P_{10} indicated a low transition probability in the driest period, i.e., rates close to zero. This transition increased significantly in stations located at the mouth. This may be explained by the type of climate of the region (*"Am"*), characterized by a brief dry season and intense rains during the rest of the year. Figure 11 also reveals that P_{11} rates were higher when compared to those of P_{10}. According to Baú *et al.* (2013), these results tend to confirm the hypothesis of persistence of the preservation of rainfall data from the previous day in the generation of probability of rainfall.

4. CONCLUSION

The Tapajos Basin region has two well-defined seasons, a dry season from May to September and a rainy season from October to April, with May and October characterized as transition periods. Factors of the probability transition matrix show variability in time and also the influence of the geographical position of the rainfall gauge stations on the determination of dry and rainy periods in specific localities of the Tapajos River Basin. Further, 8 regions with rainfall probability were identified by the clustering technique. This identification shows the difference in specific behavior of each rainfall station within the Tapajos River Basin. The insertion of the probability of occurrence analysis for different rainfall volumes according to annual variation may be recommended. For agricultural activity, the definition of these regions

assists in the identification of sites with similar dry and rainy periods, optimizing their planning. Thus, in the months with the greatest number of dry days, being June, July and August in a good part of the basin, and the months of August, September and October for cluster 4, it is necessary to use more irrigation. In defining the best sowing period, the farmer should take into account crop cycles (short or long cycle) in order to avoid crop losses due to the increase in rainy days in the region of interest.

5. ACKNOWLEDGEMENTS

The authors would like to thank ANA and INMET for kindly providing rainfall data for this analysis. The first author would like to thank CNPq for the Master's degree scholarship. The second author would like to thank CNPq for funding research productivity grant (Process 304936/2015-4). The third author would like to thank CNPq for the research productivity grant (Process 306410/2015-0).

6. REFERENCES

ALMEIDA, A. Q.; RIBEIRO, A.; PAIVA, Y. G.; RASCON, N. J. L.; LIMA, E. P. Geoestatística no estudo de modelagem temporal da precipitação. **Revista Brasileira de Engenharia Agrícola e Ambiental**, v. 15, n. 4, p. 354–358, 2011.

ANDRADE JÚNIOR, A. S. de; FRIZZONE, J. A.; BASTOS, E. A.; CARDOSO, M. J.; RODRIGUES, B. H. N. Estratégias ótimas de irrigação para a cultura da melancia. **Pesquisa Agropecuária Brasileira**, v. 36, p. 301-305, 2001.

BARRON, J.; ROCKSTROM, J.; GICHUKI, F.; HATIBU, N. Dry spell analysis and maize yields for two semi arid locations in East Africa. **Agricultural and forest Meteorology**, Boston, v. 117, n. 1-2, p. 23 – 37, 2003.

BAÚ, A. L.; AZEVEDO, C. A. V. de; BRESOLIN, A. de A. Modelagem da precipitação pluvial diária intra-anual da Bacia Hidrográfica Paraná III associada aos eventos ENOS. **Revista Brasileira de Engenharia Agrícola e Ambiental**, v. 17, n. 8, p. 883–891, 2013.

BERTONI, J. C.; TUCCI, C. E. M. Precipitação. In: TUCCI, C. E. M. **Hidrologia**: Ciência e aplicação. Porto Alegre: UFRGS, 2007. p. 177-241.

BREINL, K.; TURKINGTON, T.; STOWASSER, M. Stochastic generation of multi-site daily precipitation for applications in risk management. **Journal of Hydrology**, v. 498, p. 23-35, 2013. https://doi.org/10.1016/j.jhydrol.2013.06.015

CABRERA, J. L. B.; ROMERO, E. A.; SUCH, V. Z.; GARCÍA, C. G.; PORRÚA, F. E. Cluster analysis for validated climatology stations using precipitation in Mexico. **Atmosfera**, v. 25, n. 4, p. 339-354, 2012.

CALGARO, M.; ROBAINA A. D.; PEITER, M. X.; BERNARDON, T. Variação espaço-temporal dos parâmetros para a modelagem estocástica da precipitação pluvial diária no Rio Grande do Sul. **Engenharia Agrícola**, v. 29, n. 2, p.196-206, 2009.

CARVALHO, A. L. de; SOUZA, J. L. de; LYRA, G. B.; WANDERLEY, H. S. Aplicação da Cadeia de Markov para Dias Secos e Chuvosos. **Revista Brasileira de Meteorologia**, v. 32, n. 2, 207-214, 2017. http://dx.doi.org/10.1590/0102-77863220001

COLLISCHONN, B.; COLLISCHONN, W.; TUCCI, C. E. M. Daily hydrological modeling in the Amazon basin using TRMM rainfall estimates. **Journal of Hydrology**, v. 360, n. 1-4, p. 207–216, 2008. https://doi.org/10.1016/j.jhydrol.2008.07.032

CONAB. **Séries históricas relativas às safras 1976/77 a 2018/2019 de área plantada, produtividade e produção**. 2019. Available at: https://www.conab.gov.br/info-agro/safras/serie-historica-das-safras?start=20 Access: 16 Fev. 2019.

DAMÉ, R. DE C. F.; TEIXEIRA, C. F. A.; LORENSI, R. P. Simulação de precipitação com duração horária mediante o uso do modelo Bartlett-Lewis do pulso retangular modificado. **Revista Brasileira de Agrociência**, v. 13, n. 1, p. 13-18, 2007. http://dx.doi.org/10.18539/cast.v13i1.1304

DASH, P. R. A Markov Chain modelling of daily precipitation occurrences of Odisha. **International Journal of Advanced Computer and Mathematical Sciences**, v. 3, n. 4, p. 482-486, 2012.

DETZEL, D. H. M.; MINE, M. R. M. Generation of Daily Synthetic Precipitation Series: Analyses and Application in La Plata River Basin. **The Open Hydrology Journal**, v. 5, 2011.

DOURADO NETO, D.; ASSIS, J. P.; TIMM, L. C.; MANFRON, P. A.; SPAROVEK, G.; MARTIN, T. N. Ajuste de modelos de distribuição de probabilidade a séries históricas de precipitação pluvial diária em Piracicaba-SP. **Revista Brasileira de Agrometeorologia**, v. 13, n. 2, p. 273-283, 2005.

FERNANDES, H. C.; HAMAKAWA, P. J.; LANÇAS, K. P. Metodologia e cálculo dos dias trabalháveis com máquinas florestais na região de Botucatu, SP. **Engenharia Agrícola**, v. 22, n. 1, p. 68-74, 2002.

GARCIA, R. G.; DALLACORT, R.; KRAUSE, W.; SERIGATTO, E. M.; FARIA JÚNIOR, C. A. Calendário agrícola para a cultura do milho em Sinop (MT). **Pesquisa Agropecuária Tropical**, v. 43, n. 2, p. 218-222, 2013. http://dx.doi.org/10.1590/S1983-40632013000200014

GONÇALVES, M. F.; BLANCO, C. J. C.; SANTOS, V. C. dos.; OLIVEIRA, L. L. dos S.; PESSOA, F. C. L. P. Identification of Rainfall Homogenous Regions taking into account El Niño and La Niña and Rainfall Decrease in the state of Pará, Brazilian Amazon. **Acta Scientiarum**, v. 38, n. 2, p. 209-216, 2016. https://dx.doi.org/10.4025/actascitechnol.v28i2.26534

JEONG, D. I.; ST-HILAIRE, A.; OUARDA, T. B. M. J.; GACHON, P. Projection of future daily precipitation series and extreme events by using a multi-site statistical downscaling model over the great Montréal area, Québec, Canada. **Hydrology Research,** v. 44, n. 1, 2013. https://doi.org/10.2166/nh.2012.183

JOHNSON, R. A.; WICHERN, D. W. **Applied Multivariate Statistical Analysis**. 6th ed. Upper Saddle River: Pearson Prentice Hall, 2007.

KELLER FILHO, T.; ZULLO JUNIOR, J.; LIMA, P. R. S. R. Análise da transição entre dias secos e chuvosos por meio da Cadeia de Markov de terceira ordem. **Pesquisa Agropecuária Brasileira**, v. 41, n. 9, p. 1341-1349, 2006. http://dx.doi.org/10.1590/S0100-204X2006000900001

KOTTEK, M.; GRIESER, J.; BECK, C.; RUDOLF, B.; RUBEL, F. World map of the Köppen-Geiger climate classification updated. **Meteorologische Zeitschrift,** v. 15, n. 3, p. 259–263, 2006.

LENNARTSSON, L.; BAXEVANI, A.; CHEN, D. Modelling precipitation in Sweden using multiple step markov chains and a composite model. **Journal of Hydrology**, v. 363, p. 42-59, 2008. http://dx.doi.org/10.1127/0941-2948/2006/0130

LYRA, G. B.; OLIVEIRA-JÚNIOR, J. F.; ZERI, M. Cluster analysis applied to the spatial and temporal variability of monthly rainfall in Alagoas state, Northeast of Brazil. **International Journal of Climatology**, v. 34, n. 3, p. 3546-3558, 2014. https://doi.org/10.1002/joc.3926

MANCUZZO, F. F. N.; MELO, D. C. R.; ROCHA, H. M. Distribuição espaço-temporal e sazonalidade das chuvas no estado do Mato Grosso. **Revista Brasileira de Recursos Hídricos**, v. 16, n. 4, p. 157-167, 2011. http://dx.doi.org/10.21168/rbrh.v16n4.p157-167

MARCELINO, A. S.; ARAÚJO, L. E.; ANDRADE, E. C. A.; ALVES, A. S. Avaliação temporal da climatologia do litoral norte da Paraíba. **Revista Brasileira de Geografia Física**, v. 5, n. 3, p. 467-472, 2012.

MARENGO, J. A.; SCHAEFFER, R.; ZEE, D.; PINTO, H. S. **Mudanças climáticas e eventos extremos no Brasil**. Available at: http://www.fbds.org.br/cop15/FBDS_MudancasClimaticas.pdf. Access: Mar. 2017.

MARTIN, T. N.; STORCK, L.; DOURADO NETO, D. Simulação estocástica da radiação fotossinteticamente ativa da temperatura do ar por diferentes métodos. **Pesquisa Agropecuária Brasileira**, v. 42, n. 9, p. 1211-1219, 2007.

MEHROTRA, R.; SHARMA, A. Assessing rainfall availability over the Sydney region in a future climate using stochastic downscaling. In: WORLD IMACS / MODSIM CONGRESS, 18. 2009, Cairns. **Anais[...]** Cairns: MODSIM, 2009.

MENDONÇA, F.; DANNI-OLIVEIRA, I. M. **Climatologia**: Noções básicas e climas do Brasil. São Paulo: Oficina de Texto, 2007.

MENEZES, F. P.; FERNANDES, L. L.; ROCHA, E. J. P. da. O uso da estatística para regionalização da precipitação no Estado do Pará, Brasil. **Revista Brasileira de Climatologia**, v. 16, 2015. http://dx.doi.org/10.5380/abclima.v16i0.40023

MORAES, B. C. de; COSTA, J. M. N. da; COSTA, A. C. L. da.; COSTA, M. H. Variação espacial e temporal da precipitação no Estado do Pará. **Revista Acta Amazônica**, v. 35, n. 2, p. 207 – 214, 2005.

MOREIRA, P. S. P.; DALLACORT, R.; MAGALHÃES, R. A.; INOUE, M. H.; STIELER, M. C.; SILVA, D. J. da; MARTINS, J. A. Distribuição e probabilidade de ocorrência de chuvas no município de Nova Maringá-MT. **Revista de Ciências Agro-Ambientais**, v. 8, n. 1, p. 9- 20, 2010.

PIZZATO, J. A.; DALLACORT, R.; TIEPPO, R. C.; MODOLO, A. J.; CREMON, C.; MOREIRA, P. S. P. Distribuição e probabilidade de ocorrência de precipitação em Cáceres (MT). **Pesquisa Agropecuária Tropical**, v. 42, n. 2, p. 137-142, 2012. http://dx.doi.org/10.1590/S1983-40632012000200006

RAZIEI, T.; BORDI, I.; PEREIRA, L. S. Regional drought modes in Iran using the SPI: the effect of time scale and spatial resolution. **Water Resources Management**, v.27, n.6, p.151–159, 2012. https://doi.org/10.1007/s11269-012-0120-3

SALAS, J. D.; RAJAGOPALAN, B.; SAITO, L.; BROWN, C. Special Section on Climate Change and Water Resources: Climate Nonstationarity and Water Resources Management. **Journal of Water Resources Planning and Management**, v. 138, n. 5, p. 385–388, 2012.

SANTOS, C. A. C.; BRITO, J. I. B.; RAMANA RAO, T. V.; MENEZES, H. E. A. Tendências dos índices de precipitação no Estado do Ceará. **Revista Brasileira de Meteorologia**, v. 24, n. 1, p. 39-47, 2009.

SANTOS, C. A. dos; SERRÃO, E. A. O.; GONÇALVES, L. de J. M.; WANZELER, R. T. S.; LIMA, A. M. de. Zoneamento da Distribuição da Precipitação Pluviométrica na Bacia Hidrográfica do Rio Tapajós. **Enciclopédia Biosfera**, v. 10, n. 18; p. 3092-3106, 2014.

SELVARAJ, R. S.; SELVI, S.T. Stochastic modeling of daily rainfall at Aduthurai. **International Journal of Advanced Computer and Mathematical Sciences**, v. 1, n. 1, p.52-57, 2010.

SEMENOV, M. A. Simulation of extreme weather events by a stochastic weather generator. **Climate Research**, v. 35, n. 3, p. 203-212, 2008. http://dx.doi.org/10.3354/cr00731

SHARIF, M.; BURN, D. H.; WEY, K. M. Daily and Hourly Weather Data Generation using a K-Nearest Neighbour Approach. In: CANADIAN HYDROTECHNICAL CONFERENCE, 2007, Winnipeg. **Proceedings[...]** Winnipeg: CHC, 2007. p. 1-10.

STOWASSER, M. Modelling rain risk: a multi-order Markov chain model approach. **The Journal of Risk Finance**, v. 13, n. 1, p. 45 – 60, 2012. https://doi.org/10.1108/15265941211191930

SUKLA, M. K.; MANGARA, A. K. J.; SAHOO, L. N. Markov Chain Modeling of Daily Rainfall Occurrence in the Mahanadi Delta of India. **Journal of Applied Mathematics and Statistical Sciences,** v. 1, n. 1, p. 21-30, 2016.

SZYNISZEWSKA, A. M.; WAYLEN, P. R. Determining the daily rainfall characteristics from the monthly rainfall totals in central and northeastern Thailand. **Applied Geography**, v. 35, n. 1-2, p. 377-393, 2012. https://doi.org/10.1016/j.apgeog.2012.09.001

VASCONCELLOS, S. L. B.; ANDRÉ, R. G. B.; PERECIN, D. Probabilidade de ocorrência de dias secos para a região de Jaboticabal-SP. **Revista Brasileira de Agrometeorologia**, v. 11, n. 2, p. 321-325, 2003.

VELA, R. H. N.; DALLACORT, R.; NIED, A. H. Distribuição descendial, mensal e totais de precipitação na região de Tangará da Serra - MT. *In:* CONGRESSO BRASILEIRO DE ENGENHARIA AGRÍCOLA, 36., 2007, Bonito. **Anais[...]** Bonito: SBEA, 2007. p. 1-4.

VIANA, T. V. A.; AZEVEDO, B. M.; BOMFIM, G. V.; ANDRADE JUNIOR, A. S. Probabilidade de ocorrência de períodos secos e chuvosos, em Pentecoste, CE. **Irriga (Botucatu)**, v. 7, n. 03, p. 226-229, 2002. https://doi.org/10.15809/irriga.2002v7n3p226-229

WARD JR.; J. H. Hierarchical grouping to optimize an objective function. **Journal American Association**, v. 58, n. 301, p. 236–244, 1963. http://dx.doi.org/10.1080/01621459.1963.10500845

YANG, T.; SHAO, Q.; HAO, Z.; CHEN, X.; ZHANG, Z.; XU, C.; SUN, L. Regional frequency analysis and spatio-temporal pattern characterization of rainfall extremes in the Pearl River Basin, China. **Journal of Hydrology**, v. 380, n. 3-4, p. 386-405, 2010. https://doi.org/10.1016/j.jhydrol.2009.11.013

YOO, C.; LEE, J.; RO, Y. Markov Chain Decomposition of Monthly Rainfall into Daily Rainfall: Evaluation of Climate Change Impact. **Advances in Meteorology**, v. 2016, 10 p., 2016. http://dx.doi.org/10.1155/2016/7957490

ZIEGLER, A. D.; GIAMBELLUCA, T. W.; TRAN, L. T.; VANA, T. T.; NULLET, M. A.; FOX, J.; VIEN, T. D.; PINTHONG, J.; MAXWELL, J. F.;EVETT, S. Hydrological consequences of landscape fragmentation in mountainous northern Vietnam: evidence of accelerated overland flow generation. **Journal of Hydrology**, n. 287, p. 124-146, 2004. https://doi.org/10.1016/j.jhydrol.2003.09.027

Ambiente & Água - An Interdisciplinary Journal of Applied Science
ISSN 1980-993X – doi:10.4136/1980-993X
www.ambi-agua.net
E-mail: ambi.agua@gmail.com

Flow distribution and trends in the Das Velhas River Basin

ARTICLES doi:10.4136/ambi-agua.2289

Received: 06 Jun. 2018; Accepted: 29 Mar. 2019

Larissa Silva Melo[1*]; João Carlos Ferreira Borges Júnior[1]; Ana Paula Coelho Madeira Silva[2]

[1]Universidade Federal de São João del-Rei (UFSJ), Sete Lagoas, MG, Brasil
Departamento de Ciências Agrárias (DCIAG).
E-mail: lalasmelo@yahoo.com.br, jcborges@ufsj.edu.br
[2]Universidade Federal de São João del-Rei (UFSJ), Sete Lagoas, MG, Brasil
Departamento de Ciências Exatas e Biológicas (DECEB). E-mail: anapaula@ufsj.edu.br
[*]Corresponding author

ABSTRACT

In the management of water resources, it is necessary to balance the demands of multiple uses of water and water availability, while enabling use in an environmentally sustainable way. Probability distributions of flow rates are essential tools for assessing water availability. The objectives of this work were to analyze the best probability distribution that conforms to the annual minimum daily average discharge for periods of seven consecutive days (Q_7) for 14 stream gauging stations in the Das Velhas River Basin and to identify possible trends in Q_7 time series and in bi monthly and annual sets of daily discharges in three key stream gauging stations. The quality of fit was verified by the Anderson-Darling test (A-D). The selection of the models that presented the best fit was done according to the Bayesian Information Criterion (BIC). The Mann-Kendall test was used to verify trends in time series of discharge. In general, better measures of quality of fit were obtained for the probability distributions Gumbel and Rayleigh. Negative trends in discharge distributions were verified in the three stations. For the Várzea da Palma station, the closest to the river mouth, negative and significant trends were found for the Q_7 data and daily average discharge for every bimester except the first.

Keywords: Mann-Kendall, model selection, water resources.

Distribuições e tendências de vazões na bacia hidrográfica do Rio das Velhas

RESUMO

Na gestão dos recursos hídricos se deve buscar a harmonização entre as demandas dos usos múltiplos da água e a disponibilidade hídrica, entendendo-se esta como o quantitativo a ser utilizado de forma ambientalmente sustentável. Distribuições de probabilidade de vazões são ferramentas essenciais para avaliar a disponibilidade hídrica. Os objetivos deste trabalho foram analisar qual a melhor distribuição de probabilidade que se ajusta aos dados mínimos anuais de vazão diária média em períodos consecutivos de sete dias (Q_7) de 14 estações fluviométricas da Bacia do Rio das Velhas e identificar possíveis tendências nas séries de Q_7 e em conjuntos bimestrais e anuais de vazões diárias em três relevantes estações. O ajuste das distribuições foi verificado pelo teste de Anderson-Darling (A-D). A seleção dos modelos que apresentaram

melhor ajuste foi feita segundo o Critério de Informação Bayesiano (BIC). Para analisar a tendência das vazões, foi utilizado o teste estatístico Mann-Kendall. As distribuições que em geral melhor se ajustaram aos dados e ocuparam a melhor posição no ranking foram Gumbel e Rayleigh. Constataram-se tendências negativas nas três estações. Para a estação de Várzea da Palma, a mais próxima da foz do rio, foram encontradas tendências negativas e significativas para os dados do Q_7 e vazão média diária para todos os bimestres, exceto o primeiro.

Palavras-chave: Mann-Kendall, recursos hídricos, seleção de modelos.

1. INTRODUCTION

Concerns about sustainability of water resources arise frequently in discussions related to environmental and socioeconomic issues at global, regional and local levels. The exploitation of natural resources, without regard for sustainability, negatively impacts relationships between water availability and demand, limiting regional strategies of social and economic development covering multiple uses, among them public water supply and irrigation.

The growing importance given to rational water use has been motivating evolutions in systems of planning, administration and use of the water resources, in the search for an effective answer to social demands. To adequately manage water potential, it is fundamental to know the hydrological characterization of the basin, considering temporal and spatial variability. Knowledge of flow distribution, identifying the probability of maximum and minimum discharges events, is a fundamental aspect of this characterization.

In the management of water resources, it is necessary to continually balance water demands and availability, in an environmentally sustainable way. Mello *et al.* (2010) emphasizes the importance of the study of the probability distribution of hydrological variables, since from this knowledge it is possible to determine the appropriate reference values of discharge to estimate regional water availability.

Each state in Brazil has adopted specific criteria for the establishment of minimum reference flows that will inform studies on the granting of water-use rights. For situations in which water catchment will occur in rivers, the hydrological regime or discharge probability distributions should be considered in the analysis. For perennial rivers, the grant request is usually analyzed based on a percentage of the minimum discharge for a period of seven consecutive days and return period of ten years ($Q_{7,10}$) or minimum flows associated with the 95% (Q_{95}) or 90% (Q_{90}) of probability.

From time series of discharges, it is possible to evaluate water availability and significant changes in the hydrological regime in the long run. Best-fit analysis to identify probability distribution can be applied to these series (Silva *et al.*, 2015).

Santos (2010) argues that the randomness of hydrological processes make it difficult to predict. However, a quality of fit analysis of flow time series can be carried out for probabilistic or stochastic models. From this analysis, it is possible to infer (at a certain level of confidence) extreme flow values that are useful to the management of water resources.

On the other hand, trend analysis of discharges gives a basis to understand the impact of climate change and variations in the executed demands of multiple water uses, supporting the development and improvement of hydrological models applicable to water-resource management and scenario forecasting (Joseph *et al.*, 2013).

The trend study of the components of the hydrological cycle is fundamental in the management of water resources. Through this analysis, government management councils can seek adjustments and courses of actions to ensure sustainability in the supply of water resources in harmony with the demand dynamics (Vilanova, 2014b; Kibria *et al.*, 2016).

The identification of flow trends also contributes to the understanding of global climate

variability and is essential for the development of hydrological models, hydrological forecasting and water-resource management. Climatic variability and disorderly use of the soil affect several components of the hydrological cycle, impacting the pattern of time series (Salvadori, 2013; Damázio and Costa, 2014; Tan and Gan, 2015; Agevap, 2016).

Statistical tests such as Pettitt and Mann-Kendall can be applied to trend analysis in the time series of meteorological and hydrological variables (Barua *et al.*, 2013; Uliana *et al.*, 2015). The Mann-Kendall test (MK) is recommended by the World Meteorological Organization (WMO) and widely applied (Blain, 2010; Caloiero *et al.*, 2011; Lima *et al.*, 2011; Suhaila *et al.*, 2010; Tao *et al.*, 2011). The Mann-Kendall test has been used in several studies of hydrological trends, mainly in flow-trend analysis. Its use is justified by the fact that it presents greater robustness regarding deviations of normality and non-stationarity of the data of the time series when compared to parametric tests. In addition, this test allows the detection and approximate location of the starting point of a certain trend (Costa *et al.*, 2015; Salviano *et al.*, 2016). Dale *et al.* (2015) applied the Mann-Kendall seasonal trend analysis method to test mean daily streamflow in gauging stations from 1948 through 2010 in the Cimarron-Skeleton Watershed (North Central Oklahoma), with a drainage area of 8275 km^2. They verified the importance of adjusting irrigation to mitigate the impact of increasing climate variability on streamflow. Soares *et al.* (2018) performed the Mann-Kendal test to analyze climatic indicators of desertification in the Pajeú River Basin in the State of Pernambuco, Brazil, identifying trends for rainfall and dryness indexes.

In the State of Minas Gerais, Brazil, the Das Velhas River Basin and some others the criterion adopted was a maximum limit of 30% of $Q_{7,10}$ to be granted for consumptive water use in the hydrographic basin portion bounded by each section considered under natural conditions. In Das Velhas River Basin, there are no studies related to probability distributions and flow trends. Segmentation of these analyses on a bimonthly basis makes it possible to identify critical periods in terms of management. The Das Velhas River is the largest tributary of the São Francisco River. In its basin is the region with the highest population density in the hydrographic unit of the São Francisco River, having significant economic importance for the State of Minas Gerais. The largest water catchment in the entire basin occurs at the upper reaches of the Das Velhas River channel, responsible for supplying about 74% of the urban demand in the Belo Horizonte and Metropolitan Region. In Strategic Territorial Units (STUs) of the high Das Velhas River region, the sectors that most draw water are industry and mining, except for the STU Nascentes, which has significant demand for irrigation. Irrigation is also the main sector responsible for the withdrawal of water in the STUs of the regions Middle Low and Lower of the Das Velhas River Basin.

The present work contributes to the updating of base studies for the management of water resources in the Das Velhas River Basin, from the perspective of expansion of irrigated agriculture, especially, among multiple uses. This study therefore analyzed the quality of fit of probability distribution models to data of annual minimum of average daily discharge for a period of seven consecutive days (Q_7) for 14 stream-gauging stations in Das Velhas River Basin and identified possible trends in Q_7 time series and in bi monthly and annual sets of daily discharges in the stream gauging stations at Ponte Raul Soares, Santo Hipólito and Várzea da Palma.

2. MATERIAL AND METHODS

2.1. Study Area

The study area was the Das Velhas River Basin, located between the latitudes 17°15' S and 20°25' S and longitudes 43°25' W and 44°50' W, in the central region of the state of Minas Gerais, comprising an area of 27,850 km^2, which corresponds to 5% of the state area. The basin has a significant drainage density that feeds the main water course, which is 806.84 km long.

Considering data of the current master plan of the basin (Comitê da Bacia Hidrográfica do Rio das Velhas, 2015), the $Q_{7,10}$ is 48.31 $m^3 s^{-1}$. The lower Das Velhas River stretch is the one with the highest water availability in relation to $Q_{7,10}$ (31.54 $m^3 s^{-1}$), followed by stretches medium-high (25.94 $m^3 s^{-1}$), middle-lower (17.46 $m^3 s^{-1}$) and high (13.58 $m^3 s^{-1}$). The main segments responsible for effective water consumption are urban supply and irrigation, which account for 50.48% and 36.44% of total consumption, respectively. The water consumption by irrigation prevails especially in the STUs of the regions Middle and Low of the Das Velhas River Basin. In the STUs of the High region of the Das Velhas River Basin, the consumption of water for mining, industry and urban supply prevails.

According to information on the portal HidroWeb (2013), in this area there are 54 stream gauging stations, 14 are the responsibility of ANA, 30 of IGAM, 5 of CEMIG, 4 of CODEVASF and 1 of DNOS. The focus of the work was on the 14 stations that are the responsibility of the National Water Agency (ANA), whose dispositions in the basin are presented in Figure 1, for which discharge data are available.

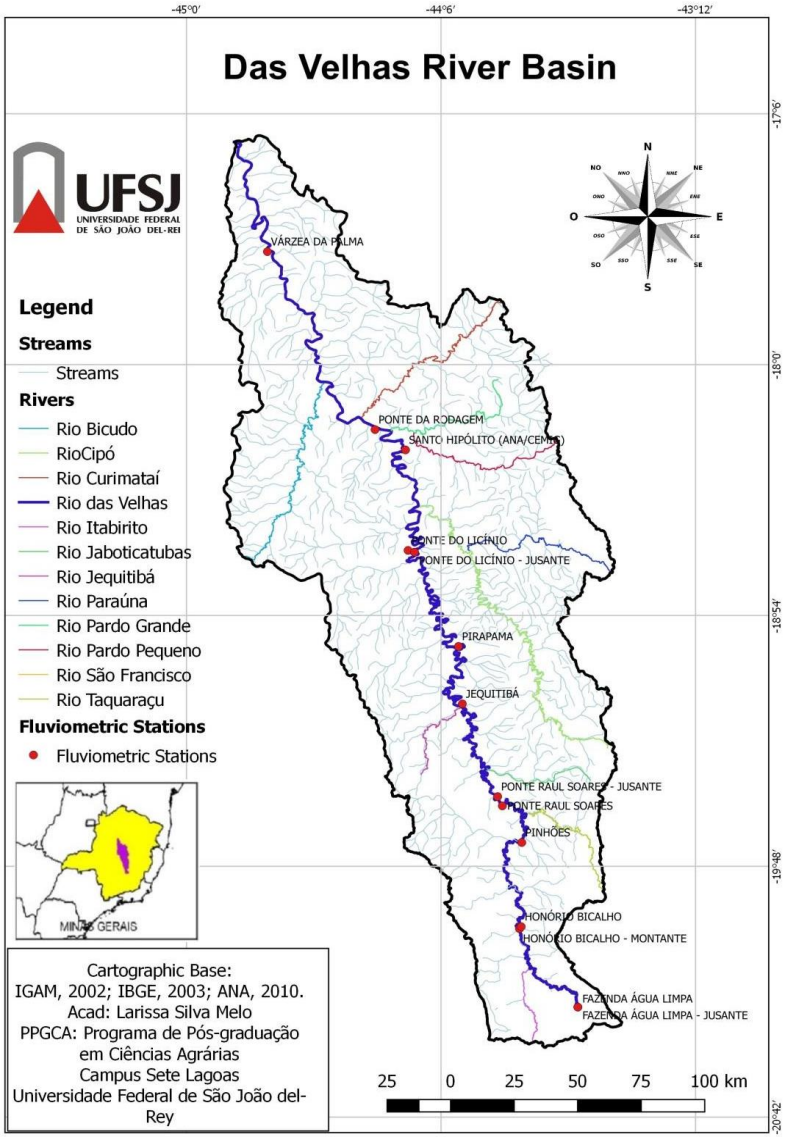

Figure 1. Location of the 14 stream gauging stations considered in the study.

The time series of discharge data was obtained from the HidroWeb system of the ANA. The stream gauging stations considered in this study are shown in Table 1. Data of the stream gauging stations and characteristics of the data set are presented in Table 1 and Table 2, respectively.

Table 1. Stream gauging stations in Das Velhas River Basin considered working, for which the National Water Agency (ANA) is responsible.

Name	Code	County	Latitude (º)	Longitude (º)	Altitude (m)	Drainage area (km^2)
Fazenda Água Limpa [(1)]	41150000	Ouro Preto	-20.30528	-43.61639	965	175
Fazenda Água Limpa Jusante [(2)]	41151000	Ouro Preto	-20.30528	-43.61639	965	175
Honório Bicalho ANA [(1)]	41200000	Nova Lima	-20.01667	-43.81667	721	1550
Honório Bicalho Montante [(2)]	41199998	Nova Lima	-20.02389	-43.82278	721	1550
Jequitibá [(2)]	41410000	Jequitibá	-19.22222	-44.02472	650	7080
Pinhões [(2)]	41260000	Santa Luzia	-19.70500	-43.81472	671[(3)]	3730
Pirapama [(2)]	41600000	Cordisburgo	-19.01111	-44.03833	616	8050
Ponte da Rodagem [(1)]	41840000	Santo Hipólito	-18.23333	-44.33333	464	19000
Ponte do Licínio [(1)]	41650000	Presidente Juscelino	-18.66667	-44.21667	560	10700
Ponte do Licínio Jusante [(2)]	41650002	Presidente Juscelino	-18.67278	-44.19389	560	10700
Ponte Raul Soares [(2)]	41340000	Lagoa Santa	-19.55972	-43.91111	637	4860
Ponte Raul Soares Jusante [(1)]	41340005	Jaboticatubas	-19.55000	-43.90000	637	4860
Santo Hipólito [(2)]	41818000	Santo Hipólito	-18.30611	-44.22583	499	16600
Várzea da Palma [(2)]	41990000	Várzea Da Palma	-17.59472	-44.71389	464	26500

Source: Adapted of HidroWeb (2013). [(1)] operator ANA; [(2)] operator CPRM, [(3)].
Source: Google Earth.

Table 2. Characteristics of discharge data sets of the stations in the Das Velhas River Basin.

Stations	Start	End	Total Data	Total Failures	% Failures	Failures in 7-day datasets
Fazenda Água Limpa	01/06/1956	31/05/1994	13745	134	0.974	380
Fazenda Água Limpa Jusante	01/05/1994	31/01/2015	7410	171	2.307	323
Honório Bicalho ANA	01/09/1963	31/12/1970	2669	10	0.374	58
Honório Bicalho Montante	01/04/1971	31/01/2015	15646	366	2.339	668
Jequitibá	01/06/1965	31/12/2014	17998	113	0.627	449
Pinhões	01/09/1975	31/12/2014	13801	566	4.101	860
Pirapama	01/07/1956	31/01/2015	19323	2076	10.743	2521
Ponte da Rodagem	01/07/1965	31/12/1970	1912	98	5.125	134
Ponte do Licínio	01/08/1941	31/12/1976	12385	552	4.457	901
Ponte do Licínio Jusante	01/05/1976	31/01/2015	13862	293	2.113	592
Ponte Raul Soares (*)	01/02/1938	30/04/2013	24045	3437	14.294	3996
Ponte Raul Soares Jusante	01/11/1976	31/01/1983	2172	111	5.110	165
Santo Hipólito (*)	01/06/1938	31/01/2015	26278	1726	6.568	2437
Várzea da Palma (*)	01/06/1938	31/01/2015	27754	250	0.900	887

(*) Stations selected for trend study.

2.2. Calculation of the minimum flow Q_7

The moving average of seven consecutive days of mean daily discharge was calculated. For each station, the annual lowest values of the moving averages for seven consecutive days (Q_7) were classified in ascending order forming a series for which the statistical analyses were carried out.

For non-complete consecutive seven-day sets of discharge values, it would not be possible to calculate the moving average without filling-in fail procedures. It was chosen in this work to not fill-in failures, discarding incomplete data sets, in order to not insert new sources of uncertainties in data series. The number of failures in seven-day datasets was counted for each station (Table 2).

2.3. Goodness of fit analysis and model selection

The probability distribution models were selected from bibliographic review (Almeida *et al.*, 2014; Silvino *et al.*, 2007; Silva *et al.*, 2015; Smakhtin, 2001; Lopes *et al.*, 2016; Rossi and Thebaldi, 2017; Pereira and Caldeira, 2018) and preliminary tests. Thus, the theoretical probability distributions used for the Q_7 data were: Erlang, Gumbel (Extreme Value), Gamma, Inverse Gaussian, Weibull, Normal Log, Pearson 5, Log Logistics, Rayleigh, Triangular. Models parameters were estimated by the Maximum Likelihood Method (Mood *et al.*, 1974).

Anderson-Darling test (Razali and Wah, 2011) at 5% significance level was applied to assess the quality of fit between empirical and theoretical distributions, i.e., for model selection. P-values and critical values were obtained by using the technique of parametric bootstrapping. The possibility of applying the technique of parametric bootstrapping due to the computational procedures programmed in the software used was considered as an additional criterion for selecting models. After that, the Bayesian Information Criterion (BIC) (Emiliano *et al.*, 2009; Detzel *et al.*, 2014; Pinto *et al.*, 2015) was applied to rank the selected models. The software @Risk version 7.0.1 (Palisade, 2016) was employed to run the tests.

2.4. Trend analysis

The mean daily discharge (volumetric flow rate) time series were analyzed in three stream gauging stations: Ponte Raul Soares, Várzea da Palma and Santo Hipólito. The data were grouped in the following categories: discharge Q_7 (minimum average daily discharge in a period of seven consecutive days, for each year); general (daily discharge over the study period); daily discharges grouped in bimesters, that is: 1st bimester (January and February); 2nd bimester (March and April); 3rd bimester (May and June); 4th bimester (July and August); 5th bimester (September and October); and 6th bimester (November and December).

The Mann-Kendall test was applied at a 5% significance level. The analyses were performed using the software R version 3.3.1 (R Core Team, 2016), with the "Kendall" package (McLeod, 2011).

Rainfall trend was also investigated by using the Mann-Kendall test for the three INMET (Brazilian National Institute of Meteorology) conventional meteorological stations in the Das Velhas River Basin. The data were obtained in the database BDMEP (Meteorological Database for Teaching and Research). The time series cover periods from 1961 to 2018 for the stations of Belo Horizonte (19.93° S, 43.93° W) and Curvelo (18.75° S, 44.45° W), and to 2016 for the station of Sete Lagoas (19.46° S, 44.25° W).

3. RESULTS AND DISCUSSION

3.1. Model fit and selection

Probability distributions that were fit to the data of annual minimum discharge for a period of seven days (Q_7) according to the Anderson-Darling test are presented in Table 3.

The probability distributions of Gumbel and Rayleigh were highlighted, since they fit to 8 and 5 stations of 14, respectively, according to the Anderson-Darling test and the possibility to apply the technique of parametric bootstrapping by the @Risk software. Quality of fit was observed for the distributions of Inverse Gaussian, Log Logistic, Log Normal, Pearson 5 and Weibull for two stations. Adjustment to Q_7 data was not verified for the Erlang, Gamma and Triangular distributions. No distribution was suitable to describe the data for the stations Água Limpa Farm, Água Limpa Fazenda, Honório Bicalho Montante, Pinhões and Ponte Raul Soares (p-value <0.05).

After checking the quality of fit of the models to the observed data, the ranking of these distributions was done through the BIC selection criterion, as presented in Table 4. The Gumbel distribution was highlighted, for which the best performance was verified for 4 of the studied stations, followed by the Rayleigh distribution.

Table 3. Probability distributions that fit to Q_7 data according to the Anderson-Darling test (α = 5%).

Stations	Erlang	Gama	Gumbel	Inversa Gaussiana	Log Logística	Log Normal	Pearson 5	Rayleigh	Triangular	Weibull
Fazenda Água Limpa										
Fazenda Água Limpa Jusante										
Honório Bicalho Montante										
Honório Bicalho ANA			X					X		
Jequitibá			X					X		
Pinhões										
Pirapama			X					X		
Ponte da Rodagem			X					X		
Ponte do Licínio			X	X	X	X	X			
Ponte do Licínio Jusante			X							
Ponte Raul Soares			X							X
Ponte Raul Soares Jusante										
Santo Hipólito			X					X		X
Várzea da Palma				X	X	X	X			

Table 4. Ranking of probability distributions applied to the data of Q_7 (annual minimum discharge with duration of seven days) according to the criterion of Bayesian classification (BIC).

Stations	Erlang	Gama	Gumbel	Inversa Gaussiana	Log Logística	Log Normal	Pearson 5	Rayleigh	Triangular	Weibull
Fazenda Água Limpa										
Fazenda Água Limpa Jusante										
Honório Bicalho Montante										
Honório Bicalho ANA			#2					#1		
Jequitibá			#1					#2		
Pinhões										
Pirapama			#2					#1		
Ponte da Rodagem			#2					#1		
Ponte do Licínio			#5	#4	#1	#3	#2			
Ponte do Licínio Jusante			#1							
Ponte Raul Soares			#1							#2
Ponte Raul Soares Jusante										
Santo Hipólito			#1					#2		#3
Várzea da Palma				#3	#4	#2	#1			

In a similar study, Silvino *et al.* (2007) used the Normal, Log-Normal, Exponential Range and Weibull probability distributions to estimate the minimum discharges of the Paraguay River. The distributions for which the data of the time series were best fitted were Weibull and Normal. Almeida *et al.* (2014) verified the quality of fit of the distributions Normal, Log Normal to 2 parameters, Weibull, Gumbel and Log Gumbel to data of time series of Q_7 in the Miranda River Watershed. Among the studied distributions, Log Gumbel was the one that provided the best fit to the time series, proving to be the most reliable in the determination of minimum flows in the reference sub-basin. On the other hand, the Normal Log distribution was the worst distribution regarding the adjustment to the series data.

In a study on minimum flows, Victorino *et al.* (2014) used the Gumbel distributions for minimums, Fréchet, Log 2p, Log 3p, Gamma 2p, Gamma 3p and Weibull. The Log 2P, Log 3P and Gama 2P distributions were considered statistically adequate for the series of minimum annual discharges of the Grande River in the region of Barreiras (Bahia, Brazil), and Log 2P presented a more accurate adjustment than the others.

Silva *et al.* (2006) applied the Log Normal 3P, Weibull and Gumbel probability distributions to time series of annual minimum daily and Q_7 discharges from the region of the high Grande River. The best fit was observed for the distribution Log Normal 3P.

Descriptive statistics measures for the empirical distributions of Q_7 of the stream gauging stations are presented in Table 5. The minimum discharge values ranged from 0.25 $m^3 s^{-1}$ (Fazenda Água Limpa) to 44.94 $m^3 s^{-1}$ (Ponte da Rodagem). Maximum values of Q_7 varied from 1.66 $m^3 s^{-1}$ for the Fazenda Água Limpa station to 180.03 $m^3 s^{-1}$ for the Ponte do Licínio station. The lowest Q_7 was verified for the Ponte Raul Soares Jusante station (1.21 $m^3 s^{-1}$) and the highest for the Várzea da Palma station (69.64 $m^3 s^{-1}$). The range of mode was from 0.8221 (Ponte Raul Soares Jusante) to 72.7039 $m^3 s^{-1}$ (Santo Hipólito). For the median, values from 0.99 (Ponte Raul Soares Jusante) to 60.06 $m^3 s^{-1}$ (Várzea da Palma) were verified. The lowest value of standard deviation was 0.22 $m^3 s^{-1}$ (Fazenda Água Limpa Jusante station) and the highest value was 25.89 $m^3 s^{-1}$ (Ponte do Licínio station).

Table 5. Descriptive statistics for empirical distributions of Q_7 ($m^3 s^{-1}$) from stream gauging stations in the Das Velhas River Basin.

Station	Minimum	Maximum	Mean	Mode	Median	Standard Deviation	Asymmetry	Kurtosis
Fazenda Água Limpa	0.25	2.24	1.47	1.76	1.44	0.43	-0.70	4.36
Fazenda Água Limpa Jusante	0.75	1.66	1.26	1.28	1.29	0.22	-0.52	3.23
Honório Bicalho Montante	4.26	21.54	14.43	12.86	14.44	3.69	-0.21	3.02
Honório Bicalho ANA	10.05	17.27	13.18	11.31	12.54	2.60	0.82	2.44
Jequitibá	17.14	58.69	33.05	31.08	31.24	8.47	0.83	3.88
Pinhões	4.26	36.82	22.97	19.73	24.03	7.15	- 0.44	3.57
Pirapama	17.87	70.08	37.99	32.41	35.06	11.99	0.69	3.21
Ponte da Rodagem	44.94	71.30	58.17	52.19	56.57	10.18	0.11	1.40
Ponte do Licínio	21.56	180.03	45.81	31.34	40.24	25.89	4.17	24.37
Ponte do Licínio Jusante	17.53	76.16	44.15	49.67	43.14	13.26	0.57	3.72
Ponte Raul Soares	10.74	51.74	29.08	23.41	27.31	8.51	0.55	2.90
Ponte Raul Soares Jusante	0.64	3.07	1.21	0.82	0.99	0.77	2.56	9.89
Santo Hipólito	24.25	105.73	60.57	72.70	57.65	17.53	0.67	3.24
Várzea da Palma	30.68	159.27	70.81	57.40	60.73	27.47	1.38	4.81

Água Limpa Farm, Água Limpa Fazenda Jusante, Honório Bicalho Montante and Pinhões stations have a negative asymmetry. The range of values was from -0.70 (Fazenda Água Limpa) to 4.17 (Ponte do Licínio). Values of kurtosis close to the normal distribution, that is, near 3 (mesokurtic), were found for most stations. However, high values of kurtosis, indicating a higher concentration of discharge values near the center of the distribution, were verified for the Ponte do Licínio and Ponte Raul Soares Jusante stations. Probability density functions for the empirical (input) and theoretical distributions for the stations of Santo Hipólito and Várzea da Palma are presented in Figure 2. Higher asymmetry and kurtosis indexes were observed in Várzea da Palma, characteristics that influenced the fitting of a different set of distributions in relation to that obtained for Santo Hipólito. The morphology of the upstream basin, relief, soil types, transmissivity and dimensions of aquifers, as well as rainfall patterns (intensity, duration and frequency) are some factors that can influence the characteristics of the distribution of flow values in a stream gauging such as asymmetry and kurtosis. These characteristics will determine the potential of theoretical probability models to fit to distributions of empirical data.

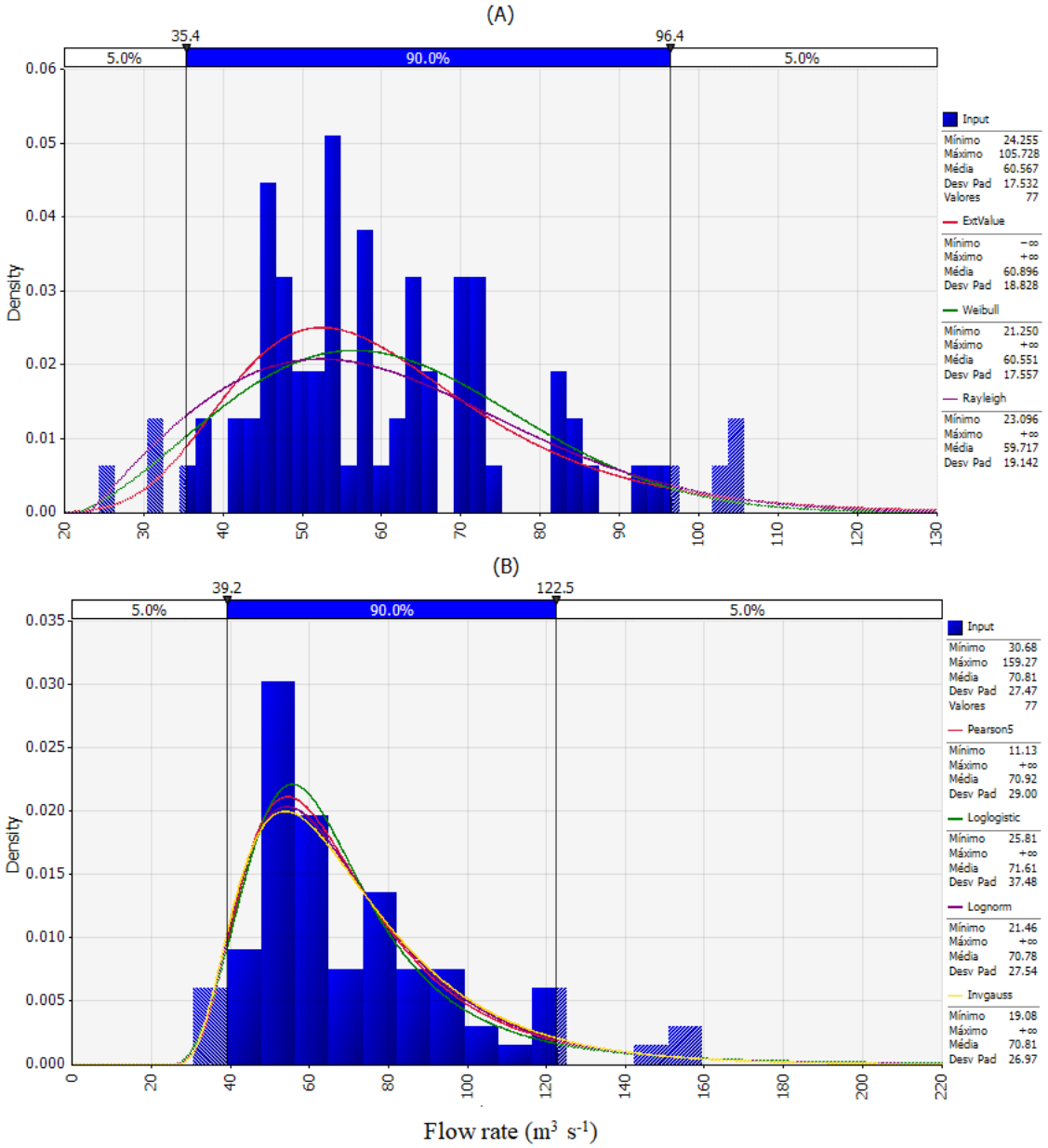

Figure 2. Empirical (input) and theoretical probability density functions for distributions of Q_7 for the gauging stations of Santo Hipólito (A) and Várzea da Palma (B).

3.2. Trend Analysis

The results of the trend analysis for the Ponte Raul Soares, Santo Hipólito and Várzea da Palma stations are presented in Tables 6 to 8. For the stream-gauging station Ponte Raul Soares (Table 6), negative trends were observed in all data sets, except for the 1st and 6th bimester (S positive). However, the negative trend was significant for the Q_7 and 4th bimester. Negative (decreasing) trends in all data sets (S negative) were detected for the Santo Hipólito station (Table 7). Based on the Mann-Kendall test, there were significant trends (p-value <0.05) for Q_7, 4th and 5th bimesters. For the Várzea da Palma station (Table 8), negative (decreasing) trends for all data sets (S negative) were pointed out. Only for the 1st bimester this trend was not significant (p-value> 0.05).

Table 6. Trend analysis of flow rate in the stream gauging station Ponte Raul Soares (S statistic, S variance (VAR (S)), denominator (D), Kendall correlation coefficient (τ)).

	S	VAR(S)	D	τ	p-value
Q_7	-499*	40588.33	2485	-0.201	0.0134
General	-83	40588.33	2485	-0.033	0.6840
1st bimester	31	34147.67	2211	0.014	0.8710
2nd bimester	-225	34147.67	2211	-0.102	0.2254
3rd bimester	-364	37275.33	2346	-0.155	0.0601
4th bimester	-632*	49716.67	2850	-0.222	0.0047
5th bimester	-352	37275.33	2346	-0.150	0.0691
6th bimester	99	34147.67	2211	0.045	0.5959

* Significant by the Mann-Kendall test at the level of 5%.

Table 7. Trend analysis of flow rate in the stream gauging station Santo Hipólito (S statistic, S variance (VAR (S)), denominator (D), Kendall correlation coefficient (τ)).

	S	VAR(S)	D	τ	p-value
Q_7	-576*	51692.67	2926	-0.197	0.0114
General	-324	51692.67	2926	-0.111	0.1554
1st bimester	-261	47791.67	2775	-0.094	0.2343
2nd bimester	-301	45917.00	2701	-0.111	0.1615
3rd bimester	-415	45917.00	2701	-0.154	0.0534
4th bimester	-489*	45917.00	2701	-0.181	0.0228
5th bimester	-555*	45917.00	2701	-0.205	0.0097
6th bimester	-145	47791.67	2775	-0.052	0.5101

* Significant by the Mann-Kendall test at the level of 5%.

Table 8. Trend analysis of flow rate in the stream gauging station Várzea da Palma (S statistic, S variance (VAR (S)), denominator (D), Kendall correlation coefficient (τ)).

	S	VAR(S)	D	T	p-value
Q_7	-823*	51689.67	2924,5	-0.281	0.0003
General	-583*	53720.33	3003	-0.194	0.0120
1st bimester	-424	51692.67	2926	-0.145	0.0628
2nd bimester	-444*	49716.67	2850	-0.156	0.0469
3rd bimester	-526*	51692.67	2926	-0.180	0.0209
4th bimester	-612*	51692.67	2926	-0.209	0.0072
5th bimester	-810*	51692.67	2926	-0.277	0.0004
6th bimester	-466*	51692.67	2926	-0.159	0.0408

* Significant by the Mann-Kendall test at the level of 5%.

The lowest mean daily flows occurred in the fourth bimester in 65.0%, 61.6% and 61.3% of the years with all bimonthly sets in the stations of Raul Soares, Santo Hipólito and Várzea da Palma, respectively. The fifth bimester is second in relevance in the concentration of low flows. Significant negative trends for the Q_7 and fourth bimester were indicated for the three stream-gauging stations. The time series of flow and nonparametric lowess (locally weighted scatterplot smoothing) regression (Lindsey and Sheather, 2010) for these two sets are shown in Figure 3. More pronounced decreases are observed in the first- and final thirds of the series.

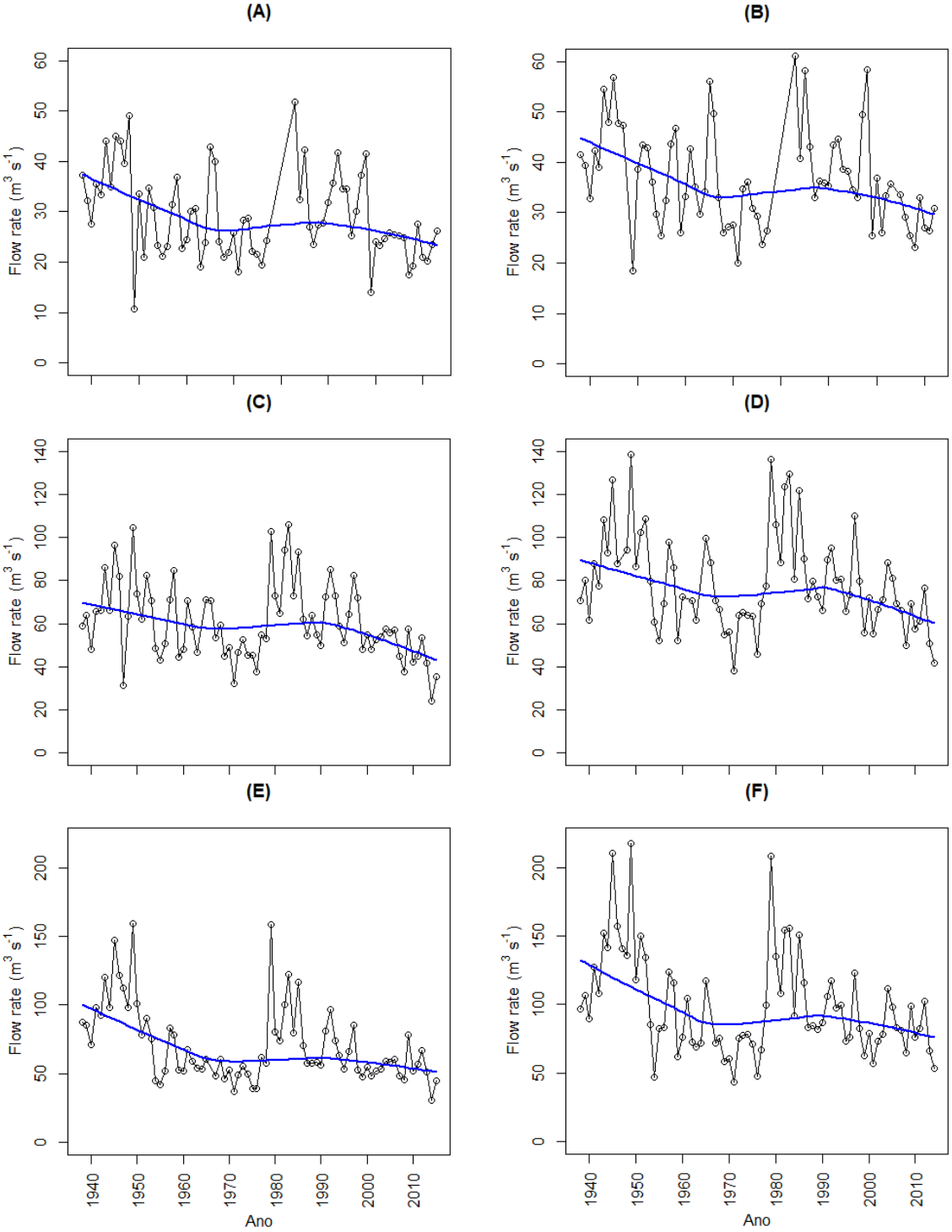

Figure 3. Time series of mean daily flow rate and nonparametric lowess regression for the stream-gauging stations of Ponte Raul Soares (A and B), Santo Hipólito (C and D), and Várzea da Palma (E and F); A, C, and E are series for Q_7; B, D, and F are series for 4th bimester.

Changes in hydrological series can occur due to different causes, such as variations in rainfall amounts and water withdrawals to meet multiple uses. The lowest values of S are in the 4th and 5th bimesters, showing trends of decreasing flows. During these periods droughts occur, which contribute to a significant increase in irrigation demand. In Q_7 data, a strong downward trend was also observed for the three stations, which is a worrisome factor regarding the management of water resources in the basin. According to the Water Resources Master Plan of the Das Velhas River Basin of 2015, for the strategic territorial units (STUs) Rio Bicudo, Ribeirão Picão, Ribeirão da Mata, Ribeirão Jequitibá, Rio Itabirito, Carste and high stretch of Das Velhas River, channel water withdrawal has already exceeded the criterion used (30% of $Q_{7,10}$), preventing new grants (Comitê da Bacia Hidrográfica do Rio das Velhas, 2015).

There is a perspective of advancing irrigated agriculture in regions such as the lower Rio das Velhas. This advance imposes pressure on the demand for water resources with significant effects on water availability, which was partially detected at the Várzea da Palma station. The milder relief in this region favors the use of irrigation methods as a central pivot, among others, as can be observed in Figure 4. The presence of irrigated agriculture is also observed in the region of the county of Sete Lagoas (STU Ribeirão Jequitibá) in the region of the Middle Velhas - High Stretch, as shown in Figure 5. This figure also shows the great urban conglomerate of the capital of the state of Minas Gerais (Belo Horizonte) in the region of High Velhas.

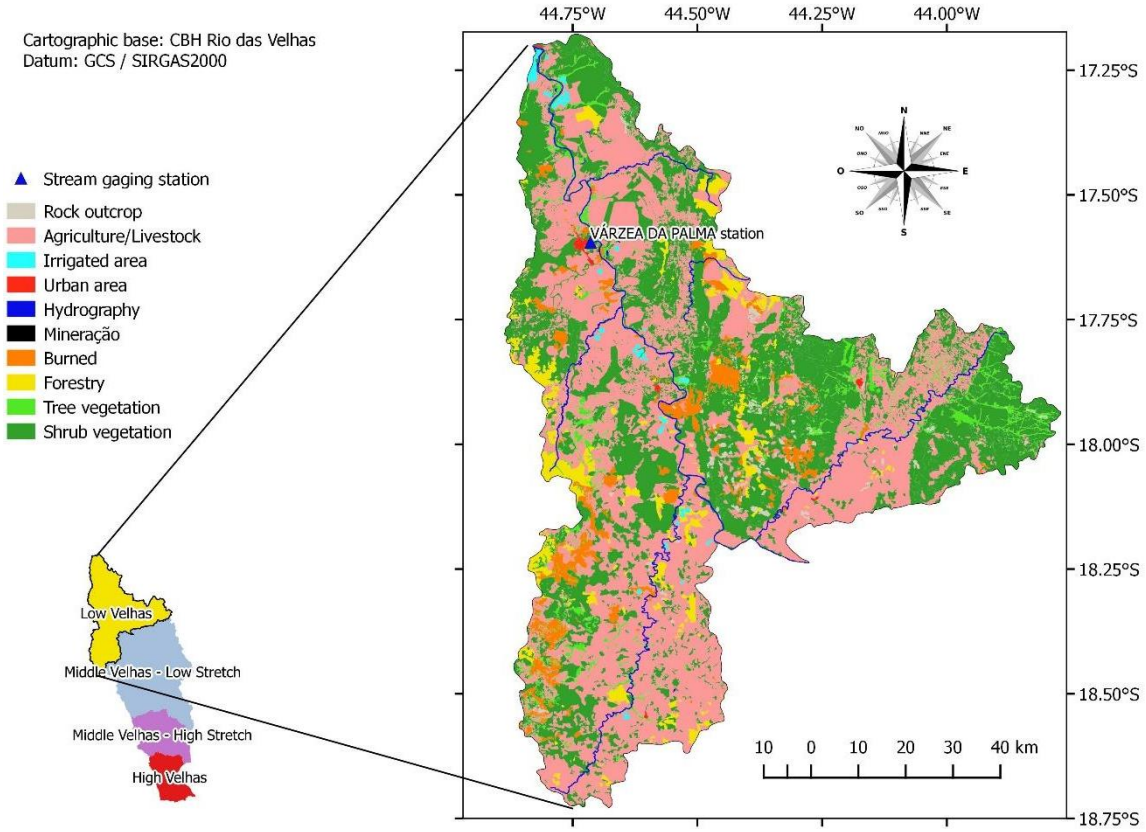

Figure 4. Land cover in the Low Velhas region, year 2013.

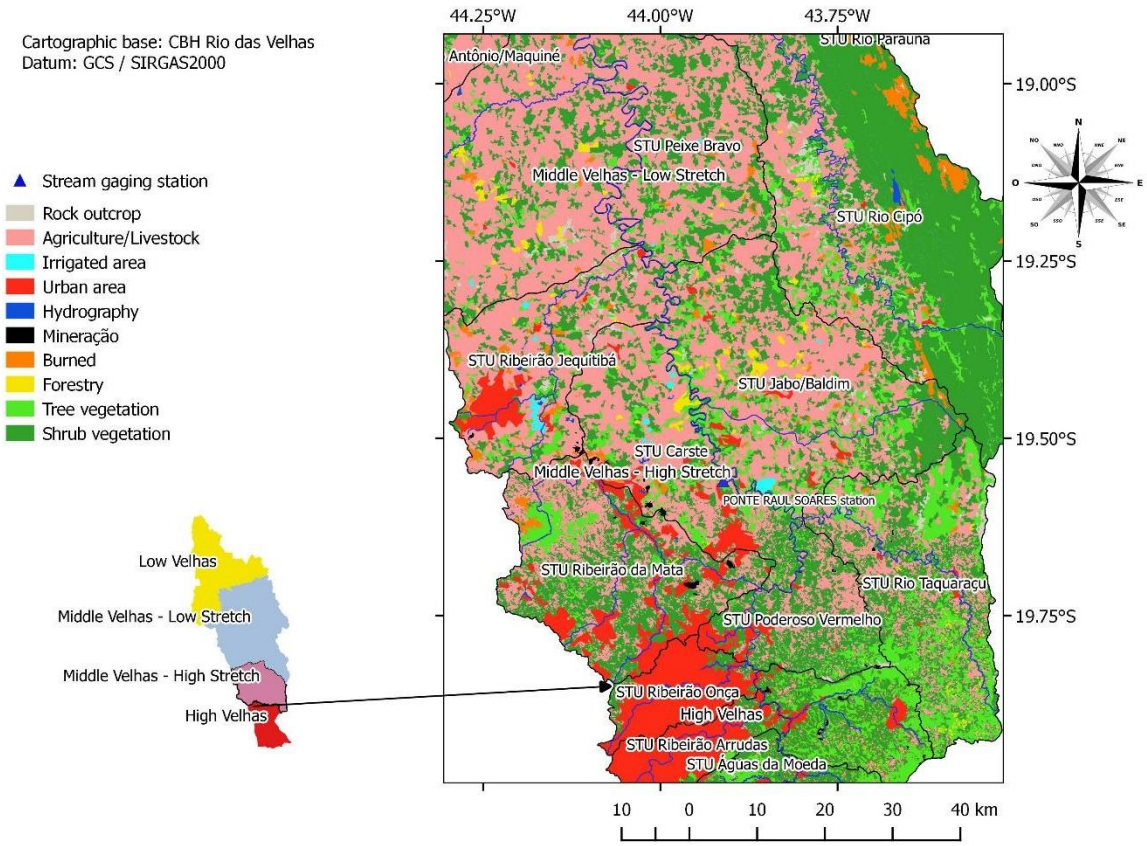

Figure 5. Land cover in the region Middle Velhas-High Stretch and parcial in the regions Middle Velhas-Low Stretch and High Velhas, year 2013.

Results from Mann-Kendall test for rainfall time series for annual totals and for bimesters indicated significant negative trends only for the fifth bimester for Sete Lagoas meteorological station (p-value = 0.0497). Significant positive trends were detected for the second bimester in the meteorological stations of Belo Horizonte (p-value = 0.0034) and Sete Lagoas (p-value = 0.0118). However, some remarks should be considered. The time series of rainfall began in the early 1960s and the series of flow rate began in the late 1930s. In addition, there are only three INMET old conventional stations in the basin. These aspects impose a certain level of uncertainty in the understanding of the effects of rainfall variability on the flow distributions in the studied area.

In their study on streamflow trend, Marengo and Alves (2005) concluded that the discharges of the Paraíba do Sul River, observed in stream gauging stations of the states São Paulo and Rio de Janeiro, has a negative trend for the last 50 years. The study pointed to a possible impact of anthropic influence (energy generation, irrigation and demand associated to population growth) as possible causes for these trends and not to a climate change of the rainfall distribution in the basin. Nevertheless, Santana *et al.* (2014) evaluated time series of rainfall and discharge in the Paraguay River Basin in the stations Barra do Bugres, Cáceres and Descalvado during the period of 1980-2005. According to the analyses, the discharge is basically a function of precipitation.

Rosin *et al.* (2015) studied five stream-gauging stations located in the interior of the Rio das Mortes Basin, in the State of Mato Grosso, Brazil. The authors verified a strong connection in relation to the type of use and withdraw of water resources for the station whose analyzes showed a negative trend in all series.

Uliana *et al.* (2015) studied trends in time series of rainfall and flow data for the city of Alegre, in the state of Espirito Santo, Brazil, and found that flow rate in October had increased

by 34.2% since 1963. They also detected a tendency of increase in rainfall for the months of August and September, since the years of 1967 and 1964, respectively, and concluded that this trend, among other possible factors, may have influenced the increase of the average flow rate for the month of October.

In a similar work, Vilanova (2014a) evaluated the existence of trends in time series of discharge and rainfall in the high Mogi-Guaçu region from 1973 to 2006. A negative trend was detected in both time series. The author suggests that the identified trends may be the result of climate change, initially affecting the region's rainfall and possibly generating a similar response at the discharges.

4. CONCLUSIONS

Among the probability distributions studied to describe discharge data of Q_7, the best fits, in general, were verified for Gumbel and Rayleigh distributions, based on Anderson Darling and Criterion of Bayesian Information tests. However, the quality of fit by different distributions was differentiated for each stream gauging station.

Significant negative trends for the three stream gauging stations were detected for time series of Q_7 and mean daily flow in the 4th bimester. There were significant negative trends for the Santo Hipólito station also for the 5th bimester. For the Várzea da Palma station, located near the mouth of the Das Velhas River, only for the first bimester significant negative trend in the flow series were not detected. Corresponding negative trends were not observed for the rainfall series from the studied meteorological stations.

5. ACKNOWLEDGMENT

The authors are grateful for the support of Fundação de Amparo à Pesquisa do Estado de Minas Gerais (FAPEMIG) and the financial support which was granted for the development of the project (CAG - APQ-03182-13).

6. REFERENCES

AGEVAP. **Plano integrado de Recursos Hídricos – PIRH – da Bacia Hidrográfica do Rio Paraíba do Sul e planos de Ação de Recursos Hídricos – PARH – das Bacias Afluentes**. Resende, 2016. 122p.

ALMEIDA, I. K.; SOBRINHO, T. A.; SANTOS, B. B.; STEFFEN, J. L.; BACCHI, C. G. V. Métodos estatísticos na determinação de vazão de referência. **Comunicata Scientiae**, v. 5, n. 1, p. 11-17, 2014.

BARUA, S.; MUTTIL, N.; NG, A. W. M.; PERERA, B. J. C. Rainfall trend and its implications for water resource management within the Yarra River catchment, Australia. **Hydrological Processes**, v. 27, n. 12, p. 1727-1738, 2013. https://dx.doi.org/10.1002/hyp.9311

BLAIN, G. C. Tendências e variações climáticas em séries anuais de precipitação pluvial do Estado de São Paulo. **Bragantia**, v. 69, n. 3, p. 765–770, 2010. https://dx.doi.org/10.1590/S0006-87052010000300031

CALOIERO, T.; COSCARELLI, R.; FERRARI, E.; MANCINI, M. Trend detection of annual and seasonal rainfall in Calabria (Southern Italy). **International Journal of Climatology**, v. 31, n. 1, p. 44–56, 2011. https://dx.doi.org/10.1002/joc.2055

COMITÊ DA BACIA HIDROGRÁFICA DO RIO DAS VELHAS. **Plano Diretor de Recursos Hídricos da Bacia Hidrográfica do Rio das Velhas 2015**: Resumo Executivo. Belo Horizonte, 2015. 233 p.

COSTA, V. J.; FERREIRA, M.; CORDEIRO, M. T. A. Análise de séries temporais climáticas. **Revista de Ciências Agroveterinárias**, v. 14, n. 2, p. 169-177, 2015.

DALE, J.; ZOU, C. B.; ANDREWS, W. J.; LONG, J. M.; LIANG, Y.; QIAO, L. Climate, water use, and land surface transformation in an irrigation intensive watershed—Streamflow responses from 1950 through 2010. **Agricultural Water Management**, v. 160, p. 144–152, 2015. https://dx.doi.org/10.1016/j.agwat.2015.07.007

DAMÁZIO, J. M.; COSTA, F. S. Stationarity of annual maximum daily streamflow time series in South-East brazilian rivers. **Cadernos do IME. Série Estatística**, v. 37, p. 29-30, 2014. https://dx.doi.org/10.12957/cadest.2014.18302

DETZEL, D. H. M.; MINE, M. R. M.; BESSA, M.; BLOOT, M. Cenários Sintéticos de Vazões para Grandes Sistemas Hídricos Através de Modelos Contemporâneos e Amostragem. **RBRH – Revista Brasileira de Recursos Hídricos**, v. 19, n. 1, p. 17-28, 2014. https://dx.doi.org/10.21168/rbrh.v19n1.p17-28.

EMILIANO, P. C.; VIVANCO, M. J. F.; MENEZES, F. S. M.; AVELAR, F. G. Fundamentos e comparação de critérios de informação: Akaike and Bayesian. **Revista Brasileira Biomatemática**, v. 27, n. 3, p. 394-411, 2009.

HIDROWEB. **Séries históricas de estações**. 2013. Available in: http://www.snirh.gov.br/hidroweb/publico/medicoes_historicas_abas.jsf. Access in: April 2018.

JOSEPH, J. F.; FALCON, H. E.; SHARIF, H. O. Hydrologic Trends and Correlations in South Texas River Basins: 1950–2009. **Journal of Hydrologic Engineering**, v. 18, n. 2, p. 1653-1662, 2013. https://dx.doi.org/10.1061/(ASCE)HE.1943-5584.0000709

KIBRIA, K. N.; AHIABLAME, L.; HAY, C.; DJIRA, G. Streamflow Trends and Responses to Climate Variability and Land Cover Change in South Dakota. **Hydrology**, v. 3 n. 1, 2016. https://doi.org/10.3390/hydrology3010002

LIMA, J. R. A.; NEVES, D. J. D.; ARAÚJO, L. E.; AZEVEDO, P. V. de. Identificação de tendências climáticas no Estado da Bahia. **Revista de Geografia**, v. 28, n. 3, p. 172–187, 2011.

LINDSEY, C.; SHEATHER, S. Model fit assessment via marginal model plots. **The Stata Journal**, v. 10, n. 2, p. 215-225, 2010. https://dx.doi.org/10.1177/1536867X1001000203

LOPES, T. R.; PRADO, G. Do; ZOLIN, C. A.; PAULINO, J.; ANTONIEL, L. S. Regionalização de vazões máximas e mínimas para a bacia do rio Ivaí - PR. **Irriga**, v. 21, n. 1, p. 188-201, 2016. https://doi.org/10.15809/irriga.2016v21n1p188-201

MARENGO, J. A.; ALVES, L. M. Tendências Hidrológicas da Bacia do Rio Paraíba do Sul. **Revista Brasileira de Meteorologia**, v. 20, n. 2, p. 215-226, 2005.

MCLEOD, A. I. **Kendall**: Kendall rank correlation and Mann-Kendall trend test. 2011. Available in: https://CRAN.R-project.org/package=Kendall. Access in: April 2018.

MELLO, C. R.; VIOLA, M. R.; BESKOW, S. Vazões máximas e mínimas para bacias hidrográficas da região Alto Rio Grande, MG. **Ciência e Agrotecnologia**, v. 34, p. 494-502, 2010. https://dx.doi.org/10.1590/S1413-70542010000200031

MOOD, A. M.; GRAYBILL, F.; BOES, D. C. **Introduction to the Theory of Statistics.** 3th ed. New York: McGraw-Hill, 1974. 480 p.

PALISADE CORPORATION. **Guide to Using @Risk. Risk Analysis and Simulation Add-In for Microsoft® Excel - Versão.7.0.1**. New York, 2016. 880 p.

PEREIRA, G. S.; CALDEIRA, F. C. Evaluation of the distribution of Gumbel in the determination of minimum flows of the Rio Negro sub-basin. **Águas Subterrâneas**, v. 32, n. 1, p. 11-16, 2018. https://dx.doi.org/10.14295/ras.v32i1.28926

PINTO, A. P.; LIMA, G. B.; ZANETTI, J. B. Análise comparativa de modelos de séries temporais para modelagem e previsão de regimes de vazões médias mensais do Rio Doce, Colatina - Espírito Santo. **Ciência e Natura**, v. 37, n. 4, p. 1–11, 2015. https://dx.doi.org/10.5902/2179460X17143

R CORE TEAM. **R-3.3.1 for Windows (32/64 bit).** 2016. Available in: https://cran.r-project.org/bin/windows/base/old/3.3.1/. Access in: April 2018.

RAZALI, N. M.; WAH, Y. B. Power comparisons of Shapiro-Wilk, Kolmogorov-Smirnov, Lilliefors and Anderson-Darling tests. **Journal of Statistical Modeling and Analytics**, v. 2, n. 1, p. 21-33, 2011.

ROSIN, C.; AMORIM, R. S. S.; MORAIS, T. S. T. Análise de tendências hidrológicas na bacia do rio das Mortes. **Revista Brasileira de Recursos Hídricos**, v. 20, n. 4, p. 99-998, 2015. https://dx.doi.org/10.21168/rbrh.v20n4.p 991-998

ROSSI, M. S.; THEBALDI, M. S. Vazões de referência do Rio São Miguel em Arcos (MG). **Revista Agrogeoambiental**, v. 9, n. 1, p. 77-86, 2017. https://dx.doi.org/10.18406/2316-1817v9n12017927

SALVADORI, N. **Evaluation of non-stationarity in annual maximum flood series of moderately impaired watersheds in the upper Midwest and Northeastern United States**. 2013. Dissertation (Master of Science in Environmental Engineering) – Department of Civil and Environmental Engineering, Michigan Technological University, Michigan, 2013.

SALVIANO, M. F.; GROPPO, J. D.; PELLEGRINO, G. Q. Análise de tendências em dados de precipitação e temperatura no Brasil. **Revista Brasileira de Meteorologia**, v. 31, n. 1, p. 64 –73, 2016. http://dx.doi.org/10.1590/0102-778620150003

SANTANA, M. F.; SOUZA, C. A.; OLIVEIRA JUNIOR, E. S. Análise de séries temporais de vazão e precipitação na bacia do rio Paraguai. **Revista GeoPantanal**, v. 8, n. 14, p. 67-89, 2014.

SANTOS, L. C. C. **Estimativa de Vazões Máximas de Projeto por Modelos Determinísticos e Probabilísticos.** 2010. 80 p. Dissertação (Mestrado) – Universidade Federal do Espírito Santo, Espírito Santo, 2010.

SILVA, A. M.; OLIVEIRA, P. M.; MELLO, C. R.; PIERANGELI. C. Vazões mínimas e de referência para outorga na região do Alto Rio Grande, Minas Gerais**. Revista Brasileira de Engenharia Agrícola e Ambiental**, v. 10, n. 2, p. 374-380, 2006. https://dx.doi.org/10.1590/S1415-43662006000200019

SILVA, B. M. B.; SILVA, D. D.; MOREIRA, M. C. Influência da sazonalidade das vazões nos critérios de outorga de uso da água: estudo de caso da bacia do rio Paraopeba. **Revista Ambiente & Água**, v. 10, n. 3, p. 623-634, 2015. https://dx.doi.org/10.4136/ambi-agua.1587

SILVINO, A. N. O.; SILVEIRA, A.; MUSIS, C. R.; WYREPKOWSKI, C. C.; CONCEIÇÃO, F. T. Determinação de vazões extremas para diversos períodos de retorno para o Rio Paraguai utilizando métodos estatísticos. **Geociências**, v. 26, p. 369-378, 2007.

SMAKHTIN, V. U. Low flow hydrology: a review. **Journal of Hydrology**, v. 240, n. 3, p. 147-186, 2001. http://doi.org/10.1016/S0022-1694(00)00340-1

SOARES, D. B.; NÓBREGA, R. S.; GALVÍNCIO, J. D. Indicadores climáticos de desertificação na bacia hidrográfica do Rio Pajeú, Pernambuco. **Revista Brasileira de Climatologia**, v. 22, 2018. http://dx.doi.org/10.5380/abclima.v22i0.58557

SUHAILA, J.; DENI, S. M.; WAN ZIN, W. Z.; JEMAIN, A. A. Spatial patterns and trends of daily rainfall regime in Peninsular Malaysia during the southwest and northeast monsoons: 1975–2004. **Meteorology and Atmospheric Physics**, v. 110, n. 1, p.1–18, 2010. https://dx.doi.org/10.1007/s00703-010-0108-6

TAN, X. Z.; GAN, T. Y. Nonstationary analysis of annual maximum streamflow of Canada, **Journal of Climate**, v. 28, p. 1788-1805, 2015. https://doi.org/10.1175/JCLI-D-14-00538.1

TAO, H.; GEMMER, M.; BAI, Y.; SU, B.; MAO, W. Trends of streamflow in the Tarim River Basin during the past 50 years: Human impact or climate change? **Journal of Hydrology**, v. 400, n. 1, p. 1–9, 2011. http://dx.doi.org/10.1016/j.jhydrol.2011.01.016

ULIANA, E. M.; SILVA, D. D. da; ULIANA, E. M.; RODRIGUES, B. S.; CORRÊDO, L. P. Análise de tendência em séries históricas de vazão precipitação: uso de teste estatístico não paramétrico**. Revista Ambiente & Água**, v. 10, n. 1, 2015. https://dx.doi.org/10.4136/ambi-agua.1427

VICTORINO, E. C.; MATIAS, G. C.; SILVA, T. B. S. DA; ALVES, R. C. P.; CARVALHO, L. G. de. Adequabilidade de diferentes distribuições de probabilidade aplicadas a uma série histórica de vazões mínimas para o rio Grande, na região de Barreiras (BA). *In:* CONGRESSO BRASILEIRO DE ENGENHARIA AGRÍCOLA, 42., 1-8 Jul., Campo Grande. **Proceedings[...]** Campo Grande: SBEA, 2014.

VILANOVA, M. R. N. Tendências Hidrológicas na região do Alto Rio Mogi-Guaçu, Sul de Minas Gerais. **Revista Agrogeoambiental**, v. 6, n. 3, p. 63-70, 2014a. https://dx.doi.org/10.18406/2316-1817v6n32014601

VILANOVA, M. R. N. Trends in Mean Annual Streamflows in Serra da Mantiqueira Environmental Protection Area. **Brazilian Archives of Biology and Technology**, v. 57, n. 6, p. 1004-1112, 2014b. https://dx.doi.org/10.1590/S1516-8913201402109

Ambiente & Água - An Interdisciplinary Journal of Applied Science
ISSN 1980-993X – doi:10.4136/1980-993X
www.ambi-agua.net
E-mail: ambi.agua@gmail.com

Application of Markov chains to Standardized Precipitation Index (SPI) in São Francisco River Basin

ARTICLES doi:10.4136/ambi-agua.2311

Received: 08 Aug. 2018; Accepted: 12 Apr. 2019

Esdras Adriano Barbosa dos Santos[1*]; Tatijana Stosic[2]; Ikaro Daniel de Carvalho Barreto[2]; Laélia Campos[3]; Antonio Samuel Alves da Silva[2]

[1]Universidade Federal de Sergipe (UFS), São Cristóvão, SE, Brasil
Departamento de Estatística e Ciências Atuariais (DECAT).
E-mail: esdras.adriano@gmail.com
[2]Universidade Federal Rural de Pernambuco (UFRPE), Recife, PE, Brasil
Departamento de Estatística e Informática (DEINFO).
E-mail: tastosic@gmail.com, daniel.carvalho.ib@gmail.com, samuelmathematical@gmail.com
[3]Universidade Federal de Sergipe (UFS), São Cristóvão, SE, Brasil
Departamento de Física (DFI). E-mail: lpbcampos@gmail.com
[*]Corresponding author

ABSTRACT

This work evaluated dry and rainy conditions in the subregions of the São Francisco River Basin (BHSF) using the Standardized Precipitation Index (SPI) and Markov chains. Each subregion of the BHSF has specific physical and climatic characteristics. The data was obtained from the National Water Agency (ANA), collected by four pluviometric stations (representative of each subregion), covering 46 years of data, from 1970 to 2015. The SPI was calculated for the time scales of six and twelve months and transition probabilities were obtained using the Markov chain. Transition matrices showed that, at both scales, if the climate conditions were severe drought or rainy, switching to another class would be unlikely in the short term. Correlating this information with the probabilities of the stationary distribution, it was possible to find the regions that are most likely to be under rainy or dry weather in the future. The recurrence times calculated for the stations that belong to the semi-arid region were smaller when compared to the value of the return period of the representative station of Upper São Francisco that has higher levels of precipitation, confirming the predisposition of the semi-arid region to present greater chances of future periods of drought.

Keywords: drought, Markov chains, standardized precipitation index.

Aplicação de Cadeias de Markov no Índice de Precipitação Padronizado (SPI) em estações da Bacia do Rio São Francisco

RESUMO

Este trabalho objetivou avaliar períodos secos e chuvosos nas sub-regiões da Bacia Hidrográfica do Rio São Francisco (BHSF) utilizando o Índice de Precipitação Padronizado (SPI) e cadeias de Markov. Cada sub-região da BHSF possui características físicas e climáticas

específicas, dessa forma foram utilizadas quatro estações pluviométricas contendo dados com 46 anos, de 1970 a 2015, obtidas na Agência Nacional de Águas (ANA), representativas de cada sub-região. O SPI foi calculado para as escalas de tempo de seis e doze meses e as matrizes de probabilidades de transição foram obtidas utilizando as cadeias de Markov. As matrizes de transição mostraram que, em ambas as escalas, caso a condição climática estivesse em classe de seca severa ou chuvosa, a mudança para outra classe seria pouco provável a curto prazo. Correlacionando esta informação com as probabilidades da distribuição estacionária, foi possível encontrar as regiões que têm maiores possibilidades de no momento futuro estar sob clima chuvoso ou de seca. Os tempos de recorrência calculados para as estações inseridas no semiárido foram menores quando comparado com o valor do tempo da estação representativa do Alto São Francisco que possui maiores níveis de precipitação, confirmando a predisposição do semiárido em apresentar maiores chances de períodos futuros de seca.

Palavras-chave: cadeias de Markov, índice de precipitação padronizado, seca.

1. INTRODUCTION

Water is considered a renewable natural resource because it is constantly recovering through the processes of the hydrological cycle. However, due to its great potential for use, with demands for different uses, water grows increasingly more scarce. The São Francisco River Basin has experienced this shortage.

The basin is very important to Brazil, not only for the volume of water transported in a semi-arid region, but also for the potential uses of the water and for its historical and economic contributions to the region. The basin covers an area of about 634,000 km^2. The São Francisco River is approximately 2,700 km long and originates in the Serra da Canastra in Minas Gerais, flowing south-north through Bahia and Pernambuco, where it changes course until it reaches the Atlantic Ocean at the border between Alagoas and Sergipe (Brasil, 2018).

The Northeast Region of Brazil demands special attention in relation to water supply, in particular Ceará, Rio Grande do Norte, Paraíba and Pernambuco, which has 87.8% of its territory in the semi-arid region. Due to little rainfall, the irregularity of its regime, high temperatures throughout the year, strong insolation and high evaporation rates, in addition to some hydrogeological characteristics, water has been very scarce (Brasil, 2018).

Drought is a phenomenon characterized by the absence, scarcity, reduced frequency, limited quantity, and inadequate distribution of rainfall during a year. Drought is considered a natural disaster, being a phenomenon that affects economic, social and political areas. Drought is random phenomenon, since its onset, end and severity are unpredictable (Mishra and Singh, 2010). According to the Brazilian Atlas of Natural Disasters from 1991 to 2012 (UFSC, 2013), drought is the disaster that most affects the Brazilian population, because it is the most frequent, representing 51% of the total records, followed by flood, with 21%.

In order to reduce the vulnerability of populations affected by drought, it is of fundamental importance to develop techniques to monitor this phenomenon, proposing indexes to standardize drought periods (Blain *et al.*, 2010; Mckee *et al.*, 1993; Tsakiris and Vangelis, 2004; Tonkaz, 2006; Sadeghi and Shamseldin, 2014), or evaluating conditions to predict droughts using Markov chains (Keller Filho *et al.*, 2006; Paulo and Pereira, 2007; Lennartsson *et al.*, 2008; Sanusi *et al.*, 2015).

In this context, this work evaluated the periodicity of the drought, and classified the intensity of the drought classes using the Standardized Precipitation Index (SPI) and Markov chains applied to 4 meteorological stations distributed in the subregions of the São Francisco Basin.

2. MATERIALS AND METHODS

2.1. Study area and data

The study area is located in the São Francisco River Basin and the data was provided by the National Water Agency-ANA through the National Information System on Water Resources (SNIRH, 2018).

In this work, 4 stations (one station in each basin sub-region) were used with daily rainfall data for the period from January 1970 to December 2015, which corresponds to 46 years of rainfall records. Table 1 below presents the information about the chosen stations.

Table 1. Description of pluviometric stations.

Sub-region	Latitude	Longitude	Code	Station	State
Upper	-20.178889	-45.700278	2045002	Iguatama	MG
Middle	-10.002222	-42.474167	1042015	Pilão Arcado	BA
Sub-middle	-8.520278	-39.640833	839034	Fazenda Tapera	PE
Lower	-10.215278	-36.823889	1036048	Propriá	SE

2.2. Standardized Precipitation Index (SPI)

The Standardized Precipitation Index was proposed and developed by Mckee *et al.* (1993) as a versatile tool in the monitoring and analysis of periods of drought and rain. The SPI is used to estimate the drought condition based on precipitation. To obtain the index, the monthly precipitation values for each meteorological station should be calculated for the desired time scale, which can be 1, 3, 6, 12 and 24 months (Mahmoudzadeh *et al.*, 2016).

Regarding the time scale, the SPI of one month is associated with short-term conditions, the three-month SPI depicts soil moisture conditions in the short- and medium term, in addition to estimating seasonal precipitation. The six-month SPI is associated with irregularities of water supply and river flows, and twelve- and twenty-four-month SPIs express long-term precipitation patterns and are directly associated with water scarcity, with water levels in groundwater flows (Sousa *et al.*, 2016).

With the accumulated monthly precipitation series, the SPI calculation consists of adjusting the Gamma probability density function to the frequency distribution of the precipitation of each of the rainfall stations. The Gamma distribution model has a good fit for continuous variables that do not have an upper limit, being widely used for studies of historical series of precipitation (Wilks, 2011). The probability density function Gamma is given by the Equation 1:

$$f(x) = \frac{1}{\beta^{\alpha}\Gamma(\alpha)} x^{\alpha-1} e^{-\frac{x}{\beta}},\ x > 0 \quad (1)$$

Where $\alpha > 0$ is the shape parameter, $\beta > 0$ is the scale parameter, x is the precipitation and $\Gamma(\alpha)$ is Gamma function, defined as Equation 2:

$$\Gamma(\alpha) = \int_0^{\infty} y^{\alpha-1} e^{-y} dy \quad (2)$$

The parameters α e β of probability density function are estimated for each station by the Maximum Likelihood (Wilks, 2011) (Equations 3, 4 and 5).

$$\hat{\alpha} = \frac{1}{4A}\left(1 + \sqrt{1 + \frac{4A}{3}}\right) \quad (3)$$

$$\hat{\beta} = \frac{\hat{x}}{\hat{\alpha}} \quad (4)$$

$$A = \ln(\bar{x}) - \frac{\sum_i^n x_i}{n} \quad (5)$$

Where: n, x, x_i and A are, respectively, the sample size of the precipitation records, the arithmetic mean, the precipitations observed, and a measure of distribution asymmetry (Husak *et al.*, 2007).

In this work, the SPI was used to assess agricultural drought as well as water scarcity in these regions of the São Francisco Basin. In this way, the SPI was used for six- (SPI-06) and twelve months (SPI-12), being an important index in arid and semi-arid regions (Blain, 2012). In order to calculate the SPI, the Gamma probability density function must first be adjusted to the series of monthly precipitation totals. In addition, the Kolmogorov-Smirnov goodness of fit test adapted by Lilliefors, as described in Blain (2014), was used to test the suitability of the gamma distribution to the data set. The software used in the calculations was the R (R Core Team, 2019). Then, the cumulative probability of occurrence of each monthly total is estimated and the inverse Normal function is applied to this probability resulting in the SPI values. According to Mckee *et al.* (1993), the drought period begins when the SPI becomes negative and ends when it returns to positive values (rainy season). Table 2 presents the classification of SPI values used in this study as states in a Markov chain.

Table 2. Classification of SPI values.

Class	SPI values
Extreme drought	$-\infty \leq SPI < -2$
Severe drought	$-2 \leq SPI < -1.5$
Moderate drought	$-1.5 \leq SPI < -1$
Mild drought	$-1 \leq SPI < 0$
Rain	$0 \leq SPI < \infty$

Source: McKee *et al.* (1993).

2.3. Markov Chains

A Markov chain is a stochastic process X_t, such as the probability that X_{t+1} takes a value j at time t +1 depends on the past only through its most recent value X_t at time t (Equation 6):

$$P(X_{t+1} = j|X_0, X_1, X_2, \dots, X_t) = P(X_{t+1} = j|X_t = i) = p_{ij} \quad (6)$$

For any one of the $i, j \in S$ and $t \in T$ (Paulo and Perreira, 2007). The transition probability p_{ij} is the probability that the Markov chain is in state j at the next time point, given that it is in state i at the present time point.

The transition probabilities can be expressed in the form of a matrix, namely (Equation 7):

$$p_{ij} = \begin{pmatrix} p_{11} & p_{12} & \cdots & p_{1n} \\ p_{21} & p_{21} & \cdots & p_{2n} \\ p_{31} & p_{31} & \cdots & p_{3n} \\ \vdots & \vdots & & \vdots \\ p_{n1} & p_{n2} & \cdots & p_{nn} \end{pmatrix} \quad (7)$$

Where: $0 \leq p_{ij} \leq 1$ e $\sum p_{ij} = 1; \quad i = 1,2,3,4 \cdots n.$

The Maximum Likelihood method was used to calculate the transition probabilities. The Maximum Likelihood Estimator (MLE) of p_{ij} is given as Equation 8.

$$p_{ij} = \frac{n_{ij}}{\sum_j n_{ij}}, \forall i, j \in S \quad (8)$$

Where n_{ij} is the number of times the observed data went from state *i* to state *j* (Mishra *et al.*, 2009).

In long-term processes, the transition probabilities of the Markov chain states are independent of the initial state. Thus, the equilibrium probabilities π_j could be obtained by successive multiplications of the transition matrix itself or by the resolution of the linear system of equations, namely (Equation 9 and 10):

$$\pi_j = \sum_{k \in S} \pi_k p_{kj}, j \in S \quad (9)$$

$$\sum_{j \in S} \pi_j = 1 \quad (10)$$

Where π_j is the long-term probability of drought class *j*.

The probability of stay, during m months, in class *i*, is calculated as (Equation 11):

$$P(X_1 = i | X_0 = i) \dots P(X_{m-2} = i | X_{m-1} = i) P(X_m \neq i | X_{m-1} = i) = P_{ii}^{m-1}(1 - P_{ii}) \quad (11)$$

Knowing the probabilities of stay in each drought class *i* during *m* months, the expected residence time in any class *i*, is (Equation 12):

$$E(T_i \mid X_0) = \sum_k kP(m = k \mid X_0 = i);\ m = 1,2, \dots, k \quad (12)$$

An important measure that helps in the process of assessing drought periods is the recurrence time to a given state. This average time represents the time required for a specific drought class to occur again. This time is then calculated (Equation 13):

$$t_{ii} = \frac{1}{\pi_i} \quad (13)$$

3. RESULTS AND DISCUSSION

The selected stations are distributed in the four subregions of the basin, and therefore have different climates and rainfall levels. For each season, mean precipitations were calculated for all months of the year, as can be seen in the bar chart in Figure 1. Precipitation totals were: 1317 mm for Iguatama station, 715 mm for Pilão Arcado, 481 mm for Fazenda Tapera and 832 mm for the Propriá station, confirming the expected difference between the sub-regions of the basin (Brasil, 2018).

Observing Figure 1, the Iguatama station has higher average precipitations in the months of November to January, especially with average rainfall over 200 mm in the months of December and January. The Pilão Arcado and Fazenda Tapera stations present the same behavior with average monthly rainfall in these months less than 150 mm. The exception is the Propriá station (Lower São Francisco), which assumes its maximum precipitation values in the months of May to June, intercepting the months of least precipitation (from June to August) of the other stations. In particular, the Pilão Arcado, Fazenda Tapera and Propriá stations, although located in different subregions, (Middle, Sub-middle and Lower São Francisco, respectively), are part of the Northeastern Semi-arid, according to the new delimitation of the Semi-arid (Brasil, 2005).

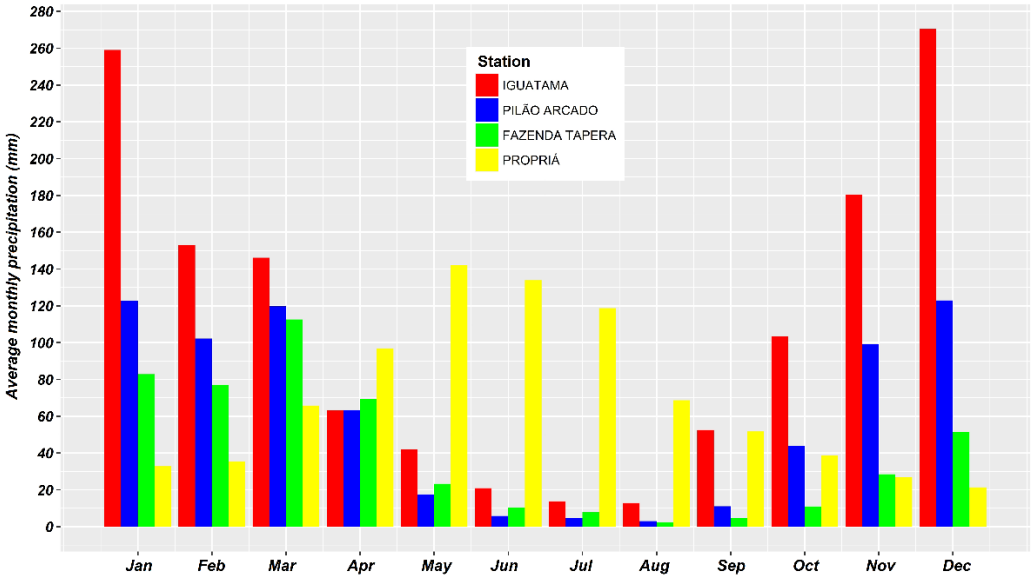

Figure 1. Average monthly precipitation of basin stations.

The SPI is widely used to characterize meteorological droughts (Blain, 2012). For the analysis of drought in the subregions of the basin, the time scales of six- and twelve months were chosen. The six-month SPI compares the precipitation of this period with the same six-month period over historical record, being associated with water storage irregularities and river outflows. The twelve-month SPI expresses long-term precipitation patterns and is directly related to water scarcity (WMO, 2012).

The adequacy of the historical series to the gamma distribution evaluated by the Kolmogorov-Smirnov test adapted by Lilliefors (Blain, 2014) indicated a good fit, as shown in Table 3.

Table 3. P-values of the Kolmogorov-Smirnov test adapted by Lilliefors to time scales of six- (SPI-06) and twelve-month (SPI-12) for basin stations.

	Iguatama		Pilão Arcado		Fazenda Tapera		Propriá	
Month	SPI-06	SPI-12	SPI-06	SPI-12	SPI-06	SPI-12	SPI-06	SPI-12
Jan	0.727	0.728	0.728	0.729	0.727	0.728	0.724	0.727
Feb	0.535	0.540	0.939	0.939	0.273	0.273	0.315	0.314
Mar	0.738	0.737	0.764	0.772	0.339	0.337	0.904	0.905
Apr	0.689	0.691	0.117	0.114	0.143	0.144	0.295	0.294
May	0.665	0.666	0.451	0.452	0.617	0.621	0.583	0.581
Jun	0.043	0.043	0.110	0.110	0.293	0.291	0.476	0.474
Jul	0.402	0.405	0.031	0.032	0.979	0.977	0.310	0.309
Aug	0.195	0.195	0.002	0.002	0.882	0.879	0.916	0.912
Sep	0.062	0.059	0.752	0.753	0.294	0.293	0.546	0.541
Oct	0.131	0.131	0.553	0.552	0.352	0.351	0.700	0.702
Nov	0.039	0.038	0.072	0.067	0.144	0.144	0.011	0.011
Dec	0.400	0.400	0.381	0.381	0.039	0.040	0.506	0.505

Next, SPI values will be presented using the six- (SPI-06) and twelve-month (SPI-12) time scales for the 4 stations representative of the subregions of the basin, for the period from 1970 to 2015, which totals a historical series of 46 years (Figures 2, 3, 4 and 5). For drought classes, the values of SPI are negative, whereas for the rainy condition the values are positive, according to the classification in Table 2.

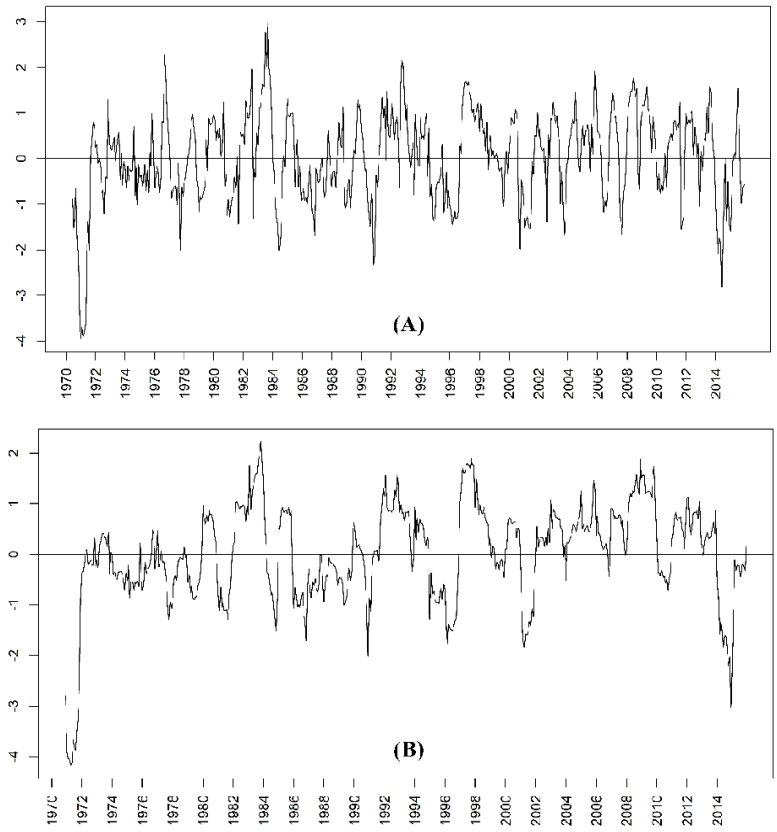

Figure 2. SPI-06 (A) and SPI-12 (B) for Iguatama station.

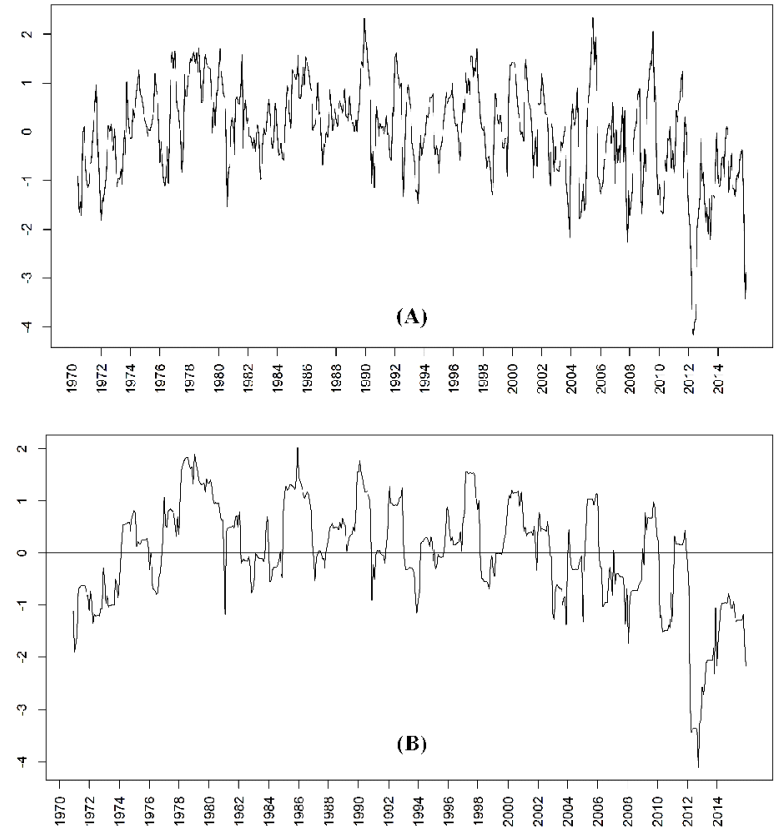

Figure 3. SPI-06 (A) and SPI-12 (B) for Pilão Arcado station.

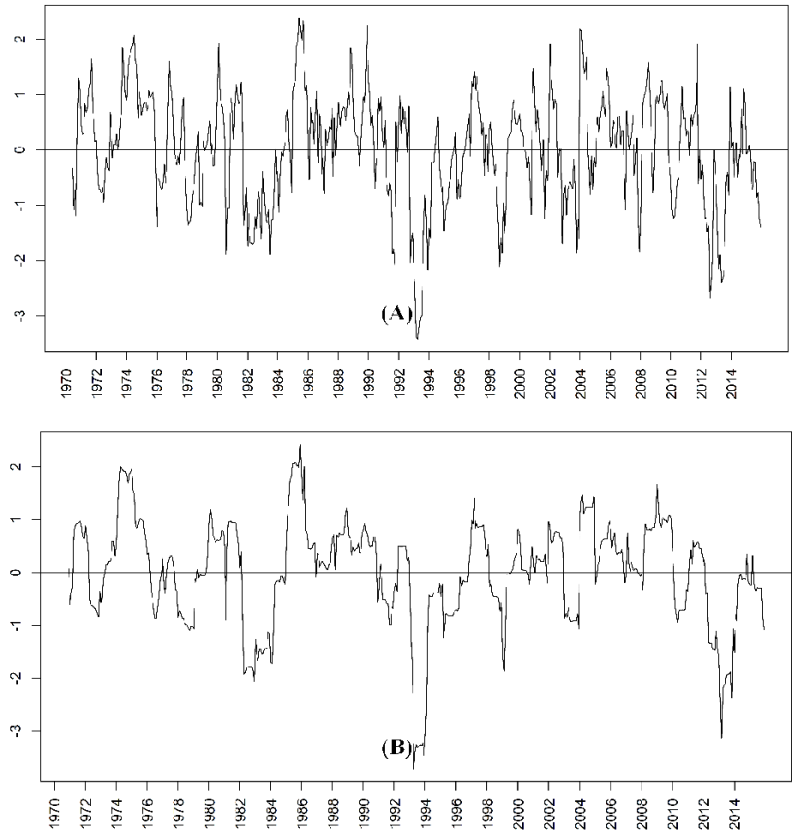

Figure 4. SPI-06 (A) and SPI-12 (B) for Fazenda Tapera station.

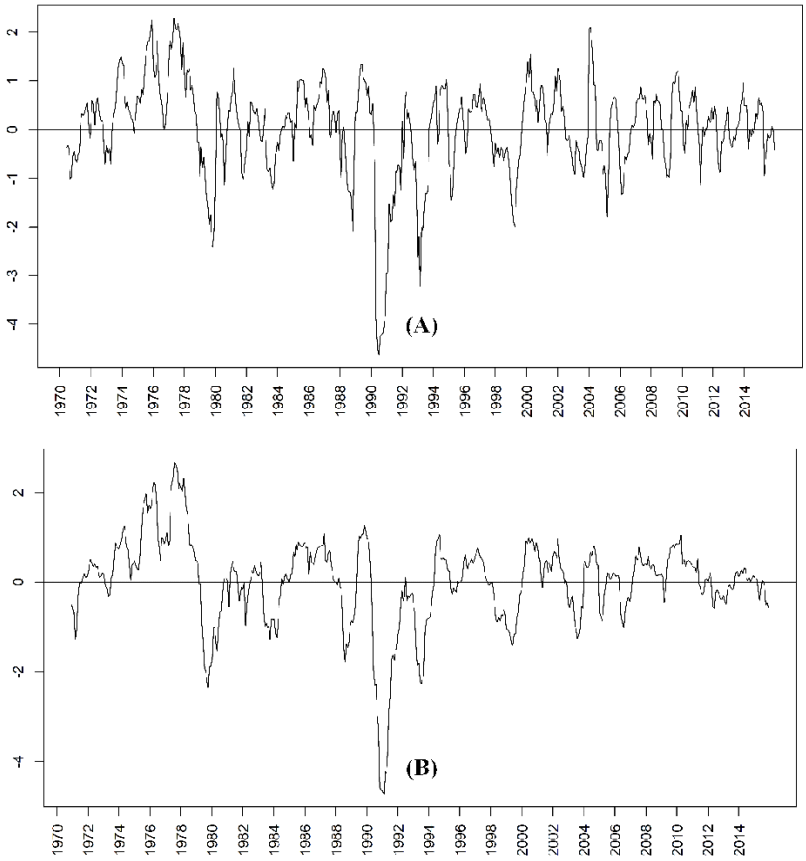

Figure 5. SPI-06 (A) and SPI-12 (B) for Propriá station.

In Figure 2 (A and B), it is possible to identify the drought years, due to the low values of SPI: the extreme drought in 1971 (with large negative peaks of SPI, -3.95 and -4.17 for the time scales of six and twelve months, respectively), and severe and moderate drought (SPI values between -1.0 and -2.0) in some years. It is important to emphasize that this station belongs to the Upper São Francisco region, where the occurrence of extreme and severe droughts is not expected.

In Figure 3 (A and B), for the Pilão Arcado station, four peaks of extreme droughts are identified for the years 2003, 2007, 2012 and 2013 with SPI values between -2.10 and -4.16 for the scale of period of six months (SPI-06). In the twelve-month scale (SPI-12), there are three extreme drought peaks for the years 2012, 2013 and 2014. The presence of severe dry and moderate drought can be observed in some years, with SPI values between -1.0 and -2.0. This station belongs to the region of the Middle San Francisco, where the occurrence of extreme and severe droughts is not expected, and the precipitation values are not so high.

In Figure 4 (A and B), the Fazenda Tapera station, there are several peaks of extreme drought. For the six-month scale (SPI-06) there are eight records of extreme dry spikes with values between -2.04 and -3.42 between 1991 and 2013; and also eight peaks for the twelve-month scale (SPI-12) between the years 1983 and 2013. In addition to extreme drought, several years presented severe drought and moderate drought with SPI values between -1.0 and -2.0, and mild drought with SPI ranging from 0.0 to -1.0 Since this station belongs to the sub-middle region, with a predominance of semi-arid and arid climate, extreme droughts, severe droughts and even mild droughts are expected due to the low precipitation values in this subregion of the basin.

In Figure 5 (A and B), three extreme drought peaks were identified, in 1980, 1991 and between 1993 and 1994 for the two time scales (SPI-06 and SPI-12). There are also some years with severe and moderate droughts in the categories of SPI-06 and SPI-12 with SPI values between -1.0 and -2.0, in addition to several years presenting mild drought with SPI between 0.0 and -1,0. It is worth noting that this station belongs to the Lower São Francisco subregion, whose expected occurrence of extreme and severe droughts is lower than in the Sub-middle, although Propriá is also part of the Northeastern Semi-arid (Brasil, 2005).

The transition probabilities for each of drought classes were calculated, representing the probabilities of state change from month to month, and presented in Table 4 (SPI-06) and Table 5 (SPI-12).

It is seen in Table 4 that for six-month, scale (SPI-06), the transition probabilities of the rainy state in the current month for the same rainy state in the subsequent month are greater than 0.800 (80%). It is also noted that the transition probabilities of drought conditions to rainy conditions are small, varying in the range of 0.00 (0.0%) to 0.262 (26. 2%).

Another important fact that the matrix exposes is that if a locality is under the condition of extreme drought, the probability that in the following month the condition changes to rainy is zero. This is expected, because weather conditions do not change suddenly. In addition, the probability for an extreme drought to continue in the following month increases as it moves towards the river mouth, with values ranging from 0.500 (50%) to 0.789 (78.9%).

For the twelve-month scale (SPI-12), shown in Table 5, the probability that a locality is currently under a rainy state and in the next month remains in this same condition, is greater than 0.900 (90%). Likewise, the probability that a locality is under extreme drought conditions and the next month remains in this same condition, are higher than 0.778 (78.8%).

Table 4. Transition probability matrices for SPI-06 for basin stations.

Iguatama station Code: 2045002					
	Extreme drought	Severe drought	Moderate drought	Mild drought	Rainy
Extreme drought	0.500	0.286	0.000	0.143	0.071
Severe drought	0.176	0.118	0.412	0.294	0.000
Moderate drought	0.038	0.135	0.327	0.404	0.096
Mild drought	0.011	0.017	0.108	0.602	0.261
Rainy	0.000	0.003	0.031	0.146	0.819
Pilão Arcado station Code: 1042015					
	Extreme drought	Severe drought	Moderate drought	Mild drought	Rainy
Extreme drought	0.545	0.091	0.273	0.000	0.091
Severe drought	0.167	0.278	0.444	0.111	0.000
Moderate drought	0.057	0.151	0.340	0.377	0.075
Mild drought	0.000	0.018	0.114	0.611	0.257
Rainy	0.000	0.003	0.017	0.141	0.838
Fazenda Tapera station Code: 839034					
	Extreme drought	Severe drought	Moderate drought	Mild drought	Rainy
Extreme drought	0.556	0.222	0.167	0.000	0.056
Severe drought	0.095	0.238	0.381	0.238	0.048
Moderate drought	0.104	0.125	0.354	0.292	0.125
Mild drought	0.000	0.024	0.109	0.618	0.248
Rainy	0.003	0.007	0.010	0.146	0.833
Propriá station Code: 1036048					
	Extreme drought	Severe drought	Moderate drought	Mild drought	Rainy
Extreme drought	0.789	0.105	0.053	0.053	0.000
Severe drought	0.154	0.462	0.308	0.077	0.000
Moderate drought	0.037	0.148	0.296	0.370	0.148
Mild drought	0.006	0.006	0.081	0.705	0.202
Rainy	0.000	0.000	0.000	0.124	0.876

Table 5. Transition probability matrices for SPI-12 for basin stations.

Iguatama station Code: 2045002					
	Extreme drought	Severe drought	Moderate drought	Mild drought	Rainy
Extreme drought	0.824	0.000	0.059	0.118	0.000
Severe drought	0.063	0.563	0.250	0.125	0.000
Moderate drought	0.031	0.156	0.375	0.438	0.000
Mild drought	0.000	0.010	0.072	0.778	0.139
Rainy	0.000	0.000	0.004	0.089	0.907
Pilão Arcado station Code: 1042015					
	Extreme drought	Severe drought	Moderate drought	Mild drought	Rainy
Extreme drought	0.857	0.095	0.048	0.000	0.000
Severe drought	0.222	0.333	0.222	0.222	0.000
Moderate drought	0.022	0.067	0.556	0.333	0.022
Mild drought	0.005	0.005	0.077	0.798	0.115
Rainy	0.000	0.000	0.007	0.071	0.922
Fazenda Tapera station Code: 839034					
	Extreme drought	Severe drought	Moderate drought	Mild drought	Rainy
Extreme drought	0.778	0.056	0.111	0.056	0.000
Severe drought	0.167	0.583	0.167	0.083	0.000
Moderate drought	0.000	0.269	0.577	0.115	0.038
Mild drought	0.000	0.011	0.034	0.835	0.119
Rainy	0.000	0.000	0.000	0.078	0.922
Propriá station Code: 1036048					
	Extreme drought	Severe drought	Moderate drought	Mild drought	Rainy
Extreme drought	0.842	0.105	0.053	0.000	0.000
Severe drought	0.214	0.429	0.357	0.000	0.000
Moderate drought	0.000	0.152	0.485	0.364	0.000
Mild drought	0.000	0.006	0.071	0.753	0.169
Rainy	0.000	0.000	0.000	0.081	0.919

Tables 6 and 7 show stationary distribution for the six- and twelve-month scales. From Table 6, it can be seen that for all stations the probability for the rainy condition is higher than 0.526 (52.6%), and that the probabilities of drought conditions decrease with the degree of severity. Particularly for the extreme drought category, the probabilities are greater than 0.025 (2.5%) and increase as it moves towards the river mouth. The same occurs for the twelve-month scale whose probabilities for rainy condition are greater than 0.513 (51.3%), while for the extreme drought category the odds are greater than 0.021 (2.1%).

Table 6. Stationary distributions for SPI-06 for basin stations.

Station	Extreme drought	Severe drought	Moderate drought	Mild drought	Rainy
Iguatama	0.026	0.095	0.031	0.322	0.526
Pilão Arcado	0.025	0.099	0.034	0.302	0.541
Fazenda Tapera	0.034	0.091	0.039	0.299	0.537
Propriá	0.035	0.049	0.024	0.317	0.575

Table 7. Stationary distributions for SPI-12 for basin stations.

Station	Extreme drought	Severe drought	Moderate drought	Mild drought	Rainy
Iguatama	0.021	0.058	0.029	0.356	0.536
Pilão Arcado	0.054	0.081	0.019	0.333	0.513
Fazenda Tapera	0.038	0.056	0.05	0.327	0.53
Propriá	0.035	0.061	0.026	0.285	0.593

The recurrence time for each drought class is shown in Tables 8 and 9 for the six- and twelve-month scale, respectively.

Table 8. Recurrence time for SPI-06 for basin stations.

Station	Extreme drought	Severe drought	Moderate drought	Mild drought	Rainy
Iguatama	38.5	10.5	32.3	3.1	1.9
Pilão Arcado	40.0	10.1	29.4	3.3	1.8
Fazenda Tapera	29.4	11.0	25.6	3.3	1.9
Propriá	28.6	20.4	41.7	3.2	1.7

Table 9. Recurrence time for SPI-12 for basin stations.

Station	Extreme drought	Severe drought	Moderate drought	Mild drought	Rainy
Iguatama	47.6	17.2	34.5	2.8	1.9
Pilão Arcado	18.5	12.3	52.6	3.0	1.9
Fazenda Tapera	26.3	17.9	20.0	3.1	1.9
Propriá	28.6	16.4	38.5	3.5	1.7

At the six-month scale, the lowest recurrence times found for the extreme drought class were for the Fazenda Tapera and Propriá stations, with values close to 29.4 and 28.6, respectively. These stations belong to Sub-middle and Lower Sao Francisco, respectively where severe droughts occur frequently as a result of low rainfall and high evapotranspiration (Bezerra *et al.*, 2018).

For the twelve-month scale, the highest return time for the extreme drought class was found to be 47.6 months for the Iguatama station, meaning that among the other stations this is the one with the least possibility of being under this type of climate. It is important to point out that this station belongs to the Upper São Francisco subregion, with a predominance of tropical humid and temperate climate, reflecting a greater amount of precipitation, that is, the chances of drought must be lower than in other subregions.

Still in the twelve-month time scale (SPI-12), the lowest recurrence times for the extreme drought class were for the Pilão Arcado, Fazenda Tapera and Propriá stations. This fact indicates that these stations are more susceptible to drought, as expected, since they are located in the semi-arid region, according to the last update of the municipalities of that region made in 2005 by the Ministry of National Integration (Brasil, 2005).

The expected residence time (which is the average time the process stays in a particular drought class before migrating to another class and represents the duration of that drought class) is shown in Tables 10 and 11, for the six- and twelve-month scales, respectively.

Table 10. Expected residence times for SPI-06 for basin stations.

Station	Extreme drought	Severe drought	Moderate drought	Mild drought	Rainy
Iguatama	2.0	1.5	1.1	2.5	5.5
Pilão Arcado	2.2	1.5	1.4	2.6	6.2
Fazenda Tapera	2.3	1.6	1.3	2.6	6.0
Propriá	4.8	1.4	1.9	3.4	8.1

Table 11. Expected residence time for SPI-12 for basin stations.

Station	Extreme drought	Severe drought	Moderate drought	Mild drought	Rainy
Iguatama	5.7	1.6	2.3	4.5	10.8
Pilão Arcado	7.0	2.3	1.5	5.0	12.8
Fazenda Tapera	4.5	2.4	2.4	6.1	12.9
Propriá	6.3	1.9	1.8	4.1	12.3

It can be observed in Tables 10 and 11 that the longest residence time for both six- and twelve-month scales, is obtained for the rainy condition, greater than and equal to 5.5 months. This information can be used, for example, to plan the sowing of a given crop, since the beginning of the rainy season is known. Also, in water management projects, such as the planning of water drainage systems or irrigation projects, it is extremely important to know the probability of rainy conditions above or below a certain value (Pereira *et al.*, 2007).

4. CONCLUSIONS

The modeling of the SPI for six- and twelve-month scales through Markov chains proved useful in the search for a better understanding of the stochastic characteristics of the climatic behavior of the subregions of the São Francisco Basin, providing (through the probability analysis for each drought class) recurrence time and expected value of residence time in each class. It was possible to observe that the results for the two scales are similar, but each one has its specific purpose. The six-month scale is recommended for the observation of agricultural drought, while the twelve-month scale is better for hydrological drought assessment (WMO, 2012).

For both scales, the transition matrix showed that switching from severe drought or rainy conditions to another class is unlikely in the short term. Correlating this information with the probabilities of the stationary distribution, it is possible to find the regions that are most likely to be in the future under rainy weather or under drought conditions. In all cases studied, and for both scales, the probability of extreme drought was low even for the semi-arid region, represented by Fazenda Tapera station. The lowest recurrence times for the extreme drought class was found for Fazenda Tapera and Propriá stations that belong to the semi-arid region.

The evaluation of the expected value of the time of residence rectifies the information of the period of duration of each climatic condition. The shortest residence time for extreme drought and the longest residence time for rainy condition was again obtained for the Fazenda Tapera station, located in semi-arid region. This information can be used for planting a particular crop, knowing the beginning of the rainy season or for the planning of the use of water resources for the generation of energy or for reservoir- and dam construction.

5. ACKNOWLEDGEMENTS

The authors thank the Coordination for the Improvement of Higher Education Personnel (CAPES) for her PhD scholarship and the Interinstitutional Doctorate (DINTER) between Federal University of Sergipe (UFS) and Federal Rural University of Pernambuco (UFRPE).

6. REFERENCES

BEZERRA, B. G. *et al.* Changes of precipitation extreme indices in São Francisco River Basin, Brazil from 1947 to 2012. **Theoretical and Applied Climatology**, p. 1-12, 2018. https://doi.org/10.1007/s00704-018-2396-6

BLAIN, G. C. Revisiting the probabilistic definition of drought: strengths, limitations and an agrometeorological adaptation. **Bragantia**, v. 71, p. 132-141, 2012. http://dx.doi.org/10.1590/S0006-87052012000100019

BLAIN, G. C. Revisiting the critical values of the Lilliefors test: towards the correct agrometeorological use of the Kolmogorov-Smirnov framework. **Bragantia**, v. 73, p. 192-202, 2014. http://dx.doi.org/10.1590/brag.2014.015

BLAIN, G. C. *et al.* Índice padronizado de precipitação aplicado às condições de seca no Estado do Espírito Santo. **Revista Brasileira de Engenharia Agrícola e Ambiental**, v. 14, n. 10, p. 1067-1073, 2010. https://dx.doi.org/10.1002/joc.1441

BRASIL. Ministério da Integração Nacional. **Rio e Seus Números**. Available at: http://www.integracao.gov.br/web/projeto-sao-francisco/o-rio-e-seus-numeros Access in: July 2018.

BRASIL. Ministério da Integração Nacional. Secretaria de Políticas de Desenvolvimento Regional. **Nova Delimitação do Semi-Árido Brasileiro**. Brasília, 2005.

HUSAK, G. J.; MICHAELSEN, J.; FUNK, C. Use of the gamma distribution to represent monthly rainfall in Africa for drought monitoring applications. **International Journal of Climatology**, v. 27, p. 935-944, 2007.

KELLER FILHO, T. *et al.* Análise da Transição entre Dias Secos e Chuvosos Usando Cadeias de Markov de Terceira Ordem. **Pesquisa Agropecuária Brasileira**, v. 41, n. 9, p. 1341-1349, 2006.

LENNARTSSON, L. *et al.* Modelling precipitation in Sweden using multiple step Markov chains and a composite model. **Journal of Hydrology**, v. 363, p. 42-59, 2008. https://doi.org/10.1016/j.jhydrol.2008.10.003

MAHMOUDZADEH, H. *et al.* Applying First-Order Markov Chains and SPI Drought Index to Monitor and Forecast Drought in West Azerbaijan Province of Iran. **International Journal of Geosciences and Environment Planning**, v. 1, n. 2, p. 44-53, 2016.

MCKEE, T. B. *et al.* The Relationship of Drought Frequency and Duration Times Scales. *In:* CONFERENCE ON APPLIED CLIMATOLOGY, 8., 17-22 Janvier, Anaheim. **Proceedings[…]** Massachusetts: AMS, 1993. p. 179-184.

MISHRA, A. *et al.* Drought characterization: a probabilistic approach. **Stochastic Environmental Research and Risk Assessment**, v. 23, p. 41-55, 2009. https://doi.org/10.1007/s00477-007-0194-2

MISHRA, A.K.; SINGH, V.P. A review of drought concepts. **Journal of Hydrology**, v. 391, n. 1-2, p. 202-216, 2010. https://doi.org/10.1016/j.jhydrol.2010.07.012

PEREIRA, A. R. *et al.* **Meteorologia agrícola**. São Paulo: USP, 2007.

PAULO, A. A.; PEREIRA, L. S. Prediction of SPI Drought Class Transitions Using Markov Chains. **Water Resources Management**, v. 21, n. 10, p. 1813-1827, 2007. https://doi.org/10.1007/s11269-006-9129-9

SADEGHI, L.; SHAMSELDIN, A. Y. Application of the Standardized Precipitation Index (SPI) in Hawke's Bay, New Zealand. *In*: ANDREU, J. (Ed.). **Drought**: Research and Science-Policy Interfacing, 2014. p. 139.

R CORE TEAM. **R**: A language and environment for statistical computing. Vienna, 2019. Available at: https://www.R-project.org/

SANUSI, W. *et al*. The drought characteristics using the first-order homogeneous Markov chain of monthly rainfall data in peninsular Malaysia. **Water Resources Management**, v. 29, n. 5, p. 1523-1539, 2015. https://doi.org/10.1007/s11269-014-0892-8

SNIRH. **Informações sobre recursos hídricos**. Available at: http://www.snirh.gov.br/portal/snirh Access in: July 2018.

SOUSA, F. A. S. *et al*. O Índice de Precipitação Padronizada (IPP) na identificação de extremos de chuvas e secas na bacia do rio Paraguaçu (BA). **Ambiência Guarapuava (PR)**, v. 12, n. 2, p. 707-719, 2016.

TONKAZ, T. Spatio-temporal assessment of historical droughts using SPI with GIS in GAP Region, Turkey. **Journal of Applied Sciences**, v. 12, n. 6, p. 2565-2571, 2006.

TSAKIRIS, G.; VANGELIS, H. Towards a Drought Watch System based on Spatial SPI. **Water Resources Management,** v. 18, p. 1-12, 2004. https://doi.org/10.1023/B:WARM.0000015410.47014.a4

UFSC. Centro Universitário de Estudos e Pesquisas sobre Desastres. **Atlas brasileiro de desastres naturais: 1991 a 2012**. 2nd ed. Volume Brasil. Florianópolis: CEPED UFSC, 2013.

WILKS, D. S. **Statistical Methods in the Atmospheric Sciences**. 3rd Ed. Oxford: Elsevier, 2011.

WMO. **Standardized precipitation index user guide.** Geneva, 2012. Available at: http://www.wamis.org/agm/pubs/SPI/WMO_1090_EN.pdf Access in: July 2018.

Ambiente & Água - An Interdisciplinary Journal of Applied Science
ISSN 1980-993X – doi:10.4136/1980-993X
www.ambi-agua.net
E-mail: ambi.agua@gmail.com

Heavy metals in the São Mateus Stream Basin, Peixe River Basin, Paraiba do Sul River Basin, Brazil

ARTICLES doi:10.4136/ambi-agua.2329

Received: 13 Sep. 2018; Accepted: 31 Mar. 2019

Cézar Henrique Barra Rocha[1*]; Hiago Fernandes Costa[1]; Leonardo Pimenta Azevedo[2]

[1]Universidade Federal de Juiz de Fora (UFJF), Juiz de Fora, MG, Brasil
Faculdade de Engenharia. Núcleo de Análise Geo Ambiental (NAGEA).
E-mail: barra.rocha@gmail.com, hiagofc@hotmail.com
[2]Instituto Estadual de Florestas (IEF/MG), Viçosa, MG, Brasil
Agência de Florestas e Biodiversidade. E-mail: leopimentaz@yahoo.com.br
[*]Corresponding author

ABSTRACT

Large-scale enterprises with high potential to pollute need to be licensed, properly supervised and monitored during and after their operations to avoid and/or mitigate impacts in their areas of influence. The São Mateus Stream Basin (SMSB), located in rural area of Juiz de Fora (MG), is impacted by several activities, highlighting a deactivated landfill and an industrial park. This study monitored the concentration of heavy metals in the waters of the main tributaries of the SMSB. Strategic points were selected in each sub-basin, before the mouth and meeting of the Bocaina, Salvaterra and São Mateus Streams, measured monthly between January and December 2014 using the Metalyser probe, and applying the Contamination Index (CI). The CI results showed that the enterprises located in this basin, especially the Park Sul and Salvaterra Landfill in the Bocaina and Salvaterra Streams, respectively, are negatively impacting the quality of these waters. Metals such as Hg, Cu, Pb and Zn were the ones that most violated CONAMA Resolution 357/2005, directing management in order to control the sources of these metals, which are cumulative in organisms and damage the whole trophic chain. The inhabitants of this rural area are not served by any water concessionaire and make use of springs and wells below the level of these streams.

Keywords: contamination index, environmental impacts, environmental monitoring, landfill, water quality.

Metais pesados na Bacia Hidrográfica do córrego São Mateus, Bacia do rio do Peixe, Bacia do rio Paraíba do Sul, Brasil

RESUMO

Empreendimentos com porte e potencial poluidor precisam ser licenciados adequadamente, fiscalizados e monitorados durante e após suas operações de forma a evitar e/ou mitigar impactos nas suas áreas de influência. A Bacia Hidrográfica do córrego São Mateus (BHCSM), situada em zona rural de Juiz de Fora (MG), é impactada por várias atividades, destacando um aterro sanitário desativado e um parque industrial. O objetivo desse artigo foi monitorar as águas dos principais tributários da Bacia Hidrográfica do córrego São Mateus em

relação à concentração de metais pesados. Escolheram-se pontos estratégicos em cada sub-bacia, antes da foz e encontro dos córregos Bocaina, Salvaterra e São Mateus, mensurados mensalmente entre janeiro e dezembro de 2014 através da Sonda Metalyser, aplicando-se o Índice de Contaminação (IC). Os resultados do IC permitiram verificar que os empreendimentos localizados nesta Bacia, em especial, o Park Sul e o Aterro Sanitário Salvaterra nos córregos Bocaina e Salvaterra, respectivamente, estão impactando negativamente a qualidade dessas águas. Metais como Hg, Cu, Pb e Zn são os que mais violaram a Resolução CONAMA 357/2005, direcionando desta forma a gestão, de modo a controlar as fontes destes metais que são acumulativos nos organismos e geram prejuízos a toda cadeia trófica. A população que habita essa região rural não é atendida por nenhuma concessionária de água, fazendo uso de nascentes e poços abaixo do nível desses córregos.

Palavras-chave: aterro sanitário, impactos ambientais, índice de contaminação, monitoramento ambiental, qualidade da água.

1. INTRODUCTION

Population growth coupled with high consumption patterns and lack of recycling and reuse programs leads to increasing waste generation and the need for disposal areas. Due to the flaws in choosing these locations, undersized treatment projects and lack of maintenance, slurry is generated which flows into nearby areas, contaminating water resources. Santana and Barroncas (2007) define slurry as a dark-colored liquid resulting from the decomposition of organic matter present in garbage. The slurry is highly toxic; its composition is varied, and depends on factors such as the type of waste and the age of the landfill site. The release of slurry can also reach underground waters, contaminating these waters compromising their use.

Particularly, heavy metals are often found in the composition of much industrial and urban waste taken to municipal landfills. The high levels of toxicity of heavy metals to organisms, associated with their relative ease of entering and accumulating along trophic chains for a long time, underlies the importance of studies that determine their concentrations in aquatic environments. Manoj *et al.* (2012) reinforce that heavy metals enter the food chain and cause metabolic and physiological disturbances in organisms.

In this context, the monitoring of the São Mateus Stream Basin (SMSB) is important, considering all the negative impacts already created by the Salvaterra Landfill in the stream mentioned above. This basin also includes the Industrial District Park Sul, with emphasis on the exploitation of gravel and industrial sand in the Pedra Sul Quarry with the discharge of mineral tailings in the Bocaina Stream Basin, one of the tributaries of the Salvaterra Stream. The latter flows into the São Mateus Stream, which has its mouth in the Peixe River, a tributary of the Paraibuna River, one of the main ones in the Paraíba do Sul River Basin (Figure 1).

From January 1999 to 04/11/2010, the date of deactivation of the landfill, all domestic, hospital and industrial waste from Juiz de Fora was deposited at Salvaterra Landfill, about 500 tons/day. Initially as a dump, intermediately as a Controlled Landfill and only in the final years, since 05/30/2005, as a landfill on the right slope. The area is on the banks of BR040, has rugged relief and had several springs, contrary to the technical and legal requirements for locating an enterprise for this purpose. During the period of operation of the Salvaterra landfill there were several irregularities, such as burial, contamination of springs and water table, risk of accidents with trucks that transported the slurry produced by the landfill to the Sewage Treatment Station (STS) in the Barbosa Laje Neighborhood, and health risks to the local population due to contamination of the shallow wells of the region, since it does not have a water supply and therefore depends on the water of wells and springs, almost always at a lower elevation than this landfill. The possible lack of compatibility between the treatment of slurry

in the Barbosa Laje STS and the accumulation capacity of the percolated tanks present in this landfill may explain possible spillages of manure in the waters of the Salvaterra Stream, which also has two of its sources within the limits of Salvaterra Landfill.

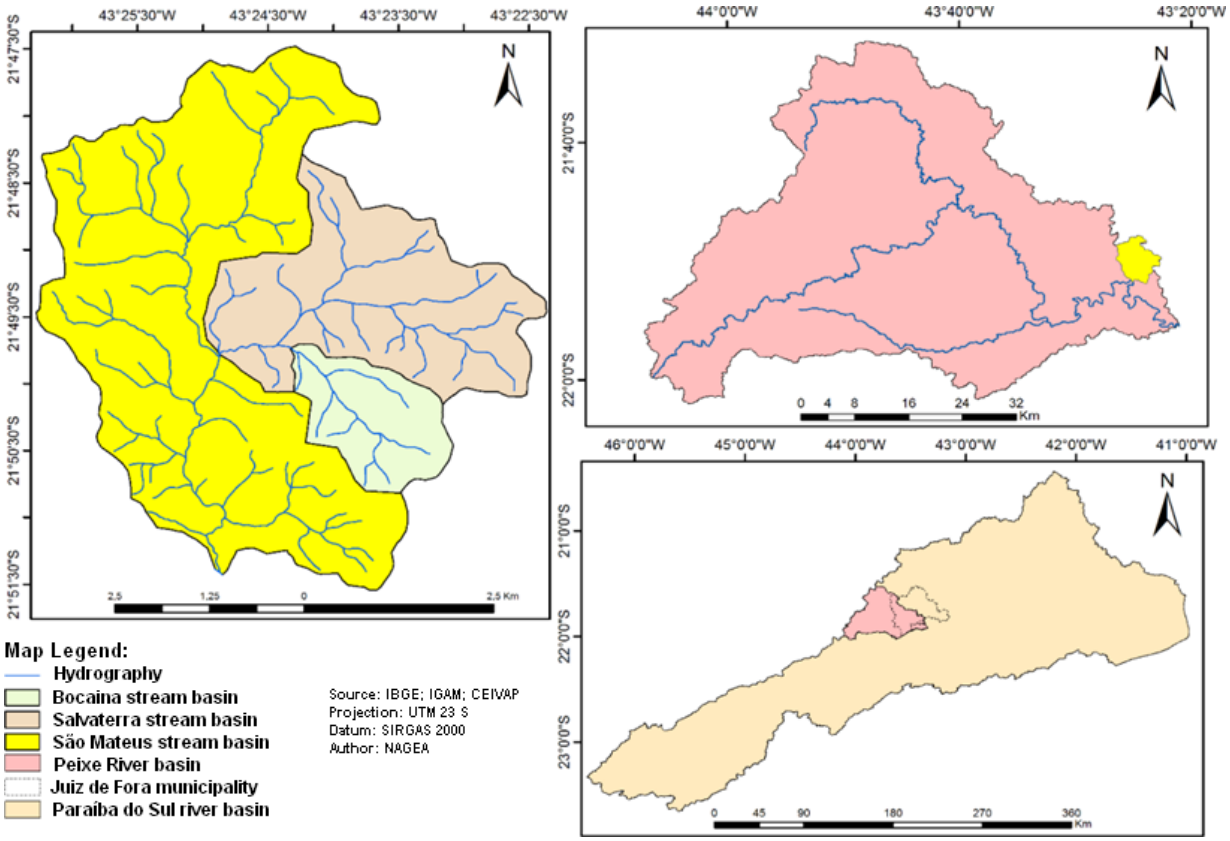

Figure 1. Location of the São Mateus River Basin in the Rio do Peixe watershed, Juiz de Fora and Paraíba do Sul River Basin.

For Guedes *et al.* (2012), Rocha *et al.* (2014) and Rocha and Pereira (2016), the monitoring of water quality is one of the main instruments for sustaining and managing water resources, functioning as a tool to identify the effects of use on water quality, assisting in environmental control actions.

Therefore, this study monitored the waters of the main tributaries of the São Mateus Stream to determine the concentrations of heavy metals by applying the Contamination Index (CI).

2. MATERIAL E METHODS

In order to verify and understand the processes that affect the São Mateus Stream Basin, monthly collections were carried out from January to December 2014 at three strategic points: Point 1 (P1) in the São Mateus Stream prior to the encounter with the Salvaterra Creek; Point 2 (P2) in the Salvaterra Stream before the encounter with the Bocaina Stream; and Point 3 (P3), mouth of the Bocaina Stream before the encounter with Salvaterra. The three points monitored, as well as the location of the Salvaterra Landfill and the Park South complex are illustrated in Figure 2.

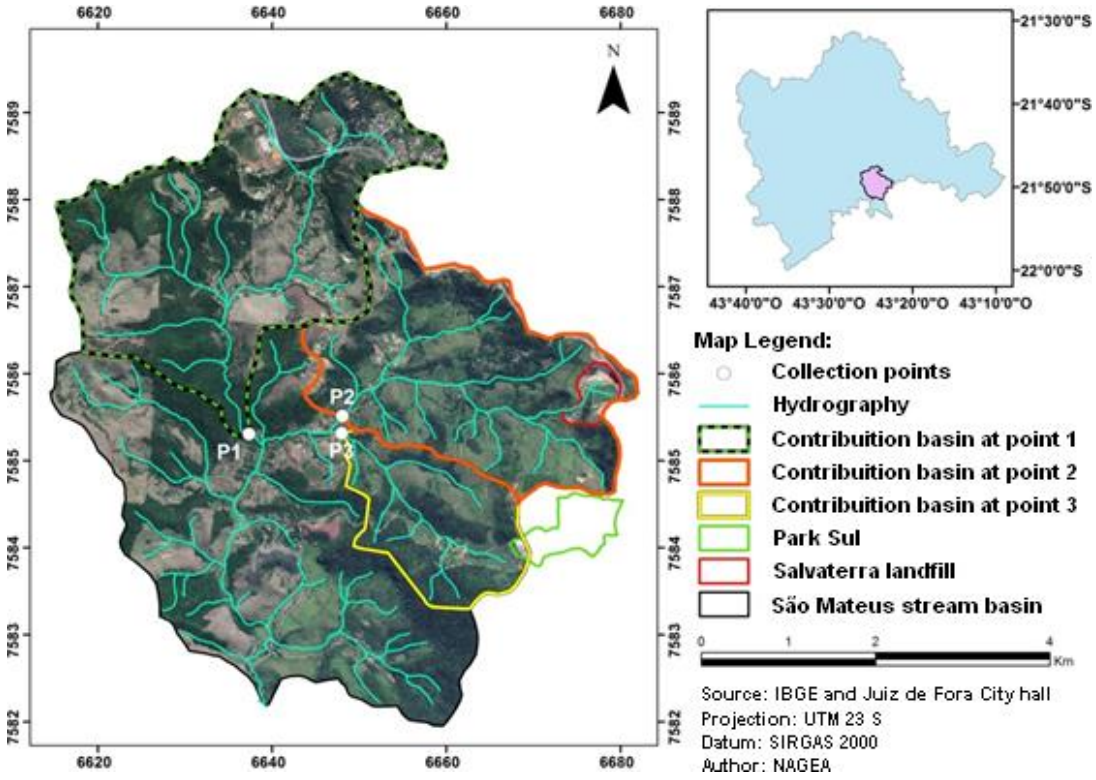

Figure 2. São Mateus Stream Basin, contribution basins of collection points, Salvaterra landfill and Park Sul within the limits of Juiz de Fora.

The São Mateus Stream Hydrographic Basin extends from the source of the São Mateus Stream, located in Nova California neighborhood, to the mouth of Peixe River, which is classified as Class 1, according to the COPAM (State Council for Environmental Policy) Normative Resolution Number 16 of September 25, 1996 (Copam, 1996). According to this classification, Peixe River can be used for human supply after simplified treatment, recreation of primary contact and irrigation. The watershed area of the São Mateus Stream is approximately 30 km², and its two main tributaries are the Salvaterra (P2 sub-basin) and Bocaina (P3 sub-basin) Streams.

The BR-040 and MG-353 are the main highways that cross the São Mateus Basin, which also includes the Salvaterra Valley Private Natural Heritage Reserve (RPPN). This RPPN is formed by natural environments typical of the remnants of the Atlantic Forest, this being the important private reserve of the municipality of Juiz de Fora with considerable vegetation, as shown in Figure 2.

The samples were collected in plastic containers with a capacity of 2 liters and later analyzed in the laboratory. Only heavy metals were monitored by means of the CLEAN Metalyser HM 1000 probe that determines 6 parameters in parts per billion (ppb) or Micrograms / liter ($\mu g\ L^{-1}$), being: Arsenic III (As III), Total Cadmium (Cd), Total Lead (Pb), Total Copper (Cu), Total Mercury (Hg) and Total Zinc (Zn). The detection limit of the probe for As (III), Cu, Hg, Pb and Zn metals ranges from 5 ppb up to 500 ppb and for Cd ranges from 3 ppb up to 500 ppb.

After obtaining the results, the data were tabulated in Microsoft Office Excel 2010 and analyzed through the application of descriptive statistics and application of the Contamination Index.

For the calculation of the Contamination Index (CI), the Contamination Factor (CF) was first determined through the method used by Manoj *et al.* (2012). Ribeiro *et al.* (2012) proposed using the relationship between the concentrations of the metals found in the sample and

reference concentrations, that is, concentrations that would be expected for that particular site, as shown in Equation 1. Thus, as in Ribeiro *et al.* (2012), in this work, the limits established by CONAMA Resolution 357/2005 (Conama, 2005) for fresh waters classified as Class 1 were used as reference values. These limits were converted from mg / L to ppb by multiplying by 1000. The contamination factors were determined for each of the metals, for each month and for each of the three points sampled.

$$\frac{\text{CF} = (\text{Concentration of sampled point (ppb)})}{(\text{Maximum concentration allowed by CONAMA 357/2005 (ppb)})} \quad (1)$$

The Contamination Factor seeks to determine the number of times the limit value established by environmental legislation, in the case of CONAMA 357/2005, has been exceeded or not. Therefore, if CF> 1, the reference value exceeds the concentration found in the sample; but if CF = 1, both concentrations, that is, found in the sample and allowed in the legislation, are equal; and CF <1, indicates that the concentration of the metals determined in the sample was lower than that established in the legislation.

After the calculation of the Contamination Factor (CF), the Contamination Index (CI) was calculated, which sums up the sum of the contamination factors of the six metals analyzed in each month for each of the three points according to Equation 2.

$$CI = \sum_{i=1}^{n} CF \quad (2)$$

The Contamination Index accumulates the contamination factors, which the greater they appear, that is, the more they exceed the maximum concentration allowed by CONAMA 357/2005, the more they contribute to the high value of the Contamination Index, and the worse the degree of contamination in the water studied.

It is worth noting that the probe used gives the total concentrations of the metals Cu, Cd, Zn, Pb and Hg and the concentration of As III, and that the CONAMA 357/2005 resolution establishes limits for dissolved copper and not total copper and total arsenic and not arsenic III. In spite of this difference, in this work the Cu data obtained by the probe were compared to the limit of the CONAMA resolution 357/2005 for dissolved Cu, since its presence or absence would little change the Contamination Indices and would change the classification only for the months of Sep / 14 in the São Mateus Stream and Dec / 14 in Salvaterra Stream that would pass from the average classification to good, but this data was maintained to highlight the presence of the same in the studied waters. As for As III, when only a fraction of the metal is compared to the total and this ratio is higher than 1, we will be underestimating the presence of Arsenic, since the Arsenic V (As V) fraction that together with As III form As Total is not being detected by the probe, which if detected could raise the Contamination Index.

In order to perform the calculations, it was considered that values below the detection limit would be equal to zero, which ultimately underestimates the results, since although the concentrations in this case are very low, the metals may be present and not contribute to the IC. Furthermore, values above the limit of detection were considered as 500 ppb.

After the calculations, the months of each point were classified according to the four categories proposed by Ribeiro *et al.* (2012), described in Table 1.

Table 1. Classification of Contamination Index.

Contamination index	Classification
0 <=10	Good
10 <= 50	Average
50 <= 100	Uncertain

Source: Adapted from Ribeiro et al. (2012).

3. RESULTS AND DISCUSSION

According to Figure 3b and 3e, Cu and Hg were repeatedly above legal limits at all three points. For Hg (Figure 3e), concentrations up to 90, 80 and 10 times the CONAMA 357/2005 limit were punctually observed for P3, P2 and P1, respectively. Zn (Figure 3a) and Cu (Figure 3b) were detected in almost all water samples, being most of the time above than the CONAMA limit for Cu at the three points while Zn was generally inferior. Cadmium (Figure 3c), Lead (Figure 3d) and Arsenic III (Figure 3f) were not always detected, but were almost each time over the legal limit when they were. The points most-impacted by Cd and Pb were P2 and P3. During all the sampling, As (III) was only detected three times: two times at P1 (São Mateus Stream) and one at P2 (Salvaterra Stream).

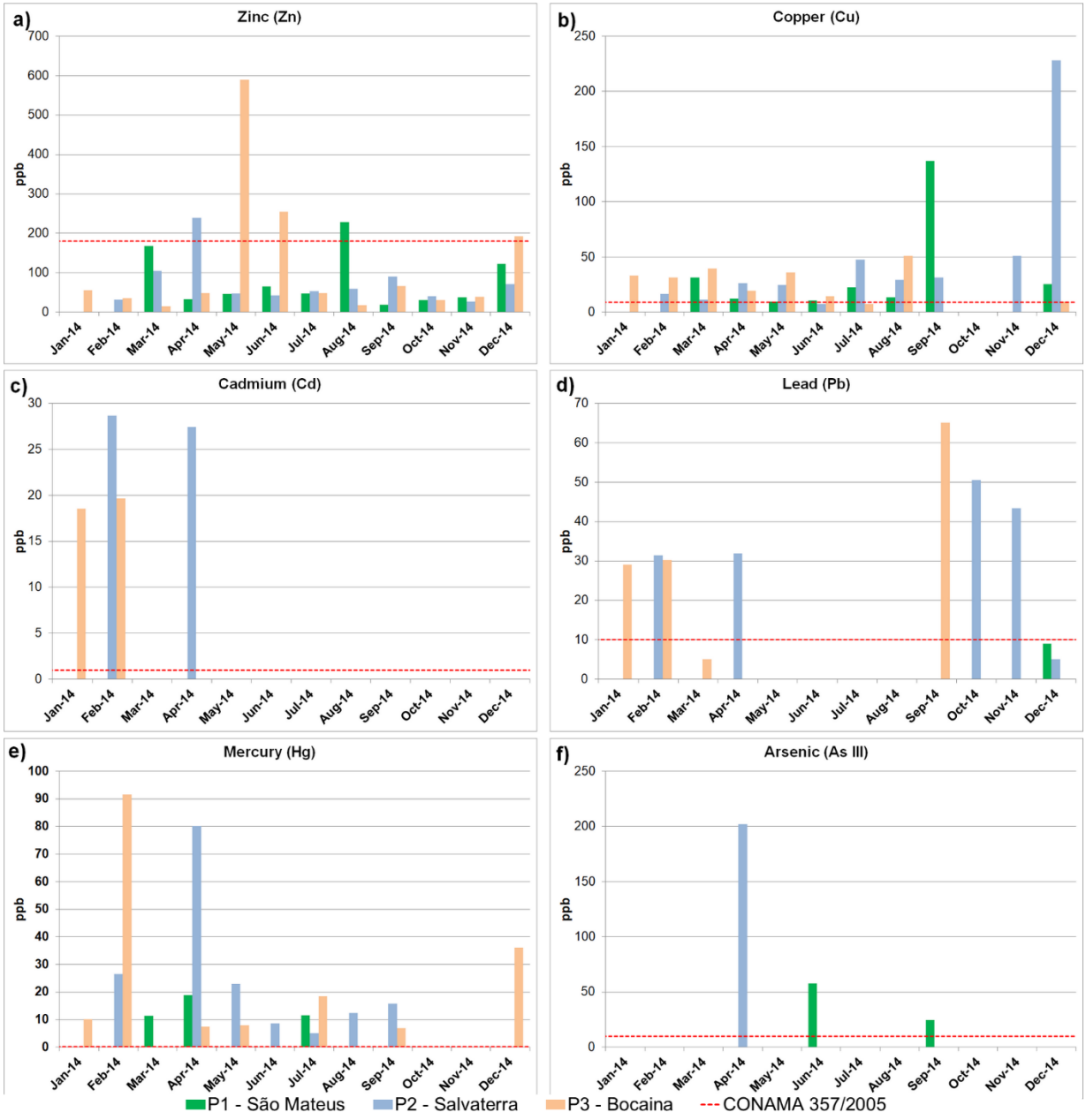

Figure 3. Monthly evolution of Zinc (a), Copper (b), Cadmium (c), Lead (d), Mercury (e) and Arsenic (f) concentrations at three points during the year 2014.

From the results obtained in the calculation of the Contamination Factor (FC) for the three

points studied, it was possible to detect that 31.3% of the concentrations of the metals analyzed were above the limits established by CONAMA resolution 357/2005, since they presented values of CF above 1. After the calculations of the Contamination Indices for all the points monitored during the study period, several results were obtained, with indices of good quality and bad quality found, as shown in Table 2, which shows the average of the Contamination Indices of each point, resulting in an average quality for the São Mateus Stream and an uncertain quality for the Salvaterra and Bocaina Streams. Salvaterra's index was slightly higher than that of Bocaina. There is also a very marked variation between the Contamination Indices from one month to the other in the points studied, which is due to possible variations in the flow of water courses, the variation of manure discharges in the case of the Salvaterra Creek and the incorporation of the metals in the sediments and their resuspension, which are quite random factors that depend on the dynamics of the basin. According to Cotta *et al.* (2006), after sedimentation, metals may again become available in water due to oxy-reduction reactions or resuspension processes caused by the current or activity of organisms that inhabit the sediment.

Table 2. Contamination Index found in the three monitored points.

Contamination index			
	São Mateus	Salvaterra	Bocaina
Months	P1	P2	P3
Jan-14			76
Feb-14		167	484
Mar-14	61	2	5
Apr-14	96	455	40
May-14	1	118	47
Jun-14	7	45	3
Jul-14	61	31	94
Aug-14	3	65	6
Sep-14	18	83	42
Oct-14	0	5	49
Nov-14	0	10	0
Dec-14	4	26	182
Average of each stream	25	92	86

The average CIs in the rainy months, which according to the Urban Development Master Plan of the city of Juiz de Fora (Juiz de Fora, 2000) are the months of October to April, are worse than in the dry months, which possibly due to the loading of materials into the body of water, such as household waste, residues from the Pedra Sul quarry, transport of fertilizers and domestic sewage and other elements that include heavy metals. According to Vasco *et al.* (2011), surface runoff of water on the ground during rainfall is the main diffuse source of pollution of water bodies. This fact denotes the importance of maintaining the riparian forests, which according to Rocha and Costa (2015) are similar to the safety bands of highways and firebreaks in parks, as they function as safety bands for the quality of the water body, reducing the impact of pollution sources through the "filter" effect, highlighting the improvement of air quality, the retention of fine sediments, toxic products and nutrients carried by precipitation, minimizing the silting of the waterbody, avoiding erosion and stabilizing the soils of the margins, constituting of a true physical barrier. Lima and Santos (2012) attributed the increase in the concentration of metals in the waters of Claro River in the state of Goiás to the absence of riparian forest at its margins.

Based on the average results found in the points, it was possible to observe that P2 and P3

are actually more impacted because they present the highest contamination indexes, which is due in large part to the ventures present in their sub-basins. This contamination can spread not only by surface water, but also can reach the water table, a possible source of water for the local population. Oliveira and Pasqual (2004), Lopes *et al.* (2007) and Nakamura *et al.* (2014), verified the contamination of the water table by heavy metals in their stidies.

Arsenic, Cadmium, Lead, Copper, Mercury and Zinc are systematically referred to as sources of urban waste deposited in landfills or dumps, domestic sewage, mining, industrial dumping and agricultural activities (Campos *et al.*, 2009; Coelho, 2012; Cotta *et al.*, 2006; Egreja Filho *et al.*, 1999; Jesus *et al.*, 2004; Lima and Santos, 2012; Macêdo, 2007; Marins *et al.*, 2004; Nakamura *et al.*, 2014; Nriagu e Pacyna, 1988; Ribeiro *et al.*, 2012; Santana and Barroncas, 2007; Silva *et al.*, 2016; WHO, 2004; 2007; 2010a; 2010b; 2010c; Yu *et al.*, 2014).

P1 in the São Mateus Stream was the point that presented a better quality of water, and bad quality was not detected at any time despite having high Contamination Indices in the first two months studied (March and April / 2014). Hg was presence in high concentrations. In addition, Cu and Zn were also detected more frequently, and occurred together with Hg in the formation of almost all Contamination Indices. As was most relevant only in the month of July, possibly associated with agricultural use in the Sub-basin of contribution of the São Mateus Stream, since Arsenic is present in elements such as fertilizers, herbicides and pesticides.

Despite the use of fertilizers and sewage, these sources did not significantly influence the presence of Pb in water, since it was detected only in December and at a concentration below the limits established by CONAMA Resolution 357/2005. At this point, Cadmium was not found in any sample, possibly due to the fact that it occurs in very low concentrations in natural waters. Cu is also not found significantly in natural waters; however, it was not present only in two months of the year, and when it was found it was always above the limit established by CONAMA 357/2005.

In this way, it can be noticed that the contribution of domestic sewage and agricultural activities to the concentrations of heavy metals in P1 occurs due to the high concentration of Hg, Cu and Zn, which have domestic sewage as a common source (Jackson, 1992), and agricultural activities, through the use of pesticides, fertilizers, insecticides, among others (Gonçalves Júnior *et al.*, 2014; Nacke *et al.*, 2013; Silva *et al.*, 2016; 2018).

P2 was the point that presented the most months classified as bad and the lowest number of months classified as good, which in fact confirms the degradation of the same, mainly because it was the only point in which were present all of the metals analyzed in the samples, i.e., the heavy metals Hg, Cu, Zn and Pb, the main ones responsible for the formation of Contamination Indices throughout the studied period. In April, in P2 a dark was detected at the time of collection. This supposedly was a spill of slurry occurred near dawn. According to Celere *et al.* (2007), several organic and inorganic substances are carried by slurry. Campos *et al.* (2009) highlights that slurry is an extremely polluting and damaging liquid with high organic load and heavy metals, the latter with bioaccumulative characteristics. Heavy metals in large concentrations deserve greater attention because of their non-degradability, remaining in the environment for a long time (Cotta *et al.*, 2006).

Hg is a highly toxic metal and harmful to human health even in low concentrations. Due to the low concentration allowed in legislation for this heavy metal, when present it was primarily responsible for values of the Contamination Index, mainly in the points P2 and P3, revealing that the index is coherent, since the presence of Hg in the water is extremely dangerous and undesirable. At P2 in April, the month in which the spill was supposed to have occurred, the Hg exceeded by about 400 times the limit of legislation, while at P3 in February the limit was exceeded 457 times.

Thus, the presence of metals Hg, Cu, Zn and Pb with higher frequency and higher

concentrations in P2, as well as the dark water in the month of April at the time of collection, which presented all the heavy metals analyzed in this work, indicate that Salvaterra Landfill would be the main source of contamination of the Salvaterra Stream, mainly due to the disposal of materials such as batteries, light bulbs, electronic garbage, metal alloys, health care waste, and ferrous metals in general which partly comprise the slurry and subsequently reach the bodies of water. There may also be a contribution from domestic sewage and agricultural activities, but they become insignificant due to the contribution of Aterro Salvaterra.

Sisinno and Moreira (1996) found Pb above that allowed by regulation in wells and springs in the area of influence of the Controlled Landfill of Morro do Céu in Niterói in the state of Rio de Janeiro. Pb was one of the main elements responsible for the values of the P2 Contamination Index; this fact is possibly due to the deposition of residues such as batteries, electric appliances, cables and paints in the Salvaterra Aterro that include this element, and that eventually leach into the waters of the stream. According to CETESB (2009), Pb can affect almost all organs of the body, especially the nervous system, both in adults and children, besides accumulating in the body causing toxification. Once absorbed, it can be found in blood, soft tissues and bone (ATSDR, 2012).

It is interesting to note that Arsenic is very much attributed to the spillage of manure, since the only time it was found in P2 was the month in which the dark waters were observed, presumably due to the presence of manure, although we underestimated such concentration due to the detection of only one of the fractions of As Total. Soon, As was one of the smallest contaminants in the analyzed waters. According to Macêdo (2007), Arsenic is rare in natural waters.

In P3, the Contamination Index was also high, presenting water as of bad quality at two different times, in February and December, both in the rainy season and as good quality in four months of the year. At this point, only Arsenic was not found, whereas the other metals, mainly, Hg, Cu and Zn formed a large part of the Contamination Indices. The possible cause of Hg contamination was not clearly found, but it is possible that domestic sewage was discharged into this stream, which is the possible source of this metal that was detected more frequently at this point. Cu may be associated with mining, that is, the production of industrial sand and gravel in the sub-basin, since this metal appears very frequently in this stream. Zn was the only metal that exceeded the detection limit of the probe, although this occurred only once in May at P3. This metal is found in the natural waters, and if it presents with concentrations above 5 mg L^{-1}, it can affect water taste. This was the only metal that was present in the monitored points every month, and in a few months, Zn exceeded the limit of Conama Resolution 357/2005. It is possible to explain the presence of this heavy metal in all samples, since according to Coelho (2012), Zn is readily transported in natural waters, being one of the most mobile heavy metals. According to Coelho (2012), Zinc is an essential and beneficial element to the human organism, but is toxic in high concentrations.

The occurrence of Cd only in the months of January and February in P3 may be associated with the exploitation of industrial sand and gravel in Pedreira Pedra Sul or the excessive use of fertilizers (Benson *et al.*, 2014; Balkhair and Ashraf, 2016) in agricultural activities that also occur in this sub-basin. Cd contamination was not associated with the domestic sewage discharge because it was not seen in P1 and had not been continuously detected in other months, considering that domestic sewage is continuously released. This metal had little influence on the formation of P2 and P3 Contamination Indices, but when it was present in these points the limit established by CONAMA Resolution 357/2005 was exceeded. Manoj *et al.* (2012) reports that, in addition to Hg and Pb, Cd is toxic even in minimal concentrations. According to Mcgrath *et al.* (2006), it may cause poisoning if ingested through water or food, in addition to being a carcinogenic element (Kumar Sharma *et al.*, 2007).

In P3, although quarrying was one of the possible origins of Arsenic, this metal was not

detected, possibly due to the absence of this metal in the rock formations. Therefore, in P3, mining from the South Park or agricultural activities in the sub-basin of the Bocaina Stream may contribute to the contamination by heavy metals.

4. CONCLUSION

The evaluation of Contamination Indices made it possible to verify that the ventures located in the São Mateus Stream Basin, especially the South Park and the Salvaterra Landfill in the Bocaina and Salvaterra Stream sub-basins, respectively, are in fact negatively impacting water quality. This impact may harm the entire trophic chain in the sub-basins of these two streams, more seriously than in the São Mateus Stream that is impacted by sewage and agricultural activities. Thus, the Contamination Index allowed us to identify that metals like Hg, Cu, Pb and Zn most violate CONAMA Resolution 357/2005, thus identifying the need for management in order to control the sources of these metals that are cumulative in organisms and generate losses in the medium- and long term.

5. ACKNOWLEDGMENTS

The authors would like to thank a Federal University of Juiz de Fora for research grants awarded and the researchers of Environmental Geo Analysis Core.

6. REFERENCES

ATSDR. **Public Health Service.** Atlanta, 2012.

BALKHAIR, K. S.; ASHRAF, M. A. Field accumulation risks of heavy metals in soil and vegetable crop irrigated with sewage water in western region of Saudi Arabia. **Journal of Biological Sciences**, v. 23, n. 3, p. 32–44, 2016. https://doi.org/10.1016/j.sjbs.2015.09.023

BENSON, N. U.; ANAKE, W. U.; ETESIN, U. M. Trace Metals Levels in Inorganic Fertilizers Commercially Available in Nigeria. **Journal of Scientific Research & Reports**, v. 3, n. 4, p. 610–620, 2014.CAMPOS, A. E. L.; NUNES, G. S.; OLIVEIRA, J. C. S.; TOSCANO, I. A. S. Avaliação da contaminação do Igarapé do Sabino (Bacia do Rio Tibiri) por metais pesados, originados dos resíduos e efluentes do aterro da ribeira, em São Luís, Maranhão. **Revista Química Nova**, v. 32, n.4, p.960-964, 2009. http://dx.doi.org/10.1590/S0100-40422009000400025

CELERE, M. S.; OLIVEIRA, A. da S.; TREVILATO, T. M. B.; MUÑOZ, S. I. S. Metais presentes no chorume coletado no aterro sanitário de Ribeirão Preto, São Paulo, Brasil, e sua relevância para saúde pública. **Caderno saúde Pública**, v. 23, n. 4, p. 939-947, 2007.

CETESB. **Significado ambiental e sanitário das variáveis de qualidade das águas e dos sedimentos e metodologias analíticas e de amostragem no Estado de São Paulo**. São Paulo: SMA, 2009.

COELHO, V. M. B. **Paraíba do Sul: um rio estratégico**. Rio de Janeiro: Casa da Palavra, 2012. p. 143-182.

CONSELHO NACIONAL DE MEIO AMBIENTE. Resolução nº 357 de março de 2005. Dispõe sobre a classificação dos corpos de água e diretrizes ambientais para o seu enquadramento, bem como estabelece as condições e padrões de lançamento de efluentes, e dá outras providências. **Diário Oficial [da] União**, Brasília, n. 53, 18 mar. 2005.

COMISSÃO DE POLÍTICA AMBIENTAL (MG) - COPAM. Dispõe sobre o enquadramento das águas estaduais da bacia do rio Paraibuna. **Deliberação Normativa n. 16, de 24 de setembro de 1996.** Available at: http://www.siam.mg.gov.br/sla/download.pdf?idNorma=113. Access: 9 Feb. 2015.

COTTA, J. A. O.; REZENDE, M. O. O.; PIOVANI, M. R. Avaliação do teor de metais em sedimento do rio Betari no Parque Estadual Turístico do Alto Ribeira – PETAR, São Paulo, Brasil**. Revista Química Nova**, v. 29, n. 1, p. 40-45, 2006.

EGREJA FILHO, F. B.; REIS, E. L.; JORDÃO, C. P.; NETO, J. T. P. Avaliação quimiométrica da distribuição de metais pesados em compostos de lixo urbano domiciliar. **Revista Química Nova**, v. 22, n. 3, p. 324-328, 1999.

GONÇALVES JÚNIOR, A. C.; NACKE, H.; SCHWANTES, D.; COELHO, G. F. Heavy metal contamination in brazilian agricultural soils due to application of fertilizers. *In*: HERNANDEZ-SORIANO, M. C. (Ed.). **Environmental risk assessment of soil contamination**. Rijeka: Intech Open, 2014. p. 105–135.

GUEDES, H. A. S.; SILVA, D. D.; ELESBON, A. A. A.; RIBEIRO, C. B. M.; MATOS, A. T.; SOARES, J. H. P. Aplicação da análise estatística multivariada no estudo da qualidade da água do Rio Pomba, MG. **Revista Brasileira de Engenharia Agrícola e Ambiental**, v. 16, n. 5, p. 558-563, 2012. http://dx.doi.org/10.1590/S1415-43662012000500012

JACKSON, J. Heavy metals and other inorganic toxic substances. *In*: MATSUI, S. (Ed.). **Guidelines of lake management. v. 4. Toxic substances management in lakes and reservoirs.** Otsu: ILEC/UNEP, 1992. p. 65-80.

JESUS, H. C.; COSTA, E. de A.; MENDONÇA, A. S. F.; ZANDONADE, E. Distribuição de metais pesados em sedimentos do sistema estuarino da Ilha de Vitória-ES. **Revista Química Nova**, v. 27, n. 3, p. 378-386, 2004.

JUIZ DE FORA. **Lei nº 9.811 de 27 de junho de 2000**. Institui o plano diretor de desenvolvimento urbano de Juiz de Fora. 2000. Available at: http://www.jflegis.pjf.mg.gov.br/c_norma.php?chave=0000023630. Access: 07 May 2014.

KUMAR SHARMA, R.; AGRAWAL, M.; MARSHALL, F. Heavy metal contamination of soil and vegetables in suburban areas of Varanasi, India. **Ecotoxicology and Environmental Safety**, v. 66, n. 2, p. 258–266. 2007. https://doi.org/10.1016/j.ecoenv.2005.11.007

LIMA, A. M.; SANTOS, F. F. Análise das propriedades físico-químicas e de metais potencialmente tóxicos na água do rio Claro, próximo a cidade de Jataí – GO. **Revista Ciências Exatas e Naturais**, v. 14, n. 2, p. 239-255, 2012.

LOPES, A. A.; BRIGANTE, J. SCHALCH, V. Influência do aterro sanitário de São Carlos (SP), Brasil, na qualidade das águas superficial e subterrânea. **Journal of Brazilian Society of Ecotoxicology**, v. 2, n. 2, p. 115-127, 2007.

MARINS, R. V.; PAULA FILHO, F. J.; MAIA, S. R. R.; LACERDA, L. D.; MARQUES, W. S. Distribuição de Mercúrio Total como indicador de poluição urbana e industrial na costa brasileira. **Revista Química Nova**, v. 27, n. 5, p. 763-770, 2004. http://dx.doi.org/10.1590/S0100-40422004000500016

MACÊDO, J. A. B. **Águas & águas**. 3. ed. Belo Horizonte: CRQ-MG, 2007. p. 137-288.

MANOJ, K.; KUMAR, B. PADHY, P. K. Characterisation of Metals in Water and Sediments of Subarnarekha River along the Project's Sites in Lower Basin, Índia. **Universal Journal of Environmental Research and Technology**, v. 2, n. 5, p. 402-410, 2012.

MCGRATH, S. P.; LOMBI, W.; GRAY, C. W.; CAILLE, N.; DUNHAM, S. J.; ZHAO, F. J. Field evaluation of Cd and Zn phytoextraction potential by the hyperaccumulators Thlaspi caerulescens and Arabidopsis halleri. **Environmental Pollution**, v. 141, n. 2, p. 115–125, 2006. https://doi.org/10.1016/j.envpol.2005.08.022

NAKAMURA, C. Y.; MARQUES, E.; VILELA, P.; ODA, T.; LIMA, L.; COSTA, R. AZEVEDO, I. C. Avaliação da qualidade da água subterrânea no entorno de um aterro sanitário. **Revista Águas Subterrâneas**, v. 28, n. 2, p. 28-40, 2014. https://doi.org/10.14295/ras.v28i2.27399

NACKE, H.; GONÇALVES JÚNIOR, A. C.; SCHWANTES, D.; NAVA, I. A.; STREY, L.; COELHO, G. F. Availability of heavy metals (Cd, Pb and Cr) in agriculture from commercial fertilizers. **Archives of Environmental Contamination and Toxicology,** v. 64, n. 3, p. 537–544, 2013. https://doi.org/10.1007/s00244-012-9867-z

NRIAGU, J. O.; PACYNA, J. M. Quantitative assessment of worldwide contamination of air, water and soils by trace metals. **Nature**, v. 333, p.134-139, 1988. https://doi.org/10.1038/333134a0

OLIVEIRA, S.; PASQUAL, A. Avaliação de parâmetros indicadores de poluição por efluente líquido de um aterro sanitário. **Revista Engenharia Sanitária e Ambiental**, v. 9, n. 3, p. 240-249, 2004.

RIBEIRO, E. V.; JUNIOR, A. P. M.; HORN, A. H.; TRINDADE, W. M. Metais pesados e qualidade da água do rio São Francisco no segmento entre Três Maria e Pirapora – MG: Índice de Contaminação. **Revista Geonomos**, v. 20, n. 1, p. 49-63, 2012.

ROCHA, C. H. B.; FREITAS, F. A.; SILVA, T. M. Alterações em variáveis limnológicas de manancial de Juiz de Fora devido ao uso da terra. **Revista Brasileira de Engenharia Agrícola e Ambiental**, v. 18, n. 4, p. 431–436, 2014.

ROCHA, C. H. B.; COSTA, H. F. Variação temporal de parâmetros limnológicos em manancial de abastecimento em Juiz de Fora, MG. **Revista Brasileira de Recursos Hídricos**, v. 20, n. 2, p. 543-550, 2015.

ROCHA, C. H. B.; PEREIRA, A. M. Análise multivariada para seleção de parâmetros de monitoramento em manancial de Juiz de Fora, Minas Gerais. **Revista Ambiente & Água**, v. 11, n. 1, p. 176-187, 2016. http://dx.doi.org/10.4136/ambi-agua.1590

SANTANA, G. P.; BARRONCAS, P. de S. R. Estudo de metais pesados (Co, Cu, Fe, Cr, Ni, Mn, Pb e Zn) na Bacia do Tarumã-Açu Manaus – (AM). **Revista Acta Amazônica**, v. 37, n. 1, p. 111-118, 2007.

SILVA, L. S.; GALINDO, I. C. D. L.; NASCIMENTO, C. W. A. D.; GOMES, R. P.; FREITAS, L. D.; OLIVEIRA, I. A. D.; CUNHA, J. M. D. Heavy metals in waters used for human consumption and crop irrigation. **Revista Ambiente & Água**, v. 13, n. 4, 2018. http://dx.doi.org/10.4136/ambi-agua.1999

SILVA, L. S.; GALINDO, I. C. L.; NASCIMENTO C. W. A.; GOMES, R. P.; CAMPOS M. C. C.; FREITAS, L.; OLIVEIRA, I. A. Heavy metal contents in Latosols cultivated with vegetable crops. **Pesquisa Agropecuária Tropical**, v. 46, p. 391-400, 2016. http://dx.doi.org/10.1590/1983-40632016v4641587

VASCO, A. N.; BRITTO, F. B.; PEREIRA, A. P .S.; MÉLLO JÚNIOR, A. V. M.; GARCIA, C. A. B.; NOGUEIRA, L.C. Avaliação espacial e temporal da qualidade de água na sub bacia do rio Poxim, Sergipe, Brasil. **Revista Ambiente & Água**, v. 6, n. 1, p. 118-30, 2011. http://dx.doi.org/10.4136/ambi-agua.178

WHO. **Copper in Drinking-water**: Background document for development of WHO Guidelines for Drinking-water Quality. Geneva, 2004. 23p.

WHO. **Exposure to mercury**: a major public health concern. Geneva, 2007. 4p. (Preventing disease through healthy environments).

WHO. **Exposure to lead**: a major public health concern. Geneva, 2010a. 6p. (Preventing disease through healthy environments).

WHO. **Exposure to cadmium**: a major public health concern. Geneva, 2010b. 4p. (Preventing disease through healthy environments).

WHO. **Exposure to arsenic**: a major public health concern. Geneva, 2010c. 5p. (Preventing disease through healthy environments).

YU, S.; WU, Q.; LI, Q.; GAO, J.; LIN, Q.; MA, J.; XU, Q.; WU, S. Anthropogenic land uses elevate metal levels in stream water in an urbanizing watershed. **Science of the Total Environment**, v. 488-489, n. 1, p. 61–69, 2014. https://doi.org/10.1016/j.scitotenv.2014.04.061

Ambiente & Água - An Interdisciplinary Journal of Applied Science
ISSN 1980-993X – doi:10.4136/1980-993X
www.ambi-agua.net
E-mail: ambi.agua@gmail.com

$CaTiO_3$ Perovskite in the Photocatalysis of Textile Wastewater

ARTICLES doi:10.4136/ambi-agua.2336

Received: 01 Oct. 2018; Accepted: 31 Mar. 2019

Ana Maria Ferrari[1*]; Talitha Oliveira Germiniano[1]; Jaqueline Elisabete Savoia[2]; Rubiane Ganascim Marques[1]; Valquíria Aparecida dos Santos Ribeiro[3]; Ana Cláudia Ueda[1]

[1]Universidade Tecnológica Federal do Paraná (UTFPR), Apucarana, PR, Brasil
Programa de Pós-Graduação em Engenharia Ambiental (PPGEA). E-mail: analima@utfpr.edu.br, talithaxd@hotmail.com, rubiane@utfpr.edu.br, anaueda@utfpr.edu.br
[2]Universidade Tecnológica Federal do Paraná (UTFPR), Apucarana, PR, Brasil
Coordenação de Engenharia Química. E-mail: savoia.jaqueline@gmail.com
[3]Universidade Tecnológica Federal do Paraná (UTFPR), Apucarana, PR, Brasil
Coordenação de Engenharia Têxtil. E-mail: valquiria@utfpr.edu.br
[*]Corresponding author

ABSTRACT

Perovskite-type $CaTiO_3$ material was synthesized by the polymeric precursor method and characterized. The powder was applied as a promising alternative to TiO_2 photocatalyst. Photocatalytic reaction parameters were optimized by surface analysis methodology on the degradation of methylene blue under UV radiation. After optimization, complex textile- and tannery wastewaters were treated and the COD reduction was evaluated. At optimized conditions (pH=11.2 and 1 g L^{-1} of catalyst concentration), the results obtained for the photodegradation of the real wastewater after 240 min of irradiation were 45% COD reduction for both effluents. The reactions were adjusted to the pseudo first order kinetic and the rate constants were 2.07 x 10^{-3} (min^{-1}) and 2.23 x 10^{-3} (min^{-1}) for COD reduction for textile- and tannery wastewaters, respectively.

Keywords: calcium titanate, dye, photocatalyst, real wastewater, response surface analysis.

Perovskitas do tipo $CaTiO_3$ na Fotocatálise de Efluentes Têxteis

RESUMO

O material $CaTiO_3$ do tipo perovskita foi sintetizado pelo método dos precursores poliméricos e caracterizado. Os parâmetros da reação fotocatalítica foram otimizados pela metodologia de análise de superfície de resposta na degradação do azul de metileno sob radiação UV. Após a otimização, as águas residuais têxteis e de curtume foram tratadas e a redução da DQO foi avaliada. Em condições otimizadas (pH = 11,2 e 1 g L^{-1} de concentração de catalisador), os resultados obtidos para a fotodegradação dos efluentes reais após 240 min de irradiação foram de 45% de redução de DQO para os dois efluentes. As reações foram ajustadas para a cinética de pseudo primeira ordem e as constantes de velocidade foram 2,07 x 10^{-3} (min^{-1}) e 2,23 x 10^{-3} (min^{-1}) para redução de DQO para o efluente têxtil e de curtume, respectivamente.

Palavras-chave: efluente de curtume, efluente têxtil, fotocatalisador, fotocatálise, perovskita, titanato de cálcio.

1. INTRODUCTION

It is well known that industries strongly contribute to the contamination of water bodies, particularly the textile and leather industries, since they use a large volume of water in their processes, generating large amounts of effluents. The wastewater from these industries present high organic loads, marked color and resistance to biodegradation, among other aggravating factors (Schimidt *et al.*, 2013). The dyeing of animal skin products as well as mechanical and hydrothermal resistance by the tannery industries is one of the most pollutant processes in terms of the complexity of the effluent generated, which has high organic and inorganic loads, strong color, solids, and specific pollutants such as chromium (Hasegawa *et al.*, 2014; Sauer *et al.*, 2006). Despite the conventional physical-chemical and biological treatments, most of effluents released to aquatic ecosystems present high concentrations of organic matter, toxic metals, color and total solids.

As a result, industrial wastewater has received a great deal of attention regarding its treatment. New methods are suggested, and a variety of research is conducted to offer treatment alternatives that are increasingly efficient, reduce or do not generate waste, and are economically viable. Among the alternative methods, the Advanced Oxidative Processes (AOPs) have stood out as a versatile, rapid and highly efficient pollutant degradation method. Among the AOP approaches, heterogeneous photocatalysis is one of the most promising and high potential methods for wastewater treatment (Ba-Abbad *et al.*, 2017; Lee and Hamid, 2005). The process is based on the irradiation of a semiconductor oxide, with photons whose energy is equal to or greater than the band gap energy of the semiconductor, generating holes in the valence band as electrons are promoted to the conduction band, leading to the formation of active sites capable of promoting redox reactions.

Perovskite-type oxides with ABO_3 structural formula have the orthorhombic structure in their natural form (Hu *et al.*, 1992). Calcium titanate ($CaTiO_3$) is a well-known and one of the most important perovskites and has recently attracted a lot of interest, since it covers a wide range of applications (Lozano-Sánchez *et al.*, 2015; Ye *et al.*, 2014) due to its structural characteristics: high chemical stability, low cost and ease of synthesis (Zhuang *et al.*, 2014).

Several studies have reported the degradation of pollutants using $CaTiO_3$. Huo *et al.* (2014) evaluated the photocatalytic activity of $CaTiO_3$ for the degradation of methyl orange dye and obtained a 96% removal percentage after 3 hours of UV irradiation. Zhuang *et al.* (2014) reported the photo-oxidation of Arsenic (III) to Arsenic (V) using $CaTiO_3$ and achieved excellent photocatalytic activity for As (III) removal (up to 98.4%) in aqueous solution under UV-254 nm irradiation. Otsuka-Yao-Matsuo *et al.* (2003) studied the degradation of methylene blue with the addition of calcium titanate to TiO_2 and observed an increase in photocatalytic activity. Han *et al.* (2016) evaluated the degradation of methylene blue using $CaTiO_3$ synthesized by the hydrothermal method as photocatalyst. Additionally, it has been reported that $CaTiO_3$ can exhibit superior photocatalytic performance on the removal of other organic and inorganic pollutants and formation of hydrogen and oxygen from the photolysis of water (Liu *et al.*, 2014; Mizoguchi *et al.*, 2002).

Real wastewaters are complex and contain a wide range of compounds. An overall mechanism for photodegradation of real textile industrial wastewater is proposed as follows: (I) the semiconductor must be activated by proper radiation source; (II) electron-hole pairs are generated on the surface; (III) oxidizing species such as $OH^{\bullet}$ are formed on the surface; (IV) highly reactive hydroxyl radicals oxidize the dye molecules as follows: Dye + $OH^{\bullet}$ → degradation and (V) the UV irradiation is concomitantly used in a photo sensitization process, in which the sensitizer (the dye) absorbs radiation to yield an excited state of the sensitizer. The dye radicals inject electrons to the conduction band of the catalyst and convert to dye^{-+}. The formed dye^{-+} radical ions react with dye molecules in the same way of the reaction of hydroxyl

radicals, promoting mineralization (Khan *et al.*, 2016; Akpan and Hameed, 2009).

Only a very few papers report the treatment of real effluents, such as textile and tannery wastewater. Highlighting our recent work (Ferrari-Lima *et al.*, 2017), evaluated the photodegradation of methylene blue and the combined treatment of a real textile wastewater by coagulation/flocculation/photocatalysis using the mesoporous perovskites $CaTiO_3$ and $CaTi_xZr_{(1-x)}O_3$ (x = 0. 0.25. 0.50. 0.75 and 1.0) prepared by the polymeric precursor method. The best results were achieved with $CaTiO_3$.

With this background, $CaTiO_3$ synthesized by the polymeric precursor method was applied to the photodegradation of textile and tannery wastewater, and COD reduction was adjusted to the pseudo-first order kinetics. Toxicity evaluation was performed with *Lactuca sativa* seeds. The reaction parameters have also been optimized by means of response surface analysis methodology on the photocatalysis of methylene blue.

2. METHODS

2.1. Catalyst preparation and characterization

$CaTiO_3$ powders were prepared by the polymeric precursor method, according to the previously published methodology (Ferrari-Lima *et al.*, 2017). Calcium acetate [$Ca(C_2H_3O_2)_2$] (97% Aldrich), titanium butoxide ($C_{16}H_{36}O_4Ti$) (97% Aldrich), ethylene glycol ($C_2H_6O_2$) (99.5% Synth) and citric acid ($C_6H_8O_7$) (99.5%. Dinâmica) were used as raw materials. In the experimental procedure, Ti citrate was formed by the dissolution of $C_{16}H_{36}O_4Ti$ in citric acid aqueous solution at 75°C under constant stirring. This citrate solution was then stirred and heated at 90°C, and then $Ca(C_2H_3O_2)_2$ was dissolved in stoichiometric quantity into the Ti citrate solution. After solution homogenization, $C_2H_6O_2$ was added in order to promote the citrate polymerization. The citric acid/ethylene glycol mass ratio was fixed at 60:40 (wt%). The resulting solution was heated at 90°C under constant stirring to eliminate water and form a polymeric resin, which was then placed in a conventional furnace and annealed at 350°C for 4 h. Finally, the obtained precursors were heat treated at 700°C for 2 h. XRD analysis was performed in a Rigaku diffractometer Model MiniFlex 600, with CuKα (λ = 1.5406 Å) in a 2Θ range of 3°–120°, at a nominal power source of 40 kV × 15 mA. Textural analysis was performed by nitrogen adsorption– desorption isotherms at 77 K using Quantachrome NOVA 1200 equipment. Photoacoustic spectroscopy (PAS) analysis was carried out in an self-designed apparatus and scanning electron microscopy analysis was performed on a JEOL JSM-6010 Scanning Electron Microscope equipped with an EDS System. Finally, the zero point of charge (pH_{ZPC}) was determined according to the methodology proposed by Keng and Uehara (1974).

2.2. Photocatalytic degradation studies

The photoactivity of the prepared powder was measured in the photodegradation of methylene blue (MB) 10 mg L^{-1} aqueous solution, a textile and a tannery wastewater collected after conventional biologic treatment system. Photocatalytic tests were performed under ultraviolet (UV) irradiation in a slurry bath reactor. In a typical experiment, the $CaTiO_3$ photocatalyst was suspended in 25 mL of the solution and allowed to stir for 30 min in the dark to attain adsorption equilibrium before irradiation. First, preliminary experiments were carried out in order to outline the Central Composite Design (CCD) for application on the MB photodegradation optimization. After optimization, the best values found for pH and catalyst loading were applied to the photodegradation of two types of real wastewater. All the experiments have been performed in duplicate.

2.3. Response surface methodology

The response surface methodology (RSM) has been successfully applied for the optimization of photocatalytic systems, for example by Soltani *et al.* (2014). In this study, RSM

was used to optimize the two parameters, $CaTiO_3$ loading and initial pH for the degradation of MB. Since the negative influence of the pollutant concentration on the photocatalytic reaction is well known, only $CaTiO_3$ loading and initial pH were selected as independent variables, while the degradation percentage of MB was the output response variable. Other factors, such as stirring rate, temperature and light intensity were held constant. The photocatalytic tests were carried out over a multi-position magnetic stirrer, irradiated with a 60W UV-C lamp array. Table 1 shows the ranges and levels of independent variables.

Table 1. Independent variables and experimental range for degradation of MB under UV-C radiation.

Factor	Symbol	Range				
		-α	-1	0	+1	+α
pH	x_1	2.8	4.0	7.0	10.0	11.2
$CaTiO_3$ loading (mg L^{-1})	x_2	0.3	0.5	1.0	1.5	1.7

Central composite design (CCD) was chosen to investigate the combined effect of the two independent variables by 11 sets of experiments, including three replications at the center points.

By using RSM, the results were matched to an empirical quadratic polynomial as follows (Equation 1) (Montgomery, 2008):

$$Y = \beta_0 + \sum_{j=1}^{k} \beta_j X_j + \sum_{j=1}^{k} \beta_{jj} X_j^2 + \sum_i \sum_{<j=2}^{k} \beta_{ij} X_i X_j + e_i \quad (1)$$

Where Y is the response, X_i and X_j are the variables, β is the regression coefficient, k is the number of factors studied and optimized in the experiment, and e_i is the random error.

2.3.1. Model fitting and statistical analysis

For the graphical analyses, ANOVA (Analysis of variance) has been used in order to define the interaction between the process variables and the responses for statistical parameters assessment. The statistical significance was checked by F-test and the accuracy of the fitted polynomial model was determined by the coefficient of R^2. The significant model terms were evaluated by the probability value (P-value) at 95% confidence interval. A number of statistical analyses such as the normal plot, residual analysis, main and interaction effects and contour plot was examined.

2.4. Textile and tannery wastewater photodegradation

After optimization of MB decomposition, the optimized conditions were applied to the photodegradation of two types of real wastewater: from a textile- and a tannery industry, presenting chemical oxygen demands of 148 mg L^{-1} and 323 mg L^{-1}, respectively.

Therefore, the photocatalytic tests were carried out in a 500 mL self-designed Inox Reactor (Figure 1). The temperature of the reaction was maintained around 25.0 ± 0.5°C by using a cooling jacket. A 125-W mercury lamp without a bulb was used as a UV source and inserted into the reactor chamber protected by a quartz tube. An aquarium air pump was used as an oxygen source. Aliquots were collected periodically and analyzed by chemical oxygen demand (COD).

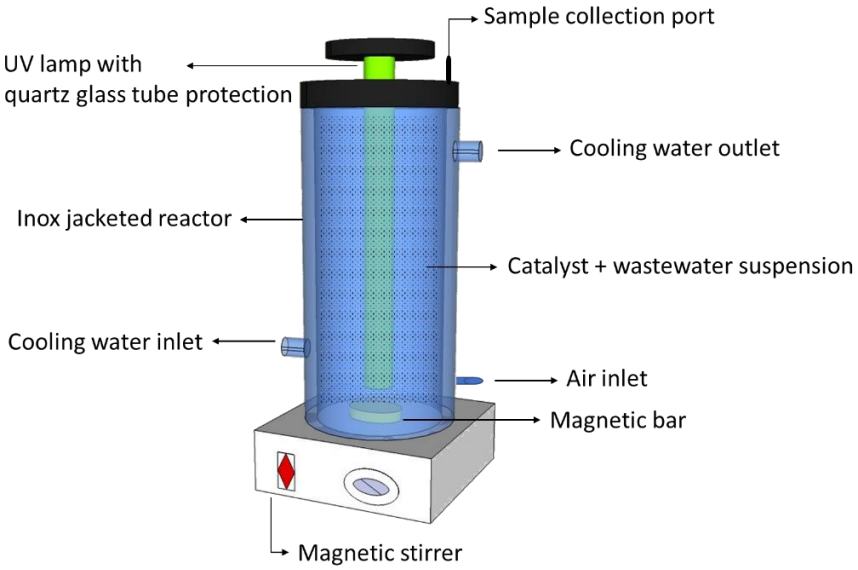

Figure 1. Schematic diagram of the photoreactor.

2.5. Phytotoxicity of real wastewater to *Lactuca sativa* seeds

Sensitive, short-term and simple ecotoxicological bioassays have been performed with *Lactuca sativa* seeds. For the phytotoxicity tests, Petri dishes were lined with a filter paper where the sample unit containing 20 lettuce seeds (*Lactuca sativa*) with 80.0% of germination index was deposited, being moistened with 7.0 mL of distilled water for the negative, NaCl (1 mol L^{-1}) for the positive control and with the samples to be tested (textile- and tannery effluents with and without photocatalytic treatment). The plates were closed and kept at room temperature for 120 h. The assay was conducted in triplicate. The percentage of relative germination (% GR) was calculated by means of Equation 2, in which SSG is the number of seeds germinated in the sample and number CSG represents the number of seeds germinated in the negative control. According to Priac *et al.* (2017), these bioassays are simple, inexpensive and only require a relatively small amount of sample. Lettuce is one of the most-common plant species recommended by the US Environmental Protection Agency and the US Food and Drug Administration for this kind of bioassay (USEPA, 1996; FDA, 1987).

$$\%RG = \frac{n^{o}SSG}{n^{o}CSG} \times 100 \quad (2)$$

3. RESULTS AND DISCUSSION

3.1. Characteristics of $CaTiO_3$

The main characteristics of the photocatalyst are presented in Table 2. The synthesized powder showed mesoporous structure with an average pore diameter of 44.8 Å and orthorhombic phase. Specific surface area and band gap energy are in good agreement with literature (Mohammadi and Fray, 2013; Lozano-Sánchez *et al.*, 2015).

Table 2. Characteristics of $CaTiO_3$.

Parameter	Value
Crystallite size (Å)	269
BET specific surface area (m^2 g^{-1})	34.6
Average pore diameter (Å)	44.8
pH_{ZPC}	10.1
Band-gap energy (eV)	3.44

Figure 1 presents the XRD and UV-Vis absorption spectra of $CaTiO_3$. The orthorhombic phase belonging to the space group Pbnm was identified by ICDD (number 01-081-0562). It can be noted that the catalyst mainly absorbs in the ultraviolet region. As shown in Figure 2, the EDS spectra of $CaTiO_3$ revealed the existence of well-distributed Ti, O and Ca in the sample. However, the material presented a non-uniform morphology. The elemental composition indicates that the presence of impurities besides carbon was not detected and the Ca/Ti ratio is 1.17:1.

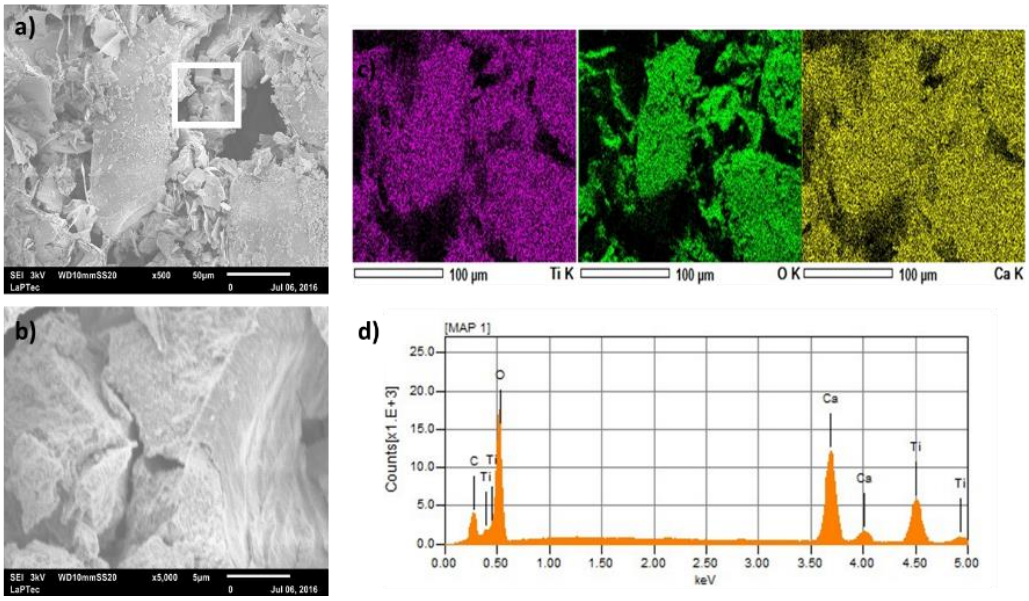

Figure 2. SEM images of $CaTiO_3$ fabricated by the polymeric precursor method: x500 (a), x5000 (b), elemental mapping (c) and (d).

3.2. Photocatalytic bleaching of methylene blue

Aiming to optimize the reaction conditions of MB degradation, a CCD with a total number of 11 experiments was applied for the response surface modelling. The software suggested quadratic model. Interactions among the two independent variables were considered in each run to investigate the validity of the photocatalytic treatment. The removal efficiencies ranged from 22% to 69% for MB. By using RSM, the results were matched to an empirical quadratic polynomial model and were written in terms of coded factors as shown in Equation 3.

$$Y = 23.01 + 34.09x_1^2 + 22.93x_2^2 \quad (3)$$

For MB removal, the quadratic terms x_1^2 and x_2^2 are significant, as the p-value for them is <0.05. From the values of the coefficients in the regression model, the order in which the independent variables affect the degradation of MB is, pH (x_1) > catalyst loading (x_2), and the effect is positive for both.

The correlation coefficient R^2 for the polynomic represented by Equation 3 had a value of 0.83, indicating a good correlation of the experimental data with the proposed model in the range studied. Values above 0.80 are acceptable for surface response modeling (Suárez-Escobar *et al.*, 2016). Additionally, the predicted R^2 (0.83) is close to the adjusted R^2 (0.89), which implies good predictability of the model (Lee and Hamid, 2015).

The optimum values for the independent variables were found using three-dimensional response surface analysis of the independent and dependent variables. The effect of the independent variables on the decolorization of MB is shown on Figure 3.

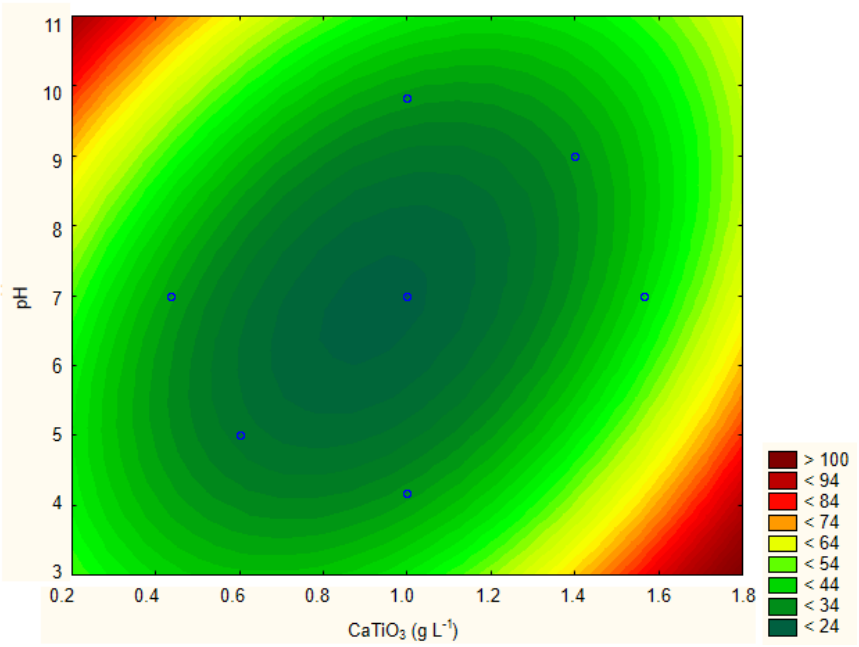

Figure 3. Contour plot of MB removal for the photocatalytic process after 180 min of UV irradiation with $CaTiO_3$.

Figure 3 depicts the influence of the $CaTiO_3$ dosage and pH on the degradation of MB. As illustrated in the plots and by Equation 3, the degradation percentage increases with increasing catalyst loading. The increase in catalyst loading enhances the number of active sites on the catalyst surface, increasing the number of hydroxyl radicals responsible for the degradation MB molecules. Degradation is also increased by increasing pH. This may be because of the higher color intensity of MB in the acidic pH range. Additionally, the pH_{ZPC} of $CaTiO_3$ is around 10, and at pH smaller than pH_{ZPC}, the surface of the catalyst is positively charged; hence, at low pH the dye forms multilayers on the catalyst particles, preventing the UV light from reaching their surface (Yang *et al.*, 2014).

3.3. Kinetic study of textile and tannery wastewater photodegradation

After 180 min of irradiation, a maximum removal for MB of 69% with a catalyst loading of 1.0 g L^{-1} and pH of 11.2 was obtained. In order to investigate the behavior of these conditions in a real situation, the kinetic study was performed for the real textile and tannery wastewater. The results are shown in Figure 4.

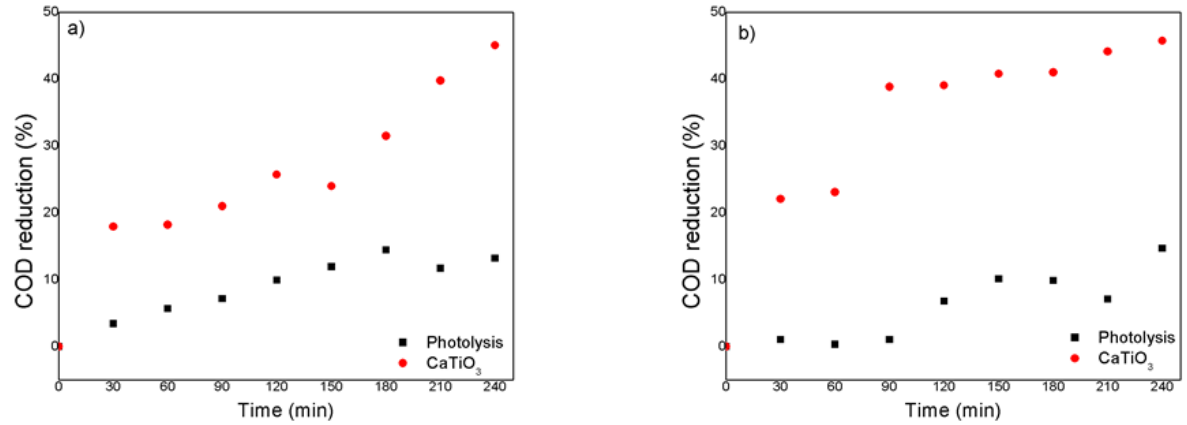

Figure 4. Kinetic behavior of the COD removal for (a) textile and (b) tannery wastewater after photocatalysis with $CaTiO_3$. Catalyst loading=1.0 g L^{-1}, pH=11.2.

A photolysis study was carried out and after a reaction time of 240 minutes about 10% of the wastewater was degraded. After that, the textile and the tannery effluents were treated by photocatalysis with $CaTiO_3$ during the same time interval. Since $CaTiO_3$ synthesized in this work has shown to be better than TiO_2 P25 in our previous study (Ferrari-Lima *et al.*, 2017), no comparison was made with this standard catalyst.

Kinetic data for COD removal were adjusted to the pseudo-first order model, obtaining an apparent kinetic constant "k" of 2.07×10^{-3} min^{-1} ($R^2 = 0.9084$) for the textile wastewater, and an apparent kinetic constant of 2.23×10^{-3} min^{-1} ($R^2 = 0.8199$) for the tannery wastewater. A maximum removal of 45% and 46% of COD was achieved for textile and tannery wastewater, respectively, after 240 min of irradiation. Yang *et al.* (2014) reported a pseudo-first order kinetic constant of 3.1×10^{-3} min^{-1} for the degradation of MB with pure $CaTiO_3$ under UV-visible light, and Han *et al.* (2016) reported a pseudo-first order kinetic constant of 1.80×10^{-3} min^{-1} for the degradation of methylene blue with the same catalyst with a Xe lamp. In our previous work (Ferrari-Lima *et al.*, 2017), a kinetic constant of 7.3×10^{-3} min^{-1} was found for the photodegradation of a coagulation/flocculation pre-treated textile wastewater with $CaTiO_3$ under UV-light at the same reactor discussed in this section. Other reports regarding the treatment of a real wastewater by photocatalysis with $CaTiO_3$ are rare.

3.4. Phytotoxicity assessment

One drawback of treating wastewater by advanced oxidation processes is the possible generation of toxic by-products. In this sense, a toxicity evaluation of the wastewater before and after treatment is mandatory. In this work, a simple phytotoxicity test was performed with the textile- and tannery wastewaters. The toxicity comparison between the effluents before and after the photocatalytic treatment was evaluated according to the percentage of germination (% RG), calculated according to Equation 2. Figure 5 shows the results.

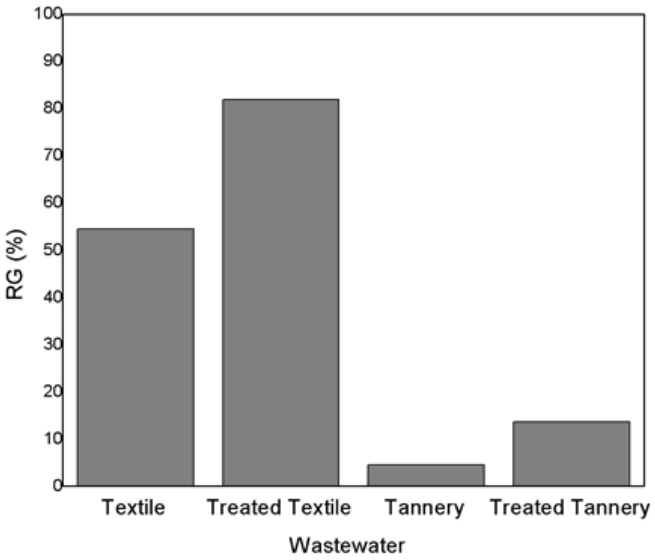

Figure 5. Percentage of relative germination of textile- and tannery wastewater before and after photocatalysis with $CaTiO_3$.

Textile wastewater, polished by photocatalysis (240 min of irradiation), showed an increase of about 27% (from 55% to 82%) in the relative germination index when compared to the wastewater without treatment. Garcia *et al.* (2009) reached 75% of germination after photocatalysis of textile wastewater with TiO_2 P25 with the same irradiation time. The treated tannery wastewater also showed an increase in RG index (9%) compared to the wastewater

conventionally treated by the industry. Considering that values of ICCR below 80% indicate a root-growth inhibition effect (Young *et al.*, 2012), the germination difference between the studied effluents is remarkable. In the tannery wastewater, the germination index was much lower than that observed for the textile wastewater even after the photocatalytic treatment. This may be due to the possible high concentration of toxic pollutants such as chromium VI, which is often used in tannery industries. High concentrations of organic matter could also explain its toxicity, as well as other concentrated components, such as salts (Elabbas *et al.*, 2016).

Hasegawa *et al.* (2014) treated tannery wastewater by photocatalysis, applying ZnO, and reached over 97% of COD while decreasing toxicity to *Artemia salina* nauplii after 240 min. However, no reference relating to a *Lactuca sativa* germination index analysis of photocatalysis-treated tannery wastewater has been found as of this writing.

4. CONCLUSION

Perovskite-type $CaTiO_3$, with mesoporous structure were synthesized and the photocatalytic degradation of methylene blue were optimized by means of response surface methodology. Degradation of 69% was achieved after 180 min of irradiation. Optimized conditions have been applied to the photodegradation of textile- and tannery wastewater after conventional treatment, and an apparent kinetic constant of about 0.002 min^{-1} was obtained for both effluents. After photocatalysis, a reduction of about 45% of COD was achieved for both textile- and tannery wastewater, and the phytotoxicity of the effluents to *Lactuca sativa* seeds was reduced.

5. ACKNOWLEDGMENTS

The authors would like to thank the Brazilian agency CNPq (459057/2014-6) for financial support.

6. REFERENCES

AKPAN, U. G.; HAMEED, B. H. Parameters affecting the photocatalytic degradation of dyes using TiO_2 based photocatalysts: A review. **Journal of Hazardous Materials**, v. 170, p. 520-529, 2009.

BA-ABBAD, M. M.; TAKRIFF, M. S.; SAID, M. *et al.* **International Journal of Environmental Research**, v. 11, p. 461, 2017. https://dx.doi.org/10.1007/s41742-017-0041-3

ELABBAS, S.; MANDI, L.; BERREKHIS, F.; PONS, M. N.; LECLERC, J. P.; OUAZZANI, N. Removal of Cr (III) from chrome tanning wastewater by adsorption using two natural carbonaceous materials: Eggshell and powdered marble. **Journal of Environmental Management**, v. 166, p. 589-595, 2016.

FERRARI-LIMA, A. M.; UEDA A. C.; BERGAMO E. A.; MARQUES R. G. *et al.* Perovskite-type titanate zirconate as photocatalyst for textile wastewater treatment. **Environmental Science and Pollution Research,** v.24, p.12529–12537, 2017. https://doi.org/10.1007/S11356-016-7590-4

GARCIA, J.C.; SIMIONATO, J.I.; ALMEIDA, V.D.C.; PALÁCIO, S.M.; ROSSI, F.L.; SCHNEIDER, M.V.; SOUZA, N.E.D. Evolutive follow-up of the photocatalytic degradation of real textile effluents in TiO_2 and TiO_2/H_2O_2 systems and their toxic effects on *Lactuca sativa* seedlings. **Journal of the Brazilian Chemical Society**, v. 20, p.1589–1597, 2009.

HAN, C.; LIU, J.; YANG, W.; WU, Q.; YANG, H.; XUE X. Enhancement of photocatalytic activity of $CaTiO_3$ through HNO_3 acidification. **Journal of Photochemistry and Photobiology A: Chemistry**, v.322-323, p.1-9, 2016. https://doi.org/10.1016/J.Jphotochem.2016.02.012

HASEGAWA, M. C.; DANIEL, J. F. S.; TAKASHIMA K.; BATISTA, G. A.; SILVA, S. M. C. P. COD removal and toxicity decrease from tannery wastewater by zinc oxide-assisted photocatalysis: a case study. **Environmental Technology**, v.35, p.1-6, 2014.

HU, M.; WENK, H-R.; SINITSYNA D. Microstructures in natural perovskites. **American Mineralogist**, v.77, p.359-373, 1992.

HUO, Y. S.; YANG, H.; XIAN, T.; JIANG, J. L.; WEI, J. Q.; LI, R. S.; FENG, W. J. A polyacrylamide gel route to different-size $CaTiO_3$ nanoparticles and their photocatalytic activity for dye degradation. **Journal of Sol-Gel Science and Technology**, v. 71, p. 254-259, 2014.

KENG, J. C. W.; UEHARA, G. **Proceedings, Soil Crop Science Society of Florida**, v. 33, p. 119-126, 1974.

KHAN, W. Z.; NAJEEB, I; ISHTIAQUE, S. Photocatalytic Degradation of a Real Textile Wastewater using Titanium Dioxide, Zinc Oxide and Hydrogen Peroxide. **The International Journal Of Engineering And Science**, v. 5, n. 7, p. 61-70, 2016.

LEE, K. M.; HAMID, S. B. A. Simple Response Surface Methodology: Investigation on Advance Photocatalytic Oxidation of 4-Chlorophenoxyacetic Acid Using UV-Active ZnO Photocatalyst. **Materials**, v. 8, p. 339-354, 2015. https://dx.doi.org/10.3390/ma8010339

LIU, S.; QU, Y.; LI, R.; WANG, G.; LI, Y. Photocatalytic activity of $MTiO_3$ (M = Ca, Ni, and Zn) nanocrystals for water decomposition to hydrogen. **Journal of Materials Research**, v. 29, p. 1295-1301, 2014. https://dx.doi.org/10.1557/jmr.2014.110

LOZANO-SÁNCHEZ, L. M.; OBREGÓN, S.; DÍAZ-TORRES, L. A.; LEE, S.W.; RODRÍGUEZ-GONZÁLEZ, V. Visible and near-infrared light-driven photocatalytic activity of erbium-doped CaTiO3 system. **Journal of Molecular Catalysis A: Chemical**, v. 410, p. 19-25, 2015. https://doi.org/10.1016/j.molcata.2015.09.005

MIZOGUCHI, H.; UEDA, K.; ORITA, M.; MOON, S. C.; KAJIHARA, K.; HIRANO, M.; HOSONO, H. Decomposition of water by a $CaTiO_3$ photocatalyst under UV light irradiation. **Materials Research Bulletin**, v. 37, p. 2401-2406, 2002. https://doi.org/10.1016/S0025-5408(02)00974-1

MOHAMMADI, M. R.; FRAY, D. J. Synthesis of highly pure nanocrystalline and mesoporous $CaTiO_3$ by a particulate sol-gel route at the low temperature. **Journal of Sol-Gel Science and Technology**, v. 68, p. 324–333, 2013. https://dx.doi.org/10.1007/s10971-013-3173-8

MONTGOMERY, D.C. **Design and Analysis of Experiments**. New York: John Wiley & Sons, 2008.

OTSUKA-YAO-MATSUO, S.; OMATA, T.; UENO, S.; KITA, M. Photobleaching of Methylene Blue Aqueous Solution Sensitized by Composite Powders of Titanium Oxide with $SrTiO_3$, $BaTiO_3$ and $CaTiO_3$. **Materials Transactions**, v.44, p.2124-2129, 2003. https://doi.org/10.2320/matertrans.44.2124

PRIAC, A.; BADOT, P-M.; CRINI, G. Treated wastewater phytotoxicity assessment using Lactuca sativa: Focus on germination and root elongation test parameters. **Comptes Rendus Biologies**, v. 340, n. 3, p. 188-194, 2017. https://doi.org/10.1016/j.crvi.2017.01.002

SAUER, T. P.; CASARIL, L.; OBERZINER, A. L. B.; JOSÉ, H. J.; MOREIRA, F. P. M. Advanced oxidation processes applied to tannery wastewater containing Direct Black 38—Elimination and degradation kinetics. **Journal of Hazardous Materials**, v. 135, p. 274–279, 2006. https://doi.org/10.1016/j.jhazmat.2005.11.063

SCHIMIDT, T. M. P.; SOARES, F.R.; SLUSARSKI-SANTANA, V.; BRITES-NÓBREGA, F. F.; FERNANDES-MACHADO, N. R.C. Photocatalytic degradation of textile effluent using ZnO/NaX and ZnO/AC under solar radiation. **Green Design, Materials and Manufacturing Processes**, p. 563-566, 2013. http://dx.doi.org/10.1201/b15002-109

SOLTANI, R. D. C.; REZAEE, A.; KHATAEE, A. R.; SAFARI, M. Photocatalytic process by immobilized carbon black/ZnO nanocomposite for dye removal from aqueous medium: Optimization by response surface methodology. **Journal of Industrial and Engineering Chemistry**, v. 20, v. 4, p. 1861-1868, 2014. https://doi.org/10.1016/j.jiec.2013.09.003

SUÁREZ-ESCOBAR, A.; PATAQUIVA-MATEUS, A.; LÓPEZ-VASQUEZ, A. Electrocoagulation—photocatalytic process for the treatment oflithographic wastewater. Optimization using response surfacemethodology (RSM) and kinetic study. **Catalysis Today**, v. 266, p. 120–125, 2016. https://doi.org/10.1016/j.cattod.2015.09.016

UNITED STATES. Environmental Protect Agency - USEPA. **Ecological effects test guidelines (OPPTS 850.4200)**: Seed germination, root elongation toxicity test. Washington DC, 1996.

UNITED STATES. Food & Drug Administration - F.D.A. **Seed germination and root elongation, Environmental Assessment Technical Assistance.** Washington DC, 1987.

YANG, H.; HAN, C.; XUE, X. Photocatalytic activity of Fe-doped $CaTiO_3$ under UV-visible light. **Journal of Environmental Science**, v. 26, p. 1489-1495, 2014. https://doi.org/10.1016/j.jes.2014.05.015

YE, M.; WANG, M.; ZHENG, D.; ZHANG, N.; LIN, C.; LIN, Z. Garden-like perovskite superstructures with enhanced photocatalytic activity. **Nanoscale**, v. 6, p. 3576-3584, 2014. https://dx.doi.org/10.1039/C3NR05564G

YOUNG, B. J.; RIERA, N. I.; BEILY, M. E.; BRES P. A.; CRESPO, D. C.; RONCO, A. E. Toxicity of the effluent from anaerobic bioreactor treating cereal residues on *Lactuca sativa*. **Ecotoxicology and Environmental Safety**, v. 76, p. 182-186, 2012. https://doi.org/10.1016/j.ecoenv.2011.09.019

ZHUANG, J.; TIAN, Q.; LIN, S.; YANG, W.; CHEN, L.; LIU, P. Precursor morphology-controlled formation of perovskites $CaTiO_3$ and their photo-activity for As (III) removal. **Applied Catalysis B: Environmental**, v. 156, p. 108-115, 2014. https://doi.org/10.1016/j.apcatb.2014.02.015

Ambiente & Água - An Interdisciplinary Journal of Applied Science
ISSN 1980-993X – doi:10.4136/1980-993X
www.ambi-agua.net
E-mail: ambi.agua@gmail.com

Modeling and hydraulic performance evaluation of a dripper device coupled to a branched water distribution network

ARTICLES doi:10.4136/ambi-agua.2340

Received: 03 Oct. 2018; Accepted: 24 Mar. 2019

Renato Braga Zanca[1]; Fernando das Graças Braga da Silva[1*]; Daniele Ornaghi Sant`Anna[1]; Alex Takeo Yasumura Lima Silva[1]; Hélcio Francisco Villa Nova[2]; Ivan Felipe dos Santos[1]; José Antônio Tosta dos Reis[3]

[1]Universidade Federal de Itajubá (UNIFEI), Itajubá, MG, Brasil
Instituto de Recursos Naturais (IRN). E-mail: renatozanca1@yahoo.com.br, ffbraga.silva@gmail.com, ornaghi@unifei.edu.br, alex.takeo@uol.com.br, ivanfelipedeice@hotmail.com
[2]Universidade Federal de Itajubá (UNIFEI), Itajubá, MG, Brasil
Instituto de Engenharia Mecânica (IEM). E-mail: helcio.villanova@unifei.edu.br
[3]Universidade Federal do Espírito Santo (UFES), Vitória, ES, Brasil
Departamento de Engenharia Ambiental. E-mail: jatreis@gmail.com
[*]Corresponding author

ABSTRACT

Irrigation is responsible for approximately 70% of the world's freshwater consumption and is one of the key factors behind the growing global water scarcity. Irrigation systems and techniques are extremely differentiated and complex. In this context, tools of computational fluid dynamics (CFD) earn relevance, allowing a detailed analysis and forecast of hydraulic behavior in different situations. In order to evaluate flow details in a dripper, this study applies CFD tools to study a drip irrigation system from three different perspectives: (i) analysis of the complete system of piping and dripper; (ii) analysis of only the isolated dripper expanded and biphasic model; and (iii) analysis of the isolated dripper operating in transient regime. Modeling results allowed a full understanding about speed fields, pressure and friction loss along the geometry. The drop formation process in the dripper output could be displayed in detail, and the obtained dripper flow output was close to the nominal value of manufacturer, in the case of the isolated dripper analysis. Although a comparison with results from experiments was not possible at the time, based on manufacturers' catalogs, results proved satisfactory, leading to successful simulations.

Keywords: computational fluid dynamics (CFD), dripper, irrigation.

Modelagem e avaliação de desempenho hidráulico de dispositivo gotejador acoplado a rede de distribuição de água ramificada

RESUMO

A irrigação é responsável por aproximadamente 70% do consumo de água doce do mundo e é um dos principais fatores por trás da crescente escassez de água global. As técnicas e sistemas de irrigação são extremamente diferenciadas e complexas. Neste contexto, as

ferramentas de dinâmica de fluidos computacional (CFD) ganham relevância, permitindo uma análise detalhada e previsão do comportamento hidráulico em diferentes situações. Com o objetivo de avaliar os detalhes do escoamento no gotejador, o presente estudo se aplica a ferramentas de CFD para um sistema de irrigação por gotejamento sob três perspectivas diferentes: (i) analisando o sistema completo composto de tubulações e gotejador; (ii) analisar apenas o gotejador isolado expandido e modelo bifásico; e (iii) com o gotejador isolado operando em regime transiente. Os resultados da modelagem e simulação mais tarde permitiu uma visão completa dos campos de velocidade e pressão e fricção perda ao longo da geometria. O processo de formação de gotas na saída do gotejador pode ser exibido com detalhes e a saída do fluxo de gotejador obtido foi próximo ao valor nominal do fabricante, no caso de análises do gotejador isolado. Embora não tenha sido possível no momento uma comparação com resultados provenientes de experimentos, com base em catálogos de fabricantes, as qualidades dos resultados foram bons e modelagem bem sucedida.

Palavras-chave: dinâmica de fluidos computacional (CFD), gotejador, irrigação.

1. INTRODUCTION

As previously noted, irrigation systems and techniques are extremely differentiated and complex. Among these techniques is micro-irrigation or localized irrigation (Tang *et al.*, 2017), which involves the application of water droplets slowly to the soil layers, the drip or micro-sprinkler technique.

Lamm *et al.* (2007) defines water system application, which consists of transmitters connected to a water supply from a low-pressure line. Li *et al.* (2018) notes that micro-irrigation not only increases the system's efficiency, but can also increase crop productivity. There are indications that drip systems, such as subsurface drip, may perform better, which may eventually expand the irrigation system's economic feasibility (Jacques *et al.*, 2018), and enable its use along with deficit irrigation. (Al-Ghobari and Dewidar, 2018).

Quingsong *et al.* (2008) explains that, in localized irrigation systems, there are several types of drippers. Multiple geometric shapes can be used, but usually the device has very small dimensions and water flow passes through micro-holes as a satellite maze, making the pressure drop. The discharge rate is usually 1 to 8 l/h and is linked to the small width and flow path depth, which is about 0.5 to 1.5 mm in height (Patil *et al.*, 2013). For low discharge rates and high uniformity in irrigated areas, many emitters adopt the hydraulic system of the path through the maze with a very low section of flow (usually less than 1 mm²).

Dripper installation can happen in two ways: (i) Drippers are attached to the polyethylene tube after drilling, which eases positioning of the transmitters under the plant tops; and (ii) Drippers are placed in polyethylene tubes, which permits formation of a wet range in the application area (Gomes, 1994). In drip systems, the liquid (usually water) is released by emitters with a very low power, so that the water flows very slowly into the soil (Palau-Salvador *et al.*, 2004). According to Gomes (1994), the hydraulic behavior of drippers is characterized in a general way, using Equation 1.

$$q = C_d \cdot h^x \quad (1)$$

Where: q = dripper flow; Cd = proportionality coefficient, which depends on the dripper, cross section size and shape; h = dripper service pressure; and x = discharge exponent dripper, which is a water flow function of emitter. The lower the "x" exponent value, the less will be the flow variation before the pressure variation at the dripper inlet. If water flow through the dripper is made in the laminar regime, x is equal to 1 and the dripper flow varies linearly with

pressure. For drippers which operate in turbulent regimes, x is approaching 0.5, meaning that the issuer flow is less sensitive to a pressure variation (q varies with the square root of h) (Gomes, 1994).

Drippers are little sensitive to low pressure variation (x), temperature variation and wear over time. These drippers are obviously more expensive, which may impact the total cost of irrigation system installation (Zanca, 2013).

There are several experimental scientific studies on drippers, especially in the agronomy field; however, mathematical modeling of drippers is infrequent.

For a better understanding and optimization of hydraulic components for irrigation systems, some authors (Tang *et al.*, 2017; Bravo-Mosquera *et al.*, 2018) have applied computational fluid dynamics tools (CFD), which allow detailed analysis of the fluid flow behavior to integrate the knowledge, fluid, mathematics and computing to solve flow equations, given by physical conservation laws and mathematical descriptions, such as the conservation of mass, Newton's second law and the first law of thermodynamics (Tu *et al.*, 2013). Computational simulation technologies are an effective way of studying a fluid behavior, since they allow results to be analyzed punctually, permitting correlation and improvement projects, even before the construction of prototypes.

Dripper characteristics of the water must be fully understood so that they can be developed with low rates of clogging in the issuers. Obtaining a complete view of field, speed, pressure and other parameters involved with drippers then becomes extremely important for designers of drippers (Wu *et al.*, 2013). In these terms, several authors (such as Wei *et al.*, 2006; Li *et al.*, 2008; Celik *et al.*, 2015; among others) have researched dripper flows by means of CFD tools.

Wei *et al.* (2006) evaluated drippers flow of different geometries using computational hydrodynamics simulation software, obtaining ratios between hydraulic quantities in dripper canals, such as discharge, pressure and flow coefficients. Li *et al.* (2008) tried to optimize the geometry of a dripper maze, suggesting improvements to the flow along the dripper, demonstrating a greater capacity for self-cleaning.

The authors also compared the results obtained through CFD with a speedometer for bi-dimensional digital tracking of particles, achieving results very close in both approaches. Wu *et al.* (2013) studied the dripper flows, comparing different turbulence models k-ε and the large-simulation and LES methods, and were able to explain the energy dissipation mechanism by speed and average pressure values of local regions for the entire course of its elimination.

In an analysis with a different focus, Celik *et al.* (2015) studied the loss of load in the piping of a drip irrigation system using 5 different CFD techniques, because they are not normally provided by the manufacturers of transmitters and are projected by estimated means and mathematical models (Gomes *et al.*, 2010), demonstrating that the CFD techniques can be used not only for dripper optimization, but also to assist in system sizing, corroborating authors such as Baiamonte (2018) which studied design optimization for each side of the drip system.

In these terms, this work proposes a mathematical modeling of this hydraulic problem (less studied in this focus) and evaluates flow through drippers from three perspectives: (i) analysis of the complete system consisting of piping and dripper; ii) analysis of only the isolated dripper and with expanded output; and (iii) analysis of the dripper operating in transient regime. The second and third perspectives aim to better visualize the formation mechanism of drops; specific papers with this approach were not found in literature.

2. MATERIAL AND METHODS

This study divides CFD tool application into 4 steps: i) specification of the problem and its geometry; ii) discretization meshes and numerical method; iii) selection of boundary conditions and (iv) evaluation of results and interpretation (Lomax *et al.*, 1999; Tu *et al.*, 2013).

The study approaches the removal of computational simulation in a dripper from three perspectives: the analysis of dripper piping system, analysis of the isolated dripper with expanded output and biphasic model, and an analysis of a similar case to the previous one, considering the transitional regime.

Dripper geometry specifications were obtained from a commercially manufactured model available in the Brazilian market, reproducing all of its geometric characteristics. The dripper has a maze format and the inserted piping has a diameter of 14 mm. Built geometry has replicated the maze format and its different surfaces (inputs, outputs and walls) were defined. The mesh was created in accordance with the principle that regions that have more pronounced speed changes should be more thoroughly studied, to provide greater accuracy in baseflow changes, since in these regions the behavior of pressure ranges, speed profiles, among others should be studied.

The following contour conditions were introduced: flow rate of 0.306 l/s along the piping and the outlet dripper pressure equal to atmospheric pressure (0). The turbulence model was the k-ε (approved by Wei *et al.*, 2006) and simulations were performed in permanent regime, since any condition of flow at the dripper output was introduced aiming to compare the result with manufacturer's model, which provided a nominal flow of 4 l/h. The residue was used to ensure that the convergence that could be reached was 10-4 (as Aguirre *et al.*, 2019) and the number of iterations required for convergence of dripper piping system was equal to 100.

There is a very large-scale difference, showing that the dripper water outlet is affected. Thus, for better visualization purposes, in the following work we performed the second perspective simulation, with the same boundary-value conditions of the first event. This new simulation was performed with the dripper operating alone, excluding the piping. In addition, we expanded the dripper output drop-formation process to obtain better visualization (Figure 1). Thus, boundary conditions were applied directly to the exit of the dripper itself.

Biphasic modeling of dripper was performed with isolated simulations, aiming to improve the visualization of the drop-formation mechanism. We modeled the dripper output as an opening to allow contact between water and air, with a surface tension coefficient between fluids of 0.0722N/m (default value for air and water to 25°C). We defined 400 as a maximum number of iterations for this scenario.

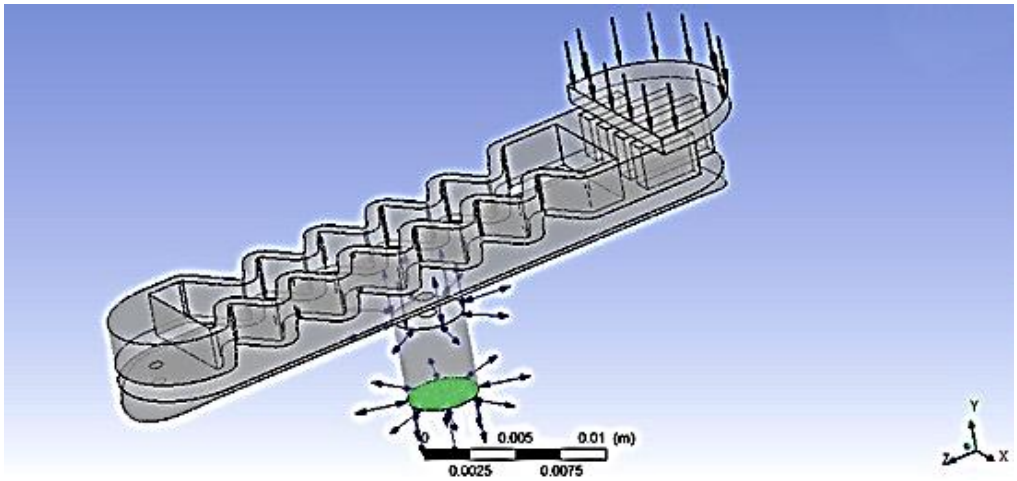

Figure 1. Analysis of geometry is defined for the scenario of insulated dripper with expanded output.

The third and last case was comparable to the second scenario, but in a transient regime, maintaining all other conditions. The total duration period adopted was 200 seconds, with increments of 1 second and 10 iterations for each second. In this scenario, the path along the

dripper and the drops formation process could be visualized in an even more complete way than in other situations.

2.1. Generation of meshes

The mesh generated in the present study was simulation of non-structured mesh and hybrids with respect to the elements' types. Generated elements among the total number of geometry elements were 4,375,853.

3. RESULTS

3.1. Results of simulation of the dripper piping system

3.1.1. Speed of fields analysis

Figure 2 illustrates the current lines along Plane 1, as if the dripper were an obstacle. Current lines were imperceptible within the dripper, although some still indicate that there is water entering the dripper. A small increase in speed of flow along the piping can still be noticed. This is accomplished by reducing the flow area, by the fact that an "obstacle" has been introduced in the center of the tubing.

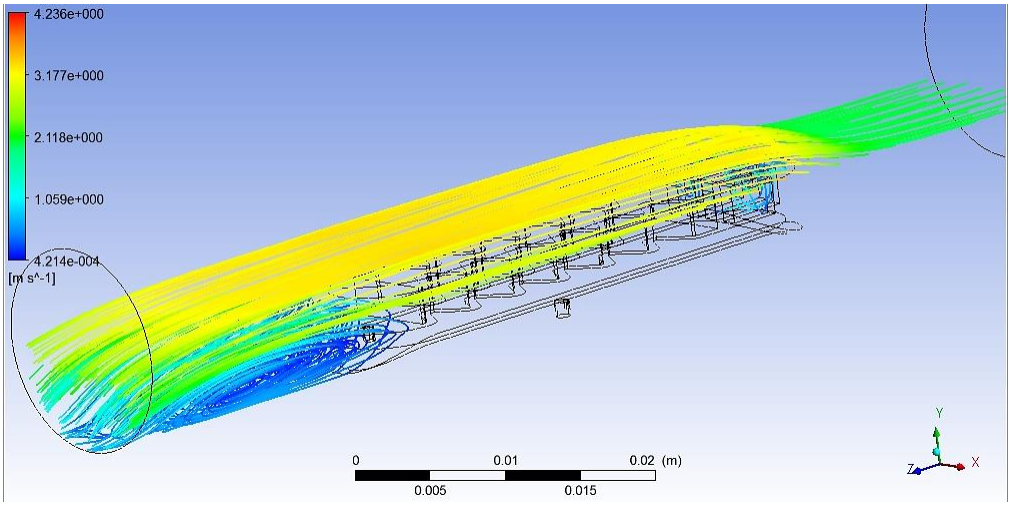

Figure 2. Current lines of the speed gradient on Plane 1.

Similarly, as the current lines of speed on Plane 1, the vectors of speed on the same plane are only inserted at the entrance of the dripper (Figure 3). In addition to the formation of vortices in the entrance of the dripper, they were also observed in speed vectors representing the mentioned shoulder (yellow).

In the YZ plane 2 (direction), the same procedures were entered for viewing the flow (observed in Figure 4).

The Figure 5 shows the speed-vector results.

Figure 6 shows the speed vectors with emphasis on the dripper, visualizing two openings. The left represents the waterflow from the hydraulic path and pours into a reservoir (lower drippers), with higher speed values. The right represents the output vector DRIPPER to the ground. There is high turbulence and vortice formation at the flow dripper's lower reservoir (left side), which can be detrimental to the equipment, damaging it. Average speed in the dripper output is 2 m/s. As the output diameter is 1 mm, it is possible to apply the continuity equation ($Q = V \cdot A$ in this region, obtaining a flow rate of 5.6 L/h close value standard deviation of 40% of nominal when compared to industrial dripper, 4 L/h - see section 2), showing the simulation's effectiveness in the dripper region, enabling expansion. In subsequent topics, we present a more detailed analysis and the need for dripper elimination.

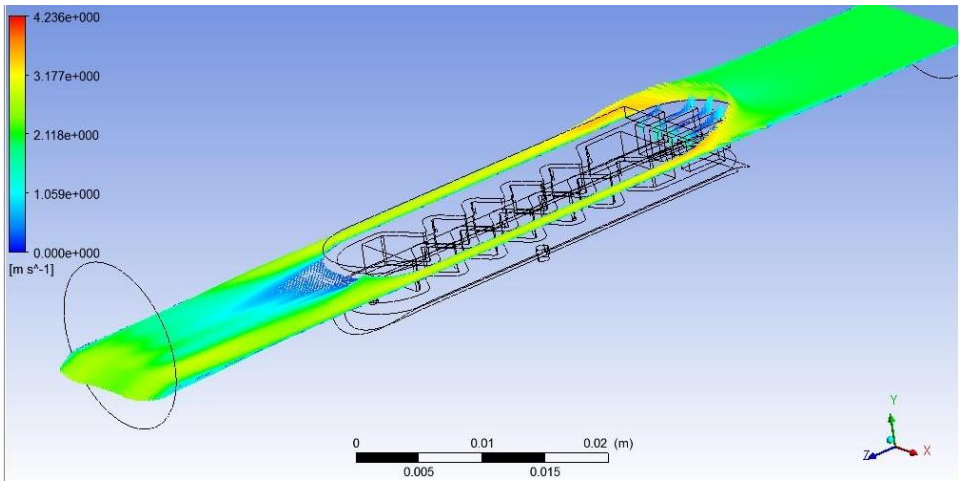

Figure 3. Speed vectors along Plane 1.

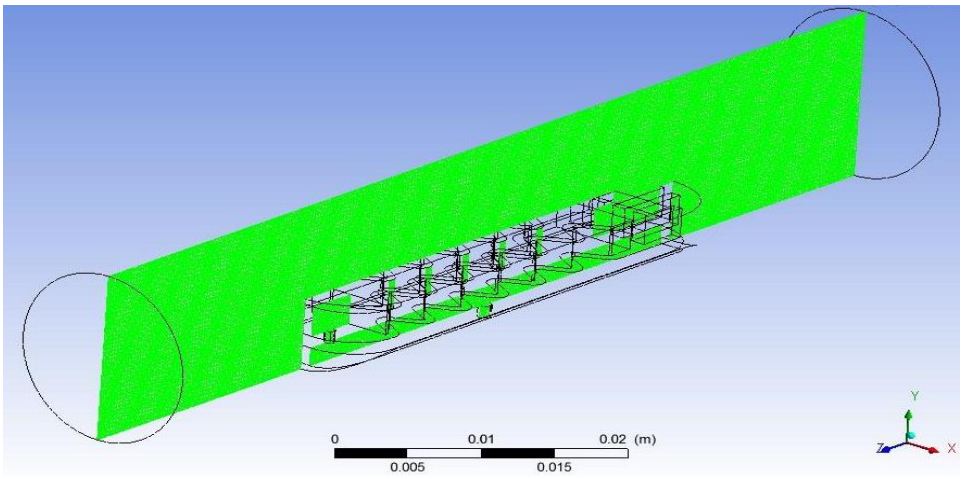

Figure 4. Speed vectors along the Plan 1.

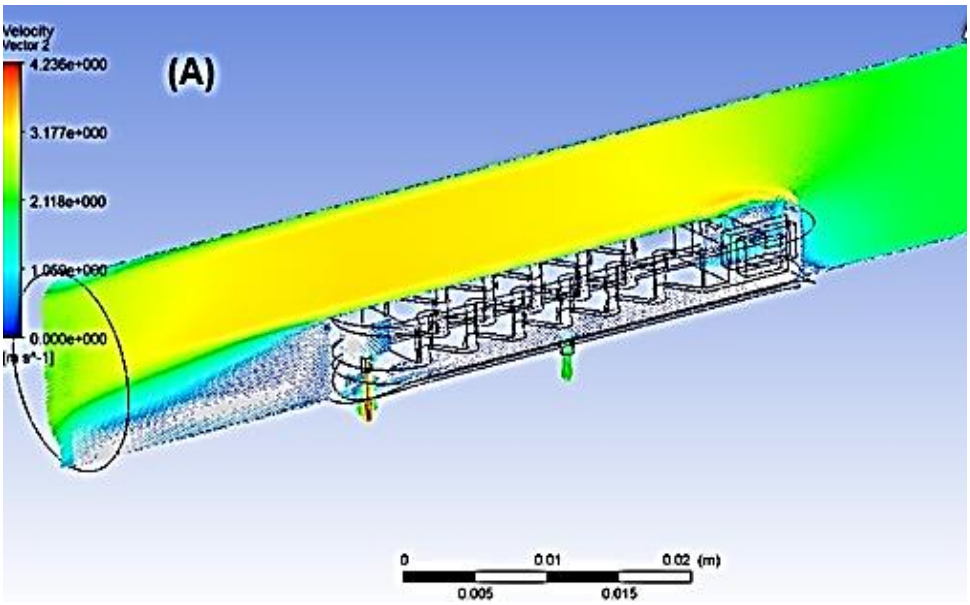

Figure 5. Dripper piping system transverse plane -. (A) analysis of speed; (b) analysis of pressure.

Figure 6 shows the fields of dripper pipe at system pressure and a transverse plane. there is a slight increase in the flow speed along the piping.

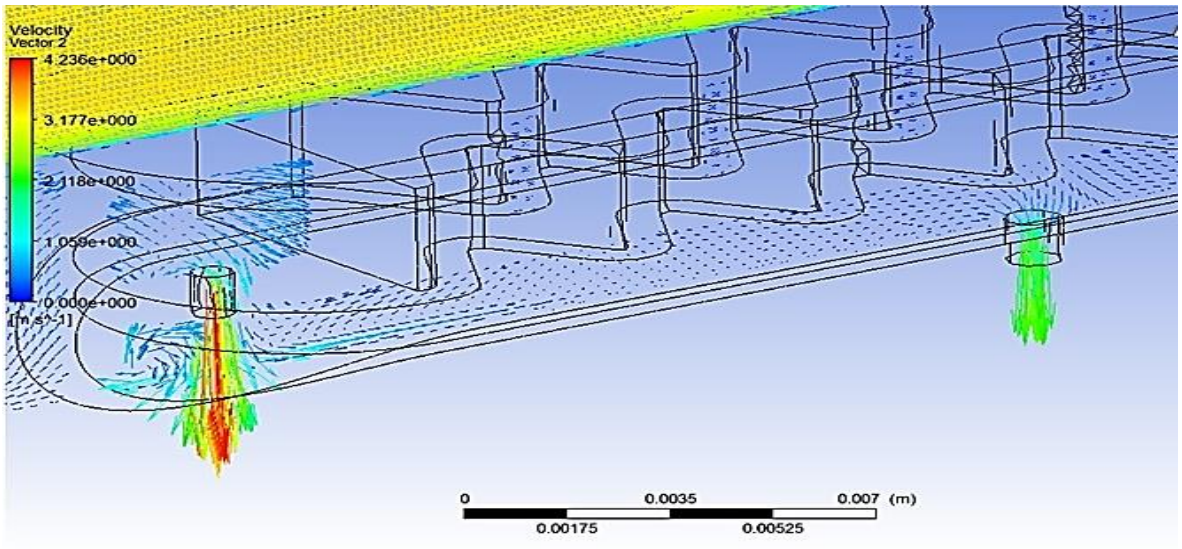

Figure 6. Speed vectors. Zoom of Dripper.

3.1.2. Analysis of pressure fields

The variation of the dripper's external pressure is very low (Figure 7). A pressure of approximately $2x10^4$Pa at the entrance of the dripper should be noticed. When the fluid reaches the region of the dripper, this Figure 7 drops to approximately $1.6x10^4$Pa. This small variation of pressure noticed in contour region follows the speed variation. The speed increased as the pressure declined, confirmed by the Bernoulli equation for horizontal tubes. In this regard, the pressure increased by a value of $1.6x10^4$Pa at the dripper entrance.

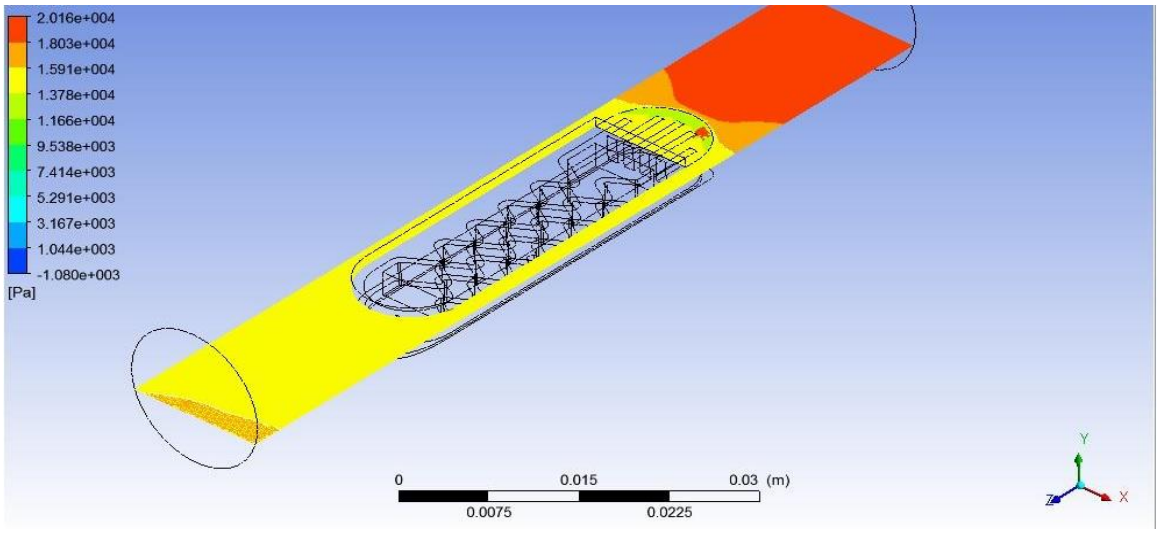

Figure 7. Current lines of the pressure gradient - Plane 1.

The pressure values presented within the dripper are very low (shown in Figure 8). This is caused because the loss of load caused by the hydraulic path is very high. The entry of the dripper (yellow) demonstrated the value of $1.6x10^4$Pa, and already in the lower part of the dripper (blue) a decrease of pressure is clearly noticed. The value in light blue is approximately 4kPa.

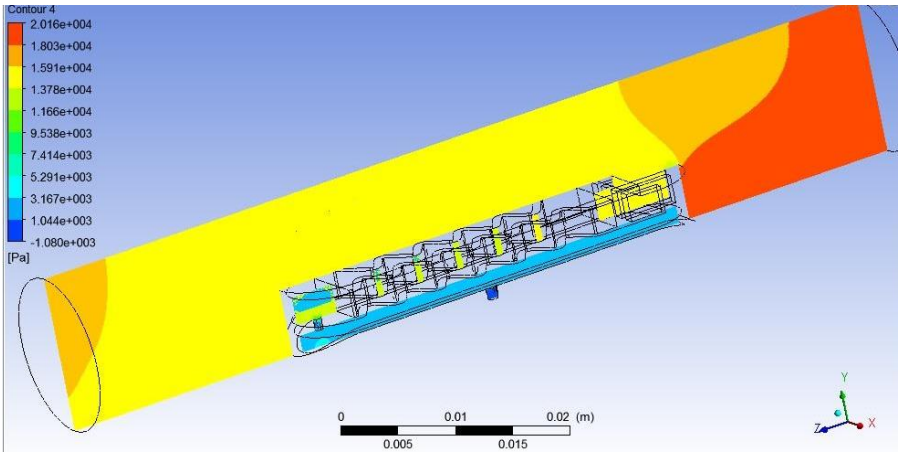

Figure 8. Current lines of the pressure gradient - Plane 2.

3.1.3. Results of isolated dripper simulation with biphasic model

In this case, we analyzed the dripper separately, with a biphasic model applied to the dripper with enlarged output to permit a more detailed view of the drop formation mechanism. Figure 9 shows the speed fields (9a) air and water volumetric fractions (9b) at the dripper output.

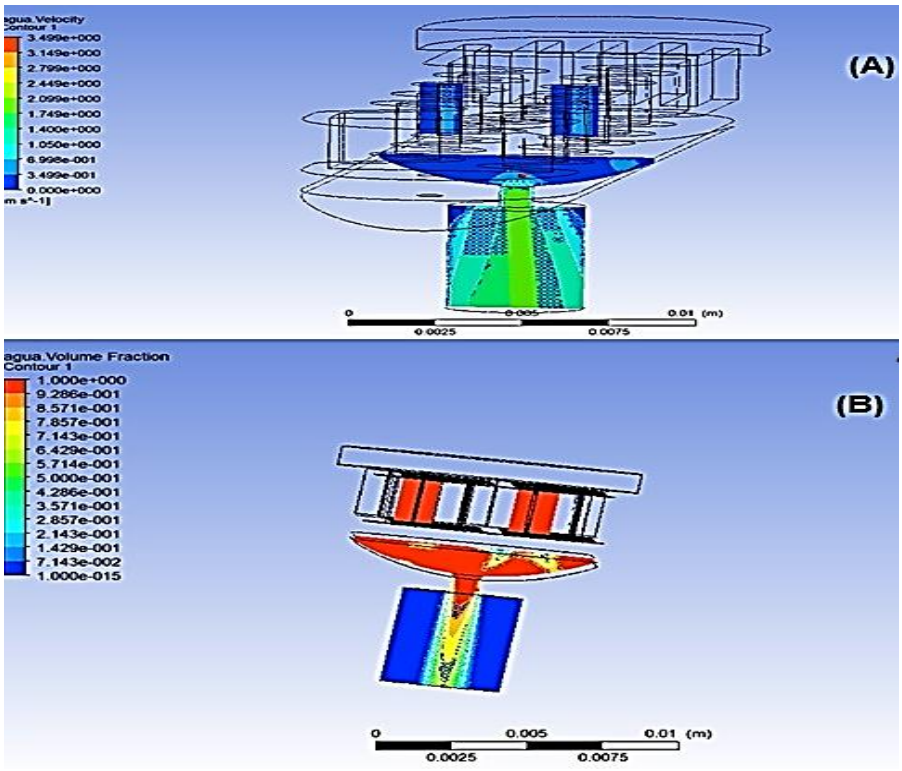

Figure 9. Insulated dripper with expanded output computational modeling. (A) speed fields; (b) air and water volumetric fractions.

As in the previous case, we can estimate that in the dripper output section velocity (Figure 9a - around 1.7 m/s) and the flow transmitter equal 4.8 L/h, which represents a deviation of 20% from the manufacturer's nominal value (4 L/h), and indicates a good estimation, since it is a small structure and difficult to simulate computationally.

In Figure 9b, the model of drop formation process by volumetric fractions of air and water, where it seems that the concentration of water is more intense in the center of the dripper output pipe (region of higher speed in Figure 4), which indicates a fall is ocurring. There is still air in

the lower part of the dripper body, which can avoid the drop-formation process and indicates a limitation of the geometry of the analyzed issuer.

3.1.4. Simulation results of the isolated dripper with biphasic model and transitional provisions

The simulation in transient regime was applied to show the drop-formation dynamics over time. Figure 10 illustrates the temporal evolution of the volumetric fraction of water in the dripper (taken from an animation) and allows the visualization of the drop formation process on the emitter from the beginning of drop formation until the complete dissipation of its heat. In the upper part of the drop formation, the intrusion of air in the dripper is observed, while the water flows from the lower part of the reservoir to the main output. At the dripper output, we observed bulb formation in different volumetric water fractions, indicating the non-uniformity of water volume along the fall. In the last frames of Figure 10, we detected very small water volumes, indicating the end of a water portion in the dripper, after the drop formation. At the end of the developed process, the dark blue color indicates a value of about 0%, caused by fall that reaches the soil.

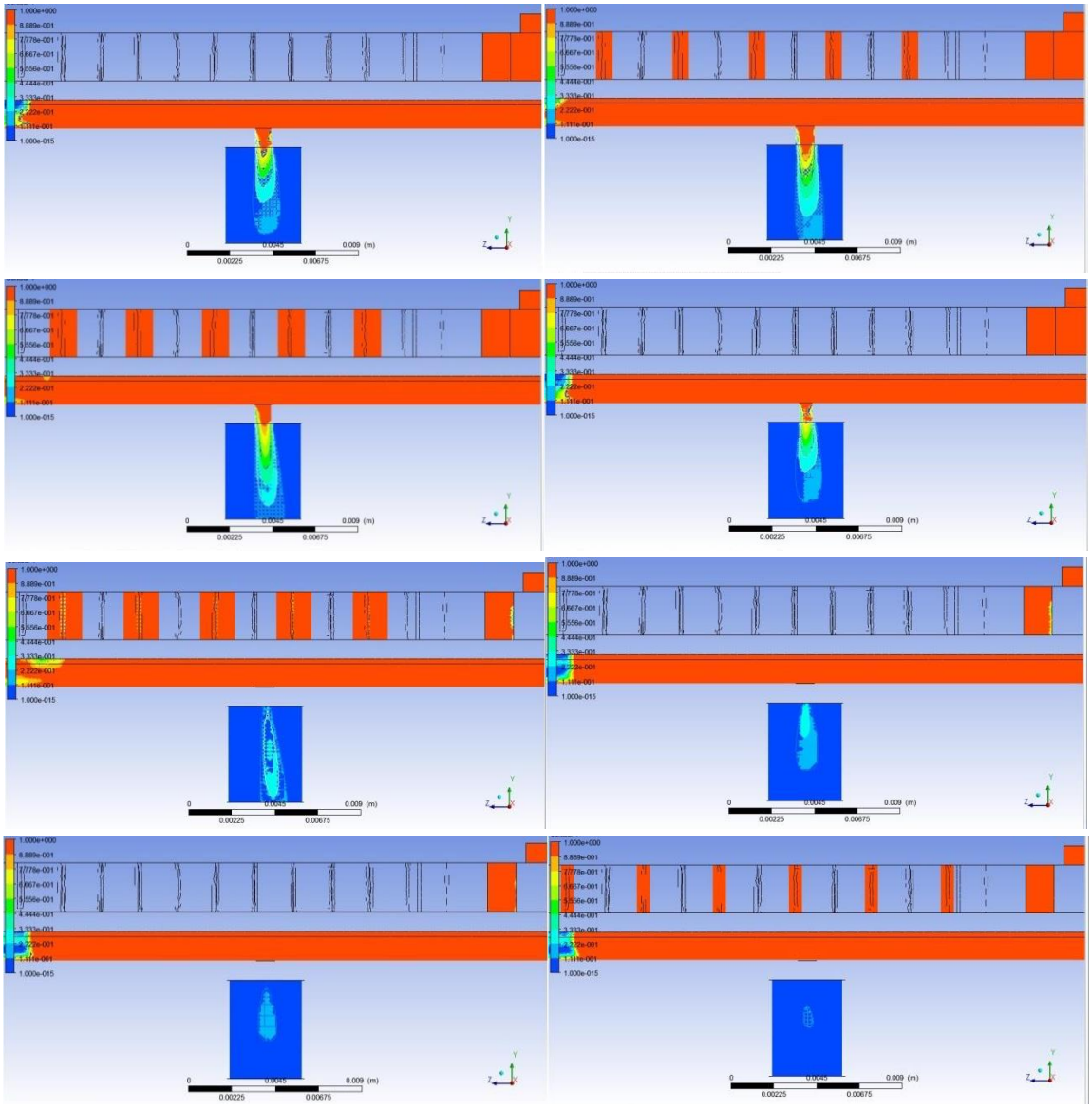

Figure 10. Temporal evolution of the volumetric fraction of water during the process of drop formation and emission.

4. CONCLUSIONS

Results permitted a full detailed view of the dripper types inline. Field studies of flow-pressure simulation along the tube dripper system enabled the load loss calculation imposed by the flow in dripper tube (close to 4 kPa). This demonstrates that the complete system of simulations, as achieved in this study, may be used to help in optimizing these structures' geometry, minimizing energy losses.

Additional simulations, focused on the dripper isolated with biphasic model and, later, with a transient regime, allowed a more detailed view within the dripper and verification of drop-formation mechanism concomitantly. The behavior of the output dripper (dripper isolated at flow output) was very close when compared to results of manufacturer. Deviations presented were 20%, considered a satisfactory value, since it is a difficult study in computational geometry.

In the simulation of transient regime, we checked the drop formation process from details until its complete heat dissipation in the dripper output. Strong air intrusion appeared, especially at the beginning of drop formation, which may indicate a geometric limitation. The drop formation mechanism would be perceived more clearly if new surface-value adaptations of water tension were adopted and/or if the number of steps for the simulation results analysis were increased. Such analyses are suggestions for future work.

Similar analyses performed in this study could be compared with laboratory analyses to optimize the dripper results, assisting a more efficient design, requiring less material and/or providing a greater speed in the drop formation mechanism, which makes the computational fluid dynamics techniques of great relevance to achieve greater efficiency in irrigation projects.

In addition, some perturbation was introduced to evaluate the sensitivity of responses; however, these studies can be presented as the continuity of work.

5. ACKNOWLEDGMENTS

The authors thank finep Redecope Project - MCT (Ref. 0983/10) - Ministry of Science and Technology entitled "Development of efficient technologies for hydro management efficiency in water supply systems" program and the researcher Miner Fapemig for the PPM - 00755-16 besides thanking NUMMARH- Nucleos modeling in simulation in Environment and Water Resources and systems of unified. Thanks to CAPES for the master's scholarship of the author 4. "Thanks CAPES, for the master's scolarship number 1764063 to the author Alex Takeo Yasumura Lima Silva".

6. REFERENCES

AL-GHOBARI, H. M.; DEWIDAR, A. Z. Integrating the deficit irrigation in surface and subsurface drip, as a strategy to save water in arid regions. **Agricultural Water Management**, v. 209, p. 55-61, 2018. https://doi.org/10.1016/j.agwat.2018.07.010

AGUIRRE, A. C.; CAMACHO, A.; OLIVEIRA, W.; AVELLAN, F. Numerical Analysis to detect loss of head on trifurcations of high head in hydropower. **Renewables**, v. 131, p. 197-207, 2019. https://doi.org/10.1016/j.renene.2018.07.021

BAIAMONTE, G. Advances in designing drip irrigation laterals. **Agricultural Water Management**, v. 199, p. 157-174, 2018. https://doi.org/10.1016/j.agwat.2017.12.015

BRAVO-MOSQUERA, P. D.; CERÓN-MUÑOZ, H. D.; DÍAZ-VÁZQUEZ, G.; CATALANO, F. M. Conceptual design and CFD analysis of the new prototype of agricultural aircraft. **Aerospace Science and Technology**, v. 80, p. 156-176, 2018. https://doi.org/10.1016/j.ast.2018.07.014

CELIK, H. K.; KARAYEL, D.; LUPEANU, M. E. *et al.* Determination of head loss in parts of drip irrigation system with emitters of cylindrical type online through the CFD analysis. **Bulgarian Journal of Agricultural Science**, v. 21, p. 703-710, 2015.

GOMES, A. W. A.; FRIZZONE, J. A.; RETTORE NETO, O.; MIRANDA, J. H. Local head losses for integrated drippers in polyethylene pipes. **Agricultural Engineering**, v. 30, n. 3, p. 435-446, 2010. http://dx.doi.org/10.1590/S0100-69162010000300008

GOMES, H. P. **Engineering of irrigation**. Recife: UFPE, 1994.

JACQUES, D.; FOX, G.; WHITE, P. Farm level economic analysis of subsurface drip irrigation in Ontario corn production. **Agricultural Water Management**, v. 203, p. 333-343, 2018. https://dx.doilorg/10.1016/j.agwat.2018.03.018

LAMM, F. R.; AYARS, J. E.; NAKAYAMA, F. S. (Eds.). **Microirrigation for crop production**: design, operation and management. Oxford: Elsevier, 2007.

LI, Y.; YANG, P.; XU, T.; REN, S.; LIN, X.; WEI, R.; XU, H. CFD and digital particle tracking to assess flow characteristics in the labyrinth flow path of a drip irrigation emitter. **Irrigation Science,** v. 26, p. 427-438, 2008. https://doi.org/10.1007/s00271-008-0108-1

LI, J.; XU, X.; LIN, G. *et al.* Micro-irrigation improves grain yield and resource use efficiency by co-locating the roots and N-fertilizer distribution of winter wheat in the North China Plain. **Science of the total environment**, v. 643, p. 367-377, 2018. https://doi.org/10.1016/j.scitotenv.2018.06.157

LOMAX, H.; PULLIAM T. H.; ZINGG, D. W. **Fundamentals of computional fluid dynamics**. Dynamics Computing, University of Toronto: Institute for Studies of Aerospaces. Nasa Ames Research, 1999, 334p. https://dx.doi.org/10.1007/978-3-662-04654-8

PALAU-SALVADOR, G.; ARVIZA-VALVERDE, J.; BRALTS, V. F. **Hydraulic flow behaviour through an in-line Emitter Labyrinth using CFD techniques**. St. Joseph: ASABE, 2004. https://dx.doi.org/10.13031/2013.16437

PATIL, S. S.; NIMBALKAR, P. T.; JOSHI, A. Hydraulic study, design and analysis of different geometries of drip irrigation emitter labyrinth. **International Journal of Engineering and Technology IJEAT**, v. 2, p. 455-462, 2013.

QUINGSONG, W.; GANG, L.; JIE, L. *et al.* Evaluations of emitter clogging in drip irrigation by two-phase flow simulations and laboratory experiments. **Computers and Electronics in Agriculture**, v. 63, p. 294-303, 2008. https://doi.org/10.1016/j.compag.2008.03.008

TANG, P.; LI, H.; ISSAKA, Z.; CHEN, C. Impact forces on the drive spoon of a large cannon irrigation sprinkler: Simple theory, CFD numerical simulation and validatio. **Biosystem Engineering**, v. 159, p.1-9, 2017. https://doi.org/10.1016/j.biosystemseng.2017.04.005

TU, J.; YEOH, G. H. LIU, C. **Computational Fluid Dynamics**: a practical approach. 2nd ed. New York: Elsevier, 2013. 439 p.

WEI, Q.; SHI, Y.; DONG, W.; LU, G.; HUANG, S. Study on the hydraulic performance drip emitters of computational fluid dynamics. **Agricultural Water Management**, v. 84, v. 1-2, p. 130-136, 2006. https://doi.org/10.1016/j.agwat.2006.01.016

WU, D.; LI, Y-K.; LIU, H-S. *et al.* Simulation of the flow characteristics of a drip irrigation emitter with large eddy methods. **Mathematical and computational modeling**, v. 58, p. 497-506, 2013. https://doi.org/10.1016/j.mcm.2011.10.074

ZANCA, R. B. **Modelagem e simulação computacional de um sistema de irrigação por gotejamento**. 2012. Trabalho de Conclusão de curso (Graduação em Engenharia Hídrica) - Universidade Federal de Itajubá, Itajubá, 2013.

Ambiente & Água - An Interdisciplinary Journal of Applied Science
ISSN 1980-993X – doi:10.4136/1980-993X
www.ambi-agua.net
E-mail: ambi.agua@gmail.com

Physicochemical, microbiological and parasitological characterization of the filter backwash water from a water treatment plant of Blumenau - SC and alternatives for treatment and reuse

ARTICLES doi:10.4136/ambi-agua.2372

Received: 05 Feb. 2019; Accepted: 12 Apr. 2019

Alinne Petris[1*]; Marcel Jefferson Gonçalves[2]; Paula Angélica Roratto[3]; Juliane Araujo Greinert Goulart[1,3]

[1]Universidade Regional de Blumenau (FURB), Blumenau, SC, Brasil
Programa de Pós-Graduação em Engenharia Ambiental (PPGEA).
E-mail: professoraalinne@gmail.com, julianeag@gmail.com
[2]Universidade Regional de Blumenau (FURB), Blumenau, SC, Brasil
Departamento de Engenharia Química (DEQ).
E-mail: marceljgoncalves@hotmail.com
[3]Universidade Regional de Blumenau (FURB), Blumenau, SC, Brasil
Centro de Ciências Exatas e Naturais (CCEN).
E-mail: p.angelica21@gmail.com, julianeag@gmail.com
[*]Corresponding author

ABSTRACT

Filter Backwash Water (FBW) from water treatment plants (WTP) is composed of raw water waste, chemicals and microorganisms. Inappropriate disposal of this residue impacts negatively in the environment and in the health of human populations. Aiming to characterize the FBW from one WTP of Blumenau-SC, physiochemical, microbiological and parasitological assessments and tests with different flocculants polymers were performed in order to propose strategies for treatment and reuse of this residue. Subsequently treated liquid is discharged into the Itajaí-Açu River (Class 2). Physicochemical and microbiological analyses showed results higher than those permitted by CONAMA Resolution n° 430/2011 and *Giardia duodenalis* (Assembly B) cysts and *Cryptosporidium* spp. oocyst positivity was observed, characterizing as polluted and contaminated residue that shouldn't be released in the hydric body. The anionic flocculant polymer showed satisfactory results in the turbidity sample reduction (99.49%), which may be a promising alternative in the treatment of this residue.

Keywords: *Cryptosporidium* spp., *Giardia* spp., wastes from WTP.

Caracterização físico-química, microbiológica e parasitológica da água de retrolavagem dos filtros de uma estação de tratamento de água de Blumenau – SC e alternativas para tratamento e reuso

RESUMO

A água de retrolavagem dos filtros (ARF) de estações de tratamento de água (ETA) é composta por resíduos da água bruta, produtos químicos e microrganismos. Seu descarte inadequado impacta negativamente o meio ambiente e a saúde da população humana. Objetivando caracterizar a ARF da ETA de Blumenau-SC, foram realizadas avaliações físico-

químicas, microbiológicas e parasitológicas e testes com diferentes polímeros floculantes, afim de propor estratégias para tratamento e reuso deste resíduo para posteriormente, o líquido tratado, ser lançado no Rio Itajaí-Açu (Classe 2). Grande parte das análises físico-químicas e microbiológicas apresentaram resultados superiores aos determinados pela Resolução CONAMA n° 430/2011, além de positividade para cistos de *Giardia duodenalis* (Assembleia B) e oocistos de *Cryptosporidium* spp., caracterizando um resíduo poluído e contaminado que não deve ser lançado in natura no corpo hídrico. O polímero floculante aniônico apresentou resultados satisfatórios na redução da turbidez da amostra (99,49%), podendo ser uma alternativa promissora no tratamento deste resíduo.

Palavras-chave: *Cryptosporidium* spp., *Giardia* spp., resíduo de ETA.

1. INTRODUCTION

Water treatment Plants (WTP) are important for the human population, because from raw water, usually unsuitable for consumption, they produce drinking water, indispensable to the survival of any living being (Achon *et al.*, 2008). Traditionally, the WTP has a complete system, consisting of steps of raw gathering water, coagulation, flocculation, decanting, filtration and disinfection. During these steps, the majority of the WTP produce a large volume of residues, generated by sedimentation of the particles in the decanters and by the filter backwash water (FBW). These residues are called sludge (Richter, 2009).

Commonly, much of the sludge generated in the water treatment plants around the world was discharged directly into hydrous bodies causing serious environmental impacts. However, the interest in new technologies for the treatment of water and waste generated is aimed at studies that promote the reuse or recycling of these effluents, such as discarding them to exclusive or sanitary landfills, discarding them in sewage systems, applying them to soil, recovering of degraded areas and even incorporation of materials from civil engineering. This reduces to just 11% the number of water treatment plants that discharge their waste into water bodies in the United States (Cornwell *et al.*, 2000), 2% in the United Kingdom (Simpson *et al.*, 2002) and absence of disposal of these residues in water bodies in France (Adler *et al.*, 2002) and Germany (Gramel, 2002).

In Brazil, 2,098 towns produce sludge in the water treatment process and present various provisions such as landfill, incineration or reuse; however, a large part discharge untreated effluent directly into water bodies (IBGE, 2010), impacting negatively the environment because of their high concentrations of WTP and solids that form sediment and isolate the benthic layer, promoting imbalance in the aquatic environment and preventing the development of biota, in addition to causing risks to the health of the human population by presenting concentrated pathogenic microorganisms (Cordeiro and Campos, 1998).

In this scenario, alternatives are sought to minimize the negative impacts caused by inadequate disposal of these residues with various strategies. Among them the recirculation of filter backwash water at the beginning of the system (Menezes *et al.*, 2005; Braga *et al.*, 2007; Freitas *et al.*, 2010; Molina and Santos, 2010; Oliveira *et al.*, 2013; Silva-Junior *et al.*, 2014; Lustosa *et al.*, 2017) and the use of sludge generated in decanters as a component of materials for civil construction (Hoppen *et al.*, 2005; 2006) are those that have been gaining greater emphasis by providing savings in natural resources and recycling of these residues.

The system and operating particularities of each WTP must be considered before making decisions to mitigate the problem, such as the characterization of raw water, the sludge of decanters, the filter backwash water and the chemical products used in the processes. In addition, the difficulty in managing the WTP, the ancient architecture present in many of them, the area of occupation, financial conditions and lack of specialized human resources also

hamper the solutions for the proper disposal of these wastes (Di Bernardo *et al.*, 2012; Richter, 2009; Januário and Ferreira-Filho, 2007).

Blumenau has four water treatment plants; among them is WTP II, which has been in operation since 1970 and supplies about 70% of the population. It's formed by two wings (North and South) composing a complete treatment system. It uses coagulant Polychloride Aluminum (PCA) and polymers as flocculation auxiliators when necessary. The filters are the fast descending type and, at the end, gaseous chlorine, fluosilicic acid and calcium hydroxide are added for disinfection, fluoridation and pH correction, respectively, before the water is distributed to the population (Samae, 2016).

As in the vast majority of Brazil's WTPs, WTP II generates residues during daily filtering using treated water from the cistern. An average of 130 m³ of water is spent in the washing of each filter, generating a monthly volume of 39,000 m³ of treated water. The wastewater is discharged directly into the Itajaí-Açu River (Class 2 according to CONAMA Resolution n° 357/2005) (Samae, 2016).

The filter backwash water is a residue described as a polluter and contaminate due to the fact that its composition presents the chemical substances used in the previous stages of water treatment, dirt from raw water and various structures infected by microorganisms, among them cysts of *Giardia* spp. and oocyst of *Cryptosporidium* spp., (Oliveira *et al.*, 2013; Braga *et al.*, 2007; Freitas *et al.*, 2010) that are pathogenic protozoa with recent records of outbreaks and worldwide epidemic caused by water transmission (Baldursson and Karanis, 2011; Efstratiou *et al.*, 2017).

Based on the above considerations, this study characterized the filter backwash water regarding the physicochemical, microbiological and parasitological aspects of the water treatment station of Blumenau – WTP II, identifying alternatives for treatment and reuse to suggest improvements in this process contributing to the quality of life of the population and preservation of this natural resource.

2. MATERIALS AND METHODS

The samples of the filter backwash water were collected monthly in the two wings (North and South), from November 2016 to October 2017. All the sample collections were carried out during the night near to midnight, due to the lower use of water by the population, when the water treatment at the station is interrupted to reverse the water from the cistern for cleaning of the filters (Figure 1).

Figure 1. Image of one of the filters during the backwash process.
Source: Samae (2016).

It was chosen to work with composite samples collected at the beginning, middle and end of the washing of the filters, according to the diminished visible turbidity of the water.

The samples were collected with the aid of a collector made available by the town's autonomous water and sewage service (SAMAE) and stored in different vials, according to the requirement of each of the analyses subsequently performed. For the physicochemical characterization tests, the samples were stored in 3 L plastic containers, previously cleaned and for determination of chlorine, in glass containers with a grinding lid with a capacity of 250 mL. For microbiological analyses, 100 mL sterile bottles of were used and for the parasitological analysis, glass bottles with a capacity of 1 L previously washed with elution solution tween 80-0.01%.

The procedures for collection, preservation, preparation and physicochemical analyses of the samples followed the Standard Methods for the Examination of Water and Wastewater (Apha, 2012).

The physicochemical parameters analyzed were turbidity, pH, true color, total residual chlorine, nitrite, nitrate, phosphorus (P), chemical oxygen demand (COD), iron (Fe), manganese (Mn), copper (Cu), zinc (Zn), dissolved aluminum (Al), total solids, fixed and volatile, sedimentary solids, fixed and volatile total suspended solids and total dissolved solids.

Microbiological analyses were performed using Quanti-Tray® Cartelas and Colilert® reagent in the determination and quantification by most probable number (MPN) of total coliforms and *Escherichia coli*. In this method, the presence of total coliforms is verified when the wells have yellow coloration and for confirmation of *E. coli*, the color chart is subjected to ultraviolet light of 365 nm, and the wells with fluorescence indicate the presence of the bacterium. The result is obtained by combining the quantity of large and small positive wells in most probable number by 100 mL (100 mL^{-1}) determined by a table available along with the Quanti-Tray® Carscreen Kit.

In the parasitological analyses, the calcium carbonate flocculation technique described was used by Vesey *et al.* (1993) and Greinert *et al.* (2004). The technique of detection and quantification applied was direct immunofluorescence according to the instructions of the manufacturer of the diagnostic kit (Merifluor ®-Meridian Bioscience, Cincinnati, Ohio) employing monoclonal antibodies marked with fluorescent substances. It's currently the most widely used method for detecting and quantifying *Giardia* spp. cysts and *Cryptosporidium* spp. oocysts in high turbidity environmental samples. The microorganisms of interest were observed and quantified under the Epifluorescence microscope (Olympus-CH30) with excitation filter from 450 to 490 nm and a barrier filter of 520 nm, followed by morphological confirmation by phase contrast.

The positive samples for the parasites were subjected to molecular genotyping. The environmental DNA was extracted using the DNeasy® Blood and Tissue kit (Qiagen INC), according to manufacturer's instructions. The triose phosphate isomerase (TPI) gene amplifications were performed following a two-step nested polymerase chain reaction (PCR) protocol for genotyping of *Giardia* spp., using the AL3543 [5′-AAATIATGCCTGCTCGTCG-3′] and AL3546 [5′-CAAACCTTITCCGCAAACC-3′] primers for the primary PCR (605 pb), and the AL3544 [5′-CCCTTCATCGGIGGTAACTT-3′] and AL3545 [5′-GTGGCCACCACICCCGTGCC-3′] primers for the secondary PCR (530 pb). Reagents and cycling conditions were the same for both steps, as described in Sulaiman *et al.* (2003), with some modifications. The PCR reaction comprised 3-5.0 µL of DNA, 250 µM each of deoxynucleoside triphosphate (dNTP), 1X PCR buffer (20 mM Tris-HCl, 50 mM KCl, 2.0 mM $MgCl_2$) 1.0 U of Taq polymerase (CELLCO Biotec – Brazil Ltda), 2.0 µL of bovine serum albumin (0.1 g/10 mL), and 1.5 µM of each primer in a total of 25 µL reaction. For the secondary PCR, 4.0 µL of the primary PCR product was used as template. The reactions were performed

for 35 cycles (94°C for 45 s, 48°C for 45 s, and 72°C for 60 s), with an initial hot start (94°C for 5 min) and a final extension (72°C for 10 min).

For genotyping of *Cryptosporidium* spp., the 18s small subunit rRNA gene was amplified in a two-step nested PCR protocol according to Macarisin *et al.* (2010), with some modifications. The primary PCR amplify an 1325 bp fragment using 5.0 µL of DNA, 1X PCR buffer (10 mM Tris-HCl, 50 mM KCl), 1.5 mM $MgCl_2$, 250 µM each of deoxynucleoside triphosphate (dNTP), 2.5 U of Taq polymerase (LUDWIG Biotec – Brazil Ltda), 1.25 µL of bovine serum albumin (0.1 g/10 mL), and 1.0 µM concentrations of each Crypto-F [5'-TTCTAGAGCTAATACATGCG-3'] and Crypto-R [5'-CCCATTTCCTTCGAAACAGGA-3'] primers in a 25 µL reaction volume. The reactions were processed with an initial hot start at 94°C for 3 min, followed by 35 cycles of 94°C for 45 s, 59°C for 45 s, and 72°C for 1 min, and a final extension step at 72°C for 7 min. The secondary PCR used 5.0 µL of primary PCR product as template, in order to amplify an 830 bp fragment, and the same mixture conditions, except that the primers were AL1598 [5'-AAGGAGTAAGGAACAACCTCCA-3'] and AL3032 [5'-GGAAGGGTTGTATTTATTAGATAAAG-3']. The processing program was an initial hot start at 94°C for 1 min, 40 cycles of 94°C for 30 s, 58°C for 90 s, and 72°C for 1 min, and a final extension at 72°C for 7 min. All PCRs were performed in a AXYGEN® Maxygene II PCR thermocycler. Positive genomic DNA controls from concentrated samples of *Giardia* spp. cysts and oocyst of *Cryptosporidium* spp., provided by the FURB Parasitology Laboratory, were included with each PCR run as positive control, as well as distilled water as negative control. PCR products were analyzed on 1% agarose gel and visualized after Gel Red ® (BioLabs) staining.

The amplified products were subjected to enzymatic purification with exonuclease I and alkaline phosphatase (CELLCO Biotec – Brazil Ltda), according to the manufacturer's recommendations, and both stands were sequenced directly at Myleus Biotecnologia (MG-Brazil). The Chromas program (http://technelysium.com.au/wp/chromas/) was used to analyze the quality of the sequences. The reliable sequences were compared to those of the other assemblages using the local alignment tool BLASTN of the National Center for Biotechnology information (NCBI) database (https://blast.ncbi.nlm.nih.gov/Blast.cgi).

For the evaluation of the treatment and possible reuse of FBW, the company Projesan – environmental sanitation, located in Gaspar - SC, yielded three flocculant polymers for the development of the research: 1. PROFLOC A 100: Anionic Polymer, pH 6.0 – 8.0 and viscosity (sol 0.1% / cSt): 100 to 300; 2. PROFLOC C 209: Cationic polymer, pH 5,0 - 8,0 and viscosity (sol. 0.1% / cSt): 50.00 a 150.00; 3. PROFLOC A 110: Slightly anionic polymer, pH 6.0 - 8.0 and viscosity (sol. 0.1% / cSt): 70.0 to 130.0. All polymers presented solid granular appearance and white to slightly yellowish coloration. Preliminary tests were performed with the use of the Jar-Test and Turbidimeter aiming to determine which polymer would be more efficient for the removal of the solid particles from the filter backwash water, its ideal concentration to be added in the sample, agitation speed and effectiveness in decreasing turbidity.

Data were organized in descriptive tables containing absolute frequencies, relative averages, standard deviations and estimates in the form of range with 95% confidence. The data of the quantitative variables were tested using the normality Shapiro-Wilk Test. To compare the groups with respect to the quantitative variable, we used the Student's t-Test (Parametric Test) and the Mann-Whitney Test (Non-Parametric Test) that compares the two independent groups. Pearson's Linear correlation and Spearman's correlation were used to correlate the quantitative. In the cases of association whose variables were categorical or qualitative, Fisher's exact test was used. In all cases, the statistical significance was considered if the P value < 0.05 and the data analysis performed by the Microsoft Excel 2016 software.

3. RESULTS AND DISCUSSION

3.1. Physicochemical analyses of the filter backwash water

Comparing the results of the physicochemical analyses of the North and South wings no significant differences were observed between them. So, the results of the two wings were combined to perform the subsequent statistical analyses.

The physicochemical characteristics of the filter backwash water of WTP II, carried out in this study in general, present agreement with the results obtained in other Brazilian WTPs (Freitas *et al.*, 2010; Molina and Santos, 2010). In relation to the dissolved aluminum content, the data of this study was much lower than those recorded by other researchers. This difference can be explained due to the different dosages of aluminium-based coagulants, as well as the flow volume of the stations, the operating conditions and the characteristics of the raw water. The contents of all groups of solids, and consequently the average of turbidity, showed much higher values. These variations are probably due to differences in the quality of raw water, disposal of wastewater from domestic and industrial exhaustion, erosion rates, agricultural activities, land occupation and influence of the biotic community of the environment (Campos, 2015; Canale, 2014; Freitas *et al.*, 2010; Molina and Santos, 2010; Chaves, 2012; Scalize, 1997).

The concentrations of iron and phosphorus are expressive as compared to the studies by Freitas *et al.* (2010), Molina and Santos (2010) and Scalize (1997). High concentrations of iron may be related to the composition of solids, since this is one of the main elements of soil formation (Carneiro *et al.*, 2013). The characteristics of the filter backwash water are closely related to those of the raw water from the catchment, so the phosphorus content found in the FBW suggests the origin of sanitary sewage, since only 42% of the population is served by the sewage collection network in the Blumenau (Brk Ambiental, 2018).

It's known that filter backwash water from water treatment plants is composed of chemical substances used during the processes to achieve water potability and is closely related to the characteristics of raw water. In a recent study, Piazza *et al.* (2017) evaluated the chemical parameters of the raw water of the four water treatment plants from Blumenau and a conservation unit. Among the evaluated parameters, the raw water captured by WTP II obtained the highest rates in chloride, sulfate, sodium and total organic carbon. The authors report that, due to the watershed of the spring being large, management is difficult, since the waters come from other cities; in addition, natural causes, the use of the soil, and several other mechanisms of action exert anthropic influence on the quality of the hydric body.

Grott *et al.* (2016) evaluated the turbidity value of the raw water catchment of the water treatment plant – WTP II of Blumenau and verified values between 18.3 and 934 UNT. The authors report that this high turbidity value occurs due to the geological formations characterized by Neossolos Fulvic, which have dark coloration and varying granulations. Also, the absence of basic sanitation in part of the city causes the discharge of domestic wastewater into the water body. The high incidence of industries in the region is also responsible for this increase in both the values of chemical parameters and the turbidity index.

The raw water capture of the WTP II of Blumenau is framed as Class 2, according to the CONAMA Resolution n° 430/201, which provides classifications of bodies of water and environmental guidelines for rating, as well as establishes the conditions and standards of effluent discharge.

The results of the physicochemical parameters of the washing water of the filters evaluated in this study were compared with the values established by CONAMA Resolution nº 430/2011 to dispose of effluent in a Class 2 water body (Table 1).

Table 1. Comparison between the physicochemical parameters of the washing water of the filters of WTP II with the limits set by CONAMA Resolution n° 430/2011 for the disposal of wastewater in Class 2 water bodies.

Variables	Average	CONAMA 430/2011	Meets the established standards
Turbidity (uT)	210,08	100 uT	NO
pH	6,69	5,0 to 9,0.	YES
True Color (uH)	4,96	75 mg Pt L^{-1}	YES
Iron (mg L^{-1})	16,81	15 mg L^{-1}	NO
Manganese (mg L^{-1})	0,2	1.0 mg L^{-1}	YES
Copper (mg L^{-1})	0,01	1.0 mg L^{-1}	YES
Zinc (mg L^{-1})	0,07	5.0 mg L^{-1}	YES
Aluminum (mg L^{-1})	0,05	0.1 mg L^{-1}	YES
Phosphor (mg L^{-1})	1,15	0.050 mg L^{-1}	NO
Nitrite (mg L^{-1})	0,02	1.0 mg L^{-1}	YES
Nitrate (mg L^{-1})	3,9	10.0 mg L^{-1}	YES
Total residual chlorine (mg L^{-1})	0,16	0.01 mg L^{-1}	NO
Total solids (mg L^{-1})	575,58	-	-
Fixed total solids (mg L^{-1})	356,17	-	-
Volatile total solids (mg L^{-1})	219,42	-	-
Sedimentary solids (mL L^{-1})	42,13	1 mL L^{-1}	NO
Total suspended solids (mg L^{-1})	394,67	-	-
Fixed suspended solids (mg L^{-1})	269,08	-	-
Volatile suspended solids (mg L^{-1})	125,58	-	-
Total dissolved solids (mg L^{-1})	180,92	500 mg L^{-1}	YES
COD (mg L^{-1})	63,35	-	-

According to the results, it's observed that some of the parameters are above the maximum standards established by CONAMA Resolution n° 430/2011, for the discharge of effluents in Class 2 Rivers, making it illegal to discharge this residue in the water body.

The high turbidity of raw water resulting from the high concentration of solids from the disposal of domestic and industrial effluents and by natural phenomena such as water speed and erosion are related to the composition of the filter backwash water as these particles remain in the WTP at this stage of treatment. Returning this water to the hydric body, besides contributing to the increase of the turbidity of the raw water at the point of discharge, promotes changes in the color of the river, siltation and influence in the regional biota.

The use of natural or synthetic flocculant polymers to reduce turbidity of the filter backwash water has been studied and is proving an efficient alternative (Braga *et al.*, 2007; Freitas *et al.*, 2010). However, in addition to water clarification, it's important to characterize the clarified water in order to verify the removal of other chemical or biological compounds that can negatively impact the environment and the surrounding population.

Iron is one of the main elements of soil formation, along with oxygen, silicon and aluminum. It presents two stages of oxidation, being Fe^{+3} predominant in aerated soils, and in soils with low O_2 content, the reduction of Fe^{+3} for Fe^{+2} is highly observed, being also the form available for plants and animals, since the Fe^{+3} precipitates more easily. The high concentration of this element in the filter backwash water may be related to the soil composition of the region, and also intensified by the coagulant, since the Aluminium Polychloride (PCA) can contain concentrations of up to 0.03% of Fe (Carneiro *et al.*, 2013).

High concentrations of iron may cause irritation when inhaled or by contact with the skin or eyes (Macedo, 2001). In addition, it causes some impacts to the public water supply by conferring color and flavor to the treated water. Biological contamination can occur in the distribution network itself with the deposit of this element through plumbing and the development of iron bacteria (Oliveira *et al.*, 2013).

For the removal of iron in water, the techniques of oxidation with free chlorine, ozone or

potassium permanganate followed by filtration are used (Rönnholm *et al.*, 2001; Moruzzi and Reali, 2012). Aeration processes also promote the reduction of these compounds (Di Bernardo *et al.*, 1993; Knocke, *et al.*, 1987).

Freitas *et al.* (2010), using ionic polymers to reduce the physicochemical parameters of the filter backwash water of water treatment plant filters in Minas Gerais, obtained satisfactory results in relation to iron, decreasing the values from 3.5 to 0.1 mg L^{-1}.

The removal of this compound in water is most often impossible in practice, mainly due to the high investment cost, since an increase in the number of steps of the WTP is required. Thus, studies aimed at the removal of these ions are important to promote more efficient strategies and mainly shorter execution time and cost.

The presence of phosphorus in water is usually related to the disposition of in natura domestic sewage in the hydric body, agricultural activity, industrial effluents, among other anthropic actions (Carneiro *et al.*, 2013). Phosphorus is one of the main elements responsible for eutrophication, which consists of the excessive growth of algae damaging the use of water; moreover, the excessive consumption of oxygen by the algae causes the death of fish and other organisms in the surroundings (Klein and Agne, 2012).

The measures of phosphorus control are related to the correct application of fertilization and effective practices in the prevention of soil erosion. In sanitary sewage, where the concentration of phosphorus is high, the main removal strategies are chemical precipitation by the use of iron or aluminum salts such as coagulant, biological processes of treatment, ion exchange and adsorption (Kaveeshwar *et al.*, 2018).

The use of chlorine (Cl) for disinfection in water treatment plants is very common, its main function being the inactivation of microorganisms such as bacteria. The chlorine found in the filter backwash water comes from the water treatment, since to perform the washing volumes of water from the cistern are used. The amount of free residual chlorine found in this study is much higher than that permitted by CONAMA Resolution n° 430/2011 for disposal in Class 2 water bodies.

The problem related to this high concentration of free residual chlorine is the capacity that this compound has in forming trihalomethanes (THM) from its reaction with organic compounds (Meyer, 1994). Raw water, due to the decomposition of biological material, promotes the development of fulvic and humic acids, which in turn form haloforals due to the presence of ketone radicals in their composition and the reaction with free chlorine. These acids are the precursors of the formation of trihalomethanes (Opas, 1987; Van-Bremem, 1984). Studies establish a certain relationship between trihalomethane compounds formed during the stages of water treatment and cancer (Santos, 1987).

The strategies for the control of the formation of the THM can occur with the reduction of the concentration of precursor acids in the treatment plant by clarification of the water using on coagulants, or in the spring, by aeration, oxidation or by adsorption in activated charcoal. The use of other alternatives for disinfection, such as ozone or ultraviolet light become interesting, or even the removal of THM already formed by activated granular carbon (Laubusch, 1971; Santos, 1987).

The alternatives quoted for the removal of components that were above the values allowed by CONAMA n° 430/2011 resolution require investments in the infrastructure of the water treatment plant, as well as specialized human resources. The deterioration of raw water influences the results of the characterization of effluent generated in the water treatment plant, so it's possible to understand that public policies and more effective inspections in relation to the regulations of use and soil occupation would help to improve the quality of raw water and consequently lower generation of sludge and wastewater in the water treatment plant, being more profitable to conserve the city's water resources than to invest in the infrastructure of the water treatment station.

3.2. Microbiological analysis of filter backwash water

According to CONAMA Resolution n° 430/2011, for water bodies framed as Class 2, a limit of 1000 thermotolerant coliforms per 100 mL of water shouldn't be exceeded and *Escherichia coli* may be determined in substitution to the parameter of thermotolerant coliforms. Table 2 shows the values of total coliforms and *E. coli* found in this study in both wards and the significance between them.

Table 2. Total coliforms and *E. coli* found in the filter backwash water of the WTP II filter in the north and south wings.

Bacterias	ALA		TOTAL	P
	South (n = 12)	North (n = 12)		
Total coliforms (MPN 100 ml^{-1})				
≤ 1000	5 (41.7%)	2 (16.7%)	7 (29.2%)	0,2223
>1000	7 (58.3%)	9 (75%)	16 (66.7%)	
Missing Data	0 (0%)	1 (8.3%)	1 (4.2%)	
E. coli (MPN 100 ml^{-1})				
≤ 1000	4 (33.,3%)	4 (36.4%)	8 (34.8%)	0,6084
>1000	7 (58.3%)	6 (54.5%)	13 (56.5%)	
Missing Data	1 (8.3%)	1 (9.1%)	2 (8.7%)	

I - P: P-value of the T-Test for correlation. If $P < 0.05$ then significant correlation.

According to the results, no significant difference was observed between the total coliform values and *E. coli* between the south and north wings. Regarding the values obtained the presence of quantities higher than 1000 MPN, 100 mL^{-1} was verified for both total coliforms and *E. coli* in most analyses. Thus, the microbiological parameters of the water to wash the water treatment station filters – WTP II of Blumenau, aren't in accordance with the values established by the current norm. It's in natura disposal is inappropriate, and can cause negative impacts both to the environment and to the health of the human population.

Grott *et al.* (2016) evaluated the presence of total coliforms and *E. coli* in the raw water of the water treatment station – WTP II of Blumenau. They obtained minimum and maximum values of 240 - 600 MPN 100 mL^{-1} sample of total coliforms and 33 – 240 MPN 100 mL^{-1} of *E. coli.* The values found in this study were 9.7- > 2419,6 MPN 100 mL^{-1} for total coliforms and 22.6 - > 2419,6 MPN 100 mL^{-1} for *E. coli*.

Filtration is the main barrier for microorganisms during water treatment (Arora *et al.*, 2001; Lechevallier and Norton, 1995). The accumulation of these bacteria in the filter bed suggests the reason for this high number of microorganisms in the filter backwash water, being important information for verifying the potential functioning of the filters.

It's noteworthy that the inadequate disposal of this wastewater causes an increase in the concentration of these microorganisms in the area of discharge, which can negatively impact the population that lives near the river and uses the water without adequate treatment.

Due to the fact that the washing of the filters of the water treatment station in question occurs with the water of the cistern, which include chlorine, it's possible that during the process part of these microorganisms are inactivated. However, as shown by the results, the treatment of this residue before its disposition in the hydric body should be carried out.

There are numerous disinfection mechanisms for water, among them, disinfection by chemical agents, which is commonly performed with liquid or gaseous chlorine, or derivatives such as sodium or calcium hypochlorite and chlorine dioxide because they are easy to apply and low cost. However, these mechanisms are not efficient against cysts and oocysts of *Giardia* spp. and *Cryptosporidium* spp., since they are highly resistant (Cheung, 2017). Other

disinfection mechanisms are the use of ozone and ultraviolet (UV) radiation. The use of ozone in water treatment plants in the United States obtained satisfactory results in the inactivation of *Giardia* spp. (Thompson and Drago, 2015). Cantusio-Neto *et al.* (2006) obtained a 98.9% reduction of *Giardia* spp. cysts and 99.7% of *Cryptosporidium* spp. oocysts using activated sludge UV disinfection at a sewage treatment plant. However, the action of UV was not completely efficient in relation to the inactivation of *Giardia* spp. cysts. Trophozoites were found in a rat intestine scraping of the UV-treated group. However, the combination of the three techniques - use of chlorine, ozone and UV can play an important role in the inactivation of these protozoa (Thompson and Draco, 2015).

When a correlation analysis between turbidity and *E. coli* values was performed, it was possible to verify a moderate correlation between these parameters (P = 0,0420).

Souza and Gastaldini (2014) found no correlation between the parameters of *E. coli* and turbidity in their study carried out in hydrographic basins that suffer anthropic action. The turbidity ratio was evident with the parameters of suspended solids and flow, and *E. coli* was strongly related to the values of DBO.

Roberto *et al.* (2017) in the study on the evaluation of pH, turbidity and parasitological analysis of the water of the Guará Velho Stream, in the city of Guaraí/TO, verified a strong relationship between the results of turbidity and MPN of *E. coli* in two of the five points evaluated in the study.

The concentration of solids in water is closely related to the turbidity value, as well as the dumping of sanitary sewage. The bacterium *E. coli* is of fecal origin both of humans and other animals; thus, the absence of sewage collection networks in more than 50% of the population of the municipality of Blumenau, suggests the relationship between the turbidity and MPN parameters of *E. coli* in this study.

Due to the presence of *E. coli*, most often associated with contamination of fecal origin, another important relationship is that of these bacteria with the possible presence of pathogenic enteric protozoa, such as *Giardia* spp. and *Cryptosporidium* spp.

3.3. Parasitological analyses of the filter backwash water

The parasitological analyses for *Giardia* spp. and *Cryptosporidium* spp. in the period of one year performed in the north and south wings didn't present significant differences for *Giardia* spp., with the value of P = 0.9110 using the Mann-Whitney test after normality was determined by the Shapiro-Wilk test. Regarding the research of *Cryptosporidium* spp., it wasn't possible to perform the statistical tests since the presence of this parasite wasn't determined in one of the wings during the entire study period.

Of the 24 analyzed samples, in 11 were verified the presence of *Giardia* spp. and in only three of *Cryptosporidium* spp. The greater detection of *Giardia* spp. indicates greater circulation of this protozoan in the region. Similar results were observed by Grott *et al.* (2016) analyzing raw water from the Itajaí-Açu River in Blumenau (SC), Miglioli *et al.* (2017) in Sewage Treatment Plant sludge, also in Blumenau (SC), Greinert *et al.* (2004) in pool water in the city of Florianópolis (SC), Franco *et al.* (2001) in Campinas (SP), Cantusio-Neto *et al.* (2006) in Sewage Treatment Plant sludge also in Campinas (SP), Sato *et al.* (2013) in several springs of the state of São Paulo.

Grott *et al.* (2016), evaluated the parasitological profile of the raw water uptake of the water treatment station – WTP II of Blumenau, and the results were compared with this research (Table 3).

Table 3. Comparison between the results of the survey of *Giardia* spp. and *Cryptosporidium* spp. in the raw water and in the filter backwash water of the water treatment station of Blumenau – WTP II.

	Filter backwash water		**Raw Water (Grott *et al.*, 2016)**	
	***Giardia* spp.**	***Cryptosporidium* spp.**	***Giardia* spp.**	***Cryptosporidium* spp.**
Total Analyses	24	24	14	14
Positive	11	3	8	2
Range	200 - 600	200 - 400	40 - 70	118 - 454
Average	133.33	33.33	141.10	286
Frequency	45.83%	12.50%	57.14%	14.28%

The positivity frequency of both protozoa was similar in the analyses of raw water and in the filter backwash water. Regarding the detection of *Giardia* spp. cysts, the maximum and minimum values in the filter backwash water are much higher than those found in the raw water. This variation is probably related to the higher concentration of these organisms during the filtration stage consequently the filter backwash water also presents a greater abundance of these protozoa.

Regarding the detection of oocyst of *Cryptosporidium* spp., the amplitude found in both studies was similar. The smallest amount of positive results for the analysis of *Cryptosporidium* spp. may be related to the epidemiology of cryptosporidiosis in the area of Blumenau. In addition to the lower frequency of infection in the population, the high turbidity of the sample may interfere with the efficiency of the technique in the detection of oocyst.

No positive sample for *Cryptosporidium* spp. presented the expected two-step PCR amplification pattern, even with several attempts to optimize the protocol.

Only two of the FBW positive samples for *Giardia* spp. presented the approximately 530 pb expected amplification by two-step PCR. The sequences obtained (NCBI accession numbers MK208823 and MK208824) presented 99% homology with sequences of *G. duodenalis* - Assemblage B.

With the presented results, it was found that the filter backwash water of the WTP II presents high levels of turbidity, iron, manganese, copper, phosphorus, free residual chlorine, total coliforms and *E. coli*, being above that allowed by CONAMA Resolution nº 430/2011, in addition to the presence of *Giardia duodenalis* cysts genotype B, which is zoonotic, and *Cryptosporidium* spp. oocysts.

Karanis *et al.* (1996) detected *Giardia* spp. and *Cryptosporidium* spp. or both in 92% of the filter backwash water from a WTP in Germany. The detection rate in raw water samples was 91.7%. Karanis *et al.* (1998) observed that good elimination results were obtained by optimizing relevant water treatment processes, but a low flocculant dose following sudden variation in the raw water quality causes a breakthrough of these protozoan into the treated water.

The use of polymer flocculant to clarify the filter backwash water was evaluated, and, after preliminary tests, higher efficiency was found in the polymer Profloc A 100, with anionic character, in the concentration of 0.01% with rapid agitation of one minute, followed by slow agitation for another minute in a jar-test. The sedimentation time was 30 minutes and its efficiency in reducing turbidity reached 99.49%.

One of the main alternatives studied and applied by water treatment plants in relation to the waters of filter backwash, is its recirculation to the beginning of the system. However, the high rates of turbidity of this residue can cause losses in the treatment process. In this way, several studies aimed at the quality of reuse of this effluent propose pre-treatment with application of different polymers in order to clarify the filter backwash water before it's forwarded to the beginning of the treatment.

Freitas *et al.* (2010) also evaluated the clarification of the waters of filter backwash without and with different polymers in order to determine which is the most efficient in decreasing the physicochemical values before this water is recirculated to the system. The values of DQO, Fe, Al, Mn, pH, turbidity, solids in total suspension and sedimentary solids were significantly reduced when cationic polymer was used; turbidity was decreased from 33.5 UNT to 1.5 UNT

Braga *et al.* (2007) determined the reduction of turbidity from 33.5 UNT to 5.32 UNT and total suspended solids from 75 mg L^{-1} to 13.5 mg L^{-1} also when the cationic polymer was used in the clarification of FBW.

Molina and Santos (2010) verified the efficiency in the clarification of FBW using light and medium anionic polymer and potato starch. The three components presented similarity in results, achieving great efficiency in the removal of the flakes. The use of potato starch stands out because it's natural, inexpensive and easy to acquire.

The process of sedimentation of the filter backwash water, with or without the use of polymer generates a more concentrated sludge that, depending on its characteristics, can be incorporated into ceramic material or civil construction or then be destined to a landfill appropriate to its classification (Vitorino *et al.*, 2009).

The filter backwash water of the WTP II of Blumenau presents characteristics similar to those found in these studies that aimed to recirculate of this type of sample to the beginning of the system. However, the importance of a pre-treatment of this residue before its reuse is evident. The use of polymer is a promising alternative, since the quantity to be used and the time for the removal of solids are low, which promotes the reuse of the filter backwash water and the reduction of operating costs (Lustosa *et al.*, 2017).

4. CONCLUSIONS

The filter backwash water of the water treatment plant of Blumenau – WTP II presents some physicochemical and microbiological indices higher than the maximum limit allowed by CONAMA Resolution N° 430/2011 for in natura disposal in Class 2 water bodies, highlighting turbidity, some solids, Fe, P and Cl, Coliformes Total and *E. coli*. Therefore, it shouldn't be discarded without prior treatment.

The high concentrations observed in the microbiological and parasitological analyses can bring negative impacts both to the environment and to the health of the human population, emphasizing the importance of a pre-treatment of this residue before it's disposed of in water bodies.

The use of flocculant polymers is an interesting alternative to clarify the filter backwash water, since they have properties that reduce the physicochemical, microbiological and parasitological loads of the effluent, and through this process allow the recirculation of FBWat the beginning of treatment, being an option for the reuse of this residue.

The high concentrations of phosphorus and turbidity, which suggest a relation with the discharge of sanitary sewage, anthropic actions and erosion episodes, can be solved with investments in the basic sanitation of the city and public policies in the supervision of occupation and land use.

Investments in the conservation of the Itajaí-Açu River and maintenance of surface water quality can be more profitable than the application of new methodologies in the water treatment plants of Blumenau, since with the preservation of raw water, the physicochemical, microbiological and parasitological parameters of the effluent of the WTP tend to conform with CONAMA Resolution n° 430/2011.

5. ACKNOWLEDGEMENTS

To the Coordination of Improvement of Personnel in Superior (CAPES) Level for the concession of the master's degree to the first author. To the University Regional of Blumenau (FURB) through the Program of Master's Degree in Environmental Engineering for the orientation and use of laboratories and equipment. To the Municipal Autonomous Service of Water and Sewer (SAMAE) for authorizations and pertinent information from the water treatment system of the municipal district of Blumenau. To the company PROJESAN for providing the polymer used in the research.

6. REFERENCES

ACHON, C. L.; BARROSO, M. M.; CORDEIRO, J. S. Leito de drenagem: sistema natural para redução de volume de lodo de estação de tratamento de água. **Revista Engenharia Sanitária e Ambiental**, v. 13, n. 1, p. 54-62, 2008. http://dx.doi.org/10.1590/s1413-41522008000100008

ADLER, E. Management of wastes from drinking water treatment in Norway. *In*: CIWEM (Org.). **Management of Wastes from Drinking Water Treatment.** London, 2002.

APHA. **Standard methods for the examination of water and wastewater.** 22nd ed. Washington DC, 2012.

ARORA, H.; DI GIOVANNI, G.; LECHEVALLIER, M. Spent filter backwash water contaminants and treatment strategies. **Journal American Water Works Association**, v. 93, n. 5, p. 100-112, 2001. http://dx.doi.org/10.1002/j.1551-8833.2001.tb09211.x

BALDURSSON, S.; KARANIS, P. Waterborne transmission of protozoan parasites: review of worldwide outbreaks–an update 2004–2010. **Water research**, v. 45, n. 20, p. 6603-6614, 2011. https://dx.doi.org/10.1016/j.watres.2011.10.013

BRAGA, M. D.; BEVILACQUA, P. D.; BASTOS, R. K. X.; FREITAS, A. G.; FERREIRA, G. M. Microbiological characterization of filter washing water and evaluation of different recirculation scenarios. **Revista AIDIS de Ingeniería y Ciencias Ambientales: Investigación, Desarrollo y Práctica,** v. 1, n. 3, 2007.

BRK AMBIENTAL. **Seu esgoto.** 2018. Available in: https://www.brkambiental.com.br/blumenau/agua-e-esgoto/seu-esgoto/. Access: 24 Dec. 2018.

CAMPOS, H. L. **Caracterização das águas de lavagem de filtros em estações de tratamento de água de filtração direta.** 2015. Dissertação (Mestrado em Engenharia Sanitária) – Universidade Regional do Rio Grande do Norte, Natal, 2015.

CANALE, I. **Caracterização microbiológica, parasitológica e físico-química da água de lavagem de filtros recirculada em ETA de ciclo completo.** 2014. Dissertação (Mestrado em Tecnologia) - Universidade Estadual de Campinas, Campinas - SP, 2014.

CANTUSIO-NETO, R.; SANTOS, J. U.; FRANCO, R. M. B. Evaluation of activated sludge treatment and the efficiency of the disinfection of *Giardia* species cysts and *Cryptosporidium* oocysts by UV at a sludge treatment plant in Campinas, south-east Brazil. **Water Science and Technology**, v. 54, n. 3, p. 89-94, 2006. https://dx.doi.org/10.2166/wst.2006.453

CARNEIRO, C.; WEBER, P. S.; ROSS, B. Z. L. Caracterização do Lodo de ETA gerado no Estado do Paraná. *In*: CARNEIRO, C.; ANDREOLI, C. V. (Eds.). **Lodo de Estações de Tratamento de Água:** Gestão e Perspectivas Tecnológicas. Curitiba: Sanepar, 2013. Cap. 3. p. 132-178.

CHAVES, K. O. **Desenvolvimento e Aplicação de sistema de floco-flotação por ar dissolvido para tratamento da água de lavagem do filtro da WTP Gavião.** 2012. Dissertação (Mestrado em Engenharia Sanitária) – Universidade Federal do Ceará, Fortaleza, 2012.

CHEUNG, P. C. W. A historical review of the benefits and hypothetical risks of disinfecting drinking water by chlorination. **Journal of Environment and Ecology**, v. 8, n. 1, p. 73-151, 2017. https://dx.doi.org/10.5296/jee.v8i1.11338

CONAMA. Settlement n. 357 from March 17th 2005. It deals with the classification of water bodies and environmental guidelines for its classification, as well as establishes the conditions and standards for the discharge of effluents, and provides other measures. **Diário Oficial [da] União,** Brasília, DF, 18 Mar. 2005. Available: http://www2.mma.gov.br/port/conama/legiabre.cfm?codlegi=459. Access date: 11 May 2016.

CONAMA. Settlement n. 430 from May 13th 2011. It has on conditions and standards for the release of effluent, complements and alters the resolution No 357, of March 17, 2005. **Diário Oficial [da] União**, Brasília, DF, 16 May 2011. Available in: http://www2.mma.gov.br/port/CONAMA/legiabre.cfm?codlegi=646. Access date: 11 May 2016.

CORDEIRO, J. S.; CAMPOS, J. R. O impacto ambiental provocado pela indústria da água de abastecimento. *In:* APIS. **Gestión ambiental en el siglo XXI**. Lima, 1998. p. 1-12.

CORNWELL, D. A.; MUTTER, R. N.; VANDERMEYDEN, C. **Commercial Application and Marketing of Water Plant Residuals.** Denver: AWWA, 2000.

DI BERDARDO, L.; DANTAS, A. D.; VOLTAN, P. N. **Métodos e técnicas de tratamento e disposição dos resíduos gerados em estações de tratamento de água.** São Carlos: LDiBe, 2012.

DI BERNARDO, L.; DANTAS, DI BERNARDO, A. **Métodos e técnicas de tratamento de água.** Rio de Janeiro: ABES, 1993.

EFSTRATIOU, A.; ONGERTH, J. E.; KARANIS, P. Waterborne transmission of protozoan parasites: review of worldwide outbreaks-an update 2011-2016. **Water research**, v. 114, n. 20, p. 14-22, 2017. https://dx.doi.org/10.1016/j.watres.2017.01.036

FRANCO, R. M. B.; ROCHA-EBERHARDT, R.; CANTUSIO-NETO, R. Occurrence of *Cryptosporidium* oocysts and *Giardia* cysts in raw water from the Atibaia river, Campinas, Brazil. **Revista do Instituto de Medicina Tropical de São Paulo**, v. 43, n. 2, p. 109-111, 2001. http://dx.doi.org/10.1590/S0036-46652001000200011

FREITAS, A. G.; BASTOS, R. K. X.; BEVILACQUA, P. D.; PÁDUA, V. L.; PIMENTA, J. F. P.; ANDRADE, R. C. de. Recirculation of water to wash filters and hazards associated with protozoa. **Revista Engenharia Sanitária e Ambiental**, v. 15, n. 1, p. 37-46, 2010. http://dx.doi.org/10.1590/S1413-41522010000100005

GRAMEL, S. **Results of the Case Study on the Water Supply in the Region of Frankfurt/Germany.** In: Achieving Sustainable and Innovative Policies through Participatory Governance in a Multi-Level Context. Final Report of a Research Project funded by the European Community. Darmstadt, 2002.

GREINERT, J. A.; FURTADO, D. N.; SMITH, J. J.; BARARDI, C. R. M.; SIMÕES, C. M. O. Detection of *Cryptosporidium* oocysts and *Giardia* cysts in swimming pool filter backwash water concentrates by flocculation and immunomagnetic separation. **International Journal of Environmental Health Research**, v. 14, n. 6, p. 395-404, 2004. https://dx.doi.org/10.1080/09603120400012892

GROTT, S. C.; HARTMANN, B.; SILVA FILHO, H. H.; FRANCO, R. M. B.; GOULART, J. A. G. Detecção de cistos de *Giardia* spp. e oocistos de *Cryptosporidium* spp. na água bruta das estações de tratamento no município de Blumenau, SC, Brasil. **Revista do Instituto de Medicina Tropical de São Paulo**, v. 11, n. 3, p. 689-701, 2016. http://dx.doi.org/10.4136/ambi-agua.1853

HOPPEN, C.; PORTELLA, K. F.; JOUKOSKI, A.; BARON, O.; FRANCK, R.; SALES, A.; ANDREOLI, C. V.; PAULON, V. A. Co-disposição de lodo centrifugado de Estação de Tratamento de Água (WTP) em matriz de concreto: método alternativo de preservação ambiental. **Water research**, v. 51, n. 20, p. 85-95, 2005. http://dx.doi.org/10.1590/s0366-69132005000200003

HOPPEN, C.; PORTELLA, K. F.; JOUKOSKI, A.; TRINDADE, E. M.; ANDREÓLI, C. V. Uso de lodo de estação de tratamento de água centrifugado em matriz de concreto de cimento portland para reduzir o impacto ambiental. **Revista do Instituto de Medicina Tropical de São Paulo**, v. 29, n. 1, p. 79-84, 2006. http://dx.doi.org/10.1590/s0100-40422006000100016

IBGE. **Pesquisa Nacional de Saneamento Básico 2008.** Rio de Janeiro, 2010. Available in: http://biblioteca.ibge.gov.br/visualizacao/livros/liv45351.pdf Access: 11 Feb. 2018.

JANUÁRIO, G. F.; FERREIRA FILHO, S. S. Planejamento e aspectos ambientais envolvidos na disposição final de lodos das estações de tratamento de água da Região Metropolitana de São Paulo. **Engenharia Sanitária e Ambiental**, v. 12, n. 2, p. 117-126, 2007. http://dx.doi.org/10.1590/s1413-41522007000200002

KARANIS, P.; SCHOENEN, D.; SEITZ, H. M. Distribution and removal of *Giardia* and *Cryptosporidium* in water supplies in Germany. **Water science and technology**, v. 37, n. 2, p. 9-18, 1998. http://dx.doi.org/10.2166/wst.1998.0091

KARANIS, P.; SCHOENEN, D.; SEITZ, H. M. *Giardia* and *Cryptosporidium* in backwash water from rapid sand filters used for drinking water production. **Zentralblatt für Bakteriologie**, v. 284, n. 1, p. 107-114, 1996. http://dx.doi.org/10.1016/s0934-8840(96)80159-9

KAVEESHWAR, A. R.; PONNUSAMY, S. K.; REVELLAME, E. D.; GANG, D. D.; ZAPPI, M. E.; SUBRAMANIAM, R. Pecan shell based activated carbon for removal of iron (II) from fracking wastewater: Adsorption kinetics, isotherm and thermodynamic studies. **Process Safety and Environmental Protection**, v. 114, p. 107-122, 2018. https://dx.doi.org/10.1016/j.psep.2017.12.007

KLEIN, C.; AGNE, S. A. A. Fósforo: de nutriente à poluente. **Engenharia Sanitária e Ambiental**, v. 8, n. 8, p. 1713-1721, 2012. http://dx.doi.org/10.5902/223611706430

KNOCKE, W. R.; HOEHN, R. C.; SINSABAUGH, R. L. Using alternative oxidants to remove dissolved manganese from waters laden with organics. **Journal American Water Works Association**, v. 79, n. 3, p. 75-79, 1987. http://dx.doi.org/10.1002/j.1551-8833.1987.tb02818.x

LAUBUSCH, E. J. Chlorination and other disinfection processes. *In*: APHA. **Water quality and treatment**: a handbook of public water supplies. New York, 1971. p. 158-224.

LECHEVALLIER, M. W.; NORTON, W. D. *Giardia* and *Cryptosporidium* in raw and finished water. **Journal American Water Works Association**, v. 87, n. 9, p. 54-68, 1995. http://dx.doi.org/10.1002/j.1551-8833.1995.tb06422

LUSTOSA, J. B.; BRACARENSE, D. C.; CASTRO, F. B. S.; QUEIROZ, S. C. B.; SILVA, G. G. Tratamento e aproveitamento de água de lavagem de filtro em estação de tratamento de água. **Revista DAE**, v. 65, n. 206, p. 44-61, 2017. http://dx.doi.org/10.4322/dae.2016.027

MACARISIN, D.; SANTÍN, M.; BAUCHAN, G.; FAYER, R. Infectivity of *Cryptosporidium parvum* oocysts after storage of experimentally contaminated apples. **Journal of Food Protection**, v. 73, n. 10, p. 1824-1829, 2010. http://dx.doi.org/10.4315/0362-028x-73.10.1824

MACEDO, J. A. B. **Águas & Águas.** São Paulo: Livraria Varela, 2001.

MENEZES, A. C. L. S. M.; GADELHA, C. L. M.; SILVA-JUNIOR, W. R.; MACHADO, T. T. V.; ALMEIDA, T. M. V. Caracterização de água de lavagem de uma estação de tratamento de água, com vistas ao reuso. **Revista Brasileira de Engenharia Agrícola e Ambiental**, v. 9, p. 191-196, 2005.

MEYER, S. T. O uso de cloro na desinfecção de águas, a formação de trihalometanos e os riscos potenciais à saúde pública. **Cadernos de Saúde Pública**, v. 10, n. 1, p. 99-110, 1994. http://dx.doi.org/10.1590/S0102-311X1994000100011

MIGLIOLI, M. G.; ZUANAZZI, J. G.; SILVA, J. D.; FRANCO, R. M. B.; GREINERT-GOULART, J. A. Removal of *Cryptosporidium* spp. oocysts and *Giardia* spp. cysts at a Wastewater Treatment Plant Garcia, in Blumenau, SC, Brazil. **Revista Ambiente & Água**, v. 12, n. 6, p. 1001-1016, 2017. http://dx.doi.org/10.4136/ambi-agua.2028

MOLINA, T.; SANTOS, H. R. dos. Caracterização e tratamento de água de lavagem de filtros de ETA, com o uso de polímeros sintéticos e amido de batata. **Revista Engenharia e Tecnologia,** v. 2, n. 3, p. 28-44, 2010.

MORUZZI, R. B.; REALI, M. A. P. Oxidação e remoção de ferro e manganês em águas para fins de abastecimento público ou industrial: uma abordagem geral. **Revista de Engenharia e Tecnologia**, p. 29-43, 2012.

OLIVEIRA, C. A. de; BARCELO, W. F.; COLARES, C. J. G. Estudo das características físico-químicas da água de lavagem de filtro em uma estação de tratamento de água para fins de reaproveitamento. **Periódico Eletrônico Fórum Ambiental da Alta Paulista,** v. 9, n. 11, p. 113-130, 2013. http://dx.doi.org/10.17271/198008279112013665

OPAS. **Guias para la Calidad del Agua Potable.** Volume I, II e III. Genebra, 1987.

PIAZZA, G. A.; GROTT, S. C.; GREINERT-GOULART, J. A.; KAUFMANN, V. Caracterização espaço-temporal da qualidade das águas superficiais dos mananciais de abastecimento de Blumenau/SC. **Rega**, v. 14, n. 8, p. 1-13, 2017. http://dx.doi.org/10.21168/rega.v14e8

RICHTER, C. A. **Água:** métodos e tecnologia de tratamento. São Paulo: Blucher, 2009. 340p.

ROBERTO, M. C.; GUIMARÃES, A. P. M.; RIBEIRO, J. L.; CARVALHO, A. V.; NERES, J. C. I.; CERQUEIRA, F. B. Avaliação do pH, turbidez e análise microbiológica da água do córrego guará velho em Guaraí, estado do Tocantins. **Desafios**, v. 4, n. 4, p. 3-14, 2017. https://dx.doi.org/10.20873/uft.2359-3652.2017v4n4p3

RÖNNHOLM, M. R.; WÄRNA, J.; VALRAKARI, D.; SALMI, T.; LAINE, E. Kinetics and mass transfer effects in the oxidation of ferrous sulfate over doped active carbono. **Catalysis Today**, v. 66, p. 447-452, 2001.

SAMAE. **Revisão do Plano Municipal de Saneamento Básico de Blumenau (SC).** Volume 02/07 – Abastecimento de Água Potável - Versão Preliminar. September 2016. Available in: https://pmsbblumenau.wordpress.com/consulta-publica/ Access: Sep. 23rd 2016.

SANTOS, C. L. Trihalometanos: Resumo Atual. **Engenharia Sanitária**, v. 26, p. 190-194, 1987.

SATO, M. I. Z.; GALVANI, A. T.; PADULA, J. A.; NARDOCCI, A. C.; LAURETTO, M. S.; RAZZOLINI, M. T. P.; HACHICH, E. M. Assessing the infection risk of *Giardia* and *Cryptosporidium* in public drinking water delivered by surface water systems in São Paulo State, Brazil. **Science of The Total Environment**, v. 442, p. 389-396, 2013. http://dx.doi.org/10.1016/j.scitotenv.2012.09.077

SCALIZE, P. S. **Caracterização e clarificação por sedimentação da água de lavagem de filtros rápidos de estações de tratamento de água que utilizam sulfato de alumínio como coagulante primário**. 1997. Tese (Doutorado em Hidráulica e Saneamento) - Universidade de São Paulo, São Paulo, 1997.

SILVA-JUNIOR, I. C. S.; HARAGUCHI, M. T.; UCKER, F. E.; BORBA, W. F.; KEMERICH, P. D. C. Avaliação dos sistemas de reutilização da água de lavagem dos filtros de uma estação de tratamento de água: estudo de caso. **Revista Monografias Ambientais**, v. 13, n. 5, p. 3713-3717, 2014. http://dx.doi.org/10.5902/2236130814057

SIMPSON, A.; BURGESS, P.; COLEMAN, S. J. The Management of Potable Water Treatment Sludge: Present Situation in the UK. *In*:: CIWEM (Org.). **Management of Wastes from Drinking Water Treatment**. London, 2002. p. 29-36.

SOUZA, M. M.; GASTALDINI, M. C. C. Avaliação da qualidade da água em bacias hidrográficas com diferentes impactos antrópicos. **Engenharia Sanitária e Ambiental**, v. 19, n. 3, 2014. http://dx.doi.org/10.1590/s1413-41522014019000001097

SULAIMAN, I. M.; FAYER, R.; BERN, C.; GILMAN, R. H.; TROUT, J. M.; SCHANTZ, P. M.; DAS, P.; LAL, A. A.; XIAO, L. Triosephosphate isomerase gene characterization and potential zoonotic transmission of *Giardia duodenalis.* **Emerging infectious diseases**, v. 9, p. 1444–1452, 2003. http://dx.doi.org/10.3201/eid0911.030084

THOMPSON, C. M.; DRAGO, J. North American Installed Water Treatment Ozone Systems. **Journal-American Water Works Association**, v. 107, n. 10, p. 45-55, 2015. http://dx.doi.org/10.5942/jawwa.2015.107.0157

VAN-BREMEM, J. W. Q. **International Course in Sanitary Engineering**. Delft: IHE, 1984.

VESEY, G.; SLADE, J. S.; BYRBE, M. SHEPHERD, K.; FRICKER, C. R. A new method for the concentration of *Cryptosporidium* oocysts from water. **Journal Of Applied Bacteriology**, v. 75, p. 82-86, 1993. http://dx.doi.org/10.1111/j.1365-2672.1993.tb03412.x

VITORINO, J. P. D.; MONTEIRO, S. N.; VIEIRA, C. M. F. Caracterização e incorporação de resíduos provenientes de Estação de Tratamento de Água em cerâmica argilosa. **Revista Cerâmica**, v. 55, p. 385-392, 2009. http://dx.doi.org/10.1590/s0366-69132009000400008